S. RUMYANTSEV

INDUSTRIAL RADIOLOGY

S. RUMYANTSEV

INDUSTRIAL RADIOLOGY


INDUSTRIAL RADIOLOGY

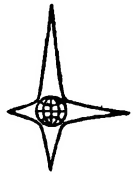

MIR
PUBLISHERS

С.В. РУМЯНЦЕВ

ПРИМЕНЕНИЕ РАДИОАКТИВНЫХ ИЗОТОПОВ В ДЕФЕКТОСКОПИИ

АТОМИЗДАТ

МОСКВА

S. RUMYANTSEV

INDUSTRIAL RADIOLOGY

Translated from the Russian
by
S. SEMYONOV

MIR PUBLISHERS • MOSCOW

1967

First Published 1962

Second Printing

На английском языке

CONTENTS

PART ONE

PHYSICAL AND ENGINEERING FUNDAMENTALS

PART TWO

METHODS OF INDUSTRIAL RADIOLOGY BASED ON THE USE OF RADIOACTIVE RADIATION

Part One

PHYSICAL AND ENGINEERING FUNDAMENTALS

CHAPTER I

STRUCTURE OF MATTER. RADIOACTIVE DECAY. RADIOACTIVE ISOTOPES EMPLOYED IN FLAW DETECTION

§ 1. Atomic structure. Electron shells and nuclear composition. Isotopes

According to the Periodic Law discovered by D. I. Mendeleyev, all known natural chemical elements are arranged in the Periodic Table in the order of increased nuclear charges and regularity of chemical properties.

The atom of any elementary substance consists of a positively charged nucleus and electrons, negatively charged particles surrounding the nucleus. The charge of an electron e is equal to 4.8029×10^{-10} electrostatic unit. The mass of an electron is about 1,840 times smaller than the atomic mass unit* and is equal to 9.108×10^{-28} g. The absolute value of the electron charge is called the elementary (smallest) charge. The atomic nucleus is about 10,000-100,000 times smaller than the atom (the linear dimension of an atom is about 10^{-8} cm and that of the nucleus—10^{-13} to 10^{-12} cm). Nearly all the mass of an atom is concentrated in its nucleus which is positively charged. The charge of a nucleus is determined by the number of protons it contains. This number is called the atomic number of the element and is denoted by Z. Z coincides with the number of the place the element occupies in the Periodic Table. When in the normal state, the atom is neutral; this means that the number of its positively charged particles is equal to the number of electrons. For example, the nuclear charge of lithium ($Z=3$) is equal to three positive charge units, hence the atom contains three electrons. Iron occupies the 26th place in the Periodic Table and has 26 electrons and a positive charge of 26 elementary charges. Attractive forces act between the positively charged nucleus and negatively charged electrons. The electrons are able to keep their orbit, if they do not receive additional energy.

---

* By definition the atomic mass unit is 1/16 the mass of an oxygen atom and is equal to 1.66×10^{-24} g.

Electron shells. The electrons surrounding the atomic nucleus are located on certain energy levels or shells. Shells are denoted according to the following system. The shell closest to the nucleus is called the *K*-shell, and is followed by *L*-, *M*-, *N*-, *P*- and *Q*-shells. The closer an electron to the nucleus, the stronger the attraction between the electron and nucleus, i.e., the higher the electron binding energy. Thus, more energy is required to remove an electron from the *K*-shell than from the *L*-shell, etc.

The maximum possible number of electrons in a shell may be determined with the aid of quantum mechanics, applying the Pauli exclusion principle: the *K*-shell contains only two electrons; the *L*-shell—8; *M*-shell—18; *N*-shell—32, etc. New electron shells are closed or filled as the number of nuclear charges increases. The number of electrons in the outer shell is repeated periodically. Thus, a lithium atom contains three electrons, two of them in the *K*-shell and one in the outer *L*-shell; the sodium atom contains 11 electrons: two are arranged in the *K*-shell, eight in the *L*-shell, one in the *M*-shell, etc.

The chemical properties of an atom are determined principally by the outer-shell electrons, for these electrons are least of all bound to the nucleus and they are more susceptible to external influence. The periodic change in the number of outer-shell electrons, as new electron shells are filled, explains the periodicity in the chemical properties of elements in the Periodic Table. For example, the outer shells of lithium, sodium, potassium and rubidium possess one electron each, and the outer shells of halogens—seven each.

The combining of atoms into molecules involves the reconstruction of outer shells only. Chemical reactions are not followed by any change in the structure of the inner shells and the nucleus.

The energy state of an atom is determined by the mutual arrangement of the nucleus and surrounding electrons. In the ground state the electrons are contained in the shells nearest to the nucleus.

Energy may be imparted to an atom in various ways, for instance, by heating the substance or by irradiation. Depending upon the amount of energy received, an electron either becomes detached from the atom, or moves from a lower to a higher energy level, where it is not so closely bound with the nucleus. Excess energy puts the atom into an excited state, i.e., into one of the several possible higher energy states. In the excited state the atom is unstable. It returns to the normal state as a result of a spontaneous rearrangement of the electronic structure of the atom, the electrons filling free spaces in the shells closest to the nucleus. The excess excitation energy is emitted as quanta or photons.

When an electron is ejected from an atom, the latter, having a prevailing positive charge, becomes a positively charged ion. The ion may become neutral by attracting the nearest free electrons. If

the removal of an electron causes a vacancy in the K-shell, the vacancy is filled by an electron from one of the outer shells.

The transition of an atom from an excited to an unexcited state is accompanied by emission of electromagnetic quanta (photons) of quite definite energies constituting the characteristic radiation of the atom. The energy of the emitted quanta is equal to the difference between the energy binding the electron to the shell it occupied after the atom returned into an unexcited state and the energy binding the electron to the shell it occupied before ejection.

Nuclear structure. Atomic nuclei are complex in structure and consist of protons and neutrons. Proton P is a positively charged elementary particle, the mass of which is $m_P = 1.007579$ amu. The proton-mass-to-electron-mass (m_e) ratio is $\frac{m_P}{m_e} = 1{,}840$. The neutron is a neutral particle of zero charge, with the mass approximating that of a proton (the mass of a neutron $m_n = 1.00898$ amu). Collectively, the protons and neutrons contained in the nucleus are sometimes called nucleons. The total number of protons and neutrons (nucleons) in the nucleus of an atom is called the mass number A of the atomic nucleus. The mass number is approximately equal to the atomic weight of the element, for the atomic weights of a proton and neutron are approximately equal to unity. The number of protons in the nucleus determines its charge and is numerically equal to the atomic number Z of the element. The number of neutrons in the nucleus is $N = A - Z$.

The nuclei of different chemical elements are denoted by an element, the chemical symbol followed by a superscript and subscript. The superscript indicates the mass number of the element and the subscript—its nuclear charge. For example, the nucleus of cobalt—Co_{27}^{59} consists of 27 protons and 32 (59 — 27) neutrons.

Isotopes. Atoms of an element with the same nuclear charge, but with different mass numbers, are called isotopes. Thus, the nuclei of isotopes possess an equal number of protons, but a different number of neutrons. Since the chemical properties of elements are primarily determined by the nuclear charge (atomic number), the isotopes of an element are similar chemically and differ only in mass numbers.

It is in rare cases only that natural elements do not possess isotopes (for example, F^{19}, Na^{23}, Tu^{169}, Ta^{181}). Generally, the number of stable isotopes of an individual element varies from 2 to 10 (tin), the relative isotopic abundance (the isotopic composition of an element) being usually of a permanent nature, irrespective of occurrence. For instance, samples of meteoritic iron have the same isotopic composition as the iron of terrestrial deposits. The atomic weights of chemical elements are averages of the masses of all the isotopes of a given element, which explains why the atomic weights of elements are not integral numbers.

D. I. MENDELEYEV'S PERIODIC

PERIODS	SERIES	ELEMENT I	II	III	IV	V
1	I	H 1 1.0080 1				
2	II	Li 3 6.940 1 2	Be 4 9.013 2 2	5 B 10.82 3 2	6 C 12.011 4 2	7 N 14.008 5 2
3	III	Na 11 22.991 1 8 2	Mg 12 24.32 2 8 2	13 Al 26.98 3 8 2	14 Si 28.09 4 8 2	15 P 30.975 5 8 2
4	IV	K 19 39.100 1 8 8 2	Ca 20 40.08 2 8 8 2	Sc 21 44.96 2 9 8 2	Ti 22 47.90 2 10 8 2	V 23 50.95 2 11 8 2
	V	29 Cu 63.54 1 18 8 2	30 Zn 65.38 2 18 8 2	31 Ga 69.72 3 18 8 2	32 Ge 72.60 4 18 8 2	33 As 74.91 5 18 8 2
5	VI	Rb 37 85.48 1 8 18 8 2	Sr 38 87.63 2 8 18 8 2	Y 39 88.92 2 9 18 8 2	Zr 40 91.22 2 10 18 8 2	Nb 41 92.91 1 12 18 8 2
	VII	47 Ag 107.880 1 18 18 8 2	48 Cd 112.41 2 18 18 8 2	49 In 114.76 3 18 18 8 2	50 Sn 118.70 4 18 18 8 2	51 Sb 121.76 5 18 18 8 2
6	VIII	Cs 55 132.91 1 8 18 18 8 2	Ba 56 137.36 2 8 18 18 8 2	La ★ 57 138.92 2 9 18 18 8 2	Hf 72 178.6 2 10 32 18 8 2	Ta 73 180.95 2 11 32 18 8 2
	IX	79 Au 197.0 1 18 32 18 8 2	80 Hg 200.61 2 18 32 18 8 2	Tl 81 204.39 3 18 32 18 8 2	Pb 82 207.21 4 18 32 18 8 2	Bi 83 209.00 5 18 32 18 8 2
7	X	Fr 87 [223] 1 8 18 32 18 8 2	Ra 88 226.05 2 8 18 32 18 8 2	Ac ★★ 89 227 2 9 18 32 18 8 2	(Th)	(Pa)

★ LANTHA

58	59	60	61	62	63	64
Ce 140.13 2 8 20 18 8 2	Pr 140.92 2 8 21 18 8 2	Nd 144.27 2 8 22 18 8 2	Pm [145] 2 8 23 18 8 2	Sm 150.43 2 8 24 18 8 2	Eu 152.0 2 8 25 18 8 2	Gd 156.9 2 9 25 18 8 2

★★ ACTI

90	91	92	93	94	95	96
Th 232.05 2 10 18 32 18 8 2	Pa 231 2 9 20 32 18 8 2	U 238.07 2 9 21 32 18 8 2	Np [237] 2 8 23 32 18 8 2	Pu [242] 2 8 24 32 18 8 2	Am [243] 2 8 25 32 18 8 2	Cm [245] 2 9 25 32 18 8 2

Figures in square brackets are mass numbers of stablest isotopes

TABLE OF ELEMENTS

GROUPS								
VI	VII	VIII						0
	(H)							He 2 4.003 2
8 O 6 2 16	9 F 7 2 19.00							Ne 10 8 2 20.183
16 S 6 8 2 32.066	17 Cl 7 8 2 35.457							Ar 18 8 8 2 39.944
Cr 24 1 13 8 2 52.01	Mn 25 2 13 8 2 54.94	Fe 26 2 14 8 2 55.85	Co 27 2 15 8 2 58.94	Ni 28 2 16 8 2 58.69				
34 Se 6 18 8 2 78.96	35 Br 7 18 8 2 79.916							Kr 36 8 18 8 2 83.80
Mo 42 1 13 18 8 2 95.95	Tc 43 2 13 18 8 2 [99]	Ru 44 1 15 18 8 2 101.1	Rh 45 1 16 18 8 2 102.91	Pd 46 0 18 18 8 2 106.7				
52 Te 6 18 18 8 2 127.61	53 I 7 18 18 8 2 126.91							Xe 54 8 18 18 8 2 131.3
W 74 2 12 32 18 8 2 183.92	Re 75 2 13 32 18 8 2 186.31	Os 76 2 14 32 18 8 2 190.2	Ir 77 2 15 32 18 8 2 192.2	Pt 78 1 17 32 18 8 2 195.23				
84 Po 6 18 32 18 8 2 210	85 At 7 18 32 18 8 2 [210]							86 Rn 8 18 32 18 8 2 222
(U)								

NIDES						
65 Tb 2 8 27 18 8 2 158.93	66 Dy 2 8 28 18 8 2 162.46	67 Ho 2 8 29 18 8 2 164.94	68 Er 2 8 30 18 8 2 167.2	69 Tu 2 8 31 18 8 2 168.94	70 Yb 2 8 32 18 8 2 173.04	71 Lu 2 9 32 18 8 2 174.99

NIDES					
97 Bk 2 8 27 32 18 8 2 [245]	98 Cf 2 8 28 32 18 8 2 [248]	99 En 2 8 29 32 18 8 2 [253]	100 Fm 2 8 30 32 18 8 2 [255]	101 Mv 2 8 31 32 18 8 2 [256]	

Atomic number

Electron layers

Atomic weight

Symbol

Besides isotopes there are atoms with the nuclei that have the same mass number, but different charges. Such atoms, called isobars, exhibit different chemical properties. Elements such as Ar_{18}^{40}, K_{19}^{40} and Ca_{20}^{40} are isobars. The existence of isobars demonstrates that the mass of an atom does not determine its chemical properties and that the latter depend primarily upon the charge of its nucleus.

§ 2. Natural radioactivity

Nuclear processes were unknown before radioactivity was discovered. In 1896, Becquerel discovered that salts of uranium emit penetrating radiation.* The discovery, in 1898 by Marie and Pierre Curie, of polonium and radium, which also emit penetrating radiation, gave an impetus to studies of nuclear transformations that came to be known as radioactive decay. Radioactive decay is a property of atomic nuclei which does not depend upon the state of aggregation of the atoms to which the nuclei belong.

At present about 40 natural radioactive elements are known. These are mostly the isotopes of very heavy elements with an atomic number Z exceeding 82. The nuclear forces of these heavy elements are not able to ensure nuclear stability, this resulting in an internal rearrangement of nuclear particles. However, there are several natural radioactive isotopes with an atomic number Z less than 83 (K_{19}^{40}, Rb_{37}^{87} and Sm_{62}^{152}). Two kinds of natural radioactivity are distinguished: alpha-activity and β^--activity. In the first case each nucleus emits an alpha-particle, and in the second case a β^--particle (electron).

Alpha-rays. Alpha-rays are a flux of alpha-particles. An alpha-particle is the nucleus of a helium atom (He_2^4) composed of two protons and two neutrons. Hence, this particle possesses a charge equal to a double elementary charge and its mass number is 4.

In the chapter dealing with nuclear structure it was mentioned that two neutrons and two protons form a very stable configuration; it may be assumed, therefore, that such combinations actually exist in a nucleus as independent components of its structure.

It was also found that in heavy nuclei of a large Z the binding force per nucleon diminishes as the nuclear charge increases. Therefore, it may be expected that at a sufficiently large Z, spontaneous emission of alpha-particles by atomic nuclei must occur. Actually no nucleus of intermediate or light mass emits alpha-particles, except Sm^{152}. In the course of radioactive decay alpha-particles escape at a velocity of up to 20,000 km/sec and the energy of a particle reaches 11 Mev. On the whole alpha-radiation of radioactive isotopes may be considered as monoenergetic. For example, the energy of

* This was the first directly observed nuclear phenomenon.

Po_{84}^{210} alpha-particles is 5.3 Mev,* that of U_{92}^{238} —4.2 Mev and Ra_{88}^{226} — 4.2 Mev, etc. The path of alpha-particles in air reaches 11 cm and in fabric —0.1 mm. Alpha-particles are absorbed by a sheet of writing paper and aluminium foil 0.006 cm thick.

Beta-rays. Beta-rays are a flux of electrons (or positrons) appearing in the course of nuclear disintegration of beta-emitting isotopes. Beta-disintegration occurs in two ways: electron disintegration (β^--disintegration) and positron disintergation (β^+-disintegration). The β^--disintegration is characteristic of natural radioactive isotopes. The generally accepted hypothesis of beta-disintegration suggests that electrons of beta-active substances are the result of neutron-proton transformation. Since there exist both β^-- and β^+-activity, it is necessary to distinguish two different transformations of elementary particles which occur in the nucleus: the transformation of neutrons into protons followed by electron emission, and transformation of protons into neutrons followed by positron emission.

As distinct from alpha-particles which are emitted by different atoms of one and the same substance always with a definite radiation energy, the radiation energy of beta-particles ranges from zero to a certain upper limit. Hence, the spectrum of beta-particles is continuous. However, the beta-particles of each radioactive element possess a quite definite maximum energy. This nature of the beta-spectrum is due to the fact that beta-disintegration yields not only a beta-particle but also a particle called neutrino which carries off a portion of the excess nuclear energy.

For various radioactive elements the maximum energy of beta-particles ranges from several hundred kev to 2-3 Mev. The path of maximum-energy beta-particles in air and fabric reaches respectively 10 m and 10 to 12 mm. Such beta-particles are fully absorbed by aluminium or lead layers 5 to 6 mm and 1.0 mm thick respectively.

Let us consider now the behaviour of atoms in the course of radioactive alpha- and beta-disintegration. Since the alpha-particle is the nucleus of helium of $Z = 2$ and $A = 4$ and the β^--particle is an electron, alpha-disintegration is followed by the number of protons and neutrons each decreasing by two unities while in the case of beta-disintegration the neutron of the nucleus is transformed into a proton and the number of protons in the nucleus increases by one unity. The atomic weight remains unchanged, for the total number of protons and neutrons in the nucleus does not change. Hence, alpha-disintegration results in the formation of a new nucleus, the atomic number and the mass number of which are smaller than those of the initial nucleus by 2 and 4 respectively. For example

---

* Polonium, however, also emits other groups of alpha-particles; the intensity of the group of alpha-particles possessing an energy of 5.3 Mev is about 5,000 times higher than the intensity of any other group in its spectrum.

alpha-disintegration of Ra_{88}^{226} yields a new element of $Z = 86$ and $A = 222$, i.e., radon Rn_{86}^{222}

$$Ra_{88}^{226} \longrightarrow Rn_{86}^{222} + He_2^4 + \gamma.$$

Electron β^--disintegration yields a new nucleus, the atomic number of which is larger than that of the initial nucleus by one unity, but of the same mass number. Thus, the new nucleus resulting from β^--disintegration of the natural radioactive isotope K_{19}^{40} contains 20 protons instead of 19 in the initial nucleus, i.e., a new element forms calcium with $Z = 20$

$$K_{19}^{40} \xrightarrow{\beta^-} Ca_{20}^{40}.$$

Sometimes the newly formed (daughter) nucleus may be in an excited state, i.e., possess excess energy. The transition of the nucleus from an excited into unexcited state is accompanied by the emission of one or several gamma-quanta, depending upon the nature of the transition; gamma-radiation energy depends upon the degree of excitation and ranges from several tens of kev to 2-3 Mev for different radioactive elements.

As a result of alpha- and beta-disintegration, the nuclei of natural radioactive elements are transformed into new nuclei, which, in turn, may also possess radioactive properties and, therefore, suffer new transformations as they disintegrate. Such a chain of radioactive transformations will continue till a stable nucleus forms. Investigations of the nature of mutual transformations of one radioactive element into another have shown that natural radioactive elements form rather long transformation chains, where each following element is the decay product of the preceding element (isotopes K_{19}^{40}, Rb_{37}^{87} and Sm_{62}^{152} are an exception to this rule). The decay products of an element became known as a radioactive series. At present three radioactive series are known. The parent element of the first radioactive series to which radium belongs is the uranium isotope U_{92}^{238} with a half-life period $T_{1/2} = 4.51 \times 10^9$ years; the parent element of the second series thorium Th_{90}^{232} has a $T_{1/2}$ equal to 1.39×10^{10} years; the actinium series includes the uranium isotope U_{92}^{235} which is referred to as actinouranium and is sometimes denoted as AcU. Its half-life is equal to 7.07×10^8 years. The end decay product of each of the three series is one of the lead isotopes: Pb_{82}^{206} — for the uranium series; Pb_{82}^{208}—for the thorium series; and Pb_{82}^{207} — for the actinium series.

§ 3. Artificial radioactivity

In 1934 F. Joliot and I. Curie discovered artificial radioactivity. They found that when aluminium is bombarded by alpha-particles of polonium, neutrons and positrons are produced and positron emission does not cease after the polonium is removed. Joliot and

Curie assumed that when Al_{13}^{27} is bombarded by alpha-particles a phosphorus isotope forms according to the following scheme:

$$Al_{13}^{27} + He_2^4 \longrightarrow P_{15}^{30} + n.$$

The artificial radioactive phosphorus isotope disintegrates emitting positrons and forming a stable silicon nucleus Si_{14}^{30}. The transformation scheme may be written as

$$P_{15}^{30} \longrightarrow S_{14}^{30} + \beta^+ + \gamma.$$

These investigations led to the discovery of the method which made possible the production of artificial radioactive isotopes which emit radiation in the same way as natural radioisotopes. Artificial nuclear transformation of elements may be induced not only by alpha-particles, but also by protons, heavy hydrogen nuclei, deuterons and neutrons, and by high-energy photon irradiation.

Nuclear reactions proceed in several successive, very rapidly alternating stages. The first stage of any reaction consists in the capture of a foreign particle which comes within a sufficiently small distance from the nucleus and in the formation of an unstable compound nucleus. The second stage consists in the transition of the unstable nucleus into a stable state. This is accompanied by the ejection of nuclear particles and emission of gamma-ray photons.

Various nuclear reactions occur when different parent isotopes are bombarded by charged particles or subjected to photon irradiation. These reactions may be classified into several principal groups. Usually, a nuclear reaction is symbolically expressed as $(x; y)$, the brackets including the particle penetrating into the nucleus and the particle resulting from the nuclear reaction.

The symbolic designation of some of the nuclear reactions is given below:

Proton induced reactions (p, n); (p, α); (p, γ)
Deuteron induced reactions (d, p); (d, n); (d, α)
Alpha-particle induced reactions (α, p); (α, n)
Neutron induced reactions (n, p); (n, α); (n, γ)
Gamma-ray induced reactions (γ, n); (γ, p); $(\gamma, 2n)$; (γ, p^n)
Heavy nuclei fission reaction (uranium, plutonium and other nuclei) accompanied by neutron capture (n, f).

Owing to its being neutral, the neutron easily penetrates the atomic nucleus and can, therefore, be most effectively utilised to induce nuclear reactions. Neutron-induced reactions are widely employed for the production of artificial radioactive isotopes.

Chain fission of uranium nuclei is effected in uranium reactors which are the most powerful neutron sources. The probability of neutron capture by the nucleus of the element depends upon neutron velocity. In most cases a decrease in neutron velocity is accompanied by an increase in its effective capture cross-section, for capture probability is proportional to the time interval during which the

neutron is positioned near the nucleus. The bombardment of stable isotopes by neutrons leads to some nuclear transformations. Neutron bombardment of atoms is accompanied by various processes. Neutron capture brings about excitation of the nucleus. Nuclear excitation energy is most commonly released through gamma-radiation. Generally, (n, γ) reactions proceed under the influence of thermal neutrons. The number of the (n, γ) reactions is very great. Practically all isotopes, except He_2^4, can capture neutrons, the result being the formation of an isotope, the mass number of which is larger than that of the parent nucleus by one unit. The reaction products may be both stable and radioactive. Neutron bombardment of Co^{59}, Ir^{191}, Tu^{169} and Ta^{181} in a reactor results in the formation of widely employed radioactive isotopes Co^{60}, Ir^{192}, Tu^{170}, Ta^{182}, etc. Such transformation may be transcribed as $Co_{27}^{59} + n \rightarrow Co_{27}^{60} + \gamma$, or $Co_{27}^{59}(n, \gamma)\, Co_{27}^{60}$ abbreviated.

The activity of radioactive isotopes produced by neutron bombardment depends upon the energy of the bombarding particles, neutron flux density, neutron effective capture cross-section, duration of irradiation and the quantity of the isotope exposed.

As decay of the produced radioactive isotope occurs simultaneously with its formation and the number of decay events rises in proportion to the total number of radioactive atoms, the activity of the radioactive isotope grows till the irradiation time reaches three-five half-life periods; then, a balance between the processes of formation and decay of the radioactive atoms is established and activity does not increase any more.

The thermalised neutrons appearing due to the collision of fast neutrons against the moderator nuclei may be captured by both U^{235} and U^{238} nuclei. Capture of slow neutrons by U^{235} nuclei, as well as fast-neutron capture, brings forth nuclear fission.

The capture of a thermal neutron by U^{238} results in the formation of U^{239}

$$U_{92}^{238} + n \longrightarrow U_{92}^{239} + \gamma.$$

The U^{239} isotope is unstable and disintegrates emitting β^--particle, a new element being formed with a periodic number 93—Np_{93}^{239}

$$U_{92}^{239} \xrightarrow{\beta^-} Np_{93}^{239}.$$

The half-life of U^{239} is 23 min.

Neptunium, in its turn, is transformed into plutonium as a result of β^--disintegration (half-life period 2-3 days)

$$Np_{93}^{239} \xrightarrow{\beta^-} Pu_{94}^{239}.$$

Like U^{235}, plutonium splits under the influence of fast and slow neutrons. Nuclear fission products are of very diverse nature. A uranium or plutonium nucleus may split in 30-40 different ways after it has captured a neutron, the mass numbers of the resulting

fission products ranging from 72 to 158. The mass numbers of most of the fission products range from 95 to 139. Most of the formed fission products are unstable and are transformed into stable isotopes as a result of one or several more beta-disintegrations. For a number of fission products such disintegration is accompanied by gamma-radiation. The half-life of different fission products ranges from fractions of a second to many thousand years. The following are the most long-lived isotopes—products of U^{235} fission: Sr^{89}, Sr^{90}, Zr^{95}, Nb^{95}, Ru^{103}, Ru^{106}, Te^{127}, Te^{129}, J^{131}, Cs^{137}, Ba^{140}, Ce^{141}, Ce^{144}, Pr^{143}, Nd^{147}, Pm^{144}. At present various nuclear reactions allow more than 100 individual radioactive isotopes and radiation sources to be produced artificially. Of these, more than ten are of practical interest for gamma-radiography, owing to their radiation and physical properties (radiation energy, half-life, specific activity and radiation intensity).

§ 4. The law of radioactive decay

Radioactive decay is the property of the nucleus and depends only upon the state of the nucleus. Radioactive decay of all radioactive isotopes is characterised by the following regularity: the average number of nuclei of a given radioactive isotope which disintegrates per unit of time always represents a definite fraction of the total number of the remaining nuclei. The fraction of the disintegrating nuclei varies for different radioactive elements, being the larger, the higher the degree of instability proper of the given nuclei. Thus, for example, only a 1.38×10^{-11} fraction of the total number of existing radium atoms disintegrates per second and about a 2.1×10^{-6} fraction in the case of radon. This means that out of each 10^{13} atoms of radium 138 atoms disintegrate per second and 20,000,000 atoms of radon out of 10^{13} atoms. Mathematically, the law of radioactive decay may be expressed by the following relationship:

$$-\Delta N = \lambda N_0 \Delta t, \tag{1}$$

i.e., the number of atoms ΔN disintegrating within a small period of time Δt is proportional to the initial total number of atoms N_0, Δt and λ. The factor λ is called the disintegration constant and determines the number of atoms disintegrating per unit time. The disintegration constant is expressed in $seconds^{-1}$, $hours^{-1}$, $days^{-1}$, $years^{-1}$, and has a definite value for each radioactive isotope: for radon $\lambda = 2.1 \times 10^{-6}$ sec^{-1}; for Co^{60} $\lambda = 4.55 \times 10^{-9}$ sec^{-1}. The minus sign preceding ΔN indicates that the disintegration process is accompanied by a decrease in the number of disintegrating atoms.

The radioactive decay law is expressed by the following exponential relationship

$$N_t = N_0 e^{-\lambda t}, \tag{2}$$

where

N_0 — the number of disintegrating atoms at the initial time $t = 0$;

N_t — the number of the same atoms at the time of observation t;

λ — decay constant;

e — base of natural logarithms.

After a certain time has elapsed, denoted as $T_{1/2}$, the number of radioactive atoms will diminish by one half, i.e., the number of the remaining atoms will be equal to:

$$N_t = \frac{N_0}{2}.$$

The time in which the number of radioactive atoms of a particular isotope is reduced by half is called the half-life period $T_{1/2}$. It is quite clear that there is a close relationship between the disintegration constant and half-life period. Indeed, if $t = T_{1/2}$ and $N_t = \frac{N_0}{2}$ we have $\frac{N_0}{2} = N_0 e^{-\lambda t}$, or $^1/_2 = e^{-\lambda T_{1/2}}$. Having taken the logarithm and replacing ln 2 by its value we will have:

$$T_{1/2} = \frac{0.693}{\lambda} \tag{3}$$

or

$$\lambda = \frac{0.693}{T_{1/2}}. \tag{4}$$

Thus, the disintegration constant of a given radioactive isotope may be determined by measuring experimentally the time in which

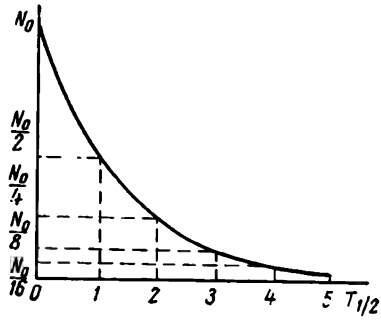

Fig. 1. Change in the number of radioactive atoms with time

radiation intensity reduces by half. If the half-life or disintegration constant is known, it is easy to plot the change with time in the number of radioactive atoms of a substance (Fig. 1). The number of atoms and initial activity of an isotope are reduced by half during

a time interval equal to the half-life period; in a time interval equal to two half-life periods the activity of the radioactive substance diminishes four times, in three half-life periods eight times, etc. In a time period equal to about ten half-life periods the activity of an isotope becomes negligible. For various radioactive isotopes the half-life periods range within wide limits (from many millions of years to one-hundredth of a second), but for a given isotope its half-life remains constant and does not depend upon the chemical or physical state of the isotope.

The mean lifetime of a radioactive isotope (radiation source) is larger than the half-life period, for this time includes the lifetime of the atoms which do not disintegrate during several half-life periods. The mean lifetime of an isotope is determined by adding up the lifetimes of all the radioactive atoms contained in the radiation source and dividing the total by the initial number of radioactive atoms. Calculations show that the mean lifetime of a radioactive source is $\frac{1}{0.693}$ times longer than the half-life period. During the mean lifetime the activity of the radiation source drops down to $\frac{1}{e}$ (0.368) of its initial activity.

All that has been said above naturally leads to the question for how long can radiation sources be employed in radiography. The answer depends upon concrete conditions and requirements (inspection efficiency, etc.). For instance, when the ionisation method of inspection is practised, minimum radiation source activity is determined by the time efficiency of the inspection unit and the given sensitivity.

§ 5. Activity of radioactive substances. Units of activity. Specific activity

The activity of a substance is characterised by the number of radioactive transformations per unit of time. It follows from this definition that the activity Q of a radioactive substance is determined by the number of radioactive atoms disintegrating per unit of time (or by the number of alpha- or beta-particles emitted)

$$Q = -\frac{\Delta N}{\Delta t}, \tag{5}$$

where ΔN is the number of radioactive atoms disintegrating per time Δt. From equations (1) and (5) it follows that the activity is equal to the product of the disintegration constant multiplied by the total number of radioactive atoms

$$Q = \lambda N_0. \tag{6}$$

Let us consider radium, for instance. It was determined by experiment that the half-life of radium is 1,586 years, therefore, according

to equation (4) $\lambda = \frac{0.693}{1.6 \times 10^3 \text{ years}}$ or 1.38×10^{-11} sec^{-1}. As the mass number of radium is 226 and one gram-atom contains $\frac{6.06 \times 10^{23}}{226}$ atoms the activity of 1 gram of radium, free from decay products, i. e., the number of radioactive nuclei N_t disintegrating in 1 gram of pure radium per second will according to equation (6) amount to $\frac{6.06 \times 10^{23}}{226} \times 1.38 \times 10^{-11} = 3.7 \times 10^{10}$ nuclei. Or 3.7×10^{10} disintegrations per second occur in 1 gram of radium. This number of disintegrations per second 3.7×10^{10} is generally adopted as the unit of activity of radioactive substances and is called a curie. Thus, the activity of a radioactive preparation is 1 curie, if 3.7×10^{10} disintegrations per second occur in this preparation. As the curie is a large unit, smaller units—millicurie and microcurie—are often used. 1 mcurie $= 3.7 \times 10^7$ dis/sec; 1μcurie $= 3.7 \times 10^4$ dis/sec; 1 mcurie $= 10^{-3}$ curie and 1μcurie $= 10^{-6}$ curie. The activity of 1 gram of pure radium is 1 curie. Therefore, the activity of radium is often expressed in grams, for in this exceptional case a unit of mass possesses a unit of activity. The recently established unit of activity (rutherford) is defined as equivalent to 10^6 dis/sec.

According to formula (2), in the course of decay the number of radioactive atoms decreases with time, therefore, the number of atoms disintegrating per second or the activity of a radioactive source diminishes. If Q_0 is the activity of a radioactive source at some initial moment, as time t elapses its activity Q_t is determined by the relationship

$$Q_t = Q_0 e^{\frac{-0.693}{T_{1/2}} \times t}, \qquad (7)$$

where $T_{1/2}$ is the half-life of the given radioactive substance. Sometimes it is necessary to determine not the absolute value of the remaining activity but the percentage value or fraction of the initial activity. By rearranging equation (7) we have

$$\frac{Q_t}{Q_0} = e^{\frac{-0.693}{T_{1/2}} \times t},$$

where $\frac{Q_t}{Q_0}$ is the ratio of the residual activity to the initial one or the fraction of the activity left after a lapse of time t. Let us assume that it is necessary to determine the activity Q_t of Co^{60} after a lapse of two years if the initial activity Q_0 of the source was equal to 100 mcurie.

$$Q_t = Q_0 e^{\frac{-0.693}{T_{1/2}} \times t}.$$

The half-life period of Co^{60} is 5.2 years, hence, Q_t will amount to $100\ e^{\frac{-0.693 \times 2}{5.2}} = 100\ e^{-0.26}$ and $Q_t = 77.1$ mcurie.

For practical purposes, specific activity is a very important characteristic of a radioactive source. Specific activity shows the relative content of radioactive atoms in the isotopic mixture of an element, or the fraction of molecules containing atoms of the radioactive isotope.

Specific activity determines the concentration of radioactive atoms in the radioactive substance and shows to what extent the isotope in question is fit to serve as a source for radiographic inspection purposes.

Specific activity is expressed by the number of curies per unit weight of the substance (gram) or per unit of its volume (litre, cu cm). When radioactive isotopes are employed as radiation sources, it is expedient to express the specific activity of the radiation source in units adopted for the measurement of radiation intensity which are characteristic of the instruments used, and the conditions under which the measurement of investigated objects is conducted. For example, when measurements are carried out by means of a meter, the specific activity is expressed by the number of impulses per minute; when a radiometer is employed—by the number of scale divisions per unit weight or volume of the substance, etc.

Specific activity depends upon the nature of the given radioactive isotope, also upon the content of the irradiated parent isotope in the isotopic mixture of the element, in the case of artificial isotopes. The higher the fraction of radioactive atoms in the irradiated substance, the higher its specific activity. Therefore, preparations of the highest specific activity are produced where the radioactive and parent isotopes are different chemical elements. The radioactive isotope may be separated in the pure form by chemical means. Naturally, the longer the half-life period of the isotope, the larger the amount of isotope required to obtain a given activity.

The number of radioactive nuclei being equal, the specific activity of a radioactive preparation is larger, the shorter the half-life period of the isotope.

§ 6. Radiation intensity

The concept of radiation intensity was introduced as a characteristic of the various radiation fluxes (number of corpuscles or quanta emitted by the substance) used for radiographic inspection. Radiation intensity is defined as the energy of particles passing through unit area perpendicular to the line of beam propagation in unit time.

The unit of gamma-ray intensity is one roentgen per centimetre per second, i.e., an intensity at which an amount of energy equal to 1 roentgen passes through each sq cm of surface arranged perpendicular to the incident gamma-rays per 1 second. Multiple units of intensity are milliroentgen (mr) per centimetre per second and

[redacted]

where P is the dose rate; D is the radiation dose; t is the exposure time. The dose rate is expressed in roentgen per second, milliroentgen per second, microroentgen per second. Dose rate units such as roentgen/hr and roentgen/min are also used in practical work.

At present new units such as the physical roentgen equivalent and the medical roentgen equivalent are introduced. The physical roentgen equivalent is defined as the dose of any ionising radiation, at which the energy absorbed by 1 g of substance is equal to the ionising energy lost by an X- or gamma-radiation dose of 1 roentgen in one gram of air.

$$1 \text{ rep} = 1.61 \times 10^{12} \text{ ion pairs/g} = 5.3 \times 10^{7} \text{ Mev/g}.$$

The physical roentgen equivalent is replaced by a new unit of radiation dose, rad, expressing the dose from any ionising radiation.

This unit corresponds to an absorbed radiation dose of 100 erg per 1 g of irradiated substance

$$1 \text{ rep} = 0.84 \text{ rad}; \quad 1 \text{ rad} = 1.19 \text{ rep}.$$

The medical roentgen equivalent is the dose of any ionising radiation that will produce the same biological effect as that produced by 1 roentgen of gamma-radiation.

The radiation dose produced by gamma-rays emitted from different radioactive preparations of a given activity depends upon the disintegration scheme, i.e., the quantity of gamma-quanta per disintegration, and the radiation spectrum. In respect to the produced gamma-radiation dose, radioactive substances are characterised by the so-called gamma-constant K_γ* showing the dose of gamma-radiation produced by a 1 mcurie point source at a distance of 1 cm per hour. K_γ is expressed in roentgen/hr millicurie cm. It was established by experiment that the gamma-constant K_γ of a radium preparation which is in equilibrium with short-lived disintegration products and enclosed in a platinum filter, 0.5 mm thick, is equal to 8.4 r/hr mcurie cm. This means that a 1 mcurie point source of radium enclosed in a platinum filter and remaining in equilibrium with short-lived disintegration products produces a radiation dose of 8.4 r/hr at a distance of 1 cm. Generally, the gamma-constant is calculated from the following relation

$$K_\gamma = K_{\gamma 1} P_{\gamma 1} + K_{\gamma 2} P_{\gamma 2} + \ldots,$$

where $K_{\gamma 1}$, $K_{\gamma 2}$ are the gamma-constants for individual lines of gamma-rays; $P_{\gamma 1}$, $P_{\gamma 2}$ —the mean quantity of the gamma-quanta of a given energy per disintegration. K_γ values may be determined from the graph (Fig. 3) where the gamma-constant is plotted as a function of the radiation energy. The radiation energy plotted on the abscissa is expressed in Mega-electron-volts, and plotted on the ordinate is the

* K_γ is often called the ionisation constant.

gamma-constant K_γ, provided 1 gamma-quanta is emitted per disintegration. For the simplest case, where each disintegration is accompanied by the emission of one gamma-quantum of a certain energy (the Pb^{95} isotope, for instance), $K_\gamma = K_{\gamma 1}$.

A disintegrating Co^{60} nucleus emits two gamma-quanta with energies of 1.17 and 1.33 Mev. From the graph in Fig. 3 we find that for 1.17 Mev gamma-quanta $K_\gamma = 6.3$ r/hr mcurie cm and for 1.33 Mev gamma-quanta $K_\gamma = 6.9$ r/hr mcurie cm.

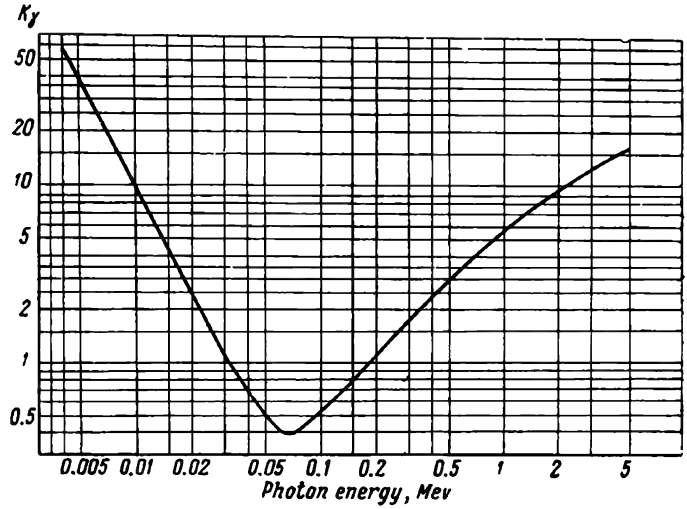

Fig. 3. Dependence of the gamma-constant on gamma-quanta energy

Thus, for Co^{60} the gamma-constant is equal to $6.3 + 6.9 = 13.2$ r/hr mcurie cm.

A comparison of the gamma-constants of radium and cobalt shows that 1 millicurie of cobalt produces a radiation dose 1.6 larger than that emitted by 1 millicurie of radium. In other words, in respect of the radiation dose produced in air 1 millicurie of Co^{60} is equivalent to 1.6 millicurie of radium or 1.6 mg of radium.

Very often, and mostly in radiography, the activity of gamma-active preparations is expressed in gram radium equivalent or in milligram radium equivalent.* The gamma-activity of any radioactive preparation is 1 milligram radium equivalent if, under given filtration and similar measurement conditions, the preparation creates a dose rate equal to that emitted by 1 milligram of radium with a platinum filter 0.5 mm thick (i.e., 8.4 r/hr). This value is called the gamma-constant and is designated $K_{\gamma(0.5;\ Pt)}$. If initial filtration is omitted, the total gamma-constant of radium $K_\gamma = 9.53$

* Sometimes the activity of a preparation expressed in gram radium equivalent is called the radium gamma-equivalent of the radioactive source.

r/hr; $K_{\gamma(1.0;\ Pt)}$ of radium is equal to 7.8 r/hr, if a platinum filter 1.0 mm thick is employed. For purposes of comparison it should be noted that platinum filters 1.0 mm and 0.5 mm thick attenuate gamma-radiation of radium the same as lead filters 2.4 mm and 1.5 mm thick respectively. Thus, the activity of preparations may be determined in milligram radium equivalent by comparing the ionising power of various radioactive isotopes with the ionising activity of 1 milligram of pure radium. In case where the gamma-constant of an isotope is known the activity of a source given in millicuries may be expressed in milligram radium equivalent with the aid of the following simple formulas:

$$M = Q\frac{K_\gamma}{8.4}, \tag{12}$$

$$Q = M\frac{8.4}{K_\gamma}, \tag{13}$$

where M—the activity of the preparation, mg radium equivalent, (or gram radium equivalent); Q—the activity of the preparation, mcurie (or curie); K_γ—the gamma-constant of the isotope, r/hr mcurie cm; 8.4—the gamma-constant of radium.

One and the same isotope may possess different gamma-equivalents, depending upon initial filtration. If a material with an atomic number Z and a thickness d is used as the initial filter instead of platinum, then it is said that the gamma-equivalent is obtained with a certain initial filtration and using a certain material for the filter. In such a case the gamma-equivalent of the given isotope, expressed in milligram radium equivalent may be calculated from the formula

$$M_{(d,\,Z)} = \frac{Q \times K_{\gamma(d,\,Z)}}{8.4},$$

where $K_{\gamma\,(d,\,Z)}$ is the gamma-constant of the isotope after an initial filter d thick made from a material with an atomic number Z.

The relation between the activity of a point source, expressed in milligram radium equivalent, and the dose created by the source at a distance R cm, may be expressed by the following formula:

$$D = \frac{8.4Mt}{R^2}, \tag{14}$$

where 8.4 is the gamma-constant of radium, M is the activity of the preparation expressed in units of milligram radium equivalent and t is the exposure time in hours.

If the activity of the preparation is expressed in millicuries, then the formula may be rewritten as follows:

$$D = K_\gamma\frac{Q \times t}{R^2}, \tag{15}$$

where K_γ is the gamma-constant of the isotope, Q is the activity expressed in millicuries, t is the exposure time in hours.

§ 8. Radioactive sources used in industrial radiography

Before we pass to the characteristics of gamma-ray sources employed in industrial radiography, let us deal with some basic facts concerning the nature and properties of gamma-rays.

Gamma-rays are identified as electromagnetic radiation emitted by atomic nuclei and having a vacuum propagation velocity of $C = 3 \times 10^{10}$ cm/sec and a certain wavelength λ. Being of a similar nature, various kinds of electromagnetic radiation (radio waves, visible light, infra-red and ultra-violet rays) differ in conditions of formation and wavelength. Thus, X-rays form as the result of electron deceleration, gamma-rays, being the result of nuclear transformations, form when the nuclei pass from an excited energy state to a lower energy state, particularly when the nuclei pass from an excited state to the ground state.

The properties of various kinds of electromagnetic radiation are determined by the wavelength or by the oscillation frequency of electrical and magnetic fields. The following relation exists between the length of a wave and its frequency:

$$\lambda = \frac{C}{\nu} = CT, \tag{16}$$

where C—the propagation velocity of electromagnetic waves in vacuum, equal to 3×10^{10} cm/sec;

T—the oscillation period, the time of one full oscillation;

λ—the wavelength, the distance through which oscillating motion propagates during one oscillation period (during a time interval T);

ν—the oscillation frequency, the number of full oscillations per second.

The oscillation frequency is inversely proportional to the oscillation period $\nu = \frac{1}{T}$. Thus, the shorter the wave, the higher its frequency (Table 2).

The electromagnetic wave spectrum is so wide that different units are employed to measure the length of the waves in various sections of the spectrum. Usually, radio waves are measured in metres, centimetres or millimetres; visible light waves—in microns or angstroms; the length of X- and gamma-rays—in angstroms and sometimes in X-units (10^{-11} cm).

Electromagnetic oscillations possess different properties, depending on the wavelength. Radiation with a wavelength ranging from 7.6×10^3 to 4×10^3 Å influences the human eye and, therefore, this range of electromagnetic oscillations is called the visible light.

Gamma-rays and X-rays occupy the shortest wave section of the electromagnetic wave range. These rays are invisible to the human

eye and possess the capacity to pass through objects which are opaque to visible light. Gamma-rays, similar to light and X-rays, falling upon a photographic plate or film, initiate a photochemical reaction resulting in darkening of the film after the latter is developed. This

Table 2

Approximate Wave and Frequency Ranges for Different Kinds of Rays

Type of electromagnetic radiation	Wavelength range	Frequency range, cps
Radio waves	30 km-0.3 mm	10^4-10^{11}
Infra-red radiation . . .	0.3 mm-7,500 Å *	3.10^{11}-4×10^{14}
Visible light rays . . .	7,500-4,000 Å	4.10^{14}-7.5×10^{14}
Ultra-violet radiation . .	4,000-200 Å	7.5×10^{14}-3×10^{18}
X-rays	20-0.05 A-50X **	0.25×10^{18}-60×10^{18}
Gamma-rays	50-1X	60×10^{18}-3×10^{21}
Cosmic rays	1.0-0.1X and above	3×10^{22} and above

* Å (angstrom) = 10^{-8} cm.
** This X-ray wavelength must be considered as conditional, for it does not take into account the latest developments in supervoltage engineering which make it possible to obtain X-rays of a high hardness.

effect and the different absorbtion of gamma-rays by various substances are employed to detect defects in metals; defects, if any, may be registered on the film by means of radiographic inspection.

Like light rays and X-rays, gamma-rays make some substances luminescent and that is why fluorescent screens are used in gamma-inspection. Gamma-rays ionise air and gases, transforming them into electric conductors. This property makes it possible to detect gamma-rays and measure their intensity. All kinds of electromagnetic radiation possess such properties as interference, refraction and difraction. However, there are a number of phenomena which cannot be explained by the wave nature of radiation.

Studies of the photoeffect, Compton effect and other phenomena have shown that electromagnetic radiation is not a continuous flux of energy, as follows from the wave theory, but consists of descrete portions of gamma-quanta, also called photons. A light quantum (photon) is the smallest quantity of light energy of a given frequency or wavelength.

The energy of a photon is proportional to the frequency of the electromagnetic oscillation

$$E = h\nu, \tag{17}$$

where $h = 6.6 \times 10^{-27}$ erg/sec—Planck's constant or one quantum of action; ν is radiation frequency.

By introducing into formula (17) the value of ν taken from formula (16) the energy of a photon is expressed as

$$E = h\frac{C}{\lambda}, \tag{18}$$

i.e., inversely proportional to the radiation wavelength.

In formulas (17) and (18) the energy of a photon is expressed in ergs. For instance, gamma-ray photons with λ equal to 10^{-11} cm have

$$E = 6.6 \times 10^{-27} \frac{3 \times 10^{10}}{10^{-11}} = 19.8 \times 10^{-6} \text{ erg.}$$

For many physical investigations it is more convenient to express radiation energy in electron-volts instead of ergs.

An electron-volt is a unit of energy equal to the energy gained by a particle having an electron charge when it passes in a vacuum through a potential difference of 1 v.

$$1_{ev} = 1.6 \times 10^{-12} \text{ erg.}$$

For practical purposes larger units of energy are used: kilo-electron-volts (1 kev = 1,000 ev) or Mega-electron-volts (1 Mev = = 1,000,000 ev).

The dependence of gamma-quanta energy, expressed in electron-volts, upon the wavelength of electromagnetic oscillation is given in Fig. 4.

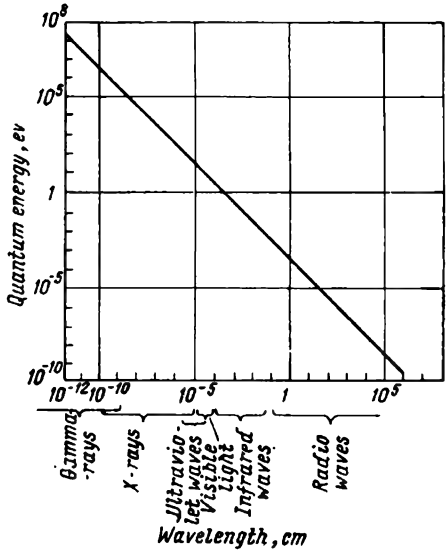

Fig. 4. Dependence of quanta energy on the wavelength of various electromagnetic radiations

Radioactive isotopes used in gamma-radiography must possess a large half-life period, high specific activity and a required radiation energy. The half-life of the isotope predetermines the effective service life of a preparation of a given activity. The specific activity determines the size of the preparation, and gamma-ray energy—the desirable thickness and density of the materials to be inspected (the effectiveness of inspection, as far as detection of defects is concerned, also depends on gamma-ray energy).

Since each radioactive isotope emits gamma-rays of one wavelength or of several strictly definite wavelengths (the possibility of energy adjustment being excluded), in order to gamma-ray an assortment of objects differing in thickness and density, one must have available a set of radioactive isotopes producing gamma-radiation of a different energy.

At present artificial radioactive isotopes are mostly used in gamma-radiography. Depending upon gamma-energy, radioactive isotopes may be divided into three groups. The first group includes isotopes emitting hard gamma-radiation with an energy of about 1 Mev; the second group—isotopes producing medium radiation at energies ranging from 0.3 to 0.7 Mev; and a third group—soft gamma-sources of an energy below 0.3 Mev.

This classification of isotopes according to gamma-radiation hardness (energy) is quite arbitrary, because in most cases radioactive isotopes are polyenergetic sources and their radiation spectrum contains very hard radiation as well as soft emission.

The following radioactive isotopes may be considered as hard radiation gamma-sources: sodium-22, potassium-40, scandium-46, iron-59, cobalt-60, zinc-65, antimony-124, and others.* At present Co_{27}^{60} is widely employed as a source of hard radiation intended for metal radiography, Ta_{73}^{182} is also used. The other radioactive isotopes listed above are not widely used, for they do not conform to the principal requirements specified for gamma-ray sources used in the inspection of metals. So, for instance, Fe_{26}^{59} possesses a relatively short half-life (45 days) and a low specific activity (0.2 to 0.3 mcurie/g); K_{19}^{40} is a natural radioactive isotope and may be separated in very small quantities from the isotopic mixture of the element (about 0.019%); preparations Zn^{65} and Sb^{124} are produced according to the (n, γ) reaction and possess a low specific activity.

The group of medium sources includes the following radioactive isotopes: cesium-137, iridium-192, silver-110, europeum-152, 154, zirconium-95, hafnium-181, cesium-134, etc. At present, out of these radiation sources, Cs^{137}, Ir^{192} and $Eu^{152, 154}$ find the widest employment in gamma-radiography, with Cs^{134} and Ag^{110} coming next. The Zr_{40}^{95} and Hf_{72}^{181} isotopes are rarely used, owing to a relatively short half-life period amounting to 65 and 46 days respectively.

The group of soft gamma-sources includes thulium-170, europeum-155, samarium-145, gadolinium-153, chromium-51, silver-105, cadmium-109, indium-114, cerium-141, cerium-144, selenium-75, etc. Of the soft gamma-sources listed above, only Tu^{170}, Eu^{155}, Se^{75} and Ce^{144} radioactive isotopes are employed in gamma-radiography.

Radioactive isotopes Cd^{109}, In^{114} and Cr^{51} have not found wide employment, owing to their small content in the isotopic mixtures from which these isotopes are separated. For example, Cd^{109} is produced by slow-neutron bombardment of Cd^{108}, only 0.18% of which is contained in the isotopic mixture of the cadmium element.

In addition, during the process of slow-neutron irradiation of natural cadmium, other radioactive isotopes form as well, including Cd^{115} with a half-life period of 43 days and a gamma-energy up to 1 Mev. As a result radioactive isotopes Cd^{109} and In^{114}, possessing

* Ta_{73}^{182}, Cs_{55}^{134} and Sb_{51}^{124} possess very wide radiation spectrum.

a high specific activity and free from considerable admixtures, may be produced only after natural elements have been enriched by the respective isotopes, such enrichment constituting a very labour-consuming and costly process. In^{114} and Cr^{24} are of no practical interest for gamma-radiography, owing to their short half-life.

The physical characteristics of the principal radioactive isotopes used in gamma-radiography are given below.

Hard gamma-emitting isotopes. *Cobalt*-60, the artificial radioactive isotope Co_{27}^{60} is obtained by bombarding the stable isotope Co_{27}^{59} with thermal neutrons. The natural mixture of the element contains 100% of Co_{27}^{59}. In the course of bombardment the neutrons are

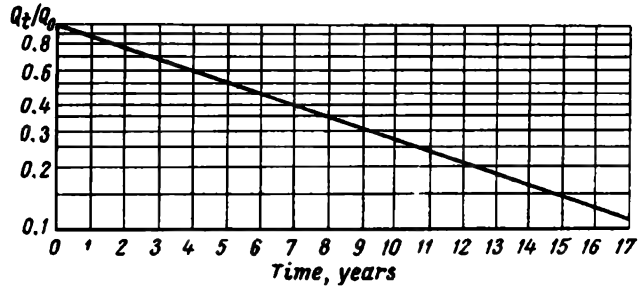

Fig. 5. Change in relative activity of Co_{27}^{60} sources with time

captured by Co_{27}^{59} nuclei, this leading to the formation of the Co_{27}^{60} isotope; the excess energy of the formed nucleus is liberated as a gamma-quantum.

The formation of Co_{27}^{60} may be written as:

$$Co_{27}^{59} + n \longrightarrow Co_{27}^{60} + \gamma$$

The Co_{27}^{60} isotope formed according to the (n, γ) reaction is in an excited state and emits a 0.059 Mev gamma-quantum as it passes to a lower energy level. The half-life of such isomeric transition is equal to $10\frac{1}{2}$ min.

The formed Co_{27}^{60} nucleus is unstable; it disintegrates emitting beta-particles of a maximum energy 0.3 Mev and converts into the Ni_{28}^{60} isotope according to the following transformation scheme:

$$Co_{27}^{60} \xrightarrow{\beta} Ni_{28}^{60} + \beta + \gamma_1 + \gamma_2.\ *$$

Two gamma-quanta of 1.17 and 1.33 Mev are emitted because the appearing Ni_{28}^{60} isotope is in an excited state. It may be assumed with a sufficient degree of accuracy that gamma-radiation of Co_{27}^{60} is monoenergetic with an average energy of 1.25 Mev. The half-life of Co^{60} is 5.24 years. The graph in Fig. 5 shows the change in the

* According to the literature, a gamma-quantum with an energy of 2.13 Mev is emitted as well. The yield of such gamma-quanta per disintegration amounts to 0.001%.

relative activity $\frac{Q_t}{Q_0}$ of Co_{27}^{60} with time. Here, Q_0—the initial activity of the preparation specified on its certificate and Q_t —activity after a certain lapse of time. If the initial activity of Co_{27}^{60} is equal to 50 gram radium equivalent, then in two years its relative activity $\frac{Q_t}{Q_0}$, as determined from the graph, amounts to 0.78 and, consequently, the activity of the preparation is $50 \times 0.78 = 39$ gram radium equivalent.

The specific activity of cobalt preparations produced according to the (n, γ) transformation scheme may exceed 37 curie/g. The ionisation constant of Co_{27}^{60} is 13.2 r/hr at a distance of 1 cm, therefore, 1 curie of cobalt will correspond to 1.57 gram radium equivalent in respect of the emitted dose of gamma-radiation.

The characteristics of gamma-radiation emitted with a zero primary filter by the isotopes treated here are given in Table 3.

Table 3

Gamma-Radiation of Isotopes with a Zero Primary Filter

Isotope	Half-life, $T_{1/2}$	Gamma-quanta energy, Mev	Yield of gamma-quanta per disintegration, %	Differentiated gamma-constant, r/hr	Total gamma-constant, r/hr	Activity, 1 millicurie, mg/equivalent of radium	Number of gamma-quanta per disintegration
Co_{27}^{60}	5.24 years	2.13	1.10^{-3}	—	13.20	1.57	2.0
		1.33	100.00	6.90			
		1.17	100.00	6.30			
Se_{34}^{75}	125 days	0.405	14.00	0.33	1.62	0.19	1.236
		0.308	0.03	—			
		0.281	5.00	0.08			
		0.269	65.20	1.01			
		0.203	0.40	—			
		0.138	21.40	0.14			
		0.124	2.30	0.01			
		0.098	0.72	—			
		0.076	14.00	0.05			
		0.066	0.50	—			
Cs_{55}^{134}	2.07 years	1.367	2.50	0.18	8.90	1.06	2.195
		1.166	1.00	0.06			
		1.038	1.00	0.06			
		0.812	7.00	0.33			

Continued

Isotope	Half-life, $T_{1/2}$	Gamma-quanta energy, Mev	Yield of gamma-quanta per disintegration, %	Differentiated gamma-constant, r/hr	Total gamma-constant, r/hr	Activity, 1 millicurie, mg/equivalent of radium	Number of gamma-quanta per disintegration
		0.796	93.00	4.28			
		0.604	90.00	3.17			
		0.569	16.00	0.53			
		0.563	9.00	0.29			
Cs^{137}_{55}	30 years	0.661	92.0	3.55	3.55	0.42	0.92
Ce^{144}_{58}	284 days	0.134	15.3	0.098	0.175	0.021	0.394
		0.100	1.5	0.007			
		0.080	7.2	0.027			
		0.054	0.5	0.002			
		0.042	6.7	0.031			
		0.034	1.5	0.010			
		0.012	Low-level	—			
Pr^{144}_{59}	17.5 min	2.185	1.44	0.14	0.32	0.038	0.056
		1.490	0.56	0.04			
		0.695	3.56	0.14			
$^{152}_{63}$	12.7 years	1.405	25.0	1.80	6.35	0.76	1.888
		1.240	2.0	0.13			
		1.210	2.0	0.13			
		1.110	12.0	0.72			
		1.100	1.5	0.09			
		1.085	13.0	0.76			
		0.963	14.0	0.75			
		0.866	6.0	0.30			
		0.778	9.0	0.41			
		0.720	1.0	0.04			
		0.690	0.3	0.01			
		0.550	0.5	0.02			
		0.442	5.0	0.13			
		0.403	2.5	0.06			
		0.344	27.0	0.54			
		0.244	9.0	0.12			
		0.122	59.0	0.34			

Continued

Isotope	Half-life, $T_{1/2}$	Gamma-quanta energy, Mev	Yield of gamma-quanta per disintegration, %	Differentiated gamma-constant, r/hr	Total gamma-constant, r/hr	Activity, 1 millicurie, mg/equivalent of radium	Number of gamma quanta per disintegration
Eu^{154}_{63}	16 years	1.116	50.0	3.00	6.23	0.74	1.5
		0.778	50.0	2.25			
		0.336	50.0	0.98			
Eu^{155}_{63}	1.7 years	0.102	32.0	0.15	0.33	0.039	0.77
		0.084	45.0	0.18			
		0.018	Low-level	—			
Gd^{153}_{64}	236 days	0.104	58.9	0.28	0.28	0.033	0.589
Tu^{170}_{63}	129 days	0.084	0.31	1.2×10^{-3}	1.2×10^{-3}	1.4×10^{-4}	0.37
		Brems-strah-lung	37.0	—	—	—	
Ir^{192}_{77}	74.37 days	1.060	0.04	—	5.46	0.65	2.473
		0.885	0.44	0.02			
		0.785	0.09	—			
		0.613	7.48	0.27			
		0.604	12.50	0.44			
		0.588	6.32	0.22			
		0.485	3.47	0.10			
		0.468	57.00	1.56			
		0.416	1.42	0.03			
		0.375	1.69	0.04			
		0.316	89.00	1.63			
		0.308	31.20	0.56			
		0.295	32.00	0.54			
		0.283	0.53	0.01			
		0.206	3.50	0.04			
		0.201	0.41	—			
		0.136	0.17	—			

For the purpose of gamma-radiography, Co^{60} radiation sources are available in metal-clad capsules of an activity and size specified in Table 4.

Table 4

Available Co^{60}_{27} Radiation Sources
(According to 1959 data)

Activity, gram radium equivalent	Specific activity, curie/g	Size, mm		Inner dimensions of capsule, mm	
		diameter	height	diameter	height
0.1	1.18	3	3	2	2
0.25	2.96	3	3	2	2
0.5	0.40	6	6	5	5
2.0	1.58	6	6	5	5
5.0	1.82	6	11	5	10
20.0	1.90	11	11	10	10
50.0	3.20	11	16	10	15
100.0	2.81	17	18	15	15
	Sources of a higher specific activity				
2.5	26.6	—	—	2	2
50.0	37.2	6	6	5	5
150.0	13.8	11	11	10	10
200.0	12.3	11	16	10	15
600.0	16.2	17	18	15	15
1500.0	22.0	11	81	9	78

Tantalum-182. The radioactive isotope Ta^{182}_{73} is produced by neutron bombardment of the stable isotope Ta^{181}_{73}. The natural element mixture contains 100% of this isotope.

$$Ta^{181}_{73} + n \longrightarrow Ta^{182}_{73} + \gamma.$$

Preparations of Ta^{182}_{73} produced according to this mode of transformation are characterised by a high specific activity ranging from 2,000 to 5,000 mcurie/year. This isotope disintegrates rapidly, its half-life period being 115,5 days.

In the process of β^--disintegration Ta^{182}_{73} is transformed into an excited W^{182}_{74}. The ground-state transition of the W^{182}_{74} nuclei is accompanied by the emission of several gamma-quanta.*

Ta^{182}_{73} emits a complex gamma-spectrum composed of 18 lines of various intensity, of an energy ranging from 0.067 to 1.188 Mev. The ionisation constant of Ta^{182} is equal to 4.3 r/hr mcurie cm.

Medium gamma-emitting isotopes. *Cesium*-137. The radioactive isotope Cs^{137}_{55} is one of the fission products of U^{235}. Nuclear fission of U^{235} yields about 6.3% of the Cs^{137}_{55} isotope. Its half-life is 30 years. During disintegration about 92% of the Cs^{137}_{55} nuclei emit

* The decay scheme of Ta^{182}_{74} has not been established exactly.

beta-particles with a maximum energy of 0.523 Mev and are transformed into the excited Ba_{56}^{137} isotope; 8.0% of the Cs_{55}^{137} nuclei emit beta-particles with an energy of 1.18 Mev and are transformed into unexcited Ba_{56}^{137} nuclei. The transition of Ba_{56}^{137} nuclei into the unexcited state is accompanied by the emission of 0.662 Mev gamma-quanta, the half-life of this isomeric transition being equal to 2.6 min.

Since the half-life of Cs_{55}^{137} is considerably longer than that of the Ba_{56}^{137} isotope during its isomeric transition, the Cs_{55}^{137} and Ba_{56}^{137} isotopes will come into equilibrium in a short time interval; while this equilibrium lasts, the number of the barium nuclei passing to

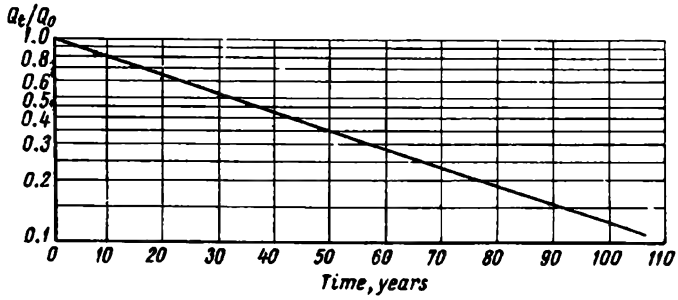

Fig. 6. Change in relative activity of Cs_{55}^{137} sources with time

the ground state per unit time and emitting gamma-radiation will be equal to the disintegration rate of the Cs_{55}^{137} nuclei. Hence, gamma-radiation intensity will also change with time, in the same way as the activity of the Cs_{55}^{137} isotope in the process of disintegration. The change in the specific activity of Cs_{55}^{137} with time is graphically shown in Fig. 6. The ionisation constant of Cs_{55}^{137} sources is 3.16 r/hr mcurie cm. Thus, in respect to the emitted gamma-ray dose, 1 curie of Cs^{137} sources is 0.38 gram radium equivalent. The specific activity of Cs^{137} preparations produced by chemical separation from U^{235} fission products may reach 20 curie/g.

For gamma-radiography Cs^{137} sources are available in metal-clad capsules of an activity and size listed in Table 5.

Cesium-134. The artificial radioactive isotope Cs_{55}^{134} is the product of the bombardment of the Cs_{55}^{133} isotope with thermal neutrons the content of which in the natural mixture is 100%. The transformation scheme is as follows:

$$Cs_{55}^{133} + n \longrightarrow Cs_{55}^{134} + \gamma.$$

This reaction yields an excited Cs_{55}^{134} isotope which passes into an unexcited state, emitting gamma-rays with an energy of 0.128 Mev. The half-life of such isomeric transition is equal to 3.15 hours. The Cs_{55}^{134} nuclei are unstable in the ground state as well. In the process

Table 5

Available Cs^{137}_{55} Radiation Sources

(According to 1959 data)

Activity, gram radium equivalent	Specific activity, curie/cu cm	Size, mm		Inner dimensions of capsule, mm	
		diameter	height	diameter	height
0.0001		6	8-10	5	5
0.0005	40*	6	8-10	5	5
0.0010		6	8-10	5	5
0.0050		6	8-10	5	5
0.01		6	8-10	5	5
0.05		6	8-10	5	5
0.10		6	8-10	5	5
0.50		7-8	14-15	5-6	8
2.0		7-8	14-15	5-6	8
10.0		16-17	18-19	10	10
20.0		16-17	24-25	10	15

* The specific activity of the Cs^{137} deposit may be raised to 60-70 curie/cu cm in certain cases.

of β^--disintegration Cs^{134}_{55} is transformed into an excited Ba^{134}_{56} isotope. The transition of the Ba^{134}_{56} nuclei into the ground state is accompanied by the emission of gamma-quanta. Each beta-disintegration of Cs^{134} yields 2.2 gamma-quanta (see Table 3) of the following energy distribution:

Gamma-quantum energy, Mev	Number of gamma-quanta per disintegration	Gamma-quantum energy, Mev	Number of gamma-quanta per disintegration
1.367	0.045	0.796	0.91
1.166	0.03	0.604	0.88
1.038	0.008	0.569	0.12
0.812	0.18	0.563	0.093

The half-life of Cs^{134}_{55} is 2.07 years. The change in its specific activity with time is graphically illustrated in Fig. 7. The ionisation constant of Cs^{134}_{55} is 8.90 r/hr mcurie cm. Thus, in respect to the emitted radiation dose, 1 curie of Cs^{134}_{55} is equivalent to 1.06 grams of radium. The specific activity of preparations produced according to the transformation scheme shown above may reach 290 mcurie/g (one millicurie of the preparation weighs 3.5×10^{-3} g).

For gamma-radiography Cs^{134}_{55} sources are available in metal-clad capsules of activities and sizes specified in Table 6.

Iridium-192. The artificial radioactive isotope Ir_{77}^{192} is produced by bombardment the stable isotope Ir_{77}^{191} with thermal neutrons. Natural iridium is a mixture of two isotopes Ir_{77}^{191} and Ir_{77}^{193}, the

Table 6

Available Cs_{55}^{134} Radiation Sources

(According to 1959 data)

Activity, gram radium equivalent	Specific activity, curie/g	Size, mm		Inner dimensions of capsules, mm	
		diameter	height	diameter	height
0.1	0.057	7	8	5	5
0.5	2.1	7	8	5	5
2.0	1.7	12	10.5	10	10

relative content of which amounts to 38.5 and 61.5% respectively. Therefore, two radioactive isotopes are formed when a natural sample of iridium ore is bombarded with thermal neutrons. Ir_{77}^{192} (according to the transformation scheme $Ir_{77}^{191} + n \rightarrow Ir_{77}^{192} + \gamma$) and Ir_{77}^{194} (according to the transformation scheme $Ir_{77}^{193} + n \rightarrow Ir_{77}^{194} + \gamma$).

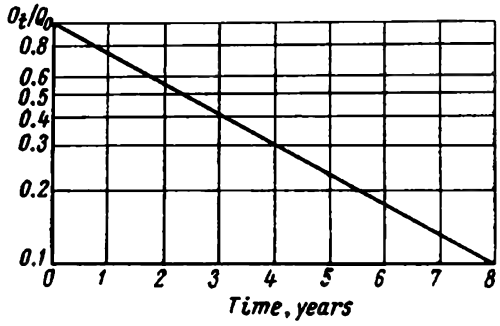

Fig. 7. Change in relative activity of Cs_{55}^{134} sources with time

However, the half-life of Ir_{77}^{194} is only 20 hours, therefore, practically all Ir_{77}^{194} disintegrates in four to five days. The specific activity of Ir_{77}^{192} preparations reaches 10,000 mcurie/g and this is one of the advantages of this isotope. The isomer Ir_{77}^{192}, produced according to the transformation scheme indicated above, is in an excited state and passes into a new state, emitting gamma-rays with an energy of 0.057 Mev. The half-life of this isomeric transition is equal to 1.42 min. The Ir_{77}^{192} isotope is unstable in this new state as well; 96% of its nuclei transform into Pt_{78}^{192} nuclei as a result of beta-disintegration and 4%—into Os_{76}^{192} nuclei, due to K-capture. The

Pt_{78}^{192} and Os_{76}^{192} nuclei formed are in an excited state and emit gamma-quanta in the process of ground-state transition. The Ir_{77}^{192} isotope emits a complex spectrum (see Table 3) consisting of 17 gamma-lines of different energies ranging from 0.136 to 1.060 Mev:

Gamma-quantum energy, Mev	Gamma-radiation intensity, %	Gamma-quantum energy, Mev	Gamma-radiation intensity, %
1.060	low-level	0.375	6.45
0.885	0.001	0.316	33.4
0.785	low-level	0.308	13.7
0.613	1.65	0.295	13.4
0.604	4.1	0.283	0.825
0.588	1.36	0.206	1.65
0.485	0.82	0.201	0.82
0.468	16.8	0.136	low-level
0.416	5.25		

The half-life of Ir^{192} is 74 days. The change of the specific activity of Ir^{192} with time is graphically shown in Fig. 8. The ionisation constant of Ir_{77}^{192} sources is equal to 4.97 r/hr mcurie cm, and, therefore, in respect of the produced gamma-radiation dose, 1 curie of Ir_{77}^{192} is equal to 0.59 gram radium equivalent.

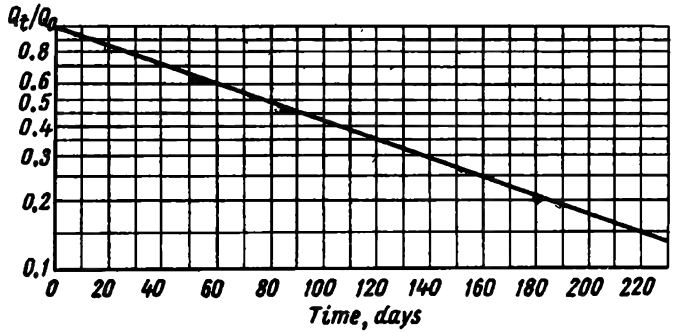

Fig. 8. Change in relative activity of Ir_{77}^{192} sources with time

The activities and sizes of capsulated Ir_{77}^{192} sources intended for gamma-radiography are given in Table 7.

Europeum-152, 154. The artificial radioactive isotope $Eu^{152,154}$ is a mixture of two isotopes: Eu_{63}^{152} and Eu_{63}^{154}. The $Eu_{63}^{152,154}$ isotope is produced by thermal-neutron bombardment of natural europeum occurring as a mixture of two isotopes Eu_{63}^{151} and Eu_{63}^{153}, the content of which amounts to 47.77 and 52.23% respectively. Isotope formation proceeds according to the following transformation scheme:

$$Eu_{63}^{151} + n \longrightarrow Eu_{63}^{152} + \gamma$$

and

$$Eu_{63}^{153} + n \longrightarrow Eu_{63}^{154} + \gamma.$$

It is possible to produce $Eu_{63}^{152, 154}$ preparations of a high specific activity. Besides, $Eu^{152, 154}$ isotopes can be separated from U^{235} fission fragments. However, the fragments contain negligible amounts of the Eu_{63}^{152} and Eu_{63}^{154} isotopes and their separation is very labour-consuming and costly.

The Eu_{63}^{152} and Eu_{63}^{154} isotopes are unstable. The Eu_{63}^{152} (26% of nuclei) isotope is transformed into Gd_{64}^{152}, emitting beta-particles

Table 7

Available Ir_{77}^{192} Radiation Sources

(According to 1959 data)

Activity, gram radium equivalent	Specific activity, curie/g	Size, mm		Inner dimensions of capsules, mm	
		diameter	height	diameter	height
0.01	0.34	4.5	5	2	2
0.10	3.4	4.5	5	2	2
0.50	17.0	4.5	5	2	2
2.0	68.0	4.5	5	2	2
5.0	170.0	4.5	5	2	2
20.0	680.0	7.5	8	5	5

with a maximum energy of 0.75 Mev. Beta-disintegration is accompanied by *K*-electron capture; as a result, Eu_{63}^{152} (74% of nuclei) is transformed into Sm_{62}^{152}. The disintegration of the Eu_{63}^{154} isotope is accompanied by beta-emission and Gd_{64}^{154} nuclei form. Beta-disintegration of Eu_{63}^{152} and Eu_{63}^{154} nuclei, as also *K*-electron capture by the Eu^{152} nuclei, is accompanied by the emission of several gamma-quanta. The $Eu^{152, 154}$ sources emit a complex gamma-spectrum (see Table 3) consisting of 20 lines of various intensity of a radiation energy ranging from 0.122 to 1.405 Mev.

Gamma-quantum energy, Mev	Gamma-radiation intensity, %	Gamma-quantum energy, Mev	Gamma-radiation intensity, %
0.341	14.5	0.871	5.9
0.421	2.4	0.958	16
0.593	1.73	1.106	20.5
0.717	3.63	1.281	7.4
0.779	10.3	1.409	17.3

The half-life of Eu_{63}^{152} is equal to 12.7 years (disintegration constant 1.408×10^{-9} cm^{-1})* and that of Eu_{63}^{154}—16 years (disintegration constant 1.37×10^{-9} cm^{-1}).

* The half-life of the isomer Eu_{63}^{152} is equal to 9.3 ± 0.2 hours.

The change in the specific activity of the $Eu_{63}^{152,154}$ preparations with time is graphically shown in Fig. 9. The ionisation constant of Eu^{152} sources is 4.3 r/hr mcurie cm. Consequently, in respect of the

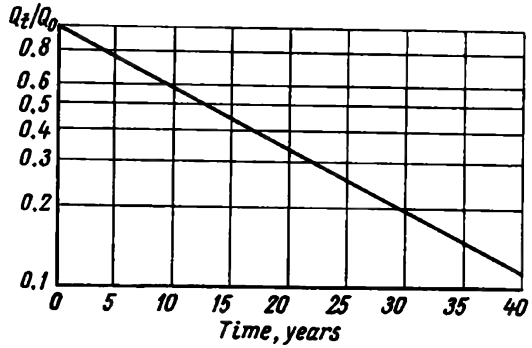

Fig. 9. Change in relative activity of $Eu_{63}^{152,154}$ sources with time

emitted gamma-radiation dose, a Eu^{152} source of an activity of 1 curie is equivalent to 0.57 gram of radium.

For gamma-radiography Eu^{152} sources are available in standard capsules of sizes and activities specified in Table 8.

Table 8

Available Eu_{63}^{152} Radiation Sources*

(According to 1959 data)

Activity, gram radium equivalent	Size, mm		Inner dimensions of capsules, mm	
	diameter	height	diameter	height
0.5	7.5	8	5	5
1.0	7.5	8	5	5
2.0	7.5	8	5	5

* The main gamma-active admixture is Eu^{154} about 10% ($I_\gamma = 6.23$); no other admixture has been observed.

Silver-110. The artificial radioactive isotope Ag_{47}^{110} is obtained by bombarding the stable isotope Ag_{47}^{109} with thermal neutrons, following the transformation scheme

$$Ag_{47}^{109} + n \longrightarrow Ag_{47}^{110} + \gamma.$$

As silver occurs in nature as a mixture of two isotopes Ag_{47}^{107} and Ag_{47}^{109}, the content of which is 51.3 and 48.7%, respectively, thermal-neutron bombardment of the isotope yields Ag_{47}^{110} and Ag_{47}^{108}. However, the latter disintegrates almost entirely in the course of

a few hours because its half-life is only several minutes. The Ag_{47}^{110} isotope is unstable and possesses a half-life of 270 days. As the isotope disintegrates, 7% of its nuclei emit gamma-quanta with an energy of 0.116 Mev and pass into the ground state. The Ag_{47}^{110} isotope is unstable in this state and is rapidly transformed into Cd^{110} ($T_{1/2}$ = 24 sec), emitting beta-particles with an energy of 2.86 Mev. The beta-disintegration is accompanied by *K*-electron capture. The other 93% of the Ag^{110} nuclei are subjected to beta-disintegration, resulting in the formation of excited Cd_{75}^{110} nuclei. The ground-state transition of Cd_{75}^{110} nuclei is accompanied by emission of gamma-quanta. Each disintegration yields three gamma-quanta of the following energy distribution:

Gamma-quantum energy, Mev	Number of gamma-quanta per disintegration	Gamma-quantum energy, Mev	Number of gamma-quanta per disintegration
0.116	0.07	0.814	0.01
0.656	0.97	0.885	0.785
0.676	0.1	0.935	0.35
0.706	0.1	1.389	0.32
0.759	0.14	1.516	0.169

The ionisation constant of Ag_{47}^{110} is equal to 14.49 r/hr mcurie cm. Consequently, in respect of the emitted gamma-radiation dose, an Ag_{47}^{110} source of an activity of 1 curie is equivalent to 1.74 gram of radium.

The specific activity of Ag_{47}^{110} preparations produced according to the (n, γ) transformation scheme reaches 1,000 mcurie/g.

Soft gamma-emitting isotopes. *Thulium*-170. The artificial radioactive isotope Tu_{69}^{170} is the product of bombarding the stable isotope Tu_{69}^{169} (100% abundance) with thermal neutrons.

$$Tu_{69}^{169} + n \longrightarrow Tu_{69}^{170} + \gamma.$$

The half-life of Tu^{170} is 129 days. The change of its relative activity with time is graphically shown in Fig. 10. When Tu_{69}^{170} disintegrates about 76% of its nuclei emit beta-particles with an energy of 0.968 Mev, such emission resulting in the formation of stable Yb_{70}^{170} nuclei. The remaining 24% of the Tu^{170} nuclei emit beta-particles with an energy of 0.886 Mev, this resulting in the formation of excited Yb_{70}^{170} nuclei which emit, during ground-state transition, gamma-quanta with an energy of 0.084 Mev. Thus, every 100 beta-disintegrations of Tu^{170} yied only 24 gamma-quanta.*

Besides the principal 0.084 Mev component, the Tu^{170} radiation spectrum contains bremsstrahlung of an energy up to 400 kev; such

* The literature also suggests other data regarding the number of gamma-quanta per 100 disintegration events, and indicates that apart from the 0.084 Mev lines the isotope spectrum contains components of 0.052, 0.01, 0.002, and 0.0005 Mev.

radiation is the result of high-energy beta-particles being slowed down by source atoms.

The low ionisation constant (K_γ for Tu_{69}^{170} is equal to 0.12 r/hr mcurie cm*) makes it expedient to use for gamma-radiography sources of a high activity amounting to several hundreds of curies (1-3 gram radium equivalent).

The low energy of Tu_{69}^{170} gamma-radiation sources is the reason for a considerable self-absorption. As a result of this self-absorption the ratio of the activity of Tu^{170} preparations expressed in curies, to that expressed in gram radium equivalent is variable and depends upon the activity of the preparation. Gamma-radiation of Co^{60},

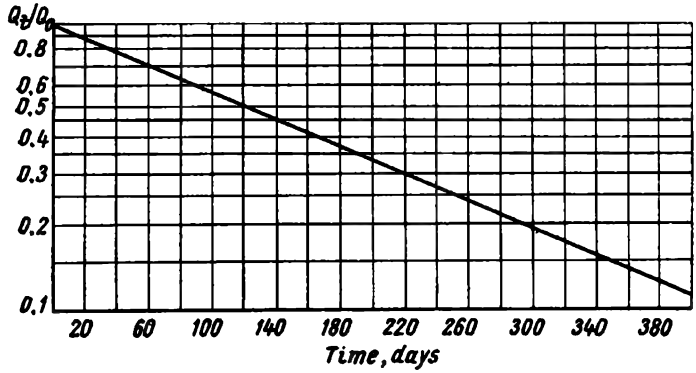

Fig. 10. Change in relative activity of Tu_{69}^{170} sources with time

Cs^{137}, Ir^{192} and other isotopes is also accompanied by self-absorption; however, for preparations used in industrial radiography source attenuation may be neglected, owing to the high-level radiation energy proper for the mentioned isotopes.

For gamma-radiography Tu^{170} sources are available in standard capsules of activities and sizes given in Table 9.

Europeum-155. The artificial radioactive isotope Eu^{155} may be separated from fission fragments of U^{235}. It is very difficult to separate pure Eu^{155} from the fission fragments, the yield only amounting to about 0.01%.

The other method of producing the Eu^{155} isotope consists in neutron bombardment of the stable isotope Sm^{154}, of which there is about 23% in the isotopic mixture of the element. During bombardment the stable isotope is transformed into Sm^{155} which, in turn, is transformed into Eu^{155} as a result of beta-disintegration and according

* Other data in relation to the Tu_{69}^{170} ionisation constant is to be found in the literature. A number of published works give for Tu_{70}^{170} an ionisation constant $K_\gamma = 0.033\text{-}0.045$ r/hr mcurie cm.

Table 9

Available Tu^{170}_{69} Radiation Sources

(According to 1959 data)

Activity, gram radium equivalent	Size, mm		Inner dimensions of capsules, mm	
	diameter	height	diameter	height
0.002	4.5	5	2	2.0
0.004	4.5	5	2	2.0
0.020	7.5	8	5	5.0
0.1	7.5	8	5	5.0
0.5	12.0	10	9	6.5

to the following scheme of transformation

$$Sm^{154}_{62}(n, \gamma)\, Sm^{155}_{62} \xrightarrow{\beta} Eu^{155}_{63} + \beta^-.$$

The half-life of Sm^{155}_{69} is about 24 min. Both enriched Sm^{154} and natural samarium may be irradiated; in the latter case, besides the Sm^{155} isotope, other radioactive isotopes are produced, of which the longest-lived Sm^{144} has a half-life of 410 days and a maximum gamma-ray energy of 950 kev (the isotopic mixture of the element contains about 3% of Sm^{144}).

Europeum-155 is unstable and disintegrates, emitting β^--particles with a maximum energy of 0.150 Mev (80% nuclei) and 250 Mev (20% nuclei). β^--disintegration of Eu^{155} results in the production of gadolinium Gd^{155}_{64} nuclei of various states of excitation. The transition of Gd^{155}_{64} nuclei into an excited state is accompanied by the emission of gamma-quanta with an energy of 0.060, 0.0870, 0.106, and 0.132 Mev. The energy of β^--particles resulting from the disintegration of Eu^{155}_{63} is considerably smaller than with the disintegration of thulium; as a result, the bremsstrahlung energy of beta-particles of Eu^{155} is commensurable with the energy of gamma-rays emitted by the isotope. However, the presence of high-energy lines in the Eu^{155} spectrum is possible (of both irradiated Eu^{155}, and Eu^{155} separated from fragments), owing to the presence of admixtures.

The half-life period of Eu^{155} is 1.7 years; therefore, the time during which it can be used effectively is about five times that of Tu^{170}. This is of special importance, bearing in mind the difficulties associated with the production of high-activity preparations which are characterised by soft gamma-emission, owing to a considerable self-absorption of the emission in the radioactive preparation. The change in the specific activity of the Eu^{155}_{63} preparation with time is graphically shown in Fig. 11.

In addition, as far as the yield of gamma-quanta per disintegration is concerned, the Eu^{155}_{63} source, for instance, is far superior to Tu^{170}_{69}. Thus, a single β^--disintegration of Eu^{155} yields 1.8 gamma-quanta, while Tu^{170} yields only 0.24. Consequently, the ionisation constant of Eu^{155} is considerably higher than that of Tu^{170} and is equal to

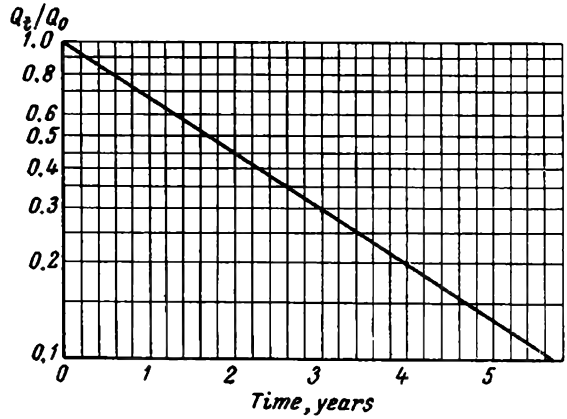

Fig. 11. Change in relative activity of Eu^{155}_{63} sources with time

about 0.65 r/hr mcurie cm. This to a considerable degree facilitates the production of high-activity sources (1 to 3 gram radium equivalent).

However, owing to the self-absorption of soft gamma-radiation in the source itself, the spectrum of Eu^{155}, as well as thulium, will change as these preparations increase in size and weight. The activities and sizes of Eu^{155} sources available for gamma-radiography are given in Table 10.

Table 10

Available Eu^{155}_{63} Radiation Sources

(According to 1959 data)

Activity, gram radium equivalent	Size, mm		Inner dimensions of capsules, mm	
	diameter	height	diameter	height
0.0001	7	9.5	3-4	5.5
0.0005	7	9.5	3-4	5.5
0.0010	7	9.5	3-4	5.5
0.0050	7	9.5	3-4	5.5
0.01	7	9.5	3-4	5.5

Cerium-144. The artificial radioactive isotope Ce_{58}^{144} is one of the fission products of U^{238}. The yeild of this isotope amounts to about 8% and, therefore, it is considerably easier to separate the isotope from fragments than to produce Eu_{63}^{155}.

The half-life of cerium is 284 days. The change in the relative activity of Ce_{58}^{144} with time is graphically shown in Fig. 12. As the isotope disintegrates, 97% of the Ce^{144} nuclei emit β^--particles with a

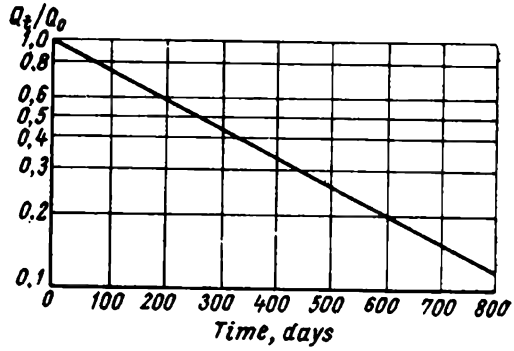

Fig. 12. Change in relative activity of Ce_{58}^{144} sources with time

maximum energy of 0.307 Mev and 3% of the nuclei—with a maximum energy of 0.446 Mev; β^--disintegration is accompanied by the emission of seven gamma-quanta of an energy ranging from 0.012 to 0.134 Mev (see Table 3).

The disintegrating Ce^{144} is transformed into an unstable isotope praseodymium Pr_{59}^{144}, the half-life of which is 17.5 min. During disintegration 85% of the Pr_{59}^{144} nuclei emit β^--particles with a maximum energy of 2.965 Mev and this results in the formation of a stable isotope Nd_{60}^{144}, 12% of the Pr_{59}^{144} disintegrating nuclei emit beta-particles with a maximum energy of 2.3 Mev; the newly formed Nd_{60}^{144} nuclei are in an excited state and emit gamma-quanta with an energy of 0.060 Mev as they pass into the ground state. The remaining 3% of the disintegrating Pr^{144} nuclei emit beta-particles with a maximum energy of 0.605 kev; the formed Nd_{60}^{144} nuclei are in an excited state and emit gamma-quanta with an energy of 2.185, 1.490 and 0.695 Mev (see Table 3) as they pass into the ground state. Thus, the Ce_{58}^{144} or $Ce_{58}^{141} + Pr_{59}^{144}$ isotopes are polyenergetic gamma-sources. Besides the very low-energy gamma-radiation, the isotope spectrum contains lines of an energy exceeding 1 Mev, such lines being the result of Pr^{144} disintegration.

Energy distribution in the $Ce_{58}^{144} + Pr_{59}^{144}$ gamma-spectrum is as follows:

Gamma-quantum energy, Mev	Specific radiation intensity, %	Gamma-quantum energy, Mev	Specific radiation intensity, %
0.134	15.4	0.042	4.3
0.1	15.4	0.034	15.4
0.094	4.5	2.185	0.18
0.080	25	1.490	0.18
0.054	15.4	0.695	3

The ionisation constant of Ce^{144} (+ Pr^{144}_{59}) sources is about 0.25 r/hr mcurie cm. The activities and sizes of isotope capsules available for gamma-radiography are listed in Table 11.

Table 11

Available Ce^{144}_{58} (+ Pr^{144}_{59}) Radiation Sources

(According to 1959 data)

Activity, gram radium equivalent	Size, mm		Inner dimensions of capsules, mm	
	diameter	height	diameter	height
0.1	10	14	8	12
0.5	10	14	8	12
2.0	20	24	8	18

Selenium-75. The radioactive isotope Se^{75}_{34} is produced by thermal-neutron bombardment of stable Se^{74}_{34} according to the following transformation scheme:

$$Se^{74}_{34} + n \longrightarrow Se^{75}_{34} + \gamma.$$

Selenium occurs in nature as a mixture of five isotopes: Se^{74}, Se^{76}, Se^{77}, Se^{78} and Se^{82}, the content of Se^{74}_{34} in the mixture amounting to only 0.86%. Therefore, when natural selenium is bombarded with thermal neutrons, other isotopes form alongside the Se^{75}_{34} isotope; however, the other isotopes disintegrate almost entirely in several hours, for their half-life is only a few minutes.

The small content of the Se^{74}_{34} isotope in natural selenium excludes the production of high-activity selenium preparations by irradiation (the specific activity of Se^{75}_{34} preparations produced by irradiating natural selenium does not exceed 10 mcurie/g).

The specific activity of Se^{75}_{34} is increased by enriching natural selenium with the Se^{74}_{34} isotope but this is a labour-consuming and costly process (at present the isotope may be enriched to 46%).

The Se^{75}_{34} isotope is unstable and disintegrates as a result of *K*-electron capture, being transformed into the isotope As^{75}_{35} in an excited state.

The ground-state transition of As^{75}_{35} nuclei is accompanied by the emission of gamma-quanta of a complex spectrum consisting of ten

lines of various intensity, their energies ranging from 0.066 to 0.405 Mev; of which the 0.269 and 0.138 Mev energy lines possess the highest intensity (see Table 3).

The half-life of Se_{34}^{75} is 125 days. The change in the specific activity of Se_{34}^{75} with time is shown in Fig. 13. The ionisation constant

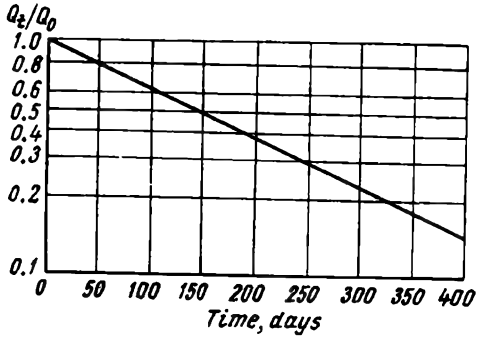

Fig. 13. Change in relative activity of Se_{34}^{75} sources with time

of a Se_{34}^{75} source is 1.49 r/hr. Thus, a Se_{34}^{75} source of 1 millicurie activity is equivalent to 0.178 gram of radium in respect of the emitted gamma-radiation dose.

Table 12 lists the activities and sizes of standard Se^{75} sources available for gamma-radiography.

Table 12

Available Se_{34}^{75} Radiation Sources

(According to 1959 data)

Activity, gram radium equivalent	Size, mm		Inner dimensins of capsules, mm	
	diameter	height	diameter	height
0.05	7.5	9.5	5	7
0.10	7.5	9.5	5	7
0.25	12.5	12.5	9	8
0.50	12.5	12.5	9	8
0.75	12.5	12.5	9	8
1.0	16.5	16.5	9	11
1.5	16.5	16.5	9	11
2.0	16.5	16.5	9	11

Radioactive sources of energies ranging from 5 to 150 kev are of great value for gamma-inspection and for measuring the thickness of low-density materials or thin sections of high-density objects.

These sources are of special value in gamma-raying parts of a complex configuration from short focal distances where it is impossible to apply a 360° panoramic roentgen tube or other methods of inspection.

In this connection let us consider the radiographic properties of Sm^{145} and Gd^{153} radiation sources. These sources are the products of the neutron bombardment of the respective enriched stable isotopes. This bombardment is effected in the following way: 8.5 mg of Sm_2O_3 enriched to 81.5% Sm^{144} and 8.4 mg of Gd_2O_3 enriched to 15% Gd^{152}, are placed in spherical quartz capsules of 2 mm inner

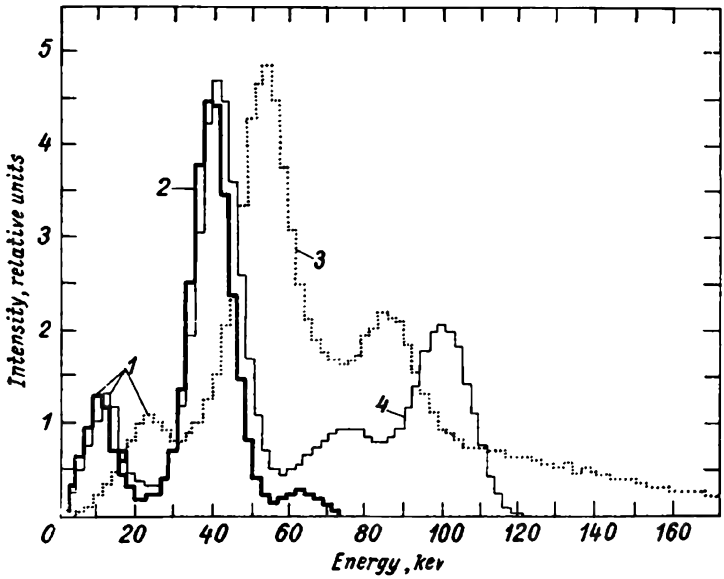

Fig. 14. Spectra of Sm^{145}, Gd^{153} and Tu^{170} sources determined with the aid of a NaI (TI) crystal detector and a hundred-channel pulse-height analyser:
1—points of maximum penetration; *2*—Sm^{145}; *3*—Tu^{170}; *4*—Gd^{153}

diameter and 0.2 mm wall thickness. Then, the capsulated isotopes are irradiated in a reactor creating a high neutron flux of $4.5 \times \times 10^{13}$ neutron/sq cm sec. Further the radioactive capsules are placed into aluminium holders with a wall 0.4 mm thick.

The photon spectra emitted by Sm^{145} and Gd^{153} and that of Tu^{170} are graphically illustrated in Fig. 14,* for purposes of comparison.

The disintegration of Sm^{145} and Gd^{153} follows the *K*-electron capture scheme; therefore, these sources do not produce the bremsstrah-

* The Tu^{170} source is produced from 50 mg of Tu_2O_3 placed into an aluminium capsule.

lung resulting from beta-disintegration. The principal photons emitted by Sm^{145} are: characteristic roentgen radiation with an energy of 38.6 kev and gamma-quanta with an energy of 61 kev, and those of Gd^{153}—the characteristic roentgen radiation with an energy of 41.5 kev and gamma-quanta of 72 and 100 kev. The half-life of these isotopes is 240 days.

The specific photon activity of any radiation source is of considerable importance for gamma-radiography and thickness measurement. True specific photon activity (photon emission rate per unit mass) may be determined only if the source disintegration scheme is precisely known.

At present it is impossible to obtain an exact determination of the specific photon activity of Sm^{145}, Gd^{153} and a number of other isotopes, owing to discrepancies in the available literature on disintegration schemes. Therefore, two new units are introduced:

1) specific photon activity which characterises the photon emission rate per unit mass of the radioactive source and is measured in source units per unit mass. One such "source unit/gram" is equal to 3.7×10^{10} emissions per second per gram;

2) unit of photon radiation intensity—the number of photons emitted by the source per unit time. One such "source unit" is equal to 3.7×10^{10} emissions per second (one "source milliunit" is equal to 3.7×10^{7} emissions per second).

The units introduced do not correspond to the curie which characterises the number of disintegrations per second. For gamma-active isotopes the number of emitted gamma-quanta rarely coincides with the number of disintegrations, i.e., when one quantum is emitted per disintegration.

The following example illustrates the relation between the photon "source units" and the curie. Let us assume that 100 millicuries of a radioactive isotope weigh 10 mg and the self-absorption is negligible. The walls of the capsule also possess a negligible absorption property. The disintegration scheme of this assumed isotopic source is known. Its disintegration time is equal to about 100% of *K*-electron capture disintegration time. In addition, the source possesses nontransformed gamma-radiation with an energy of 90 kev per disintegration. There are no other gamma-photons. Applying the introduced units to the given source, it may be established that X-radiation intensity (*K*-series) amounts to 100 *source milliunits* (or 3.7×10^{9} emissions per second). Gamma-radiation intensity with an energy of 90 kev amounts to 100 *source milliunits* (or 3.7×10^{9} emissions per second). The total photon radiation intensity amounts to 200 *source milliunits* (or 7.4×10^{9} emissions per second). But if the absorption of the source-holding capsule is not negligible in relation to X-radiation (*K*-series) and the capsule attenuates the photons by, say, 20%, then the X-radiation intensity (*K*-series) will amount to 80 *source milliunits*, etc.

As the specific photon activity is the intensity of photon emission per unit mass of the source material, the specific activity of X-radiation (K-series) is equal to $\frac{100\ source\ milliunits}{10\ mg} = 10\ source\ units/g$. The specific activity of gamma-radiation with an energy of 90 kev = = 10 *source units/g.*

The total specific photon activity is equal to 20 *source units/g.*

The terms and units introduced simplify the quantitative calculations in comparing radiation sources, for they represent the quantitative values which are employed in the practice of gamma-radiography and measurement work, for measuring, for instance, the thickness of materials, the thickness of surface coatings, etc. These new quantitative values may be easily determined in a laboratory with the aid of a gamma-ray spectrometer and a balance.

The intensity of photon radiation, and also the specific photon activity for Sm^{145}, Gd^{153} and Tu^{170} sources are shown in Table 13.

Table 13

Intensity of Photon Sources

Sources	Photons, kev	Measurement data		Maximum calculated data	
		Photon radiation dose, source milliunit*	Specific photon activity, source unit/g**	Photon radiation dose, source milliunit*	Specific photon activity, source unit/g**
Sm^{145}	39	0.85	0.100	22.1	2.60
(8.5 mg	61	0.05	0.006	1.3	0.16
Sm_2O_3)	>61	0.02	0.002	0.5	0.05
	Total	0.92	0.108	23.9	2.81
Gd^{153}	42	8.3	0.99	216	25.8
(8.4 mg	72	2.2	0.26	57	6.8
Gd_2O_3)	100	4.0	0.48	104	12.5
	Total	14.5	1.73	377	45.1
Tu^{170}	52	41	0.82	410	8.2
(50 mg	84	18	0.36	180	3.6
Tu_2O_3)	Additional bremsstrahlung	16	0.32	160	3.2
	Total	75	1.50	750	15.0

* *A source milliunit* is equal to 3.7×10^7 emissions per second.
** *A source unit/g* is equal to 3.7×10^{10} emissions per second per gram.

In addition, the table shows the maximum photon radiation intensity and specific photon activity which may be obtained in modern high-neutron flux reactors.

CHAPTER II

INTERACTION OF RADIOACTIVE RADIATION WITH MATTER

The passage of alpha-, beta- and gamma-rays through a substance is accompanied by a gradual decrease in the intensity of the rays, owing to interaction with atoms of the substance.

The nature of the atomic interaction of alpha-, beta- and gamma-rays possesses features specific to each of these kinds of radiation. Alpha- and beta-rays lose their intensity very rapidly as they pass through a substance, alpha-rays being absorbed to a higher degree than beta-rays. Gamma-rays possess a higher penetrating power, compared with alpha- and beta-radiation.

§ 1. Alpha-absorption

The loss of energy by alpha-particles as they pass through a substance is due mainly to electron interaction. During transit through the substance the alpha-particles are subjected to an enormous number of atomic collisions and form a large quantity of ions. For example, while passing through air at a temperature of 15°C and 760 mm Hg pressure, one alpha-particle creates 150-250 thousands of ion pairs along its entire path, depending on its energy. Thus, alpha-particles create about 6,600 ion pairs per 1 mm of path.

The path of an alpha-particle depends upon its energy. For the most important radioactive elements, the path of alpha-particles through air ranges from 2.6 to 8.6 cm.

The path of alpha-particles diminishes with the increase in the atomic weight and number of the absorbing element. For hard substances the penetrating power of alpha-particles is very low. The most penetrating alpha-particles of ThC′ of an energy equal to 8.8 Mev are absorbed by aluminium foil 0.0052 cm thick. Ordinary paper entirely absorbs the alpha-rays of natural radioactive elements.

Alpha-rays produce various chemical actions, the mechanism of which is determined by the ionising power of the alpha-rays. Alpha-rays decompose water, the reaction being accompanied by the liberation of hydrogen and oxygen; when exposed to alpha-radiation, hydrogen chloride, ammonia, hydrogen sulphide and other similar substances decompose into the elements of which they consist. Alpha-rays possess a high radiation-chemical activity. Therefore, they can easily be detected by the photographic technique, although the path of the alpha-rays in the photo-emulsion is not long.

Alpha-radiation produces a considerable physiological effect. It causes skin burns and other inflammatory processes. A thin layer of rubber or of a textile fabric offers adequate protection against alpha-radiation.

§ 2. Beta-absorption

As already mentioned, beta-particles are electrons or positrons emitted by the atomic nucleus. These particles may move at a very high velocity. The velocity of a 0.5 Mev electron is approximately equal to 0.9 of the velocity of light and to 0.98 of light velocity, if the energy of the moving electron is 2.0 Mev. While passing through substance the beta-particles decelerate, owing to atomic interaction.

The interaction of electrons and positrons with matter is similar in quality and consists of three principal processes: elastic scattering with atomic nuclei, scattering with shell electrons and inelastic collision with atomic nuclei.

Owing to ionisation, ion pairs are created along the electron path. On the average, it takes about 32.5 electron-volts to create one ion pair, in other words, 1 Mev of absorbed energy yields 30 thousand ion pairs in air.

Almost a linear dependency exists between the maximum path of beta-particles and their maximum energy. It is characteristic of beta- as well as of alpha-radiation that it is fully absorbed by a layer of the irradiated substance, the thickness of which is determined by the energy of the particles.

Beta-rays with a maximum energy of 3.0 Mev are entirely absorbed by a layer of water 12.5 mm thick or by a layer of aluminium 4.9 mm thick.

§ 3. Interaction of gamma-rays with matter

As gamma-rays pass through a substance, their intensity gradually diminishes, approaching zero asymptotically (unlike beta-rays, no definite maximum path is observed here).

The attenuation of radiation intensity is traced to three principal elementary processes: photoelectric absorption, scattering, and pair production. The probability of each of the specified processes depends upon the radiation spectrum, atomic number and density of the absorbing medium.

In examining the laws of radiation attenuation, a distinction is drawn between narrow-beam gamma-radiation and broad-beam gamma-radiation. A narrow beam of gamma-rays is a beam at which scattered gamma-quanta, created as the gamma-rays pass through the substance, do not penetrate into the recording unit placed behind the absorbing medium. In order to secure a narrow beam, it is necessary properly to diaphragm both the incident ray and the recording unit. The radiation beam is defined as broad, if the scattered gamma-photons get into the recording unit. In general, gamma-radiography deals with broad beams. Narrow beams are usually created for special experimental work conducted to study the nature of gamma-ray and substance interaction.

Photoelectric absorption. When passing through a substance, gamma-quanta may transfer all their energy to the electrons in the course of electron interaction. This process is called photoelectric absorption. The gamma-quanta vanish in the process of photoelectric absorption and the energy of a quantum is spent to eject an electron from its shell and to impart kinetic energy to the electron. Naturally, the process of photoelectric absorption may occur only if the energy of the gamma-quantum is higher than the electron-binding energy. A gamma-quantum may impart its energy to any of the atom electrons; thus, under conditions of one and the same incident-photon energy the kinetic energy of the electron will depend on its atomic binding energy. Owing to the formation of the photoelectron, one of the atom electron levels becomes unoccupied; this place is filled at once by one of the electrons situated on the shell farther away from the nucleus. Thus, in the process of photoelectric absorption, the characteristic radiation takes place as well.

It could have been assumed that the number of photoelectrons must be equal to the number of absorbed quanta; actually, however, the number of ejected electrons is larger than the number of absorbed gamma-quanta. The reason is that transition of the atom from an excited into the ground state may occur not only on account of photon radiation (characteristic radiation), but also by direct transfer of the excitation energy to one of the shell electrons, and the ejection of this electron. The probability of photoelectric absorption depends upon the radiation energy and the nature of the substance.

If the energy of gamma-quanta is low ($E_\gamma < 0.5$ Mev), the photoelectrons mostly escape in directions perpendicular to the direction of gamma-ray propagation. The higher the energy, the nearer the direction of the escaped photoelectrons approaches the initial line of gamma-ray propagation.

The value which characterises relative gamma-flux attenuation caused by photoelectric absorption during passage through a layer 1 cm thick is called the photoelectric absorption coefficient τ; the dimensiality of this coefficient is centimetre^{-1}. The photoelectric absorption coefficient diminishes with an increase in the radiation energy and it rises sharply as the atomic number of the absorbing substance increases (Fig. 15).

Besides the linear photoelectric absorption coefficient, a mass coefficient $\frac{\tau}{\rho}$ is also used in calculations, where ρ represents the substance density. The mass absorption coefficient shows the extent to which gamma-radiation attenuates through photoelectric absorption after having passed through a layer of substance of a mass equal to 1 g/sq cm and is measured in square centimetres per gram. Fig. 16 shows the dependency of the photoelectric absorption mass coefficient on the element's atomic number for gamma-quanta of various energies.

The photoelectric effect is mainly observed during low-energy gamma-radiation in absorbers of a high atomic number. For example, in the case of aluminium, the photoelectric absorption of gamma-rays may be considered practically negligible starting with

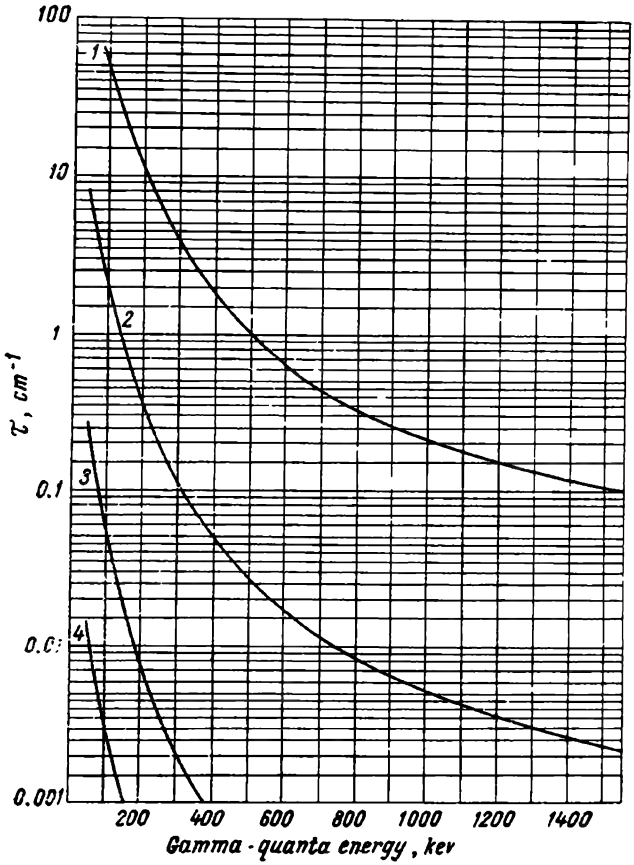

Fig. 15. Dependence of the linear photoelectric absorption coefficient on radiation energy for water, aluminium, copper and lead:
1—lead; *2*—copper; *3*—aluminium; *4*—water

a gamma-radiation energy of 150 kev, and in the case of lead starting with 2.0 Mev.

Gamma-ray scattering. In the course of gamma-ray interaction with matter, absorption is accompanied by the scattering of gamma-quanta.

Two processes of gamma-ray scattering are distinguished:

a) coherent or classical scattering;

b) incoherent or Compton scattering.

Coherent scattering is defined as gamma-quantum-electron interaction which is followed only by a change in the path of gamma-quanta (no change in the gamma-quanta energy occurs). This process of interaction is similar to an elastic collision of two balls where the mass of the stationary ball is many times larger than that of the moving ball. The small ball strikes against the stationary ball and jumps away from the latter in a direction opposite to the initial

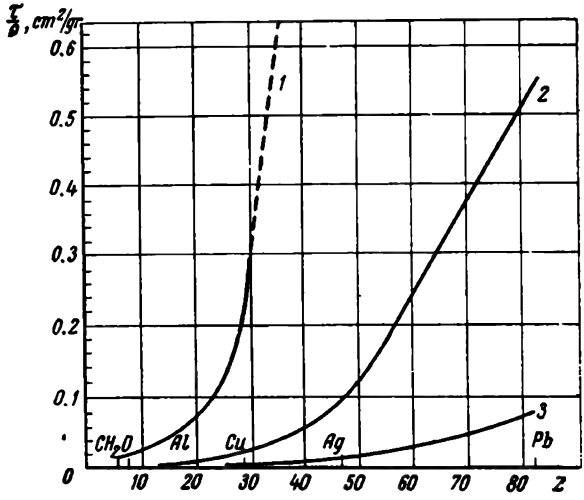

Fig. 16. Dependence of the mass photoelectric absorption coefficient on the atomic number of elements for gamma-quanta of different energies: *1*—100 kev; *2*—255 kev; *3*—500 kev

motion as from a hard wall. Coherent gamma-ray scattering is of importance only for long-wave radiation (of an energy up to 60-100 kev) or for substances of a small Z.

For radiation energies of a higher order the so-called incoherent (Compton) scattering is essential; incoherent scattering is followed by a decrease in gamma-quanta energy.

Incoherent (Compton) scattering is the gamma-quantum-electron interaction during which the gamma-quantum does not transfer all its energy to the electron (unlike the photoeffect), but only part of it, and deflects at a certain angle from its initial path in doing so. Having received a certain quantity of energy, the electron starts to move at an angle towards the direction of the gamma-quantum motion. Thus, incoherent scattering results in the appearance of the scattered gamma-quantum of a smaller energy (but of a longer wavelength) moving in a different direction and of the ejected, so-called, recoil (Compton) electron which received a portion of the gamma-quantum energy.

It should be mentioned that incoherent scattering occurs only when the energy of the gamma-quantum considerably exceeds the electron binding energy (about 10 thousand times), and the electron may be practically considered as a free electron. Moreover, in contrast to the photoeffect in which the gamma-quantum interacts mainly with the K-electron, during incoherent scattering, gamma-quanta interact with outer electrons of a minimum binding energy.

When passing through a substance, gamma-quanta may scatter at various angles ranging from 0 to 180°, while secondary electrons escape only at an angle not exceeding 90°. The propagation line of the scattered gamma-quanta depends on the energy of primary radiation.

The attenuation of radiation intensity resulting from incoherent scattering is due to the fact that gamma-quanta, interacting with substance electrons and scattering in various directions, mostly pass beyond the primary gamma-ray beam. As the scattered radiation passes through the substance, electron interaction takes place; double-, triple- and multiple-scattered gamma-quanta appear. The interaction between the scattered gamma-quanta and the substance usually ends in the photoeffect.

The value which characterises the relative attenuation of the radiation flux due to the Compton scattering phenomenon, occurring as the rays pass through a substance layer 1 cm thick, is called the linear factor of incoherent (Compton) scattering σ. The linear factor of Compton scattering is measured in centimetres^{-1}; the factor is larger, the more electrons the layer contains, for in such a case a larger portion of the gamma-quanta is subjected to scattering.

Thus, attenuation of the radiation intensity due to Compton scattering, calculated per unit length of the absorber is larger for absorbers of a higher density. For example, as radiation of one and the same spectrum passes through a layer of aluminium ($\rho = 2.7$ g/cu cm) 10 cm thick and a layer of lead ($\rho = 11.34$ g/cu cm) of a similar thickness, the number of photons scattered in the lead will be about 4.2 times greater than the number of photons scattered in the aluminium layer.

In addition, a mass factor of Compton scattering is used. This factor, designated $\frac{\sigma}{\rho}$, characterises the relative attenuation of the gamma-ray flux as it passes through a substance layer with a mass of 1 gram and is expressed in square centimetres per gram. It may be assumed with a sufficient degree of accuracy that the linear coefficient of Compton scattering is proportional to the density of the absorber.

As attenuation of gamma-radiation intensity due to scattering is the result of two processes—the partial transfer of gamma-quanta energy to the electron and gamma-quanta scattering, the summary scattering factor is the total of two components:

$$\sigma = \sigma_a + \sigma_s, \tag{19}$$

where σ_a —the scattering absorption factor,
σ_s—the scattering factor.

The attenuation of gamma-rays due to incoherent scattering, as the rays pass through a substance with a mass of 1 gram is about the same for various substances. In other words, the mass factor of incoherent scattering is about equal for all substances.

With an increase in incident radiation energy the Compton scattering factor diminishes to a smaller degree, as compared with the photoelectric absorption coefficient; the Compton scattering factor is of essential importance for energies of up to several Mega-electron-volts.

Pair production. As high-energy (over 1 Mev) gamma-rays pass through a substance, the gamma-quanta energy may be spent to form pairs, each consisting of one positive and one negative electron (positron and electron) and the gamma-quantum vanishing in the pair-production process. The transformation of the gamma-quanta into positive and negative electrons takes place in direct proximity to the nucleus and under the influence of its electrical field.

As the masses of the resting electron and positron are approximately equal and equivalent to an energy of 0.51 Mev, the gamma-quanta energy must be not less than 1.02 Mev to make pair production possible.

Gamma-ray absorption due to pair formation is governed by the following relationship:

$$\varkappa = KNZ^2(E-1.02) \tag{20}$$

where: $\varkappa$— the linear absorption coefficient, cm^{-1}, characterising the relative attenuation of radiation intensity due to pair production;
K— the factor of proportionality;
N— the number of atoms per 1 cu cm of absorber;
Z— the absorber atomic number;
E— the gamma-quantum energy.

It follows from the above relationship (20) that the coefficient of the gamma-radiation absorption due to pair formation increases with an increase in radiation energy and is proportional to Z^2 of the absorber.

It should be borne in mind that as the positron exists only during a very short time interval, pair formation is followed by the annihilation phenomenon accompanied by the emission of two gamma-quanta of an energy of 0.51 Mev.

Besides the modes of interaction of gamma-rays with matter treated above, in the case of gamma-rays of a very high energy nuclear interaction may occur. In the course of such interaction either a proton or neutron may escape from the nucleus, this resulting in the formation of a new nucleus, i.e., nuclear reaction takes place.

For example,

$$Be^9 + h\nu \longrightarrow Be^8 + n.$$

For energies running up to several Mega-electron-volts the effective cross-section of a photonuclear reaction is extremely small, therefore, the attenuation of gamma-rays due to nuclear photoeffect may be considered negligible.

§ 4. General laws governing attenuation of narrow-beam gamma-radiation

The passage of gamma-rays through a substance is accompanied by attenuation of beam intensity to an extent which depends on the thickness of the absorbing layer.

Let us examine a monochromatic narrow gamma-beam. Let the intensity of radiation at any point, as registered by an instrument in the absence of an absorber, be equal to I_0. If a thin layer of substance, dx thick, is placed between the radiation source and the instrument, then, the radiation intensity at that point will change by a small value dI and become equal to I, i.e., $I_0 - I = -dI$.*

Measurements conducted with various absorbers and radiation sources of a different energy have shown that

$$-dI = \mu I\, dx, \tag{21}$$

i.e., as radiation passes through thin layers of an absorber the change in radiation intensity is proportional to the thickness of the layer and the primary intensity (when there is no absorber); it also depends upon the value μ which, in its turn, depends upon the radiation energy and density of the substance, and is called the linear coefficient of gamma-ray absorption.

Assuming that dx is equal to 1 cm, it follows from equation (21) that

$$\mu = \frac{dI}{I}\ \text{cm}^{-1}. \tag{22}$$

Thus, the linear coefficient of gamma-ray absorption characterises the relative change in radiation intensity during the passage through a layer of substance 1 cm thick, and is measured in centimetre^{-1}.

In order to determine the attenuation of gamma-ray intensity by a layer of finite thickness, equation (21) ought to be integrated, this leading to the exponential law of gamma-ray absorption expressed as

$$I = I_0 \times e^{-\mu d}, \tag{23}$$

where I_0—the intensity of gamma-radiation in the absence of an absorbing layer ($d = 0$);

I—the intensity of gamma-radiation after passage through an absorbing layer d cm thick;

μ—the linear coefficient of gamma-ray absorption.

* The minus sign before dI indicates that attenuation of intensity takes place.

If the thickness of the absorbing layer is expressed in grams per square centimetre, instead of centimetres, equation (23) may be rewritten as follows:

$$I = I_0 e^{\frac{-\mu}{\rho} m}, \tag{24}$$

where I_0—the gamma-radiation intensity in the absence of an absorbing layer;

I—the gamma-radiation intensity after passage through an absorbing layer m thick, g/sq cm;

$\frac{\mu}{\rho}$—the mass absorption coefficient.

The mass coefficient of gamma-ray absorption characterises the relative attenuation of radiation intensity during passage through a

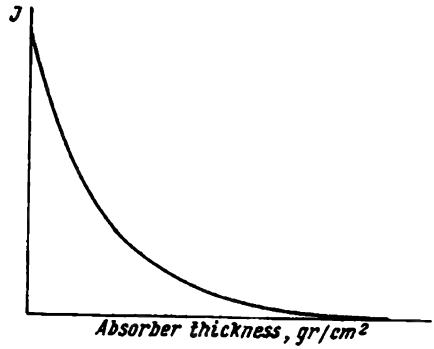

Fig. 17. Change in gamma-intensity I with absorber thickness (simple coordinates)

substance of a mass of 1 g enclosed in a cylinder with a base area of 1 sq cm. The ratio $\frac{\mu}{\rho}$ is expressed respectively in square centimetres per gram.

Fig. 17 illustrates the exponential curve characterising the variation in intensity of monochromatic narrow-beam radiation as a function of absorber thickness. The curve shows that it is impossible to absorb gamma-rays entirely; it is only possible to diminish their intensity to the desired low value. The thickness of a layer, the passage through which diminishes gamma-radiation by one half, is called the half-value layer and is usually designated $d_{0.5}$.

The following relationship exists between the half-value layer and the linear absorption coefficient:

$$d_{0.5} = \frac{0.693}{\mu}. \tag{25}$$

The thickness of the layer, the passage through which diminishes radiation intensity ten times, i.e., $I = \frac{I_0}{10}$ is called the tenth-value layer and is designated $d_{0.1}$. As with the half-value layer it can be shown that the following relationship exists between the tenth-value layer and the linear absorption coefficient

$$d_{0.1} = \frac{2.3}{\mu}. \tag{26}$$

It should be mentioned here that the laws of gamma-ray attenuation discussed above refer to monochromatic radiation.

If the gamma-ray spectrum consists of several lines, as is the case with most of the radioactive isotopes, the law of gamma-ray attenuation is expressed by the following equation:

$$I = I_1 + I_2 + \ldots = I_{0.1}e^{-\mu_1 d} + I_{0.2}e^{-\mu_2 d} \ldots, \tag{27}$$

where $I_{0.1}$ and $I_{0.2}$—the primary intensity of gamma-spectrum components;

I_1 and I_2—the intensity of gamma-spectrum components after passage through an absorbing medium d thick, cm;

μ_1 and μ_2—the linear absorption coefficients for different gamma-spectrum components for the given absorption medium.

In some cases polychromatic gamma-radiation may be considered as monochromatic radiation possessing a certain effective energy E_{ef} and an effective absorption coefficient —μ_{ef}. When passing through a substance, the intensity of such polychromatic radiation is attenuated in the same manner as the intensity of monochromatic radiation:

$$I = I_0 e^{-\mu_{ef} d}. \tag{28}$$

In contrast to the absorption coefficient of monochromatic radiation, the effective absorption coefficient of polychromatic radiation depends not only upon the kind of absorber and radiation energy, but on the absorber thickness as well. The reason is that various components of the polychromatic-radiation spectrum are absorbed in a different manner as the rays pass through the absorber; consequently, the radiation spectrum will vary with a change in absorber thickness. As small-energy gamma-quanta become attenuated to a higher degree, an increase in absorber thickness will result in an increased share in the spectrum of high-energy gamma-quanta, i.e., the hardness of radiation will be augmented and the value of μ_{ef}—diminished.

The total absorption coefficient μ may be defined as the sum of coefficients representing various processes of gamma-radiation ab-

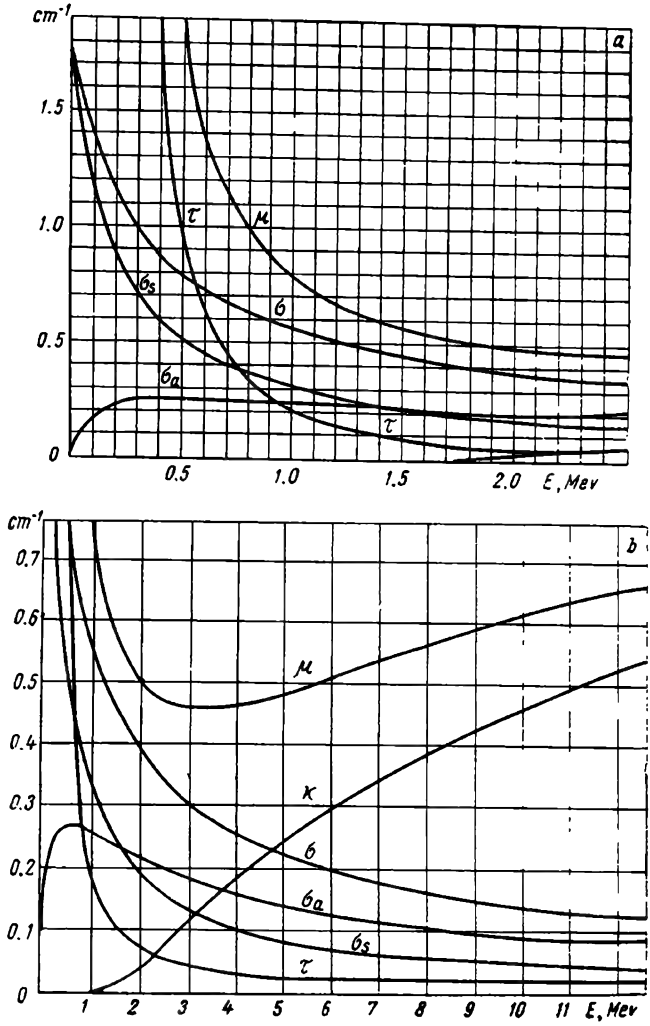

Fig. 18. Linear absorption coefficients μ, σ, τ and κ for a narrow gamma-beam of different energies in lead:

a—for energies up to 2.5 Mev; b—for energies up to 12 Mev

sorption. As attenuation of radiation intensity is mainly traced to three processes—photoelectric absorption, incoherent scattering and pair production—the total absorption coefficient μ is equal to the sum of the three factors

$$\mu = \tau + \sigma + \varkappa, \tag{29}$$

where τ, σ and $\varkappa$ characterise respectively the relative reduction in radiation intensity resulting from each of the above-mentioned processes.

A similar formula may be written for the mass absorption coefficient

$$\frac{\mu}{\rho} = \frac{\sigma}{\rho} + \frac{\tau}{\rho} + \frac{\varkappa}{\rho}. \tag{30}$$

The curves in Fig. 18 characterise the variation in μ, σ, τ and $\varkappa$ for lead, depending upon the radiation energy. The same diagram gives the respective curves for factors σ_s and σ_a. The curves of Fig. 18 show that the linear coefficients of the photoelectric absorption τ and the scattering factor σ diminish continuously with an increase in gamma-ray energy. For low-energy gamma-rays and heavy-element absorbers $\tau > \sigma$, while $\sigma > \tau$ in the case of high-energy gamma-radiation and light-element absorbers.

In the case of aluminium the gamma-absorption coefficient increases only slightly, as a result of pair production up to an energy of 10 Mev. The picture is different with lead.

In the case of lead the linear coefficient of absorption due to pair production increases so rapidly with an increase in the radiation energy that the curve of the total absorption coefficient μ, first dropping, has its minimum value at a point corresponding to an energy of 3 Mev, and then begins to rise. A similar picture is observed with a number of other heavy elements.

Appendix I lists the values of the linear absorption coefficients μ, τ, σ and $\varkappa$, also the half-value and tenth-value layers for aluminium, brick, concrete, iron and lead, depending upon radiation energy.

From the data specified (see Fig. 18 and Appendix I) it follows that for lead the photoelectric effect is observed only at radiation energies ranging from 1.5 to 2.0 Mev. When dealing with light elements (aluminium), starting with energies of 100-150 kev, the photoelectric absorption becomes extremely weak and may be ignored. In this case attenuation of radiation intensity is the result mainly of incoherent scattering for a wide range of energies up to 10 Mev, where the process of pair production begins to be felt

$$\mu = \sigma. \tag{31}$$

This relationship also holds for elements of a medium Z (copper, iron) in the energy range from 0.5 to 5.0 Mev.

§ 5. Laws governing attenuation of broad-beam gamma-radiation

The preceding section dealt with the laws governing attenuation of narrow-beam gamma-radiation. However, gamma-radiography is mainly based upon the employment of broad divergent gamma-beams. In this case a certain fraction of the scattered gamma-quanta penetrates into the registering apparatus and, therefore, the attenuation of broad-beam radiation intensity will be slower than with a narrow beam. The fraction of scattered radiation augments with an increase in the radiation field and the absorber thickness.

If the energy of the gamma-quanta is low, then, during the passage through a substance, the attenuation of radiation will chiefly be the result of photoelectric absorption. In this case the difference in the nature of narrow- and broad-beam radiation attenuation will be slight. With an increase in radiation hardness the fraction of the incoherent scattering factor σ in the total absorption coefficient μ will increase, this resulting in a significant difference between narrow- and broad-beam attenuation. For lead absorbers it may be accepted, in the first approximation, that there is no difference between narrow- and broad-beam attenuation for energies of 200-250 kev; but this difference in attenuation ought to be taken into account in the case of light absorbers beginning from a softer radiation of about 100 kev. It should be mentioned that the harder the radiation, the smaller the back scattering. For instance for gamma-radiation from a Co^{60} source ($E_{ef} = 1.25$ Mev), back scattering constitutes from 1 to 3% and may reach 20 to 40% for radiation with an energy of 200 kev.

In the general form the intensity of broad-beam radiation after passage through an absorber d cm thick may be presented by the following equation:

$$I_{br} = I_0 \times e^{-\mu d} + I_{scat}, \tag{32}$$

where $I_0 \times e^{-\mu d}$ – the attenuation of narrow-beam radiation;

μ — the linear absorption coefficient for narrow-beam gamma-radiation;

I_{scat} — the intensity of scattered radiation at a given point.

Thus, in order to calculate the attenuation of intensity of broad-beam gamma-radiation, it is necessary to determine I_{scat}. But the value of I_{scat} depends upon many parameters, such as the radiation spectrum and its variation during scattering, the absorption of scattered radiation, etc. Naturally, it is difficult to determine I_{scat} by calculation; such calculations are complicated, in addition, by the fact that the scattered gamma-quanta may be subjected to repeated scattering, i.e., it is necessary to take into consideration multiple scattering. At present several approximation methods for

the calculation of scattered radiation are being suggested. All these methods are extremely complicated and require much time.

For practical purposes the intensity of scattered radiation is determined experimentally by registering the difference between the intensity of broad- and narrow-beam gamma-radiation after passage through an absorber of a definite thickness.

The law governing attenuation of broad-beam gamma-radiation may be expressed in a form similar to that for narrow-beam radiation

$$I_{br} = I_0 \times e^{-\mu_{br} d}, \tag{33}$$

where I_{br}—the intensity of broad-beam gamma-radiation after passage through a substance d cm thick;

I_0—the intensity of broad-beam gamma-radiation at the same point in the absence of an absorbing layer;

μ_{br}—the linear absorption coefficient for broad-beam gamma-radiation, cm^{-1}.

The absorption coefficient for broad-beam gamma-radiation may be determined experimentally. For this purpose an absorption curve is plotted for broad-beam gamma-radiation passing through a certain material (the change in the intensity of a broad, divergent gamma-beam as it passes through substance is determined with the aid of ionisation chambers).

The absorption curve is employed to determine μ_{br} for layers of a different thickness according to the formula

$$\ln \frac{I_{br}}{I_0} = -\mu_{br} \times d. \tag{34}$$

Figs. 19 and 20 illustrate the absorption curves for broad-beam gamma-radiation emitted by Ir^{192}, $Eu^{152, 154}$, Eu^{155}, Tu^{170} and Ce^{144} artificial radioactive isotopes which have been widely used in practice as radiation sources in gamma-radiography.

Figs. 21 to 23 contain curves characterising the variation of the linear absorption coefficient of broad-beam gamma-radiation from Tu^{170}, Eu^{155}, $Eu^{152, 154}$, Ir^{192} and Ce^{144} sources with absorber thickness.

As already mentioned, for polychromatic radiation the narrow-beam absorption coefficient diminishes with the increase in absorber thickness, because radiation hardness grows as a result of the relatively larger filtration of soft components. The absorption coefficient for broad-beam radiation will diminish accordingly. But the linear absorption coefficient of a broad beam μ_{br} will always be smaller than the linear absorption coefficient μ of a narrow beam (Fig. 24), for the relative intensity of a broad beam is always larger than that of a narrow beam ($I_{br}/I_0 > I/I_0$).

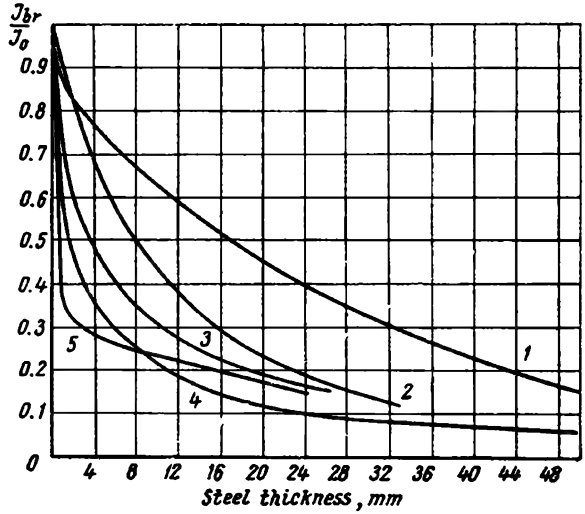

Fig. 19. Relative change in the intensity of a broad gamma-beam from $Eu^{152,154}$, Ir^{192}, Eu^{155}, Tu^{170} and Ce^{144} sources after passage through steel:
1—$Eu^{152,154}$; *2*—Ir^{192}; *3*—Eu^{155}; *4*—Tu^{170}; *5*—Ce^{144}

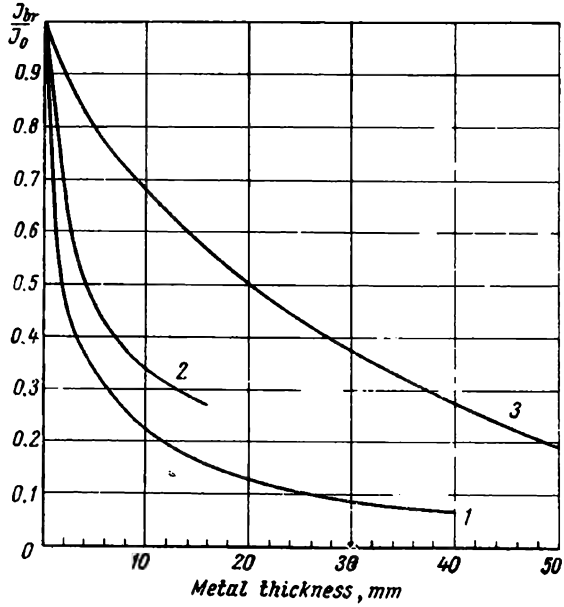

Fig. 20. Relative change in the intensity of a Tu^{170} broad gamma-beam after passage through steel, titanium and duralumin:
1—steel; *2*—titanium; *3*—duralumin

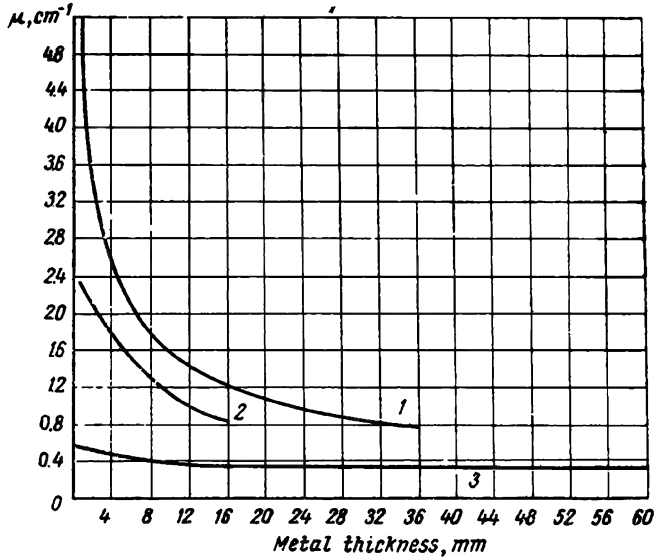

Fig. 21. Change in the linear absorption coefficient of a Tu^{170} broad gamma-beam with thickness of steel, titanium and duralumin:

1—steel; *2*—titanium; *3*—duralumin

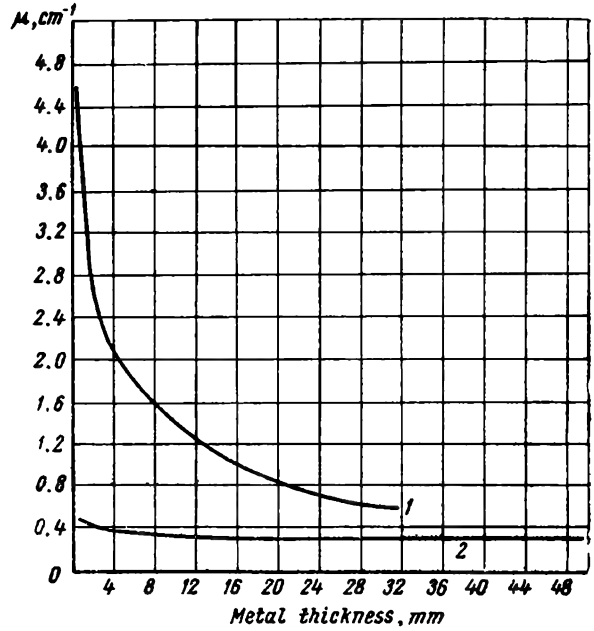

Fig. 22. Change in the linear absorption coefficient of a Eu^{155} broad gamma-beam with thickness of steel and duralumin:

1—steel; *2*—duralumin

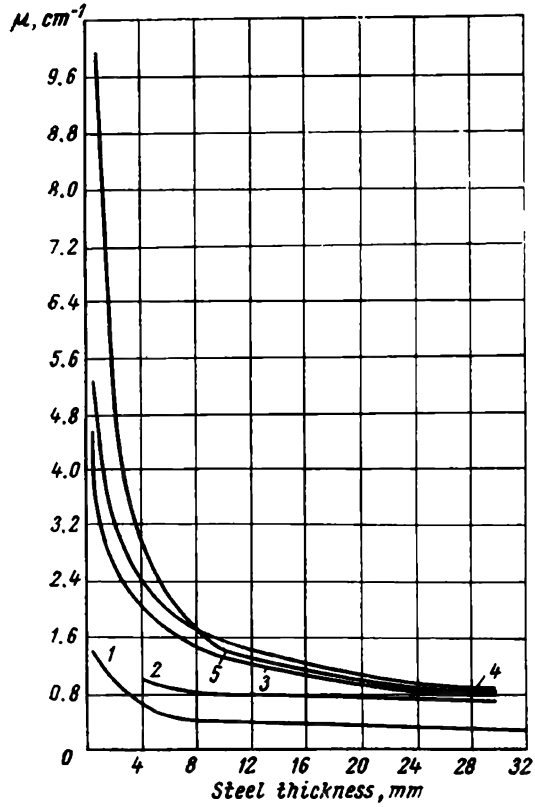

Fig. 23. Change in the linear absorption coefficient of a broad gamma-beam from $Eu^{152,154}$, Ir^{192}, Tu^{170}, Eu^{155} and Ce^{144} sources with steel thickness:

1—$Eu^{152, 154}$; *2*—Ir^{192}; *3*—Eu^{155}; *4*—Tu^{170}; *5*—Ce^{144}

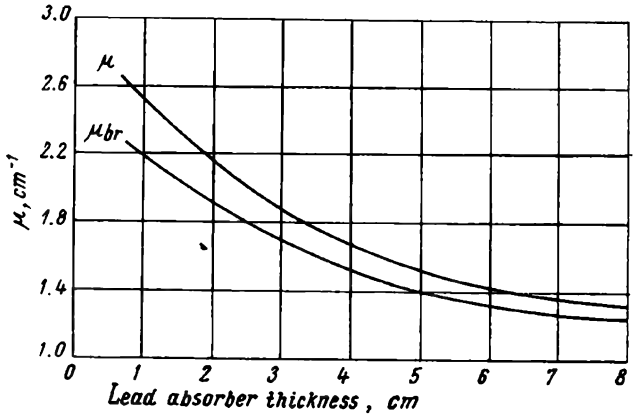

Fig. 24. Dependence of μ and μ_{br} for an Ir^{192} gamma-beam on the thickness of lead absorbers

Part Two

METHODS OF INDUSTRIAL RADIOLOGY BASED ON THE USE OF RADIOACTIVE RADIATION

Gamma-radiography is defined as the combination of methods employed to check the quality of opaque materials with the aid of gamma-rays emitted by radioactive isotopes. Beta-radiography includes methods of inspecting very thin materials (foils, etc.) with the aid of beta-rays, the exposure arrangements being similar to those employed in gamma-radiography. This book mostly deals with methods of gamma-radiography.

The use of radioactive isotopes for purposes of flaw detection is based on the law governing attenuation of the intensity of radiation emitted by radioactive isotopes as the rays pass through a substance. The penetrating radiation is attenuated to a different degree, depending upon the thickness and density of the radiographed material. The gamma-rays escape from the heterogeneous material of the inspected article in a beam of nonuniform intensity. The beam which has passed through a material of a smaller thickness or a smaller density (at the spot where the defect is located) escapes with a higher intensity, as compared with that of the adjoining gamma-beams which have passed through solid material. The internal state of the inspected material is determined by the results obtained in measuring the intensity of individual gamma-ray beams which have passed through various sections of the radiographed material. This method makes it possible to determine the presence of defects in metal ingots, castings, welds, or to detect defective parts of assembled units, etc.

The intensity of the gamma-rays may be measured by registering directly the effects produced by these rays: heat effects, electrical effects (ionisation of gases, induction of electrical current in semiconductors, variation in the electrical conductivity of solid and fluid bodies, photoeffect), physical and chemical effects (film-blackening, appearance of deposits) and luminescence.

Depending upon the technique employed to measure gamma-ray intensity, various methods of flaw detection in metals are used at present, such as: radiography, xeroradiography, ionisation, metal vision techniques and others.

In radiographic inspection the varying intensity of individual gamma-ray beams emerging from the inspected object is registered on a film. Xeroradiography consists in registering intensity with the aid of semiconductors (selenium and other plates). In the ionisation method of inspection, the intensity of individual beams of gamma-radiation is measured by means of gamma-counters or ionisation chambers, while in the metal vision method inspection of metals is carried out with the aid of gamma-radiation image converters and amplifiers, distributed over the plane of radiation fluxes, and also by means of television.

CHAPTER I

RADIOGRAPHIC INSPECTION

§ 1. Fundamentals

The radiographic method of flaw detection in metals is based on the property of gamma-rays to cause blackening of film emulsion. The higher the intensity of the gamma-rays after passage through the radiographed material, that is, the higher the intensity of the gamma-rays falling upon the film, the higher the density of the film exposed to the rays (Fig. 25). The gamma-rays passing through different sections of the inspected article are attenuated to various degrees, depending upon the thickness and density of the particular radiographed section. Fields of varying density form on the film, according to the intensity or the gamma-rays which have passed through the respective sections of the inspected material. The spots on the negative which correspond to sections of the article which have absorbed a smaller fraction of the radiation, as compared with neighbouring spots, will be darker (of a higher optical density). The film image obtained with gamma-rays is called a gamma-graph. The image appearing on the gamma-graph is the projection of the macrostructure of the radiographed metal and of the defects present in the metal. Thus, the gamma-graph depicts the "transparency" to gamma-rays of

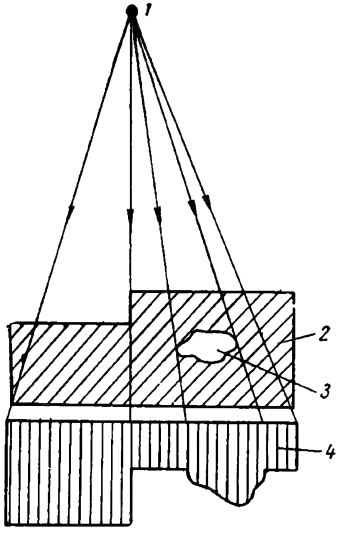

Fig. 25. Heterogeneity of gamma-ray intensity after passage through an inspected object:

1—radiation source; *2*—inspected object; *3*—defect; *4*—diagram of gamma-ray intensity after passage through object

various sections of the inspected article, the blacker spots on the negative corresponding to the more "transparent" sections of the article.

Hence, it follows that both variation in thickness of the radiographed article and nonuniformity in its density, for instance, air and slag inclusions, metallic admixtures of a different density, etc., should appear on the gamma-graphs as fields of different optical density.

The majority of defects common in metals are voids (cavities, blow holes, lack of fusion, cracks in welds, etc.). Naturally, sections of an article in which such defects are present are more "transparent" to gamma-rays than the flawless sections; on gamma-graphs these defects appear as black spots (cavities) or bands and lines (lack of penetration, lack of fusion). However, the defects may be so insignificant in size that the difference in the attenuation of gamma-rays passing through the defective and sound sections would be very small and the exposure of the film to the rays would not yield any visible difference in the density of the image. Gamma-radiography has a certain sensitivity limit, which depends on a number of factors.

§ 2. Photographic materials used in radiography

As already stated above, certain changes occur in photographic emulsion when exposed to gamma-rays. Owing to these changes, an exposed film blackens during development. The photographic emulsion is prepared from the minutest silver-bromide crystals, suspended in a gelatine water solution.* Silver bromide and other silver halogens possess a selective light-absorption property. Only blue, violet and ultra-violet rays of the spectrum actively influence silver bromide. The emulsion is made sensitive to the remaining rays of the spectrum by introducing other components, so-called sensitisers, into the emulsion. The sensitisers absorb these spectrum rays, thus forcing them to react with the silver bromide.

Photographic materials which possess the highest sensitivity to the green and yellow rays of the spectrum are called orthochromatic. Panchromatic materials are sensitive, in addition, to red rays.

Gamma-radiation and visible light affect photographic emulsion in a different manner, owing to the great quantitative difference in gamma-quanta and visible light energies. Incident visible light beams are almost entirely absorbed by the emulsion, i.e., the beams

* The emulsion is poured on to a base bearing a tanned-gelatine sublayer which binds the emulsion firmly to the base, not allowing the emulsion to separate from the base during the processing. Photographic materials such as plates, film and printing paper differ only in the material used as a base. Transparent glass or celluloid are used as a base for plates and film, and paper—for photographic printing paper.

transfer almost all the energy to the emulsion. Both gamma- and X-rays are very poorly absorbed by the emulsion and therefore their photographic action is considerably weaker.

In order to intensify the effect of gamma-rays on photographic film, it is necessary to manufacture the film in a way ensuring absorption of a larger portion of incident gamma-rays. This is achieved by increasing the thickness of the emulsion layer on both sides of the film and by introducing into the emulsion special substances contributing to an increase in gamma-ray absorption.

Usually, gamma-ray as well as X-ray inspection of metals is performed with X-ray film which, unlike the usual photographic film, is double-coated and has a somewhat thicker emulsion layer. When an X-ray film is exposed to gamma-rays, a latent image forms on the emulsion which appears in the course of subsequent processing. The latent image is the result of chemical changes occurring in the grains of silver bromide during the process of gramma-ray absorption. Recoil electrons and photoelectrons form in the film during gamma-ray absorption and scattering. Passing through the emulsion, the electrons ionise the atoms, forming new free electrons on the way. The photoelectrons, recoil electrons and the free electrons formed by the latter possess different energies. The energy of some of them is sufficient to neutralise the positive silver ion of the AgBr grain crystal lattice, transforming it into metallic silver.

Thus, under the influence of gamma-rays, individual atoms of metallic silver form in the emulsion layer of the X-ray film, the number of atoms being determined by the ionisation effect of the given radiation and gamma-ray intensity. The atoms of metallic silver are centres around which the silver bromide is reduced into metallic silver under the influence of the developer. The development proceeds more intensively at spots where there are more of these centres and more metallic silver forms at these spots. The reduced metallic silver causes the blackening of the negative, mainly in spots which have been exposed to a beam of gamma-rays of a higher intensity. The sections less influenced by the gamma-rays contain less metallic silver and therefore develop more slowly. The sections of the film not exposed to gamma-rays would also blacken a little if the developing is carried on for a long time. The difference in the density of the deposited silver creates different blackening of individual sections of the negative. Sections subjected to a stronger gamma-ray influence appear blacker and sections subjected to a weaker influence—lighter.

Developing is a complicated process involving chemical and physicochemical phenomena. It is carried out in dark-red or green-yellow light. To protect the unblackened silver bromide from the effects of daylight or electric light, the developed image is placed in a fixing bath (the fixing process consists of the dissolution of the nondeveloped silver bromide). The fixed negative is rinsed and

only metallic silver is left on it. The processing technique for X-ray film exposed to gamma-rays, the developer and the formulas for fixing, as well as the conditions required for developing, are described in § 6 of this chapter.

The density (degree of blackening) of individual sections of a negative can be determined by examining the negative against passing light. The degree to which the intensity of the visible light is reduced during passage through the negative serves as a measure of the film density. Film density D is generally defined as the common logarithm of the ratio of the intensity L_0 of the light, falling on the film at a certain point, to the intensity L of the light which has passed through the negative at the same point

$$D = \log \frac{L_0}{L}. \tag{35}$$

Thus, a film which attenuates passing light 10 times possesses an optical density of unity, and a film with an optical density of 2 attenuates passing light 100 times, etc. The density of negatives is measured with the aid of special devices—densitometers. Type МФ-2 and МФ-4 microphotometers are widely employed to measure film density.

The measurement of film density with the aid of microphotometers is carried out in passing light, i.e., is determined by the attenuation of the intensity of a passing light beam. Microphotometers make it possible to determine the density of very small sections of an exposed negative. The maximum density which can be measured exactly by means of a microphotometer does not exceed 2.5. It should be mentioned that the density D of a negative measured with the aid of a microphotometer consists of two components: the fog of the X-ray film of a density D_0, and the density traced to absorption of gamma-rays by the X-ray film emulsion D_1, i.e.,

$$D = D_0 + D_1. \tag{36}$$

The fog of the X-ray film is the result of the slow formation of metallic silver which absorbs light passing through the negative while the latter is being developed. In addition, the light passing through the negative is partially absorbed by the base. The fog of high-quality X-ray film should not exceed 0.25.

The density of a negative $D_1 = D - D_0$ caused by the absorption of the gamma-ray energy in the emulsion layer depends on the intensity I of the incident gamma-rays, exposure time t, gamma-ray wavelength λ and the Watkins development factor α. Thus, the density of a negative or the blackening of a gamma-graph is a function of I, λ, t and α:

$$D_1 = f(I \times t \times \lambda \times \alpha). \tag{37}$$

Numerous investigations have shown that the following relationship exists for gamma-rays of a definite wavelength and a con-

stant Watkins development factor:

$$D_1 = c \times I \times t^p, \qquad (38)$$

where: c — the factor of proportionality depending on the gamma-ray energy and the type of film employed;
I — the intensity of the incident gamma-rays;
t — the exposure time;
p — the index which characterises the sensitivity of the film to radiation of a given hardness.

For film densities up to 2.0 the value of p approximates unity. Therefore, for a density D smaller than 2.0 it may be accepted approximately that

$$D_1 \cong c \times I \times t. \qquad (39)$$

In other words, for gamma-radiation of a certain wavelength (energy), the density of a negative is proportional to the product of the gamma-ray intensity multiplied by the exposure time, e.g., is proportional to the energy of the gamma-rays falling on 1 sq cm of film in time t.

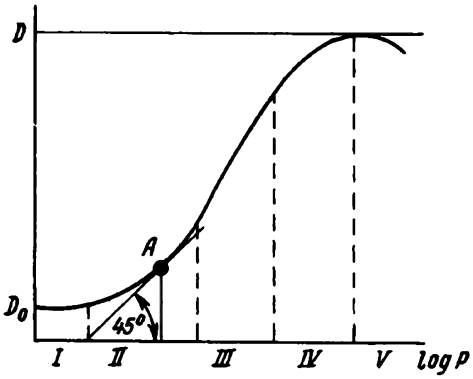

Fig. 26. Typical characteristic curve for roentgen film (in semilog coordinates); radiation dose is plotted along the abscissa and film density—along the ordinate

In so far as the physical radiation dose, which characterises the amount of energy absorbed per unit mass of the irradiated substance, is the principal value which determines the quantity of gamma-radiation, in order to evaluate the quality of film from the point of view of gamma-radiography it is essential to know the relationship existing between the film density and the radiation dose causing this density.

The curves expressing the relationship between the optical density and the radiation dose are called characteristic curves. With a constant radiation dose rate, the characteristic curves express the relationship between density and exposure time. A typical characteristic curve is shown in Fig. 26 (the dose logarithm log P is plotted along the X-axis). Along section I the radiation has practically no influence on the film density, the latter being traced only to the fog of the film. Along section II of the curve the density of the negative increases very slowly as the dose logarithm increases. The straight-line section III of the curve indicates the range in which the highest change in density occurs, depending upon exposure (the radiation dose). Along section IV of the curve the rate at which

density increases with an increase in the radiation dose diminishes; solarisation occurs along section V—density diminishes with the increase in exposure.

The ratio of the increase in the optical density to the increase in exposure is called the film contrast. The slope of the tangent to the characteristic curve at any point serves as the measure of contrast. The absolute value of contrast $\frac{\Delta D}{\Delta \log t}$ is expressed by tan α, i.e., the tangent of the angle of a slope,

$$\frac{\Delta D}{\Delta \log t} = \tan \alpha. \tag{40}$$

The maximum contrast occurs on the straight-line section of the characteristic curve. The tangent of the angle which this straight-line section of the curve forms with the abscissa is called the contrast factor α of roentgen film. The higher the contrast factor, the finer are the defects defined on gamma-graphs, all other conditions being equal.

When operating with gamma-rays of a constant energy, the contrast factor depends on the grade of emulsion and its thickness. For a given difference in the radiation dose to which an X-ray film is exposed, the difference in density increases with the increase in the thickness of the emulsion layer. Therefore, X-ray film is double coated. Films of one and the same grade developed in different developers or in one and the same developer, but for different time intervals, may possess a different contrast factor α.

The factor α is also called the development factor, because α depends not only on the grade of emulsion, but also on the conditions under which the film is processed. The contrast factor of roentgen film exposed to X-rays is 2.5.

As to the minimum difference in the density of contiguous sections perceptible to the eye, it may be assumed, on the basis of a number of investigations, that the difference in densities below $D_1 - D_2 \simeq$ $\simeq 0.02$—0.03 is generally not perceptible to the eye (it is assumed that the border line between adjacent fields is sufficiently sharply defined).

Apart from contrast, the sensitivity of X-ray film is of great importance for gamma-radiography. The sensitivity of X-ray film is expressed in reciprocal roentgens and is equal numerically to the reciprocal value of the radiation dose required to obtain a certain density at the point of the characteristic curve for which $\alpha = 1 =$ $= \tan 45°$. This point is found on the characteristic curve by constructing a tangent to the characteristic curve at a 45° angle to the abscissa. Then, the corresponding dose is read off the abscissa and its reciprocal value is taken.*

* At present this method is used to determine the sensitivity of "Roentgen XX" film produced in the U.S.S.R.

Another important characteristic of roentgen film is the maximum negative density. In factories producing X-ray film such properties as fog density, contrast, sensitivity and the maximum optical density of negatives are determined by the so-called sensitometry process, i.e., a set of operations making it possible to determine the above-mentioned properties of photographic material. For this purpose the films are exposed to X-rays obtained by applying an 80 kv voltage to the tube; then the exposed films are processed, etc. The characteristics obtained in such a way are called the sensitometric characteristics of X-ray film. Sensitometric testing of X-ray film consists in exposing the film to exact doses of roentgen radiation, this being achieved by varying exposure time and maintaining the dose rate constant. Sensitometric testing is performed with the aid of special instruments called sensitometers or sensitesters.

Films obtained in the course of sensitometry are called sensitograms. They have fields of a different optical density. Density D is determined as the function of exposure time by examining the fields of the sensitogram with the aid of a photometer. The obtained data are used to plot characteristic curves, then sensitometric characteristics of X-ray film (sensitivity, contrast factor, fog density, maximum negative density), specified on film labels, are determined.

At present, in the U.S.S.R., two grades of X-ray film are available for industrial radiology: "Roentgen X" and "Roentgen XX".

"Roentgen XX" film is called nonscreen film. The film carries a somewhat thicker emulsion layer to increase absorption of X- and gamma-radiation. "Roentgen X" film is known as a screen film, for its emulsion is specially made sensitive (sensibilised) to the light of fluorescent screens.

To determine film sensitivity expressed in reciprocal roentgens, "Roentgen X" film is irradiated in the presence of intensifying screens and the "Roentgen XX" film—without such screens; therefore, the sensitivity of these films is not comparable. In addition, since 1953, the sensitivity of "Roentgen X" film has been determined by a new method, according to which film sensitivity is equal to the reciprocal of the dose required to obtain a negative density, exceeding the density of inherent fog by 0.75.*

Sensitometric testing of "Roentgen X" film without intensifying screens (under the conditions in which "Roentgen XX" film is exposed to radiation) and employing the method of sensitivity determination used for "Roentgen XX" film shows that "Roentgen X" film possesses a sensitivity equal to 20 reciprocal roentgens, i.e., a sensitivity about 1.5-2.0 times weaker than that of "Roentgen XX" film.

---

* To obtain the sensitivity characteristic of "Roentgen X" film by the previously employed method (still used for "Roentgen XX" film), it is necessary to double the sensitivity specified in the label.

The sensitivity of roentgen film to X-radiation of an energy of about 80 kev, as determined by film manufacturers, does not fully characterise the sensitivity of film to gamma-radiation and may only be used roughly to compare the quality of different grades of film.

The curves in Fig. 27 show the dependence of specific film sensitivity (film density referred to the radiation dose) on the hardness of X-radiation. It follows from these curves that for roentgen radiation of an energy ranging from 80 to 100 kev the specific sensitivity

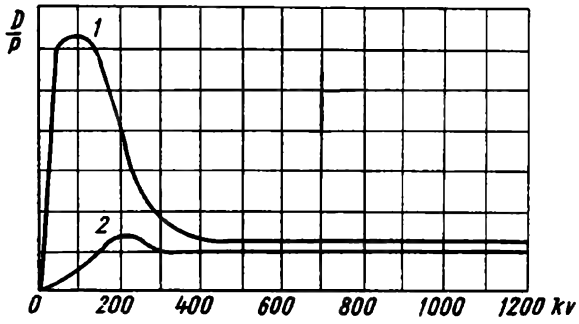

Fig. 27. Dependence of specific film sensitivity (the ratio of film density to radiation dose) on radiation hardness:
1—film without screen; *2*—film covered by a flux flattening screen (1mm Gd)

of X-ray film is the maximum; specific sensitivity diminishes as radiation energy increases to 400 kev, and, finally, sensitivity depends only slightly on radiation energy in the range of 400 to 1,400 kev.

The sensitivity of roentgen film to gamma-radiation emitted by various radioactive isotopes is determined by exposing the film to radiation (as in the case of X-radiation), individual sections of the film being exposed to a number of exactly measured doses of gamma-radiation. This is achieved by varying the exposure time and keeping both source activity and source-film distance, i.e., the physical radiation dose, constant. Individual sections of the developed film possess a different density, and photometric data are employed to plot the characteristic curves for X-ray films exposed to gamma-rays emitted by different radioactive isotopes.

These characteristic curves make it possible to determine the sensitivity of X-ray film to gamma-rays of various energies emitted by the specified radioactive isotopes and also other sensitometric characteristics of film exposed to gamma-radiation. In order to compare the sensitivity of X-ray film to the gamma-radiation emitted by different radioactive isotopes, there is no need to express

film sensitivity in reciprocal roentgens. It is of greater interest to compare the gamma-radiation doses of the various radioactive isotopes required to ensure gamma-graphs of a certain density (a density which would ensure the best detection of defects) or to compare specific film sensitivities to the gamma-rays of various radioactive emitters.

Fig. 28 illustrates the characteristic curves for "Roentgen X" film exposed to gamma-rays from Co^{60}, Cs^{137}, Ir^{192}, $Eu^{152, 154}$, Tu^{170} and Eu^{155} sources, while the graph shown in Fig. 29 characterises the dependence on gamma-radiation energy of the physical radiation dose required to ensure an optical density of 1.5.

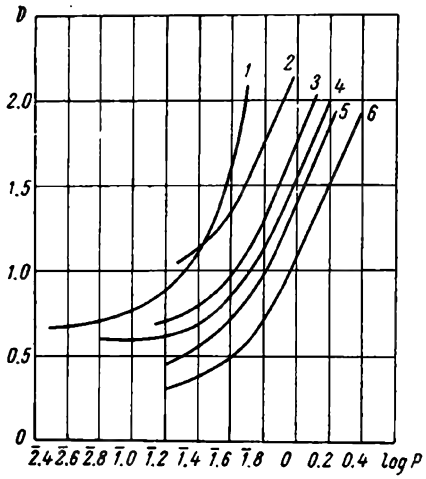

Fig. 28. Characteristic curves for "Roentgen X" film exposed to gamma-rays:
1—Eu^{155}; *2*—Tu^{170}; *3*—Ir^{192}; *4*—$Eu^{152, 154}$; *5*—Cs^{137}; *6*—Co^{60}

From the curves mentioned it can be seen that in exposing film to gamma-radiation of various energies, one and the same film density may be ensured with different physical radiation doses.

For the radioactive isotopes in question, the smaller the gamma-radiation energy, the smaller the physical radiation dose required to ensure a certain film density, i.e., a decrease in the energy of gamma-radiation is accompanied by an increase in film sensitivity to radiation. Thus, radioactive isotopes of different radiation energies, but equivalent in relation to the ionisation effect produced in air (in relation to the radiation doses produced in air), cause a different film density, i.e., a different film ionisation (as mentioned above, film density is a measure of ionisation caused by radiation). Hence, the ionisation constants of various radioactive isotopes for air and film are not equal.

Table 14 lists the ionisation constants of Cs^{137}, Ir^{192}, $Eu^{152, 154}$, Eu^{155} and Tu^{170} for air and "Roentgen X" film in regard to cobalt; thus, the ionisation constant of Co^{60} gamma-rays for air and film is accepted as unity. The relative film ionisation constants given in Table 14 have been determined by means of characteristic curves. From Table 14 it follows that the film relative ionisation constant increases more, the smaller the gamma-ray energy. As compared with air, for Tu^{170} the film relative ionisation constant increases approximately from 4 to 4.5 times, for Ir^{192}—2.35 times, for $Eu^{152, 154}$—1.6 times and for Cs^{137} about 1.5 times.

Table 14

Air and Film Ionisation Constants

Isotopes	Ionisation constant $K\gamma$, r/hr mcurie cm	Ratio of ionisation constant of isotope $K\gamma$ to the ionisation constant of cobalt $K\gamma_{Co^{60}}$	
		air	film
Cobalt-60	13.50	1.0	1.0
Cesium-137	3.55	0.262	0.39
Iridium-192.	2.7	0.2	0.47
Europeum-152, 154 . . .	6.0	0.445	0.71
Thulium-170	0.1	0.0074	0.03
Europeum-155	0.6	0.0445	—

It is exactly for this reason that equal doses of gamma-radiation emitted by isotopes of different radiation energies cause different blackening (density) of the emulsion layer, the blackening being the greater, the smaller the radiation energy. This explains certain specific features of exposure charts (different rise, crossing of curves, etc.) plotted for metals.

Comparing the radiation doses required to produce gamma-graphs of a certain optical density (1.5, for instance), we find that in exposing "Roentgen XX" film to gamma-radiation emitted by Co^{60}, Cs^{137}, Ir^{192}, $Eu^{152, 154}$, Tu^{170} and Eu^{155} sources, the required doses are about half those required for "Roentgen X" film to produce the same optical density.

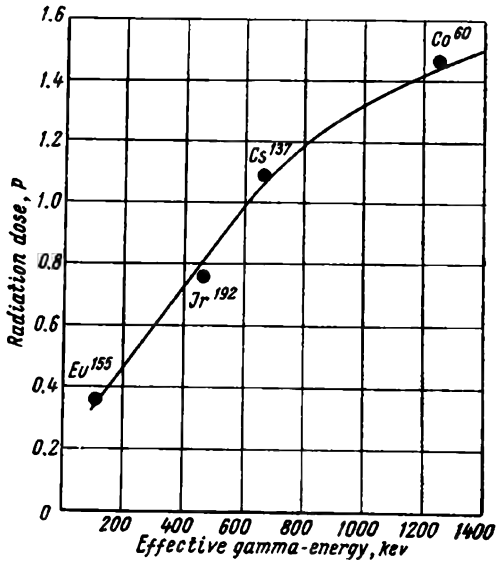

Fig. 29. Dependence of the physical radiation dose required to ensure a film density of 1.5 ("Roentgen X" film) on gamma-ray energy

The quality of the developed image depends not only on sensitometric, but also on other film characteristics, such as grain size and resolution. To the naked eye a developed image appears uniformly black over its entire surface. However, when we examine the negative through a microscope or strong magnifying glass we find

that the blackening consists of individual grains of different size. Grain size depends on a number of factors among which grain size of nondeveloped emulsion, optical density, developer composition and development time are essential. Usually, the initial bromide-silver grains of slow-speed emulsion are smaller than the grains of a high-speed emulsion. The resolving power of a film depends on emulsion grain size. The resolving power of photographic materials is defined as the maximum number of individual lines appearing per 1 mm of optical image, these lines being of a width equal to that of the interval between them. So, the resolving power of "Roentgen X" film is equal to 30-40 lines per 1 mm and for "Roentgen XX" film it is only 20 lines. It should be borne in mind that, although of a high resolving power, fine-grain film possesses a relatively low sensitivity to radiation. Therefore, such film requires longer exposures than coarse-grain film of "Roentgen XX" grade.

§ 3. Exposure time for metals in gamma-radiography

The quality of gamma-graphs and, consequently, the detection of hidden faults in metals depend to a considerable degree on the density of the image. A number of investigations has shown that flaw detection by means of gamma-radiography of metals proves most successful if the density of the produced gamma-graphs ranges from 1.4 to 2.0. The revealment of defects on gamma-images deteriorates if optical density is either increased or diminished. Thus, in the gamma-radiography of metal, it is necessary to select the exposures required to secure gamma-graphs of a density ensuring the best revealment of defects.

As mentioned above, the density of a gamma-graph depends on gamma-radiation intensity I, exposure time t, gamma-ray wavelength λ, properties of the given film and its development factors α.

$$D = f(I, t, \lambda, \alpha).$$

The intensity of the gamma-radiation to which the film is exposed depends on the energy of the gamma-rays, radioactive isotope activity, yield of gamma-quanta per disintegration, film-source distance (focal distance), thickness of the radiographed metal and the linear absorption coefficient. The latter, in turn, depends on gamma-ray energy and thickness and the density of the radiographed metal. In addition, gamma-ray energy, radioactive source activity, the yield of gamma-quanta per disintegration and film-source distance determine the intensity of gamma-radiation I_0 irrespective of the attenuation layer. The thickness of the radiographed metal and its gamma-ray linear absorption coefficient determine the attenuation of radiation intensity by the inspected metal. Many sources are not monochromatic in relation to gamma-radiation energy and emit soft components in addition to hard gamma-radia-

tion. The soft components of the gamma-spectrum are absorbed, as the thickness of the inspected metal increases, and the hardness of the radiation which has passed through the metal increases. In this connection for most radioactive isotopes the linear absorption coefficients for a broad gamma-beam depend to a considerable degree upon the thickness of radiographed metals (see Figs. 21-23).

In gamma-radiography objects are usually inspected not by a narrow parallel beam, but by a broad divergent beam. In this case the gamma-ray linear absorption coefficients depend on beam width. The narrower the beam, the smaller the number of scattered gamma-quanta added to the initial gamma-beam as the beam passes through the metal, and the larger the absorption coefficient μ_{br}. Consequently, exposure time increases with the decrease in gamma-beam width, all other conditions being equal.

Thus, for a given radioactive isotope and roentgen film of a given grade exposure time increases with the increase in the thickness and density of the examined metal object, the activity of the radioactive source and film-source distance being constant.

The exposure time chosen when gamma-radiography is performed with the aid of various radioactive isotopes (isotope activity and film-source distance being maintained constant) depends on the energy of the gamma-radiation which determines both the film sensitivity and the gamma-ray linear absorption coefficient.

In practice, exposure time is determined with the aid of exposure charts plotted on the basis of experimental data.

In order to plot exposure charts, steel, titanium, duralumin and magnesium plates of different thickness are exposed to gamma-radiation emitted by different radioactive isotopes at different film-source distances. The data obtained by studying the gamma-graphs with the aid of a photometer are used to plot curves expressing the dependence on exposure time of the density of the gamma-graphs, i.e., characteristic curves for the given grade of film (Fig. 30).

The characteristic curves are employed to determine the exposure time required to ensure gamma-images of the optimal density. The optimal density for gamma-graphs is fixed at 1.5-1.7, since defects appear best on gamma-graphs at the optimal density from 1.4 to 2.0, and it is necessary to ensure maximum efficiency of inspection.

Metal intensifying screens. In order to cut down exposure time, metal foils are used as intensifying screens in gamma-radiography. The intensifying effect produced by the foils is caused by the photoelectrons freed from the foil by gamma-rays. The photoelectrons are absorbed by the silver-bromide layer and bring about a photochemical reaction, in addition to that caused by the gamma-rays. Not all the freed photoelectrons possessing a certain kinetic energy reach the film. The path of photoelectrons (depth of penetration into the foil) depends on the energy of the gamma-radiation.

The path of the photoelectrons ejected from the lead foil by gamma-quanta of an energy E expressed in Mev can be calculated from the following approximate equations:

$$R\,\text{mm} = \frac{0.407}{10\rho} \times E^{1,38} \text{ for } 0.15 < E < 0.8 \text{ Mev}, \tag{41}$$

$$R\,\text{mm} = \frac{0.667}{10\rho} \times E^{1,67} \text{ for } 0.05 < E < 0.15 \text{ Mev}, \tag{42}$$

where ρ is the density of the inspected material.

For X-radiation of an energy equal to 350 kv the path of the photoelectrons in lead is about 0.06 mm and 0.18 mm at an energy

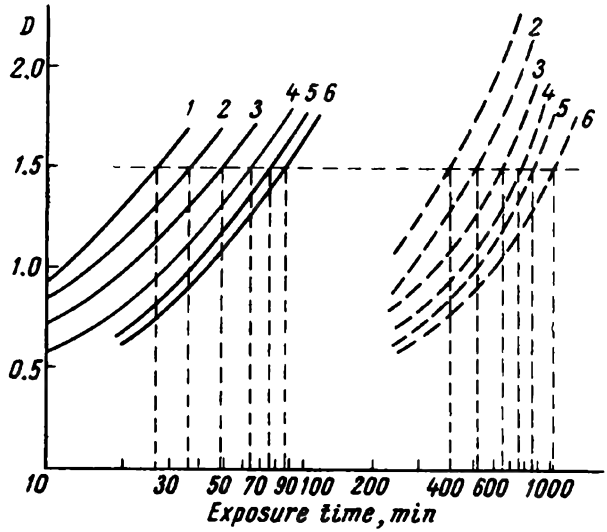

Fig. 30. Characteristic curves for "Roentgen X" film plotted on data obtained in inspecting steel with gamma-rays from a 0.16 gram radium equivalent Tu^{170} source (film is placed between lead foils 0.05 mm thick):

1—1 mm; *2*—2 mm; *3*—4 mm; *4*—6 mm; *5*—8 mm; *6*—10 mm; $F = 25$ cm—continuous lines; $F = 50$ cm—dotted lines

of 700 kv. Table 15 lists the path of the photoelectrons in lead for gamma-rays emitted by Ir^{192} and Cs^{137} sources at a back scattering angle of 180° calculated by means of equations (41) and (42).

The attenuation of intensity of hard gamma-radiation in thin foils is insignificant (about 1.5%), if the optimal foil thickness is equal to the electron path. In such foils the ejected electrons reach the opposite surface. Any decrease in foil thickness diminishes the gamma-quanta-photoelectron transformation efficiency. The X-ray spectrum is continuous and the isotope gamma-spectrum, discontinuous. Since in this case the spectrum varies as the gamma-rays

penetrate into the foil, the intensity of softer components becomes attenuated to a greater extent, as the thickness of the material is increased. Therefore, the optimum foil thickness must be determined according to the harder gamma-quanta components.

Table 15

Ejected Electron Path in Lead for Ir^{192} and Cs^{137}

Source	Gamma-quanta energy, Mev	Photoelectron energy, Mev	Photo-electron path, mm × 10⁻³	Compton 180° scattering, Mev	180° photo-electron energy, Mev	Photo-electron path, mm × 10⁻³
Ir^{192}	0.610	0.525	150	0.180	0.95	10
	0.468	0.380	100	0.165	0.80	10
	0.316	0.230	45	0.140	0.55	5
	0.295	0.215	40	0.140	0.50	5
	0.136	0.150	20	0.090	—	—
Cs^{137}	0.661	0.575	170	0.190	0 105	12

The intensifying effect of metal foils* depends on the material of which the foil is made, its thickness and radiation energy. Electron formation occurs most intensively in materials of a high Z, i.e., in materials which absorb gamma-rays intensively. Thus, lead foils possess a considerable advantage over light-metal foils (aluminium foils, for instance), for in them gamma-rays free a greater number of electrons.

For a given gamma-ray energy the number of electrons passing from a thin foil to the film is not great. With an increase in foil thickness the number of electrons reaching the film grows to a certain magnitude and then remains practically constant. But an increase in foil thickness is accompanied by greater gamma-ray attenuation; as a result a smaller number of electrons forms in the layers nearest to the film and the intensifying effect of the foil diminishes. Thus, the maximum effect is gained with foils of a certain thickness, this being very essential for soft gamma-emitting isotopes. It has been shown by experiment that it is of no advantage to use heavy-metal foils as intensifying screens for X-ray inspection, if the voltage applied to the tube is below 60-70 kv, for no appreciable reduction in the exposure time is possible with such a voltage. The energy of photoelectrons produced by such X-radiation is small and, therefore, only a small number of the photoelectrons reaches the film. In addition, the primary X-ray beam is so "soft" that it is attenuated to a considerable degree in the first layers of the foil.

* The intensification factor of a screen (metal foils or fluorescent screens) is the ratio of the exposure time without an intensifying screen to the exposure time with an intensifying screen.

Attenuation of gamma-radiation due to photoelectric absorption diminishes sharply with the increase in gamma-energy and reaches a minimum at an energy ranging from 2 to 3 Mev. Attenuation of gamma-radiation due to scattering, which is the most important kind of attenuation of such energies, depends to a lesser degree on the atomic number of the radiographed material. Consequently, with an increase in the gamma-ray energy, the difference in the intensifying effects of lead and substances of smaller atomic numbers diminishes greatly. For gamma-quanta energies exceeding 2-3 Mev the number of electron-positron pairs formed as the gamma-rays pass through matter increases greatly. This process of pair production depends upon the atomic number of the radiographed metal. In this connection the difference in the intensifying effect of lead foil and foils made of metals of a smaller atomic number Z increases again at the specified energy level.

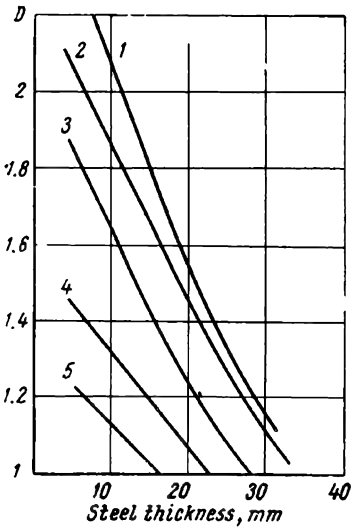

Fig. 31. Characteristic curves for fine-grain films exposed to Cs^{137} gamma-rays with different combinations of lead foils of different thicknesses. Exposure time constant:
1 150 (front) + 150 (rear); *2* 20 (front) + 150 (rear); *3* 150 (rear); *4*—150 (front); *5*—20 (front)

The emission of photoelectrons from the front and rear foils (in the direction of the inspection) produces an intensifying effect on the film. An increase in radiation hardness is accompanied by an increase in the quantity of scattered radiation. As the back scattered rays possess a smaller energy, the path of the electrons ejected by these rays is also shorter; nevertheless, these electrons contribute to film blackening.

The intensifying effect of lead foils was investigated during the radiographing of steel on fine-grain roentgen film with the aid of Ir^{192} and Cs^{137} gamma-sources and foils 20 and 150 microns thick. The foils were used as an intensifying screen in the following way: first, only a front foil; then, only a rear foil; then, a front and a rear foil together. The rear foil caused a higher film density when a steel plate 23 mm thick was exposed to gamma-radiation from a Cs^{137} source. The data given in Table 16 and the graph in Fig. 31, show the effect of foil thickness on both film density and exposure time, depending on the thickness of the radiographed steel.

Experimental data from investigations conducted to compare the intensifying effect of lead and tin foils (from 0.02 to 0.2 mm thick) in radiographing steel, titanium, aluminium and manganese alloys

with Co^{60}, Cs^{137}, Ir^{192}, $Eu^{152, 154}$, Tu^{170} and other gamma-sources, are given below. Steel, titanium, duralumin and magnesium plates of various thickness were radiographed at a constant film-source distance and with different exposure times, using "Roentgen X" film placed between lead and tin foils of a different thickness. The films were developed under similar conditions and studied with the

Table 16

Exposures, in Curie/hrs, Obtained with Lead Foil Pairs 20 and 150 Microns Thick

Radiation source	Steel thickness, mm	Foils				Saving in time, %
		front 20 microns	rear 20 microns	front 150 microns	rear 150 microns	
Ir^{192}	10	1.5		2.2		20
	20	2.2		1.75		20
	40	5.0		4.0		20
	60	11.0		8.8		20
Cs^{137}	10	1.1		0.8		27
	20	1.6		1.1		31
	40	3.2		1.9		41
	60	6.5		3.4		48
	80	13.0		6.1		53
	100	26.4		10.8		60

aid of a photometer. The photometry results were used to plot characteristic curves (Fig. 32) expressing the relation between the density of gamma-graphs and exposure time for metal objects of different thicknesses and different foils. The curves made it possible to determine the exposure time required to obtain gamma-graphs with an optical density of 1.5 under various conditions, the reduction in exposure time owing to the employment of metal foils being calculated.

The use of a front lead foil from 0.05 to 0.2 mm thick in radiographing metals with a Co^{60} source does not allow any essential reduction in exposure time. In this case the intensification factor of lead foils is about 2. A further increase in foil thickness to 0.4 mm results in a somewhat smaller reduction in exposure time. A change in the thickness of the rear foil from 0.05 to 0.5 mm hardly affects the exposure time. As it is not convenient to employ lead foils less than 0.1 mm thick (these foils crumple and wear rapidly) for metal gamma-radiography with Co^{60} sources, the use is recommended of a front lead foil 0.1 to 0.2 mm thick and a rear foil—0.2 to 0.5 mm thick.

When using Cs^{137}, Ir^{192} and $Eu^{152, 154}$ gamma-sources to inspect metals, the maximum reduction in exposure is gained with a front lead foil 0.05-0.15 mm thick. The intensification factor of lead foils of specified thickness in radiographing steel, titanium and duralumin, using "Roentgen X" film and Cs^{137}, Ir^{192} and $Eu^{152, 154}$ gamma-sources, is approximately 2.0-3.0. A rear lead foil 0.05 to 0.5 mm thick similar to that in the case of a Co^{60} source does not appreciably affect the exposure time.

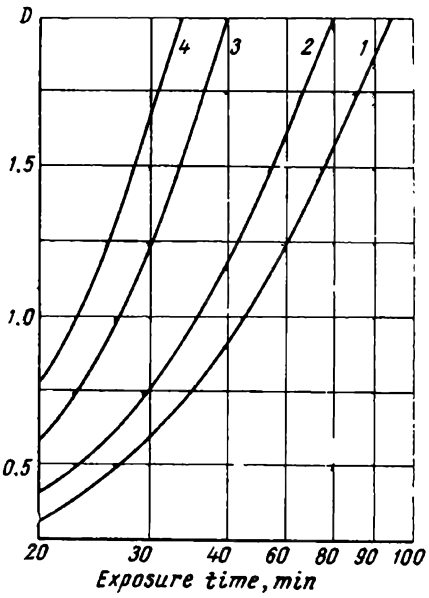

Fig. 32. Characteristic curves for "Roentgen X" film used with lead foils of different thicknesses to radiograph magnesium with gamma-rays from a 0.160 gram radium equivalent Tu^{170} source, $F = 25$ cm, magnesium thickness—30 mm:
1—without lead foils; *2*—lead foils 0.2/0.2 mm thick; *3*—lead foils 0.05 mm thick; *4*—lead foils 0.02/0.02 mm thick

Therefore, with Cs^{137}, Ir^{192} and $Eu^{152, 154}$ gamma-sources it is necessary to employ a front lead foil 0.1-0.15 mm thick and a rear foil—0.2 mm thick (0.1/0.2 mm; 0.15/0.2 mm).

The intensification factor of lead foils depends on the thickness of the inspected metal and the nature of the radiation source. Thus, for example, in the case of a Cs^{137} source (monoenergetic source) the intensification factor augments with the increase in the thickness of the radiographed metal, and the intensification factor diminishes in the case of polyenergetic sources Ir^{192} and $Eu^{152, 154}$ (Table 17). This phenomenon is traced to a change in the gamma-spectrum as the rays pass through the metal: gamma-radiation from monoenergetic sources becomes softer, as a result of scattering; and radiation from polyenergetic sources—harder, owing to the absorption of soft gamma-spectrum components.

The intensifying action of lead foils is most effective with Eu^{155} and Tu^{170} gamma-sources (as compared with other isotopes) and depends on the foil thickness, because a considerable amount of the soft radiation emitted by these sources is absorbed by the lead.

When using Tu^{170} and Eu^{155} radioactive sources in metal inspection, the maximum reduction in exposure time is obtained with a front lead foil 0.02 mm thick. An increase in foil thickness is accompanied by a considerable drop in the intensifying effect; with a front foil 0.2 mm thick there is practically no reduction in exposure time.

Table 17

Dependence of Lead Foil Intensification Factor on the Thickness of Inspected Metal

Steel thickness, mm	Intensification factor of lead foils: front 0.1 mm thick rear 0.2 mm thick		Steel thickness, mm	Intensification factor of lead foils: front 0.1 mm thick rear 0.2 mm thick	
	Cs^{137}	Ir^{192}		Cs^{137}	Ir^{192}
1-5	2.25	3.1	25	2.7	2.7
10	2.4	3.0	30	2.8	2.5
15	2.5	3.0	40	2.9	2.5
20	2.7	2.7	50	3.0	2.5

Table 18 shows the intensification factors for lead foils used in various combinations in radiographing steel 2 to 15 mm thick, employing Tu^{170}, Eu^{155} gamma-sources and grade "Roentgen X" film (in the specified thickness range, the intensification factors only slightly depend on the metal thickness).

Table 18 shows that to reduce the exposure time in radiographing metal with Tu^{170} and Eu^{155} gamma-sources it is advisable to use lead foils of the following thickness: front—0.02 to 0.05mm, rear—0.05 to 0.1 mm. For this combination of lead foils and "Roentgen X" film, the intensifying factor is 2.0. As lead foils 0.02 mm thick are inconvenient in practical work, lead foils of the following thickness are generally employed with Tu^{170} and Eu^{155} sources: front—0.05 mm thick; rear—0.1 mm thick (0.05/0.1 mm).

Table 18

Intensification Factors for Various Combinations of Lead Foils Used to Inspect Steel 2-15 mm thick

Lead foil thickness, mm		Intensification factor	Lead foil thickness, mm		Intensification factor
front	rear		front	rear	
Without foils	—	1	0.05	0.05	1.75
0.02	0.02	2.02	0.05	0.1	1.75
0.02	0.05	2	0.2	0.1	1.15
0.02	0.1	2	0.2	0.2	1.15

Fluorescent intensifying screens. The fluorescent screen used to reduce exposure time in gamma-radiography of metals is a thin cardboard sheet, one side of which is coated with a layer of luminofor—a substance which glows under the influence of gamma-rays.

At present several inorganic luminofors are known, among them: zinc sulphide ZnS, cadmium sulphide CdS with copper and silver activators, zinc and cadmium silicates with manganese activators, alkali earth tungstates, e.g., calcium tungstate ($CaWO_4$) and double salts of the BaPt $(CN_4) \times 4H_2O$ type.

The intensifying effect of a fluorescent screen consists in the influence on the film of the additional glow appearing in the presence of gamma-rays. For intensifying screens luminofors are selected on the basis of their luminescent spectra. A luminofor spectrum may contain visible light, ultra-violet and infra-red components. In metal radiography, screens intended to reduce exposure time should emit a glow to which the film is highly sensitive. Screens needed for visual observation should luminesce in the region of the spectrum best perceptible to the human eye, i.e., emit yellow-green beams of the visible spectrum.

At present, calcium-tungstate screens are most widely used as intensifying screens in gamma-radiography. These screens possess a low visible luminescence, but their luminescent spectrum is most suitable for roentgen film.

The most important characteristic of the intensifying screen is the intensification factor, which shows how many times the exposure time, required to ensure a certain film density when operating without a screen, is longer than the exposure time required to obtain a gamma-graph of the same density with an intensifying screen.

Generally, two screens are used with double-coated roentgen film, both sides of the film being placed in close contact with the sensitive layers of the screen.

There are several types of fluorescent screens, depending on the weight of the luminescent layer (coating weight). Investigations have shown that screens with coating weights of 120, 160, 300 and 400 mg/sq cm (using a front and rear screen of similar thickness) provide almost the same intensifying effect. Screens with a coating weight of 300 and 400 mg/sq cm are very inconvenient in operation, for the luminescent layer of these screens is excessively brittle and cracks rapidly.

At present radiography with hard and medium-hard gamma-radiation is carried out with a combination of two fluorescent screens, each having a 120 mg/sq cm coating weight; screens used with sources of soft gamma-radiation have a fluorescent coating weight of 60 mg/sq cm. A combination of two screens with a coating weight of 40 and 120 mg/sq cm is also used sometimes. When a combination of two screens of a different coating weight is employed, the screen of the smaller coating weight is arranged at the front in the direction of the gamma-raying. These screen combinations may serve for a long time, provided they are handled and stored with care. The intensifying effect of fluorescent screens depends on the hardness of the gamma-rays, the roentgen film quality and gamma-graph density.

Table 19 shows the intensification factors for Soviet-made tungstate fluorescent screens with a 40/120 mg/sq cm coating weight, used to inspect steel with gamma-rays from Co^{60}, Cs^{137}, Ir^{192} and Tu^{170} sources, employing grade "Roentgen X" film.

Table 19

Intensification Factors of Tungstate Fluorescent Screens for Steel Radiography

Steel thickness, mm	Intensification factor			
	Co^{60}	Cs^{137}	Ir^{192}	Tu^{170}
No material	5	7.5	10.0	6
10	5	9.2	9.5	6
25	5-6	10.0	10.0	—
50	5-6	10.0	10.0	—

The nonscreen "Roentgen XX" film is not sensitive to the light emitted by fluorescent screens; therefore, when employed with film of this grade, the intensification factors of fluorescent screens are about one half of those obtained in using such screens with grade "Roentgen X" film. Figs. 33 and 34 show the characteristic curves for "Roentgen X" and "Roentgen XX" film exposed to gamma-radiation to inspect steel with the $Eu^{152, 154}$ radioactive source.

Hence, the intensification factor or the relative reduction of exposure time gained with fluorescent screens increases with the fall in gamma-energy, the increase being about 1.5 to 2.0 times larger for Cs^{137} and Ir^{192} sources, as compared with a Co^{60} source. The Tu^{170} isotope is an exception. The intensification factors of screens when used with a Tu^{170} source are smaller than in the case of Cs^{137} and Co^{60} gamma-sources, which may be explained by the fact that the fluorescent coating of the screen absorbs a considerable amount of soft gamma-radiation emitted by thulium.

Some authors cite larger intensification factors for fluorescent screens, then those given in Table 19. Thus, for instance, according to L. K. Tatochenko and S. V. Medvedev, the intensification factor of fluorescent screens used with "Roentgen X" film and an Ir^{192} source to radiograph 70 and 15 mm steel is respectively 12 and 29.

It should be borne in mind that fluorescent screens diminish image definition. For large defects this deterioration in definition is practically imperceptible; small defects (narrow cracks, lack of fusion, etc.) show up even less clearly with fluorescent screens than with lead foils.

The poorer image definition obtained with fluorescent screens may be traced to the following causes: firstly, the grains of the screen coating are larger than the film grains; secondly, the screen is not

in close enough contact with the film, this resulting in additional scattering of luminescent light. The effect of light scattering is the more important, the larger the screen coating grains.

This is the reason why fluorescent screens are relatively rarely used in industrial radiography. Lead and tin foils have found a wider application in gamma-inspection of metal articles.

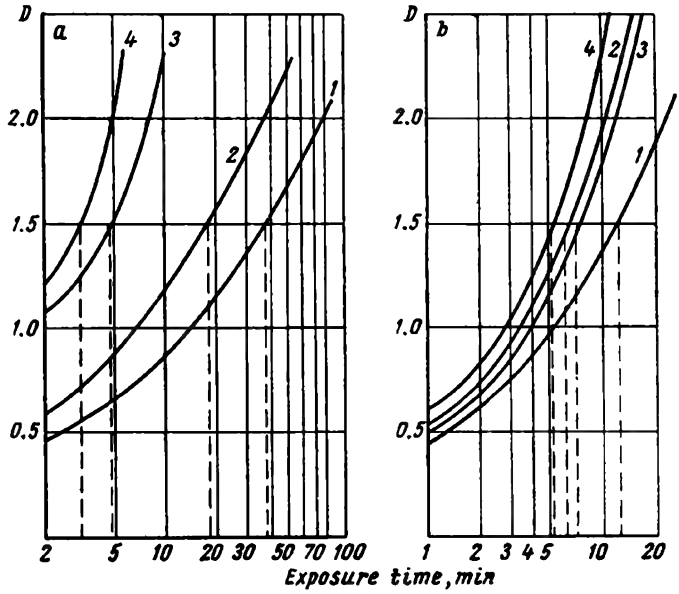

Fig. 33. Characteristic curves for "Roentgen X" (a) and "Roentgen XX" (b) films exposed to gamma-rays from a 0.55 gram radium equivalent $Eu^{152,154}$ source ($F = 50$ cm):
1—without foils and screens; *2*—with lead foils 0.1/0.2 mm thick; *3*—with fluorescent screens (coating weight is 40/120 mg/sq cm) and lead foils 0.1/0.2 mm thick; *4*—with fluorescent screens (coating weight is 40/120 mg/sq cm)

Exposure charts. In gamma-radiography exposure is usually expressed as the product of the source strength in curies or in gram radium equivalent multiplied by exposure time in hours or minutes. Knowing the radiation dose emitted by a source of 1 curie, the exposure, expressed in curie-hours, can be represented in gram radium equivalent-hours and vice versa. Thus, for instance, in regard to the gamma-radiation dose, 1 curie cesium source is equivalent to 0.48 gram of radium. Hence, when using a Cs^{137} source, the exposure expressed in curie-hours may be converted into gram radium equivalent-hours by multiplying the latter by 0.48.

Soft gamma-sources Tu^{170} and Eu^{155} are an exception. Owing to self-absorption, the relation for these sources between the strength of a source expressed in curies and in gram radium equivalent is not

constant and depends upon source weight and geometry. Hence, for Tu^{170} and Eu^{155} sources it is more correct to express exposure in gram radium equivalent-hours.

This is also true to a large extent of other radioactive isotopes, for source strength expressed in gram radium equivalent characterises the radiation dose to which the film is exposed more fully.

The exposure charts for Co^{60}, Ir^{192}, Cs^{137}, $Eu^{152, 154}$, Ce^{75}, Tu^{170} and Eu^{155} sources, used to radiograph steel articles with "Roentgen X" film at a 50 cm film-source distance are shown in Fig. 35.

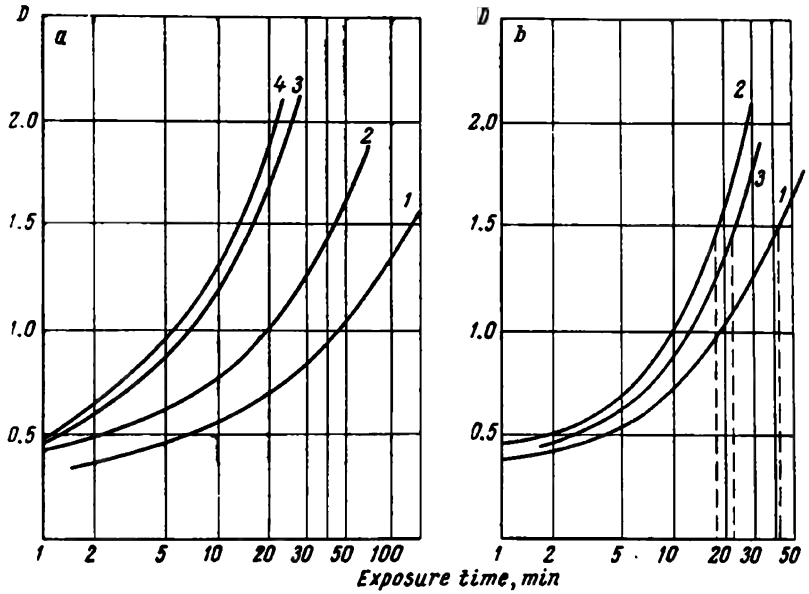

Fig. 34. Characteristic curves for "Roentgen X" (a) and "Roentgen XX" (b) films used to radiograph steel with gamma-rays from a 0.55 gram radium equivalent $Eu^{152,154}$ source (F = 50 cm, steel thickness—25 mm):
1—without foils and screens; *2*—with lead foils 0.1/0.2 mm thick; *3*—with fluorescent screens (coating weight—40/120 mg/sq cm) and lead foils 0.1/0.2 mm thick; *4*—with fluorescent screens

From the chart it follows that in radiographing thin metal articles, all other conditions being equal, the exposure time is the shorter the smaller the gamma-energy, and vice versa, for thick metal articles the exposure time increases with the fall in gamma-energy; with low gamma-energies the exposure time increases with the metal thickness at a higher rate. This explains the different slope and crossing of exposure curves plotted for various radioactive isotopes of a different radiation energy. The exposure curves for Tu^{170} and Eu^{155} sources show a steep rise for relatively small thicknesses of inspected metal and a more gradual rise with an increase in metal thickness.

This phenomenon may be explained as follows. If all inspection conditions in regard to film, foils, screens, and focal distance remain unchanged, and the film development factor and the source strength are kept constant, the exposure time required to secure gammagraphs of a constant density depends only on the energy of the gamma-radiation striking the film. The latter depends upon gamma-attenuation and the sensitivity of the film to gamma-radiation.

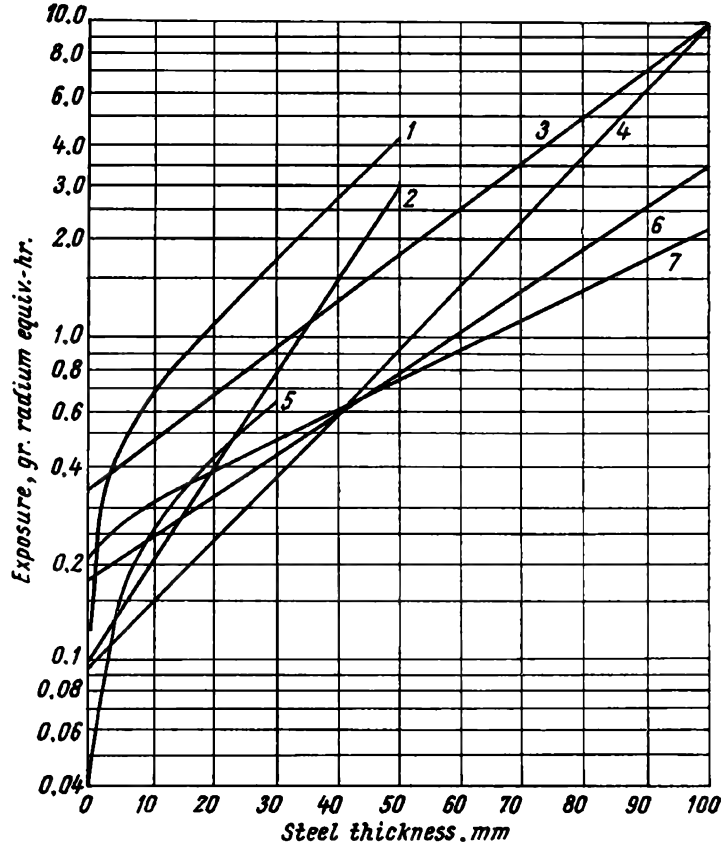

Fig. 35. Exposure curves for steel examined with gamma-rays (F = 50 cm; "Roentgen X" film; D = 1.5):

1—Tu^{170} (Pb = 0.05/0.05 mm); *2*—Ce^{75} (Pb = 0.1/0.2 mm); *3*—Co^{60} (Pb = 0.2/0.2 mm); *4*—Ir^{192} (Pb = 0.2/0.2 mm); *5*—Eu^{155} (Pb = 0.05/0,05 mm); *6*—Cs^{137} (Pb = 0.2/0.2 mm); *7*—$Eu^{152, 154}$ (Pb = 0.2/0.2 mm)

Consequently, if there is no attenuating layer, and also in the case of thin metal articles where gamma-attenuation is low, film sensitivity to the given gamma-radiation is the principal factor determining exposure time.

Accordingly, in radiographing thin metal articles, the exposure time is the shorter the higher the ionisation action produced by gamma-radiation on the film, i.e., the smaller the gamma-energy at equal isotope strength expressed in gram radium equivalent and, therefore, at an equal ionisation caused by radiation in the air (see Fig. 28 and Table 14). Besides, the sensitivity of film to gamma-radiation, for thick metal articles exposure time depends on the linear absorption coefficient of the inspected metal, because gamma-rays become attenuated with an increase in metal thickness. The rate at which exposure time increases is the higher, the greater the linear absorption coefficient for the given metal, i.e., the lower the gamma-energy. Thus, as the Ir^{192} spectrum contains soft components to which X-ray film is very susceptible, considerably shorter exposures are required when an Ir^{192} source is used to radiograph steel up to 40 mm thick and duralumin up to 80-85 mm thick, as compared with a Cs^{137} source, notwithstanding the fact that radiation from an Ir^{192} source is attenuated to a considerably greater extent than Cs^{137} radiation. But with an increase in the thickness of the inspected article the soft components of the Ir^{192} spectrum become absorbed and in this case the total intensity of radiation which passes through the metal is considerably smaller than with a Cs^{137} source; as a result for steel articles over 40 mm thick and duralumin articles more than 80-85 mm thick longer exposures are required with an Ir^{192} source, as compared with a Cs^{137} isotope. This explains the intersection of the exposure curves plotted for Cs^{137} and Ir^{192} sources (see Fig. 35).

The exposure curves for Tu^{170} and Cs^{137} also intersect. Owing to the abrupt attenuation of Tu^{170} radiation, for this source, exposures for steel 1 mm thick (and duralumin 13 mm thick) are longer than in the case of a Cs^{137} source, although the film is more susceptible to Tu^{170} radiation (see Fig. 28).

Intersection of the exposure curves plotted for Tu^{170} and Ir^{192} sources when used for the inspection of steel is to be expected. Yet no such intersection is observed, this being probably the result of using lead foils, the presence of which with a Tu^{170} source, as distinct from Ir^{192}, brings about a definite fall in intensity and a change in the radiation spectrum.

In the exposure chart* plotted for Cs^{137}, Ir^{192}, $Eu^{152, 154}$, Tu^{170}, Eu^{155} and Ce^{144} sources and shown in Fig. 36, the exposure is expressed in curie-hours.** The difference in the curves is traced to different gamma-energy and different yield of gamma-quanta per disintegration. This becomes especially clear when the exposure curves plotted for Tu^{170} and Eu^{155} sources are examined. Thus, in inspect-

* This chart may be used to determine the exposure time for Tu^{170} and Eu^{155} gamma-sources only when there is practically no self-absorption, i.e., when the used sources are small in size and possess a high specific activity.

** The Ce^{144} source employed was enclosed in a steel capsule 0.15-0.2 mm thick through which hard beta-radiation passes, in addition to gamma-radiation,

ing steel with a Eu^{155} source, the exposure, in curie-hours, required to obtain gamma-graphs with a density of 1.5 is considerably smaller than that required with a Tu^{170} source, although these two sources

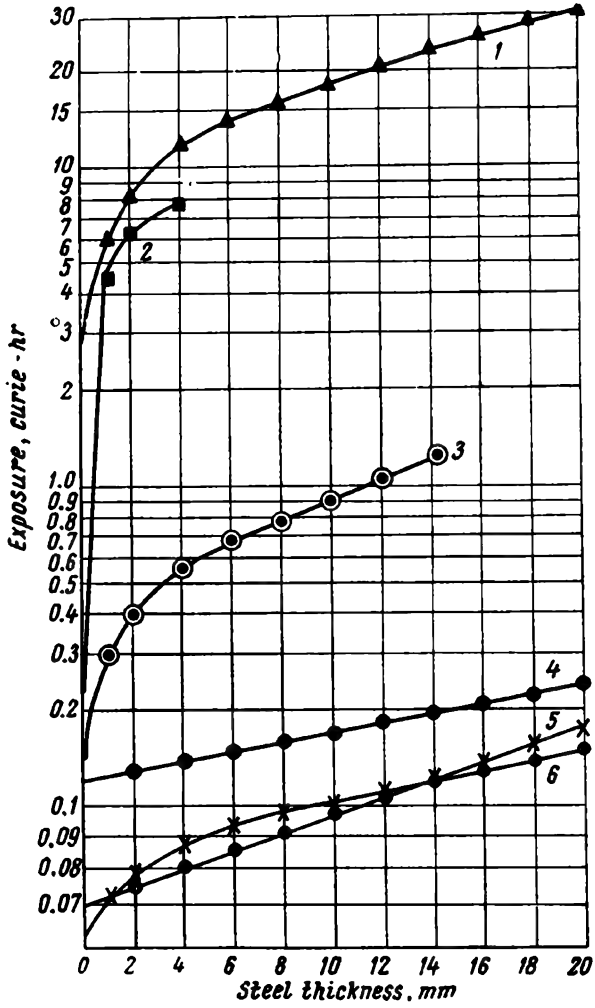

Fig. 36. Exposure curves for steel examined with gamma-rays ($F = 50$ cm; "Roentgen X" film; $D = 1.5$; film is placed between lead foils 0.1/0.2 mm thick):
1—Tu^{170}; *2*—Ce^{144}; *3*—Eu^{155} (film is placed between lead foils 0.05 mm thick); *4*—Cs^{137}; *5*—Ir^{192}; *6*—$Eu^{152,\ 154}$

emit gamma-radiation of about equal energy. This is explained mainly by the difference in the yield of gamma-quanta per disintegration. Tu^{170} yields only 25 gamma-quanta per 100 disintegrations and its ionisation constant is 0.12-0.039 r/hr mcurie cm, while the Eu^{155}

source emits 180 gamma-quanta per 100 disintegrations, and, as a result, the ionisation constant of this source is approximately 0.65 r/hr mcurie cm.

As the Tu^{170} source emits radiation of a low energy and its yield of gamma-quanta per disintegration (K_γ) is low as well, high-activity Tu^{170} sources are required to ensure efficient inspection (of the order of hundreds of curies, this amounting to 2-3 gram radium

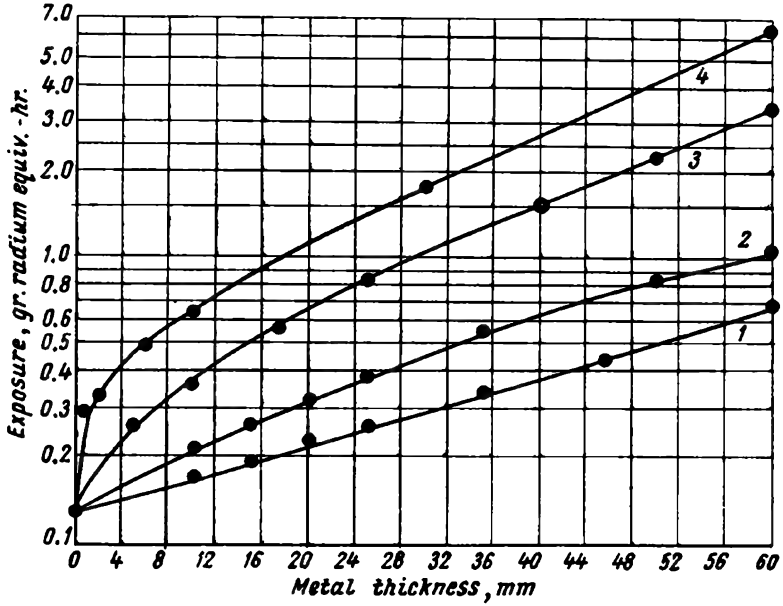

Fig. 37. Exposure curves for steel, titanium, aluminium and magnesium alloys examined with gamma-rays from a Tu^{170} source (F = 50 cm; D = 1.5; "Roentgen X" film is placed between lead foils 0.05 mm thick):

1—magnesium alloys; *2*—aluminium alloys; *3*—titanium alloys; *4*—steel

equivalent). On the other hand, owing to the high yield of gamma-quanta there is no need to use Eu^{155} sources of such high activity, in spite of the soft radiation emitted by this isotope.

Sources of an activity of the order of tens of curies ensure a sufficiently efficient inspection.

Under conditions of constant gamma-energy, source activity (expressed in gram radium equivalent), film-source distance and mode of development, and with the use of similar film and screens, the exposure time depends on the thickness and density of the inspected article (or, which is more correct, on the thickness of the article and linear absorption coefficient of the inspected metal).

From the curves shown in Figs. 35-38 it can be seen that isotopes producing soft gamma-radiation (Tu^{170} and Eu^{155}) may be employed

for the inspection of thin steel articles and articles made from light alloys. Radioactive isotopes emitting medium and hard gamma-radiation are most suitable for the inspection of medium thick and thick articles.

The exposure time for steel, titanium, aluminium and magnesium alloys, can be easily read off exposure charts plotted for Co^{60}, Cs^{137}, Ir^{192}, $Eu^{152, 154}$, Se^{75}, Tu^{170} and Eu^{155} sources and shown in Figs. 39-54, the inspection being carried out with "Roentgen X" film placed between two lead foils with various film-source distances.

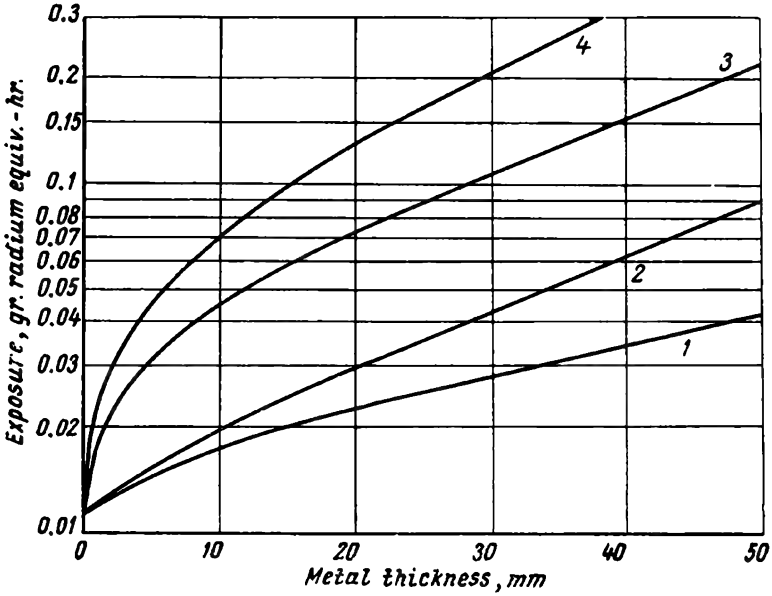

Fig. 38. Exposure curves for steel, titanium, aluminium and magnesium alloys examined with gamma-rays from a Eu^{155} source (F = 25 cm; D = 1.5; "Roentgen X" film is placed between lead foils 0.05 mm thick):

1—magnesium alloys; *2*—aluminium alloys; *3*—titanium alloys; *4*—steel

The exposure charts are based on experimental data obtained for gamma-graphs with a density of 1.5. The exposure is expressed in gram radium equivalent-hours.

A combination of foils which would ensure the maximum reduction in exposure time was used for each of the specified radioactive isotopes.

Should metal inspection be conducted with film and foils other than those for which the exposure charts were plotted, approximate exposure may be determined by multiplying the given exposure read off a chart by the respective coefficient listed in Table 20 (the exposure time read off the chart is taken as unity).

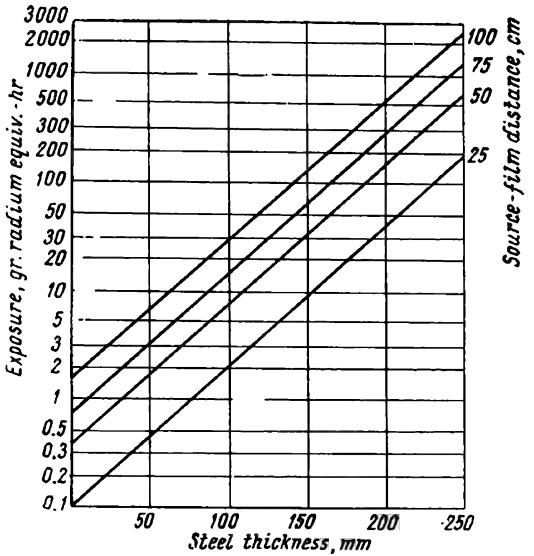

Fig. 39. Exposure chart for steel to be examined with a Co^{60} gamma-source (D — 1.5; "Roentgen X" film, lead foils 0.2 mm thick)

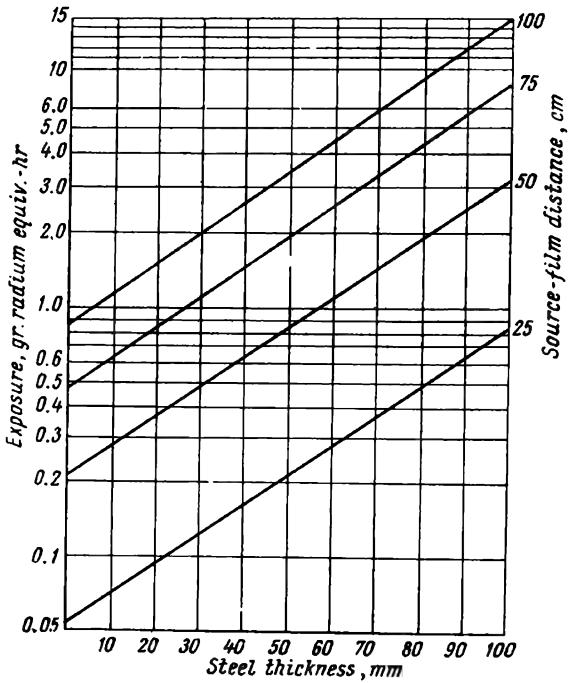

Fig. 40. Exposure chart for steel to be examined with a Cs^{137} gamma-source (D = 1.5; "Roentgen X" film, lead foils 0.1/0.2 mm thick)

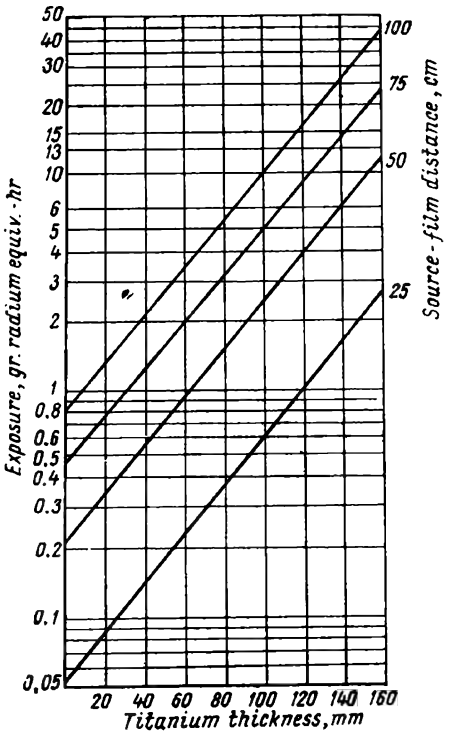

Fig. 41. Exposure chart for titanium alloys to be examined with a Cs^{137} gamma-source (D = 1.5; "Roentgen X" film, lead foils 0.1/0.2 mm thick)

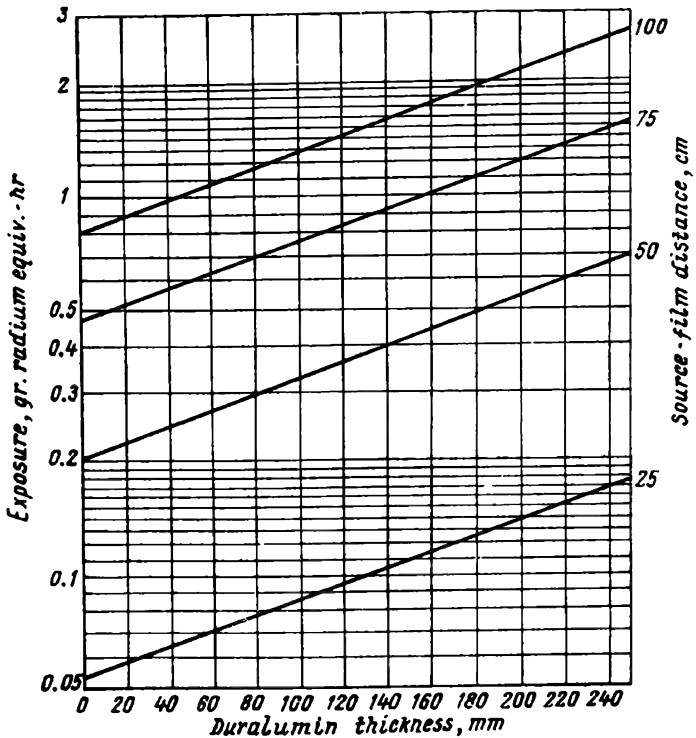

Fig. 42. Exposure chart for aluminium alloys to be examined with a Cs^{137} gamma-source (D = 1.5; "Roentgen X" film, lead foils 0.1/0.2 mm thick)

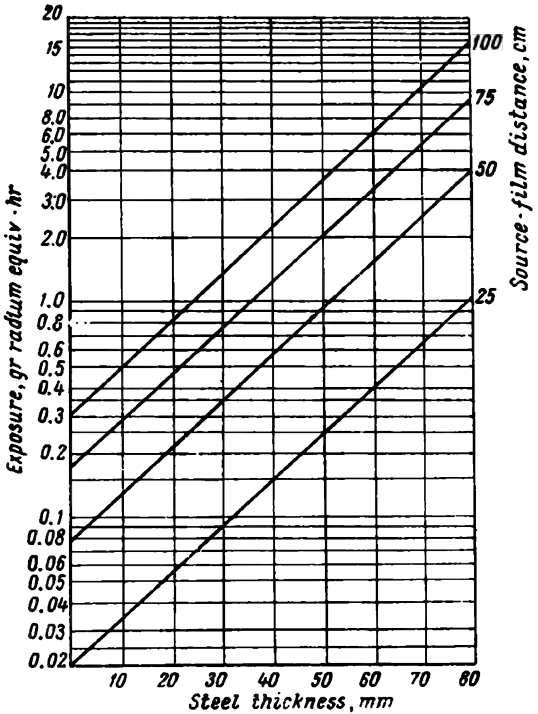

Fig. 43. Exposure chart for steel to be examined with an Ir^{192} gamma-source ($D = 1.5$; "Roentgen X" film, lead foils 0.1/0.2 mm thick)

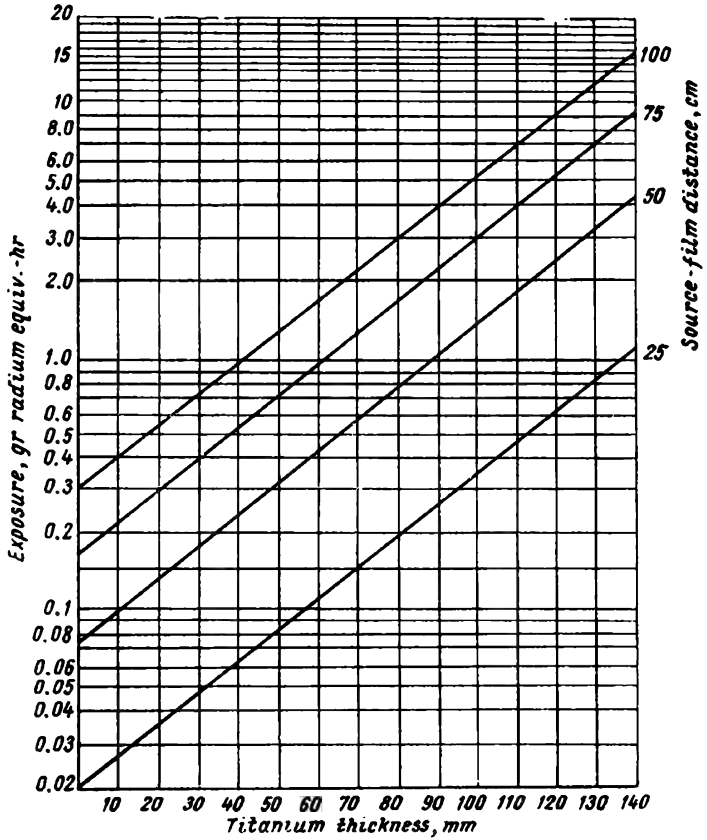

Fig. 44. Exposure chart for titanium alloys to be examined with an Ir^{192} gamma-source ($D = 1.5$; "Roentgen X" film, lead foils 0.1/0.2 mm thick)

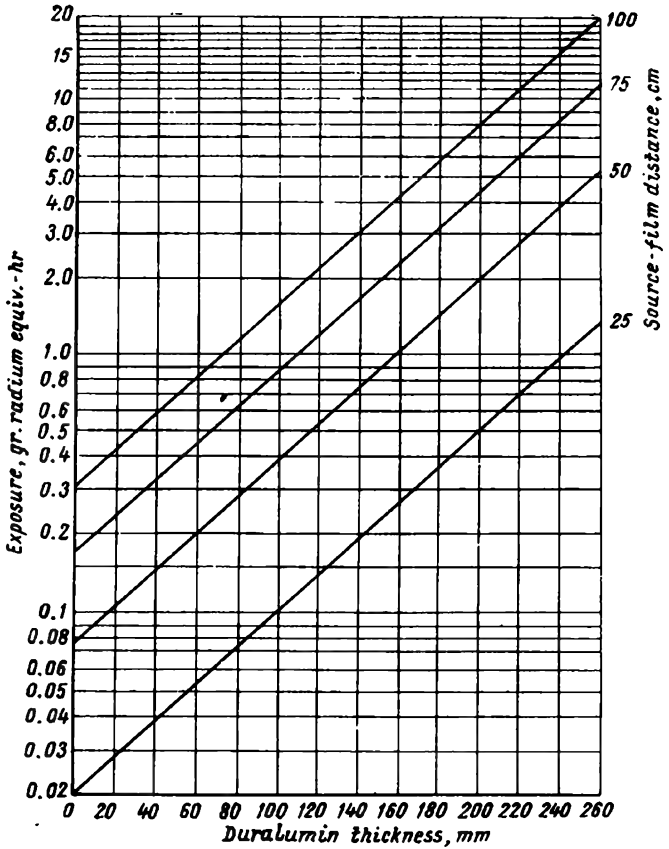

Fig. 45. Exposure chart for aluminium alloys to be examined with an Ir^{192} gamma-source ($D = 1.5$; "Roentgen X" film, lead foils 0.1/0.2 mm thick)

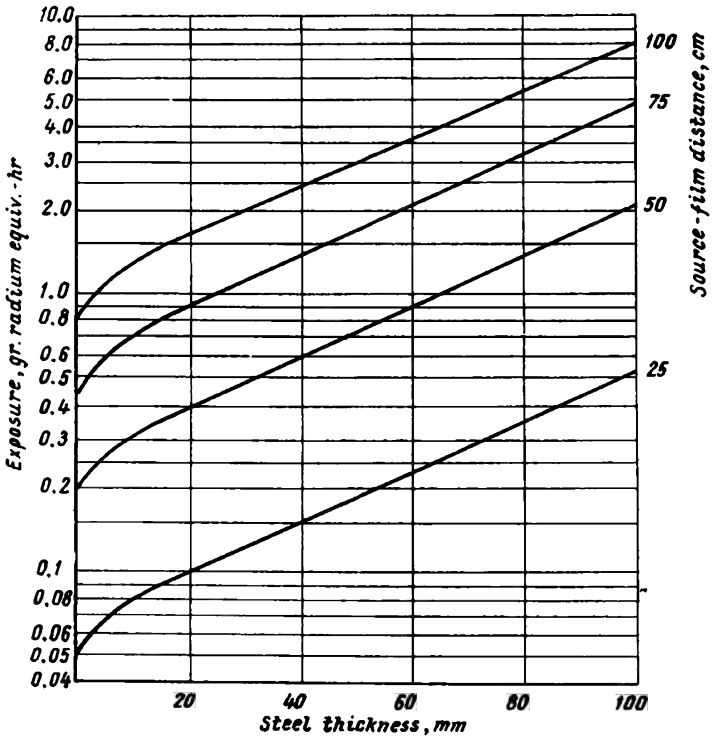

Fig. 46. Exposure chart for steel to be examined with a $Eu^{152,154}$ gamma-source ($D = 1.5$; "Roentgen X" film, lead foils 0.1/0.2 mm thick)

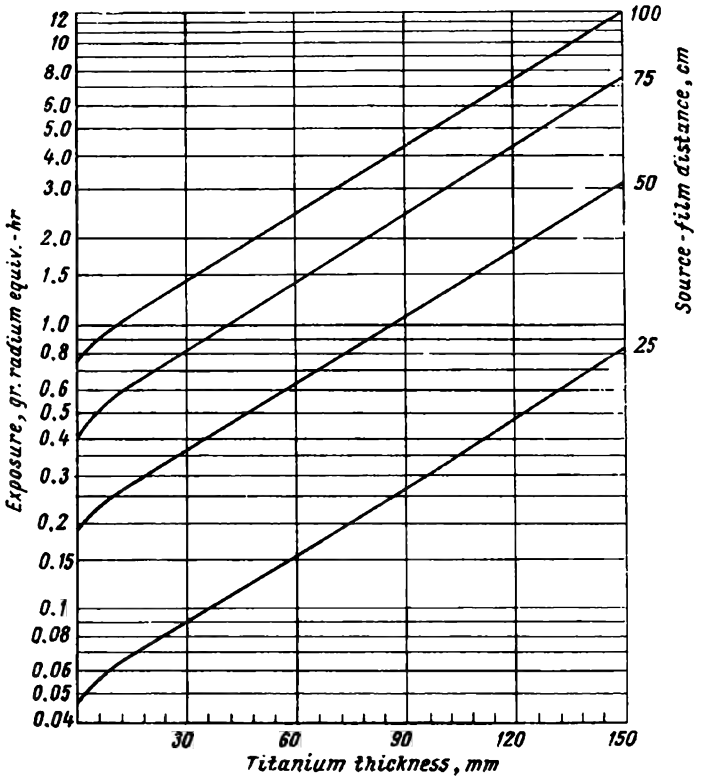

Fig. 47. Exposure chart for titanium alloys to be examined with a $Eu^{152,154}$ gamma-source ($D = 1.5$; "Roentgen X" film, lead foils 0.1/0.2 mm thick)

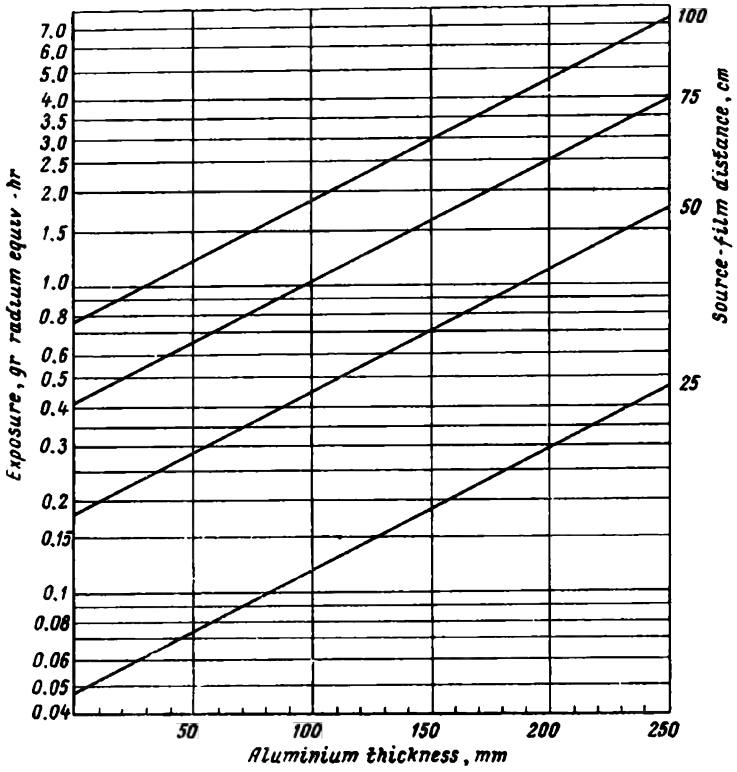

Fig. 48. Exposure chart for aluminium alloys to be examined with a $Eu^{152,154}$ gamma-source ($D = 1.5$; "Roentgen X" film, lead foils 0.1/0.2 mm thick)

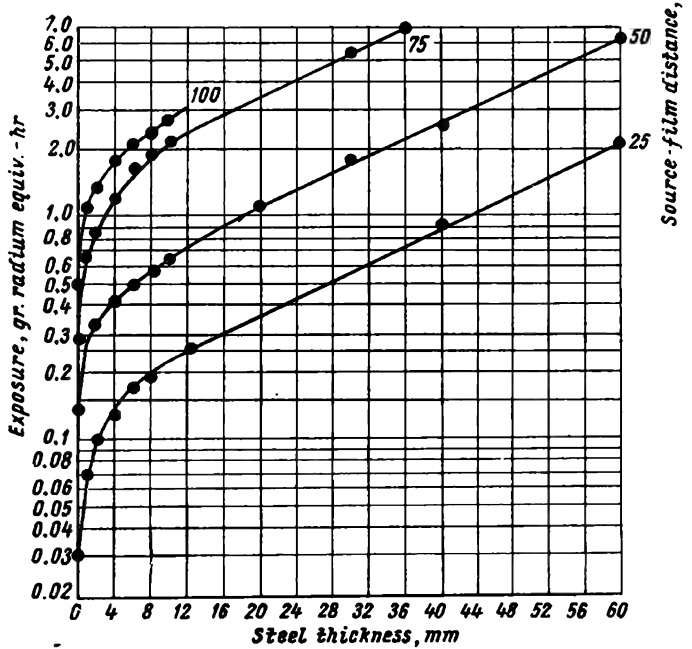

Fig. 49. Exposure chart for steel to be examined with a Tu^{170} gamma-source ($D = 1.5$; "Roentgen X" film, lead foils 0.05/0.05 mm thick)

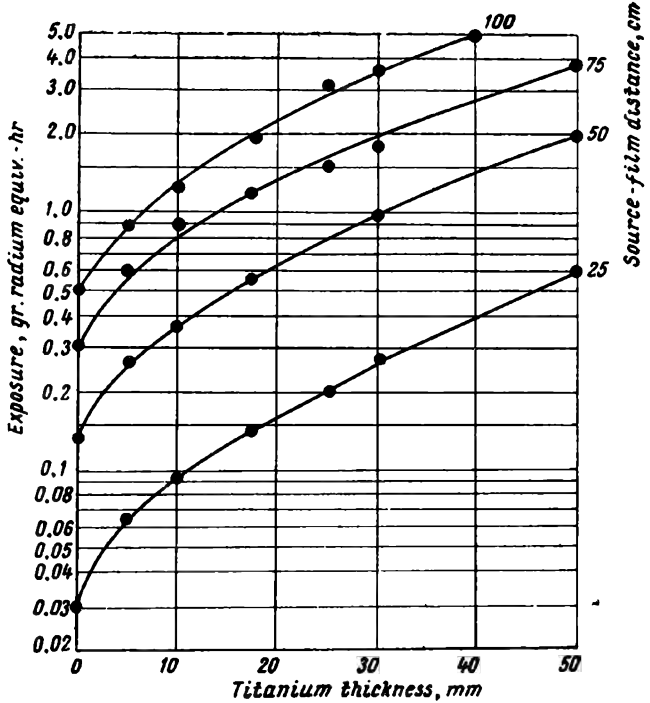

Fig. 50. Exposure chart for titanium alloys to be examined with a Tu^{170} gamma-source ($D = 1.5$; "Roentgen X" film, lead foils 0.05/0.05 mm thick)

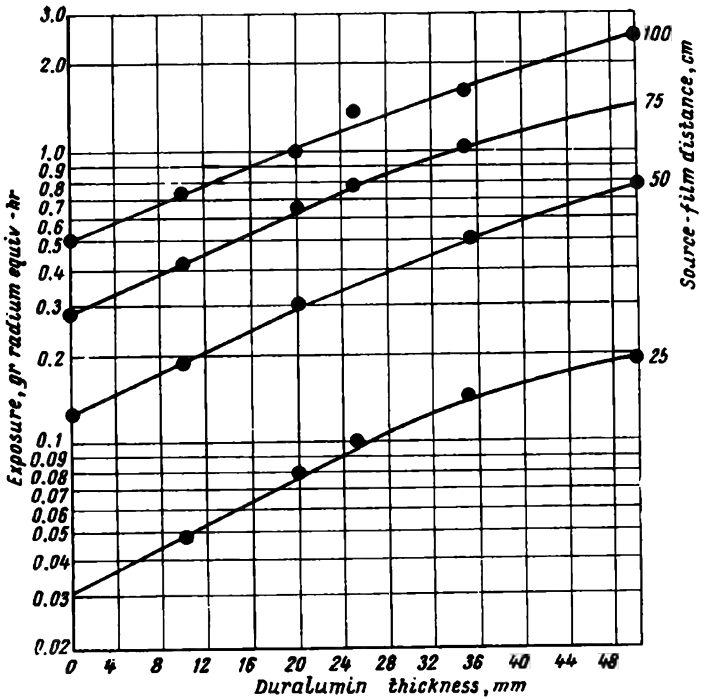

Fig. 51. Exposure chart for aluminium alloys to be examined with a Tu^{170} gamma-source ($D = 1.5$ "Roentgen X" film lead foils 0.05/0.05 mm thick)

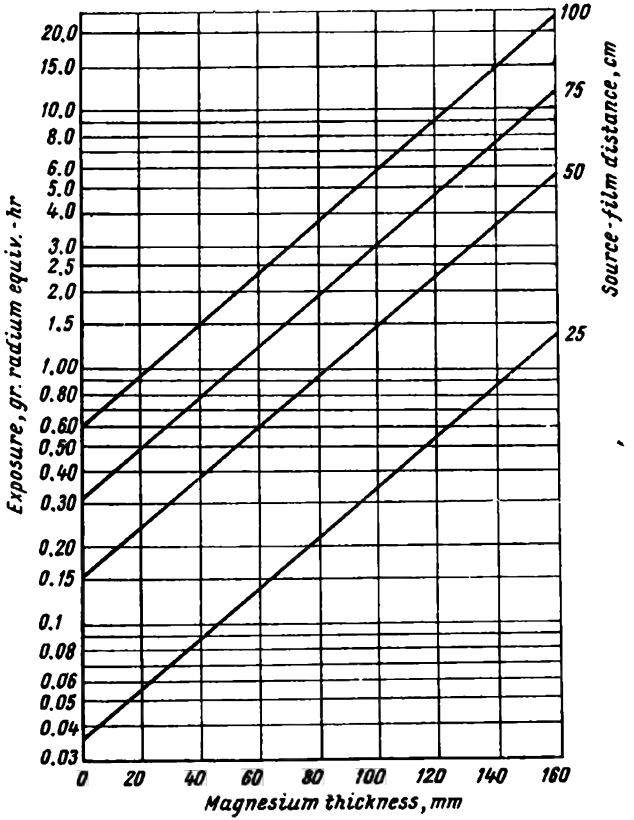

Fig. 52. Exposure chart for magnesium alloys to be examined with a Tu^{170} gamma-source ($D = 1.5$; "Roentgen X" film, lead foils 0.02/0.05 mm thick)

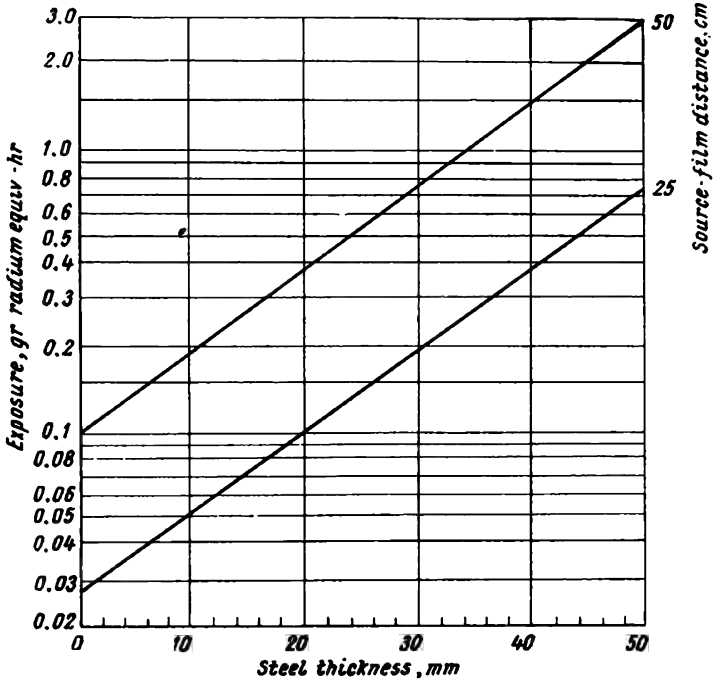

Fig. 53. Exposure chart for steel to be examined with a Se^{75} gamma-source ($D = 1.5$; "Roentgen X" film, lead foils 0.1/0.2 mm thick)

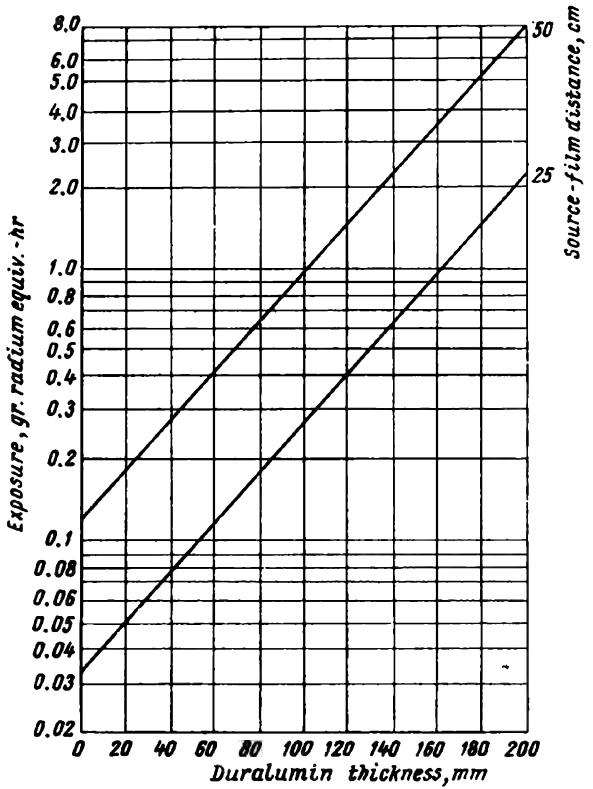

Fig. 54. Exposure chart for aluminium alloys to be examined with a Se^{75} gamma-source ($D = 1.5$; "Roentgen X" film, lead foils 0.1/0.2 mm thick)

Method of film loading	"Roentgen X" film						"Roentgen XX" film					
	Co^{60}	Cs^{137}	$Eu^{152,154}$	Ir^{192}	Eu^{155}	Tu^{170}	Co^{60}	Cs^{137}	$Eu^{152,154}$	Ir^{192}	Eu^{155}	Tu^{170}
Film without foils and screens	2	2.5	2.6	2.7	2	2	—	1.25	1.25	1.35	1	1
Film placed between 0.02/0.05 mm lead foils	—	—	—	—	0.9	0.85	—	—	—	—	0.45	0.4
Film placed between 0.05/0.05 mm lead foils	1	1	1	1	1	1	0.5	0.5	0.5	0.5	0.5	0.5
Film placed between 0.05/0.1 mm lead foils	1	1	1	1	1	1	0.5	0.5	0.5	0.5	0.5	0.5
Film placed between 0.1/0.1 mm lead foils	1	1	1	1	1.2	1.2	0.5	0.5	0.5	0.5	0.6	0.6
Film placed between 0.1/0.2 mm lead foils	1	1	1	1	1.2	1.2	0.5	0.5	0.5	0.5	0.6	0.6
Film placed between 0.2/0.2 mm lead foils	1	1.1	1.1	1.2	1.5	1.6	0.5	0.55	0.55	0.6	0.75	0.80
Film placed between fluorescent screens of a coating weight 40/120 mg/sq cm	0.4	0.28	0.3	0.3	0.28	0.33	0.4	0.25	0.25	0.28	0.25	0.35

Note: The table is compiled on the basis of the intensification factors for various combinations of foils and screens specified above.

Exposure charts for Sm^{145}, Gd^{153} and (for the sake of comparison) Tu^{170} sources used to inspect steel and aluminium are shown in Fig. 55.

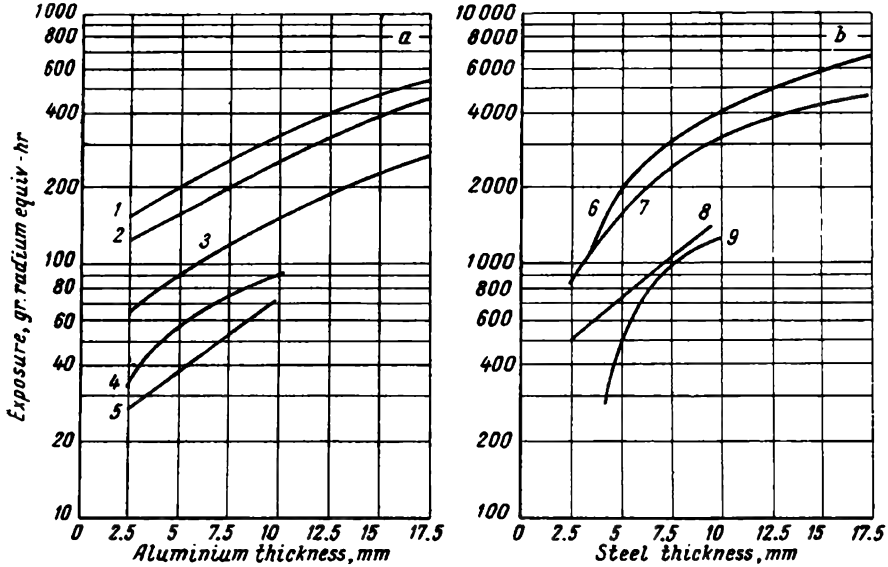

Fig. 55. Exposure curves plotted on data obtained in radiographing aluminium with Sm^{145}, Gd^{153}, Tu^{170} gamma-sources (*a*), and steel with Gd^{153} and Tu^{170} gamma-sources (*b*); $D = 1.5$; grade AA Kodak film:
1—Sm^{145} ($F = 50$ mm); *2*—Gd^{153} ($F = 50$ mm); *3*—Tu^{170} ($F = 50$ mm); *4*—Gd^{153} ($F = 25$ mm); *5*—Tu^{170} ($F = 25$ mm); *6*—Tu^{170} ($F = 50$ mm); *7*—Gd^{153} ($F = 50$ mm); *8*—Gd^{153} ($F = 25$ mm); *9*—Tu^{170} ($F = 25$ mm)

Examples of Exposure Determination

1. Determine the exposure time required to inspect a welded part 4 mm thick with a 0.5 gram radium equivalent Tu^{170} gamma-source at a film-source distance of 25 cm, using "Roentgen XX" film placed between lead foils 0.1/0.1 mm thick.

From the chart shown in Fig. 49 read off an exposure of 0.15 gram radium equivalent-hours, proper for a Tu^{170} source used to radiograph a steel article 4 mm thick with "Roentgen X" film and 0.05/0.05 mm lead foils.

The exposure time

$$t = \frac{0.15}{0.5} = 0.3 \text{ hr.}$$

With "Roentgen XX" film and 0.1/0.1 mm lead foils the exposure time is $0.3 \times 0.6 = 0.18$ hr (11 min).

2. Determine the exposure time for a steel article 30 mm thick to be radiographed with a 5.2 gram radium equivalent Ir^{192} source, "Roentgen X" film and fluorescent screens. Film-source distance is 50 cm.

From the exposure chart shown in Fig. 43 read off an exposure of 0.35 gram radium equivalent-hours proper for the given part and source, provided "Roentgen X" film and lead foils 0.1/0.2 mm thick are used.

The exposure time

$$t = \frac{0.35}{5.2} = 0.07 \text{ hr.}$$

According to the correction factor specified in Table 20 ($K_1 = 0.3$) the exposure time with "Roentgen X" film and fluorescent screens $t = 0.07 \times K_1 = 0.7 \times 03 = 0.02$ hr (1.2 min).

If the inspection is performed at a film-source distance different from that used to plot the exposure charts, the exposure may be found from the formula

$$t_{exp} = t_0 \frac{F^2}{F_0^2}, \tag{43}$$

where t_{exp} —the exposure for the specified film-source distance F, cm;
t_0—the exposure with a film-source distance F_0, cm, read off the chart.

If the inspection is performed at a large angle to the surface of the article, exposure must be determined for a thickness d_φ found from the formula

$$d_\varphi = \frac{d}{\cos \varphi}, \tag{44}$$

where d—the thickness of the inspected article;
φ—the angle formed between central beam and perpendicular to the surface of the article.

If the specific weight of the inspected metal differs from that specified in the exposure charts, the approximate exposure time may be read off the exposure chart for steel, recalculating the thickness of the inspected metal to an equivalent thickness, taking into account the specific weight of the inspected metal.

Equivalent steel thickness is determined from the formula

$$d_{equiv} = d \frac{\rho}{\rho_{st}}, \tag{45}$$

where d—the thickness of the inspected article, mm;
ρ—the specific weight of the inspected metal;
ρ_{st}—the specific weight of steel equal to 7.85 g/cu cm.

3. A copper casting 50 mm thick is radiographed with a Cs^{137} source of an activity of 10 gram radium equivalent, and at a film-source distance of 50 cm. The specific weight of copper $\rho = 8.9$ g/cu cm. Equivalent steel thickness

$$d_{equiv} = 50 \times \frac{8.9}{7.85} = 50 \times 1.13 = 56 \text{ mm.}$$

From the exposure chart shown in Fig. 40 read off an exposure of 1.2 gram radium equivalent-hours, for a steel article 56 mm thick, and find the exposure time

$$t = \frac{1.0 \text{ gram radium equivalent}}{10 \text{ gram radium equivalent}} = 0.10 \text{ hr} = 6 \text{ min.}$$

If radiographed with tungstate screens, the same copper casting would require an exposure time of only 2-3 min, for the intensifying power of such screens is three times that of lead foils.

It should be borne in mind that a considerable reduction in exposure time may be obtained by practising simultaneous inspection of several articles, arranging the articles around the circumference of a circle and placing the source at the centre, also by radiographing welds or cylindrical castings 500 to 2,000 mm dia in one exposition.

Different exposure set-ups for gamma-radiography are treated below.

§ 4. Radiographic sensitivity

Radiographic sensitivity is the ability to detect defects of the smallest size (in the direction of inspection) in the object examined. Sensitivity may be expressed in millimetres (absolute sensitivity) or in percentages of the total thickness (relative sensitivity).

The difference in attenuation of gamma-rays passing through solid metal, and through a section where a fault is located, diminishes with the decrease in the size of the fault. As a result the sharpness of the gamma-graph image diminishes.

There exists a minimum difference between the densities of two adjoining sections of an image perceptible to the human eye when viewing the gamma-graph in passing light. It has been shown by experiment that this minimum difference in densities is about 0.02-0.03. Consequently, very small defects are not revealed on gamma-graphs.

Sensitivity is the main factor which determines the application of a given inspection technique. It is not advisable to practise gamma-radiography in cases where other inspection methods yield better results in flaw detection. There are many objects in which gamma-radiography reveals defects of a size smaller than that allowed by accepted manufacturing standards. In such a case gamma-inspection may be practised, but efficiency and the cost of inspection should be considered. Sometimes, the sensitivity of gamma-radiography is inadequate; nonetheless, gamma-inspection is employed to detect large defects (it is important, however, to know the size of unrevealed flaws), for there is no other method of nondestructive inspection for these objects.

The detection of internal faults depends upon the contrast and definition of the appearing image, contrast and definition, in their turn, being a function of the penetrating power of gamma-rays, the atomic number, the density and thickness of the inspected article, the density of defect, the shape of the radioactive source, the film-source distance and field of radiation, the object-film distance, the shape of the defects, the location of the defect in regard to object thickness, gamma-graph density, intensifying screens, film quality, processing and other factors.

Since the process of gamma-ray attenuation in a substance is of a complex nature, and also owing to the great number of factors which determine image quality, it is impossible to determine the sensitivity of gamma-radiography analytically. However, sensitivity may be evaluated experimentally for each individual case. This is done with the aid of penetrameters or sensitivity gauges which imitate the artificial defects. Penetrameters are available in sets of notched plates, or plates with cylindrical holes of various depths. The notches and holes may be located on the side of the film or source or be arranged at various distances from the film along the inspected article. Penetrameters may be made from wire or metal plates of different thicknesses with holes. The plates are joined to sets so that the holes of individual plates do not coincide. A wire penetrameter is a set of wires of different diameter arranged parallel to one another and secured between glued thin rubber strips. Ball-bearings of a small diameter may also be used as penetrameters. These balls are placed on the inspected object. Another type of penetrameter is a special device making it possible to ensure a clearance of different length and width between two jointed walls of sheet material. The following section devoted to the influence of various factors on fault detection in gamma-radiography is based on known physical laws and experimental data.

Radiographic sensitivity as a function of gamma-ray hardness and density and thickness of inspected material. Let us examine the variation in radiographic sensitivity as a function of gamma-ray hardness and the density of the inspected material, all other factors remaining unchanged.

We assume that the inspected material of a thickness d possesses a linear absorption coefficient μ. Inside the material there is an imperfection Δd in size, measured in the direction of gamma-raying, with a linear absorption coefficient μ_1 (Fig. 56).

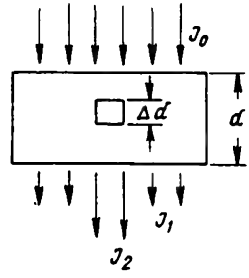

Fig. 56. Diagram showing passage of gamma-rays through metal plates

According to the law of narrow-beam, monochromatic gamma-ray attenuation, after passage through a material of a thickness d (i.e., through the flawless section), the radiation intensity I_1 will be equal to*

$$I_1 = I_0 e^{-\mu d}. \tag{46}$$

According to the same law the intensity of radiation which passed through the defect of Δd thickness may be expressed as

$$I_2 = I_0 e^{-[\mu(d-\Delta d)+\mu_1 \Delta d]}, \tag{47}$$

* Scattered radiation and geometric factors are not taken into account.

where I_0—the initial intensity of the gamma-beam;
e—the natural logarithm base.

The defect will appear on the radiograph only if there is a definite difference between the intensities of the radiation passed through the flawless and defective sections of the inspected material, i.e., I_2 must be larger than I_1. From the previous two equations it follows

$$\frac{I_2}{I_1} = \frac{I_0 e^{-\mu(d-\Delta d)+\mu_1 \Delta d}}{I_0 e^{-\mu d}} = e^{(\mu-\mu_1)\Delta d}. \tag{48}$$

As the defective article is radiographed in one exposition,

$$\frac{I_2}{I_1} = \frac{D_2 - D_0}{D_1 - D_0}, \tag{49}$$

where D_2 and D_1—respective densities of the defect image and adjoining sections on the radiograph;
D_0—fog density.

If we substitute the ratio $\frac{I_2}{I_0}$ into the equation (49) we will have:

$$\frac{D_2 - D_0}{D_1 - D_0} = e^{(\mu-\mu_1)\Delta d}. \tag{50}$$

Hence, the film density opposite the defective spot is expressed by

$$D_2 - D_0 = (D_1 - D_0)\,[e^{(\mu-\mu_1)\Delta d} - 1],$$

and the difference between the densities of the film section showing the defect and the neighbouring section exposed to the beam which passed through the solid section of the inspected metal will be

$$\Delta D = D_2 - D_1 = D_1 - D_0\,[e^{(\mu-\mu_1)\Delta d} - 1]. \tag{51}$$

Hence,

$$\Delta d = \frac{\ln\left(\frac{\Delta D}{D_1 - D_0} + 1\right)}{\mu - \mu_1}. \tag{52}$$

The possibility of revealing a defect is characterised by a definite minimum contrast ΔD of the defect image. Therefore, for a constant film density $D_1 - D_0$ it can be assumed that

$$\left[\frac{\Delta D}{D_1 - D_0}\right]_{\min} = K = \text{Const},$$

then

$$\Delta d_{\min} = \frac{\ln(K+1)}{\mu - \mu_1}. \tag{53}$$

The difference between the absorption coefficients $(\mu - \mu_1)$ increases with the increase in the difference between the densities (specific weights) of the flawless metal and the defective spot, hence, the minimum size of the revealed defect $\Delta d_{\min}$ diminishes, i.e., the inspection sensitivity increases with the increase in the density of the inspected metal and the decrease in the density of the defective spot. For an air-filled defect (air inclusions, lack of penetration, etc.)

$\mu_1 = 0$, therefore Δd_{min} can be expressed as

$$\Delta d_{min} = \frac{\ln (K+1)}{\mu}. \tag{54}$$

An increase in gamma-energy is accompanied by an increase in the penetrating ability of the radiation while the linear absorption coefficient for a given metal diminishes. This results in an increase in Δd_{min} —the minimum size of the revealed defect, i.e., in a fall in the sensitivity. Hence, the sensitivity increases with the increase in the density of the inspected material and the simultaneous decrease in the defect density, as well as with a fall in gamma-energy.

As the minimum difference in film densities perceptible to the human eye is 0.02,

$$\Delta d_{min} \approx \frac{\ln (0.02+1)}{\mu}. \tag{55}$$

This expression may be used to determine approximately the minimum revealed defect (air-filled), when inspection is carried out with a narrow (pencil) monochromatic gamma-beam. Thus, for instance, the linear absorption coefficient of Co^{60} radiation in radiographing steel is 0.413 cm^{-1}, therefore, the size of the smallest revealed defect in the direction of gamma-raying is approximately equal to

$$\Delta d = \frac{\ln (0.02+1)}{0.413} \cong 0.048 \text{ cm} = 0.48 \text{ mm}.$$

In inspecting steel with monoenergetic gamma-radiation from a 0.5 Mev source, the linear absorption coefficient of which is 0.655 cm^{-1} for steel, the minimum size of the revealed defects will be

$$\Delta d = \frac{\ln (0.02+1)}{0.655} = 0.030 \text{ cm} = 0.30 \text{ mm},$$

or 1.6 times smaller than when the inspection is carried out with hard gamma-radiation from a Co^{60} source.

These values may be used only for a comparative evaluation of the revealment of defects, when materials of various density are inspected with gamma-radiation of a different hardness.

From equations (54) and (55) it follows that the minimum size of the detected defects does not depend on the thickness of the inspected material. However, this equation does not account for the polyenergetic character of gamma-radiation from most of the radioactive isotopes and for the scattered radiation.

As polyenergetic gamma-rays pass through the inspected material, the radiation becomes harder, owing to the absorption of soft components. As a result the effective linear absorption coefficient diminishes, and, therefore, the minimum size of the revealed defects increases.

The graphs in Figs. 57—61 show the sensitivity in revealing imitated defects as a function of the gamma-energy, thickness and den-

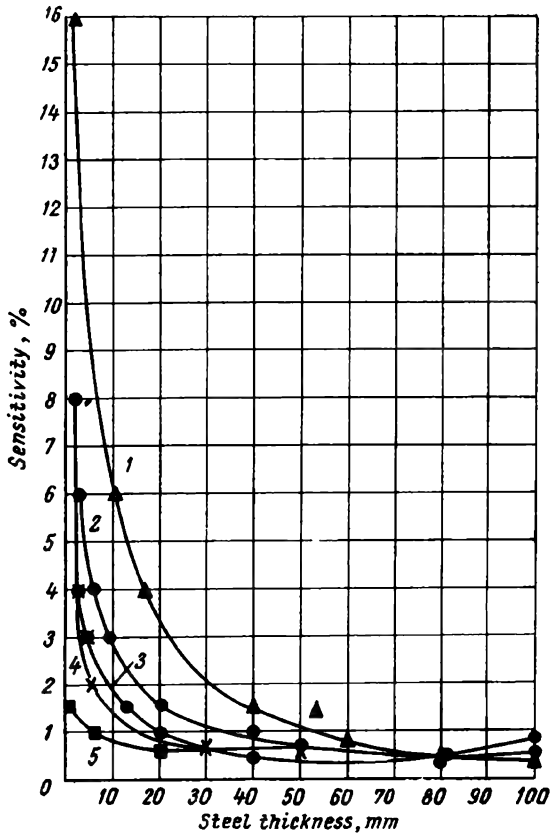

Fig. 57. Sensitivity curves based on data obtained in gamma-raying steel ($F = 50$ cm; "Roentgen X" film; $D = 1.5 \div 1.8$):
1—Co^{60}; *2*—Cs^{137}; *3*—Ir^{192}; *4*—$Eu^{152, 154}$; *5*—Tu^{170}

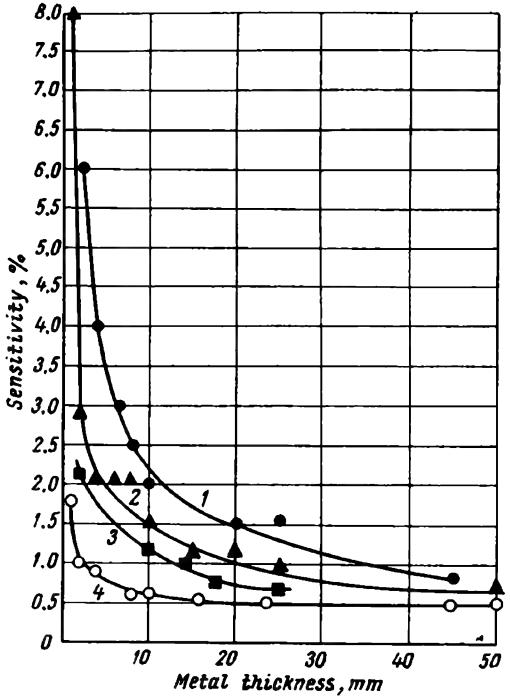

Fig. 58. Sensitivity curves based on data obtained in radiographing steel, titanium, duralumin and magnesium with a Tu^{170} gamma-source ($F = 50$ cm, "Roentgen X" film; $D = 1.5 \div 1.8$):
1—magnesium alloys; *2* aluminium alloys; *3*—titanium alloys; *4* steel

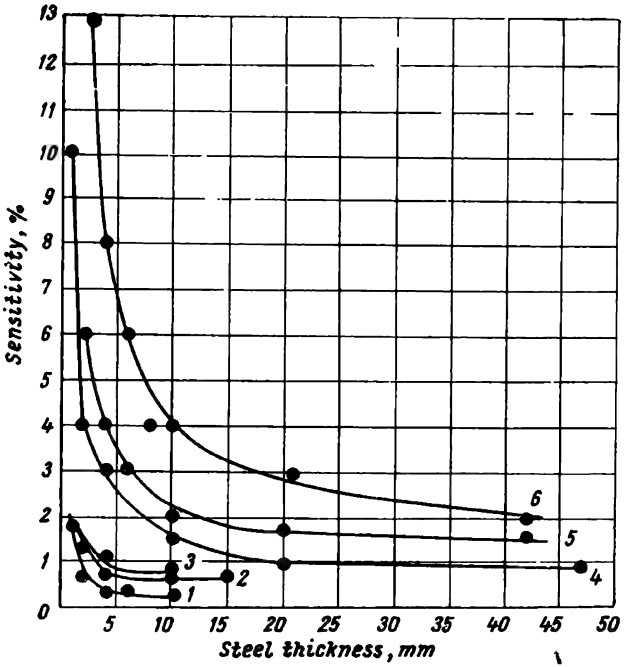

Fig. 59. Sensitivity curves based on data obtained in radiographing steel with gamma and X-rays ($F = 50$ cm; "Roentgen X" film; $D = 1.5 \div 1.8$):

1—X-rays; *2*—Tu^{170}; *3*—Eu^{155}; *4*—Ir^{192}; *5*—Cs^{137}; *6*—Co^{60}

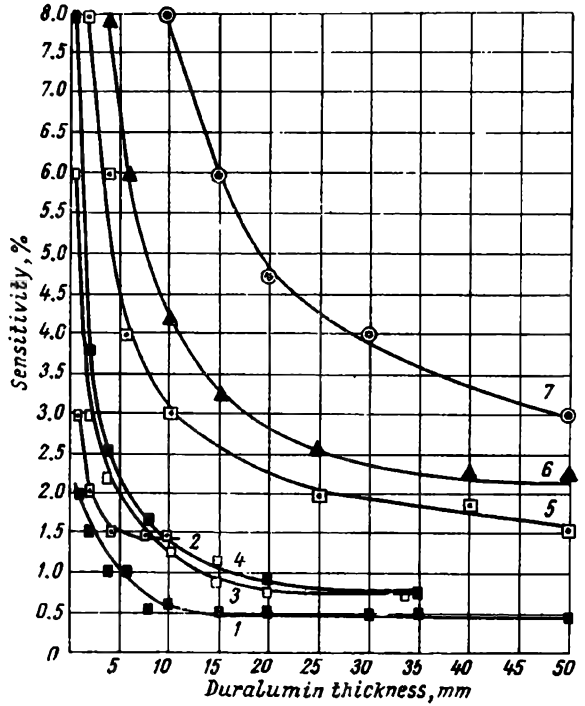

Fig. 60. Sensitivity curves based on data obtained in radiographing aluminium alloys with gamma- and X-rays ($F = 50$ cm; "Roentgen X" film; $D = 1.5 \div 1.8$):

1—X-rays; *2*—Ce^{144}; *3*—Tu^{170}; *4*—Eu^{155}; *5*—Ir^{192}; *6*—Cs^{137}; *7*—Co^{60}

sity of the inspected material. The graphs are plotted on experimental data obtained in inspecting steel, duralumin, titanium and magnesium stepped, grooved standard penetrameters with gamma-rays from Co^{60}, Cs^{137}, Ir^{192}, $Eu^{152, 154}$, Tu^{170}, Eu^{155} and Ce^{141} sources, using "Roentgen X" film placed between lead foils of a thickness ensuring maximum reduction of exposure time. The optical density

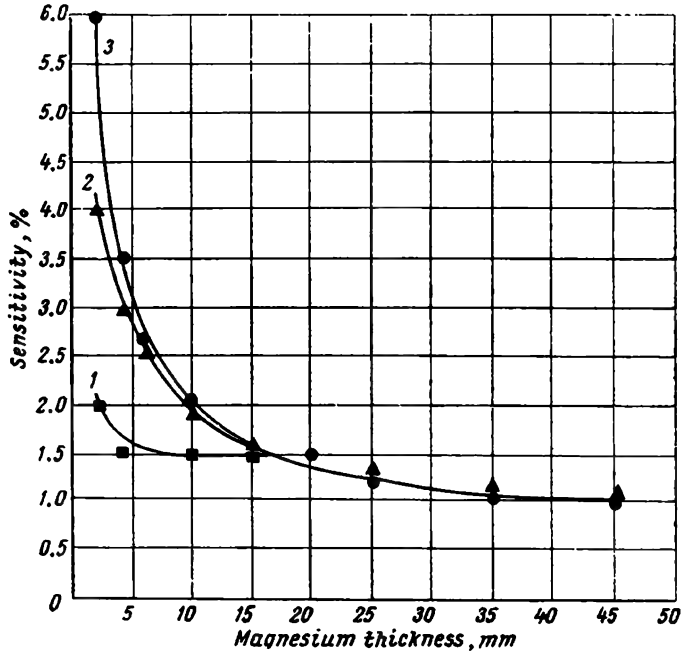

Fig. 61. Sensitivity curves based on data obtained in gamma-raying magnesium alloys ($F = 50$ cm; "Roentgen X" film, $D = 1.5 \div 1.8$):
1—Ce^{144}; *2*—Eu^{155}; *3*—Tu^{170}

o the gamma-graphs was assumed to be equal to 1.5-1.8 in all cases, groove width 3 mm, the penetrameter grooves facing the film. The inspection was performed with a broad 40° divergent gamma-beam and at a source-film distance of 50 cm.

The effect of scattered radiation on radiographic sensitivity. If the inspection is performed with a narrow, monoenergetic gamma-beam, all the appearing scattered quanta are removed from the primary beam. However, gamma-radiography is usually practised not with a narrow parallel beam, but with a broad divergent gamma-beam. In this case not all the scattered quanta leave the region in which the primary beam is active and some of them join the non-scattered quanta (Fig. 62).

The relative proportion of the scattered radiation in a broad gamma-

beam passed through a substance increases with the increase in the thickness of the inspected metal; hence, an increase in metal thickness results in heavier film fogging by scattered radiation, and the revealment of defects deteriorates.

The negative effect of scattered radiation on image contrast is pronounced in cases of large film-fault distance, especially, during the inspection of articles over 80-100 mm thick, because the proportion of scattered radiation increases with the increase in the thickness of inspected metal.

The sensitivity curves shown in Fig. 63 are based on experimental data obtained during inspection of steel, duralumin and magnesium penetrameters of various thicknesses with gamma-rays from a Tu^{170} source, the penetrameter grooves being differently arranged in respect of the film.

When variable cross-section articles are inspected, scattered rays penetrate from one section into another. As a result the intensity of the scattered radiation in each cross-section of the inspected object differs from the intensity of the scattered radiation registered in radiographing plates of uniform thickness. Therefore, radiographic sensitivity in inspection of complex-shaped articles of a variable cross-section, differs from that obtained in radiographing plates of uniform thickness. It is impossible to eliminate scattered radiation entirely. However, partial reduction of scattered radiation hitting the film may be obtained by practising small exposure fields, e.g., by orificing the gamma-beam, by diminishing the taper of the container opening, by using lead foils which absorb soft scattered radiation more actively than primary radiation. It should be mentioned that scattered radiation passes through lead foils at various angles, i.e., scattered radiation is absorbed over a longer path, than primary radiation. It should be noted that film is exposed not only to the scattered radiation originating in the inspected object, but to the radiation scattered from surrounding articles. Therefore, during exposure, the film should be protected from the scattered radiation coming from surrounding articles and the floor by placing possibly thicker lead plates below the film-charged holder.

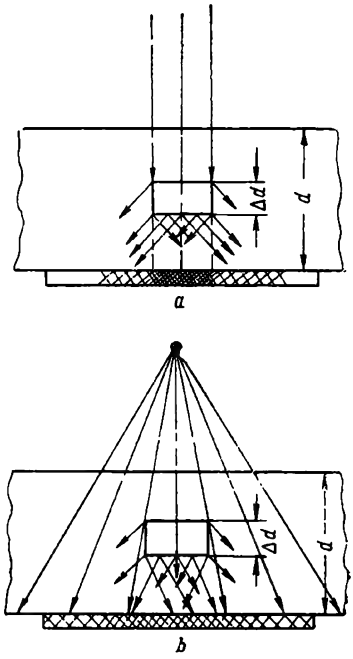

Fig. 62. Effect of scattered radiation on gamma-graph definition:
a—narrow beam; *b*—broad divergent beam

The influence of source geometry and source-film distance on sensitivity. In gamma-radiography the projection of the radioactive source on the plane perpendicular to the direction of the inspection is called the focus or focal spot of the radioactive source and the

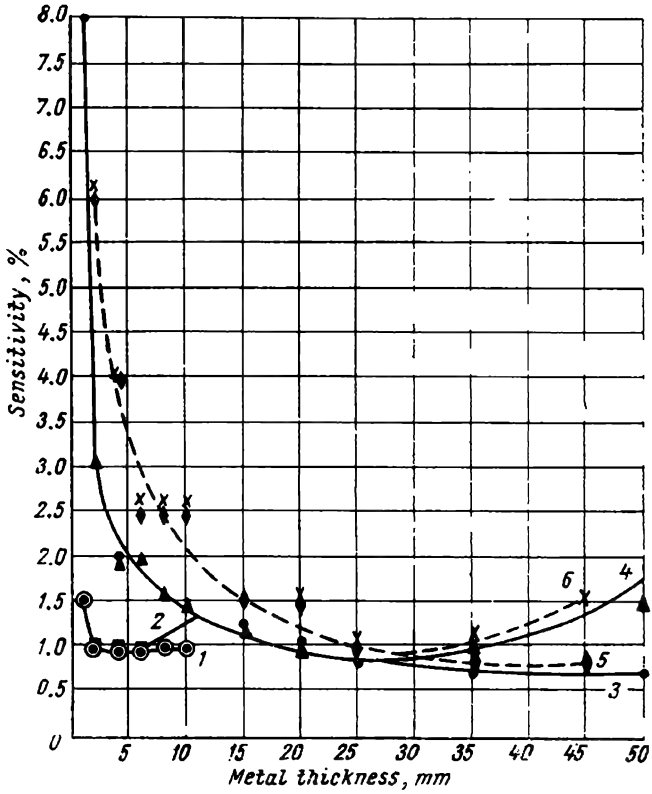

Fig. 63. Sensitivity curves based on data obtained in radiographing with a Tu^{170} gamma-source steel, aluminium and magnesium alloys in which the defects are differently located in relation to the film:

1—steel, notches face the film; *2*—steel, notches face the radiation source; *3*—aluminium, notches face the film; *4*—aluminium, notches face the radiation source; *5*—magnesium, notches face the film; *6*—magnesium, notches face the radiation source

source-film distance—focal distance. If the source capsule is not sphere-shaped, the geometry of the focal spot may change, depending on the manner the capsule is arranged in relation to the inspected object and film. The size of the focal spot and the source-film distance affect the definition of the defect on the gamma-graph.

From Fig. 64 it follows that with a point radiation source the outlines of defects are sharply defined, while in the case of a volume source each point of the source gives a projection on the film, all

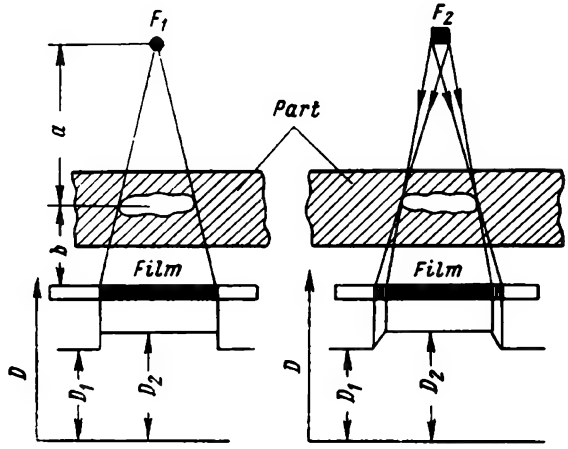

Fig. 64. The effect of the size of radioactive source on defect image definition:

F_1—point focus; F_2—line focus; D_2—density of film section underneath the defect; D_1—density of film section underneath the section of the examined article adjoining the defect; D—density

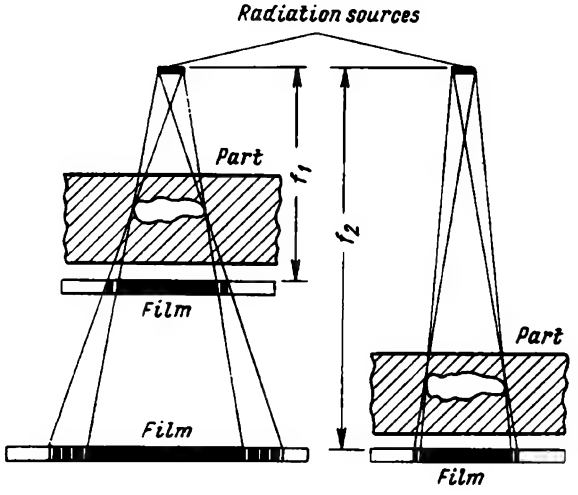

Fig. 65. Effect of source-film distance and film-object distance on the definition of defect image:

and f_2—source-film distances

other factors affecting image definition being ignored. Therefore, besides the blackening of the film caused by the rays which passed through the imperfection there would be semidark areas (transition from density D_2 to density D_1) on the gamma-graph, this resulting in the appearance of an image with blurred outlines. The width of the semidark sections is determined by the focal spot diameter F, source-film distance f and fault-film distance b and is expressed by the following equation:

$$y = F\frac{b}{f-b}. \tag{56}$$

The width of semidark sections diminishes with the increase in source-film distance and the decrease in the defect-film distance, and the image appears more sharply defined (Fig. 65).

The dependence of inspection sensitivity on the shape of defects and their arrangement in relation to the direction of inspection. Defects having straight edges running in the direction of the gamma-radiation appear much better, due to the sharp definition of the straight edges, as compared with cylindrically-, sphere-, or trapezium-shaped defects. The sharpness of an image, representing a defect with straight edges running parallel to the direction of the inspection, depends only on the extent of blurring. With a sphere-shaped defect, image density diminishes gradually and uniformly from a maximum density which depends upon the defect diameter to the density of the entire exposed film section. The defect image will not be defined sharply, owing to the gradual weakening of density. This is also true for trapezium-shaped defects and defects of other shapes.

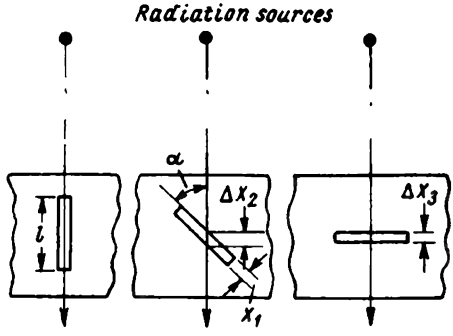

Fig. 66. Revealment of defects depending on their position in relation to ray propagation

The revealment of defects depends on the manner in which the latter are arranged in relation to the direction of the primary gamma-beam (Fig. 66). The best revealment is obtained when the gamma-rays pass along the defect; revealment deteriorates if the defects are arranged at a definite angle to the radiation beam, for in this case each ray travels over a section of the defect and not along its entire length l. Hence, sensitivity would be determined by the width x_1 of the defect exposed to radiation and the angle α formed between the plane of the defect and the direction of radiation. In practical radiography narrow defects such as cracks, defoliation in rolled stock, lack of fusion in welds are common. For such defects, although large in length, the sensitivity will be determined

by the values Δx_2 and Δx_3. The curve in Fig. 67 characterises the revealment of an imitated crack in a steel plate 40 mm

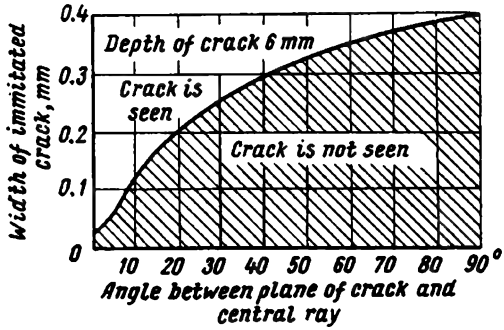

Fig. 67. Revealment of an imitated crack depending on the angle formed between the plane of the crack and the central beam (true for a 40 mm steel bar)

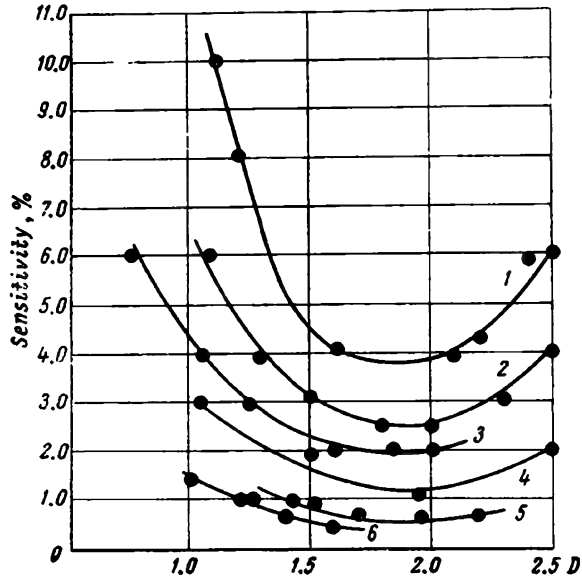

Fig. 68. Curves expressing the effect of gamma-graph density on the revealment of defects based on data obtained in examining steel of different thicknesses with a $Eu^{152,154}$ source (F = 50 cm; "Roentgen X" film; lead foils 0.1/0.2 mm thick):
1—2 mm; *2*—10 mm; *3*—20 mm; *4*—25 mm; *5*—50 mm; *6*—100 mm

thick as a function of the angle formed between the plane of the crack and the gamma-beam.

It should be mentioned that it is a little difficult to indicate the minimum width at which the defect would still be revealed, for this depends on a number of factors. When steel 40 mm thick is inspected (see Fig. 67), the minimum width of a crack running parallel to the gamma-beam, which would appear on the gamma-graph, is 0.025 mm.

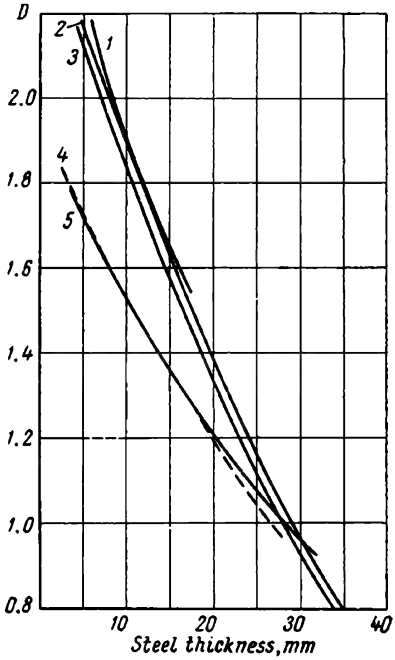

Fig. 69. Characteristic curves for steel radiographed with a Cs^{137} gamma-source using a rear foil 150 microns thick and front foils of different thicknesses; exposure time is constant:

1—front foil 300 microns; *2*—front foil 150 microns; *3*—front foil 450 microns; *4*—front foil 600 microns; *5*—front foil 20 microns

The dependence of radiographic sensitivity on gamma-graph density. As mentioned above, a contrast below 0.02 is not perceptible to the human eye, the border between neighbouring fields being sharply outlined. As there is no linear-line relationship between the density of a negative and exposure time, the density difference $D_1 - D_2$ changes with a change in exposure time. Therefore, the appearance of defects on gamma-graphs depends on negative density.

The curves in Fig. 68 show the dependence of the minimum depth at which a defect is revealed on the optical density in inspecting steel with gamma-rays from a $Eu^{152, 154}$ source. The graph is plotted on the basis of data obtained in inspecting grooved steel penetrameters; the gamma-graphs were studied in a negative viewer of medium illuminating intensity. A similar relationship is observed in inspecting steel, titanium, duralumin and magnesium with gamma-rays from Cs^{137}, Ir^{192}, Tu^{170}, Eu^{155} and other radioactive isotopes. From the curves shown in Fig. 68 it follows that the best revealment of defects on gamma-graphs, examined in a negative viewer of medium illuminating intensity, is obtained in the optical density range from 1.5 to 2.0. However, high-density gamma-graphs require long exposures which diminishes inspection efficiencies. Therefore, in practical radiography one tries to get gamma-graphs of a density ranging from 1.5 to 1.7.

The effect of lead foils and fluorescent screens on sensitivity. Apart from the intensifying effect, lead foils (or foils made of other heavy metals) improve the quality of gamma-graphs, diminishing the harmful fogging effect of scattered radiation which is of a lesser

hardness and is, therefore, absorbed by lead more intensively than primary gamma-radiation. This contributes to a cleaner image of a higher sharpness.

Different combinations of lead foils, 20, 150, 300, 450 and 600 microns thick, were used to determine the influence of such foils on contrast and sensitivity. Experimental data obtained by gamma-raying steel, using a Cs^{137} radiation source, are shown in Fig. 69. A combination of a front and rear foil, 300 and 150 microns thick

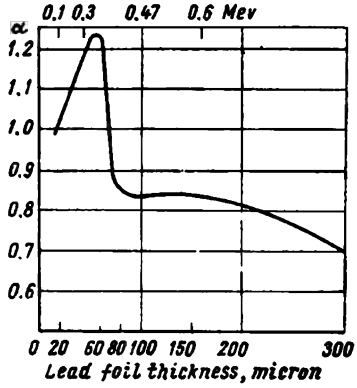

Fig. 70. Contrast curves based on data obtained in radiographing steel with an Ir^{192} gamma-source using a rear foil 150 micron thick and front foils of different thicknesses; exposure time is constant

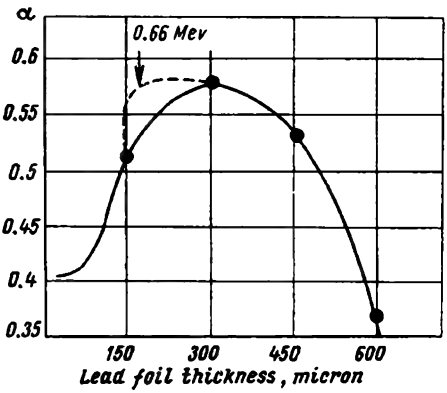

Fig. 71. Contrast curves based on data obtained in radiographing steel with a Cs^{137} gamma-source using a rear foil 150 microns thick and front foils of different thicknesses; exposure time is constant

respectively, is characterised by steeper curves. They are arranged above the curves of other foil combinations. The characteristic curve for a front and rear foil, 600 and 150 microns thick respectively, almost coincides with the characteristic curve plotted for a front and rear foil 20 and 150 mm thick respectively. The characteristic curves for steel 5 mm thick differ considerably (D ranges from 1.7 to 2.3). For steel 28 mm thick all the characteristic curves almost coincide at $D = 1.0$.

The curves shown in Figs. 70 and 71 characterise the variation of contrast α with lead foil thickness, for steel radiographed with gamma-rays from Ir^{192} and Cs^{137} sources. Contrast is expressed through $\alpha = \frac{\Delta D}{\Delta d}$, where D (density) $= 2$; d is the thickness of the radiographed steel.

For the Ir^{192} source optimal results are obtained with a front foil 80 microns thick and a rear foil—150 microns, while with the Cs^{137} source, optimal contrast is ensured with a front and rear foil 300 and 150 microns thick respectively. The specified contrast ranges depend on the theoretical path of the photoelectrons formed as

a result of gamma-ray absorption. Owing to mutual foil effect and back scattering, the optimum contrast will shift and the optimal foil thickness change (for the Cs^{137} source: front foil—180 microns, rear foil—150 microns).

As is generally known the revealment of defects depends on gamma-graph contrast. Let us consider the equation which may be employed to determine the size of a minimum defect S_D arranged in the direction of gamma-raying which may be revealed on the gamma-graph:

$$S_D = \frac{\Delta d}{d} \times 100\% = \underbrace{\left[\frac{2.3 \times \beta}{G \times C_0}\right]}_{\text{film and observation factor}} \times \underbrace{\left[\frac{1}{\mu d} + \frac{K}{\mu}\right]}_{\text{radiation factor}} \times \underbrace{[\sqrt[3]{u_D^3 + u_i^3}]}_{\text{unsharpness factor}} \times 100\% \quad (57)$$

where Δd — the size of the defect, cm, in an object d cm thick;
β — minimum noticeable change in density equal to 0.02;
G — the contrast factor;
μ — the radiation absorption coefficient, cm^{-1};
K — the primary radiation scattering factor (per cm of inspected object);
C_0 — the maximum resolving power of the eye (about 0.076 mm at a distance of 60 cm);
u_i — the inner unsharpness of film, mm;
u_D — geometric unsharpness (focal spot as a function of lighted spot-defect and defect-film distances).

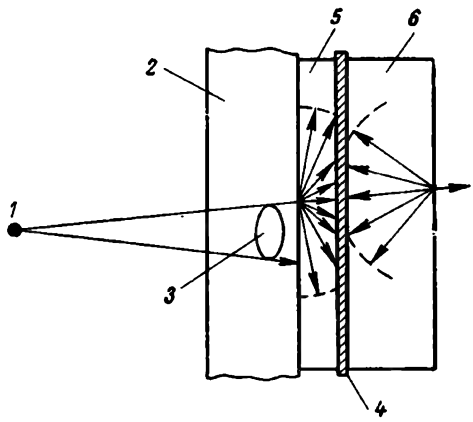

Fig. 72. The effect of scattered fluorescent light of intensifying sources on image definition:
1—radiation source; *2*—radiographed metal; *3*—defect; *4*—roentgen film; *5*—front intensifying screen; *6*—rear intensifying screen

From the equation it follows that defects are better revealed with an increase in contrast unsharpness (blurriness) remaining unchanged.

On the contrary, with fluorescent screens there is a slight deterioration in the revealment of defects, because the grains of fluorescent screens emit scattered light (Fig. 72).

§ 5. Application of radioactive isotopes in flaw detection

The application of radioactive isotopes in engineering, including industrial flaw detection, is governed by technical expediency and economic efficiency.

Any physical method of nondestructive inspection, including the use of radioactive isotopes, must satisfy the following principal technical requirements: sensitivity to flaw detection and efficiency of inspection.

Analysis of the available data on sensitivity and exposure time, industrial tests, and the introduction of radiographic inspection into different branches of industry have made it possible to determine the optimal thickness of articles made from iron-, titanium-, aluminium- and magnesium-base alloys suitable for gamma-radiography (Table 21). From the table it follows that for the inspection of metals, weldings and castings with walls 60 to 80 mm thick it is most advantageous to employ such radioactive isotopes as Eu^{155}, Tu^{170}, $Eu^{152,154}$, Se^{75}, Ir^{192} and Cs^{137} sources (this largely refers to light alloys). This recommendation is based not only on sensitivity (see Figs. 57-61) and exposure time (see Fig. 35), but also on the fact that it is easier to provide protection from gamma-radiation, as compared with Co^{60}.

However, what has been said is not sufficient to give preference to one or another radiation source, because these sources are practically interchangeable in relation to sensitivity and exposure time or application, depending on metal thickness and density, as for example, Tu^{170} and Eu^{155} for thin-walled articles and Cs^{137}, $Eu^{152, 154}$, Ir^{192} for articles with medium wall thickness.

The technical expediency of isotope application must be supplemented with economic considerations, for the economic efficiency of introducing gamma-radiography into industry is one of the most important criteria to be followed in selecting radioactive isotopes.

Investigations have shown that in choosing the type of radioactive source and its activity consideration has to be given to the specification requirements governing the production of the article, the accepted standards and the operation of inspected articles, maximum reduction of production time and inspection costs. Taking account of thickness it is desirable to inspect articles with the aid of isotopes which would meet specification requirements and incur minimum expenditures.

At the present time, industrial gamma-radiography has found wide application in the following cases:

1) inspection of thick metal articles inaccessible to X-ray inspection;

2) inspection of complex assemblies, welded and cast articles of a design excluding the possibility of X-ray inspection;

3) inspection of circular welds in large-size cylindrical and sphere-shaped welded articles, where X-ray inspection is less efficient, since remote-anode X-ray tubes are not yet employed;

4) inspection of assemblies, welds and castings under field conditions, where the possibility of X-ray inspection is excluded;

5) in all cases where no X-ray equipment is available and it is impossible to practise other inspection techniques.

Source	Most effective inspection thickness, mm				Possible inspection thickness, mm			
	Iron-base alloys	Titanium-base alloys	Aluminium-base alloys	Magnesium-base alloys	Iron-base alloys	Titanium-base alloys	Aluminium-base alloys	Magnesium-base alloys
Ce^{144}	0.5-2	0.5-4	1-8	1-15	0.5-160	0.5-200	1-300	1-500
Eu^{155}	1-10	2-15	5-40	30-150	1-15	2-30	3-60	10-150
Tu^{170}	1-10	2-20	5-50	30-150	1-20	2-40	3-70	10-200
Se^{75}	7-15	10-30	40-150	50-200	5-30	7-50	20-200	30-300
Ir^{192}	10-40	15-70	50-250	100-300	5-70	10-100	40-300	70-400
$Eu^{152,154}$	10-60	15-90	50-250	100-350	5-80	10-120	40-330	70-500
Cs^{137}	20-80	25-100	70-300	150-400	10-120	20-150	50-350	100-500
Cs^{144}	15-65	20-85	60-250	120-350	10-75	15-110	50-300	100-450
Co^{60}	60-200	100-300	250-500	—	30-300	60-400	200-600	300-700

Note: The upper and lower limit of inspected material thickness should be corrected depending on the technical specifications for the article to be inspected and the conditions of inspection.

§ 6. General procedure in gamma-radiography

The following general procedure in gamma-radiography is to be recommended irrespective of the designation of the articles to be inspected, their manufacturing processes, and also irrespective of the inspection requirements, activity and kind of radiation source: 1) preparatory work; 2) exposure; 3) gamma-graph processing; 4) interpretation of gamma-graphs and evaluation of the quality of the inspected article; 5) record keeping and filing gamma-graphs.

Preparatory work includes preparing the article, choice of a radiation source, photographic materials, screens, film-source distance; determination of exposure time, loading holders, attaching the holders to the inspected article and placing the radioactive source.

Preparing an article for inspection. The nomenclature of parts to be subject to gamma-inspection in each industrial enterprise is usually established in accordance with accepted standards.

First, it is necessary to be familiar with the article to be inspected and the quality requirements, to make a sketch of the article indicating dimensions, wall thickness and the material of which the article is made. This would determine the choice of the radioactive source, the exposure set-up, film-source distance, manner of loading the holder and attaching the latter to the article to be inspected.

The article to be inspected must conform to a number of requirements. In the case of a casting it is necessary to remove pouring gates, air gates, frame wire and burrs. Welded articles must be cleaned from slag, sand and other impurities. In welds, surface defects, such as voids, deep cavities, etc., should be eliminated, for they may appear on the processed film and hamper detection of internal defects. During external examination, one must look out for surface cracks, as such defects are not always revealed by radiography. To prevent spoilage of film-loaded paper holders, the parts must be cleaned from oil, grease and other profuse fat coatings.

If a part is to be inspected by sections, the sections must be marked strictly in accordance with the accepted exposure set-up, so as to make possible the exact location of the internal defects after exposure is completed (this marking may be done with a coloured pencil or chalk). Holders and X-ray film placed into holders are marked according to the respective sections of the article to be inspected. Film may be marked by placing lead marker-numerals on any of the two surfaces of the article under inspection (facing the source of film). The markers are attached with paste, plasticine or any other suitable material on the side of the article facing the source or film. The lead markers appear on the gamma-graphs and make possible the identification both of the inspected article and the particular section. The markers must be of different thicknesses, depending on the thickness of the material under inspection and the radiation hardness.

Inscriptions on gamma-graphs may be made with the conventional graphite pencil, for inscriptions of this kind do not wash off the film during the processing. Intensifying screens placed into holders may be properly marked with china ink. Fluorescent light does not pass through china ink and clear inscriptions appear on gamma-graphs. Gamma-graphs may be numbered with the aid of copper plates in which numerals are cut out. Two plates are used: one of aluminium and one of magnetic steel, the latter making it possible to secure the numbering device to the inspected article. With copper plates about 1 mm thick the numerals appear distinctly on gamma-graphs obtained in inspecting 1-10 mm thick steel articles with gamma-rays from Tu^{170} and Eu^{155} sources.

The thickness of the copper plates should be increased when thick-walled articles are inspected with hard gamma-rays. Copper plates may be replaced by plates made from lead with a small zinc content.

Selecting a radiation source. The radiation source for iron-, titanium-, aluminium- and magnesium-base alloys is selected in Table 21, depending on the thickness of the article. The activity of the radiation sources is determined according to the required speed of inspection and protection.

Let us consider the following case as an example. It is necessary to inspect with gamma-rays welded articles made from steel stock 40-70 mm thick. According to the data in Table 21, radiographic inspection of steel articles 40-70 mm thick may be accomplished with $Eu^{152, 154}$, Ir^{192}, and Cs^{137} sources. As the half-life of Cs^{137} is 30 years, the latter is most convenient to handle under workshop conditions. From the point of view of high efficiency of inspection a 20 gram radium equivalent Cs^{137} source would be most suitable. Radiographic inspection may be carried out in a 2×2.5 m concrete room with walls 50 cm thick. The personnel engaged on premises adjacent to the inspection room are not concerned in the inspection work, consequently, outside the room the radiation dose must not exceed 0.005 r per working day. To ensure such a safe radiation dose when using a 20 gram radium equivalent source placed at a distance of 1 m from the concrete walls, the latter must be not less than 70 cm thick. Therefore, in this particular case it is impossible to employ a Cs^{137} source of an activity amounting to 20 gram radium equivalent. The maximum activity of the source which could be employed in the room available for radiographic work is 1 gram radium equivalent. To make it possible to use a 20 gram radium equivalent source, the walls must be built-up to the required thickness.

Selecting photographic materials. It is advisable to use grade "Roentgen X" and "Roentgen XX" film for metal radiography. The storage guarantee term for the film is specified in the certificate glued to the packing case; usually, the guarantee term is for one year. As mentioned above, grade "Roentgen XX" is a higher speed film and

it therefore requires an exposure time of about one half of that required for "Roentgen X" film (if inspection is carried out without fluorescent screens). But high-speed "Roentgen XX" film rapidly loses its properties, it is therefore recommended that film that has been in prolonged storage prior to employment should be checked for fogging.

Owing to its high resolving power, "Roentgen X" film ensures a somewhat better revealment of defects than "Roentgen XX" film. The choice of film for radiographic work depends on the thickness and density of the inspected article, the required exposure time and the degree of defect revealment. Thus, for thin light-alloy articles

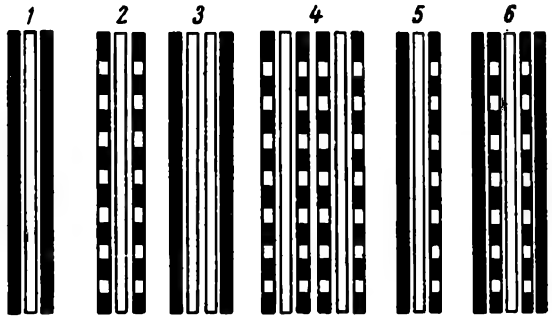

Fig. 73. Holder charging diagrams:
1—film placed between two lead foils; *2*—film placed between two fluorescent screens; *3*—two films placed between two lead foils; *4*—two films placed between fluorescent screens; *5*—film placed between lead foil and fluorescent screen; *6*—film placed between two fluorescent screens and two lead foils

where the revealment of defects is comparatively low even with soft gamma-radiation "Roentgen X" film should be used. "Roentgen XX" film is recommended for the inspection of thick alloys where the efficiency of gamma-radiography depends to a large extent on exposure time.

Loading and placing film holders. Owing to the great variety in the shape of the articles to be inspected, flexible holders, twin envelopes made from black opaque paper or leatherette, have been widely used in industrial radiography. In making and using paper holders, care should be taken not to damage the holders.

Fig. 73 shows various methods of film loading. The film may be placed between two foils. This film loading should be practised in gamma-raying thin heavy alloys and light alloys, when it is necessary to ensure the best revealment of defects, and a reduction in exposure time is not aimed at. Lead, tin and lead-tin foils have found the widest use in radiography. It was mentioned above that the intensifying effect of lead foils depends on gamma-energy, foil thickness and thickness of the material under inspection.

The film may also be placed between two fluorescent screens. This loading of the holder is recommended for cases where it is necessary to ensure the shortest possible exposure time as, for instance, in radiographing cast thick-walled articles. It should be borne in mind that although they ensure a considerable reduction in exposure time (5 to 8 times, as compared with "Roentgen X" film used without fluorescent screens), fluorescent screens somewhat impair the revealment of defects. Fluorescent screens are, therefore, not recommended for gamma-raying thin heavy-metal alloys and light alloys. It is also not advisable to use fluorescent screens with "Roentgen XX" film, for the reduction in exposure time rendered possible by such screens differs only slightly from that obtained with lead foils, while the quality of the gamma-graphs deteriorates.

To avoid the necessity of repeated exposure of especially important articles (units) due to a damaged emulsion, it is recommended in such cases to load two films into one holder.

It is not advisable to use lead foils and fluorescent screens together, for in this case the reduction in exposure time is smaller than in using fluorescent screens without lead foils because the fluorescent screen absorbs the electrons ejected from the lead foil while the quality of the gamma-graphs does not improve.

Holders must be loaded in a photographic laboratory by ruby light or in the dark on a special table, depending on the property of the film. Lead screens must have a smooth surface, free from irregularities. Fluorescent screens must be handled with care, not bent in excess, or handled directly after film developing and fixing work.

The loaded holder is attached to the article set in the proper position for inspection. It should be remembered that the nearer the defects to the film, the better they are revealed.

The design of the devices used to clamp holders is determined by the size and shape of the articles under inspection as well as by the adopted exposure scheme. The devices must ensure a tight and uniform holder-to-article fit. Film holders may be secured in place by means of a fabric band, insulating tape, plasticine and special clamps.

In all cases, a lead sheet 5-6 mm thick must be placed behind the holder (in the gamma-ray direction) to absorb scattered radiation. In radiographing hollow cylinders, the film-loaded holder is pressed against the cylinder wall by means of lead plates and spacers. Flat holders are either placed on a special bench covered with lead sheeting or on a lead sheet of a size not smaller than the exposure field.

Selecting film-source distance and exposure field. The film-source distance is determined by the thickness of the articles under inspection and the required field of exposure. In addition, when selecting a definite film-source distance, the revealment of defects and the change in exposure time with film-source distance are taken into account.

Table 22 gives the diameters for exposure fields, both on the film and on entering the article under inspection, as a function of film-source distance for various gamma-beam divergence angles and different thicknesses of the inspected metal.

Determining exposure time. Exposure time is determined with the aid of charts, depending on the thickness and density of the inspected metal, the activity of the selected radioactive source, the film-source distance, the used film, metal foils and fluorescent screens (see § 3).

Placing the radiation source. The radiation source is set in place after all other preparatory work has been done (the article prepared, holders and markers set, radiation source selected, film-source distance and exposure time determined). In cases where inspection is performed with the aid of special apparatus (see Chapter II dealing with inspection equipment) and the articles to be inspected are relatively small, it is more convenient to arrange the inspected article in relation to the source stored in a protective container. The radiation source is arranged in relation to the inspected article (or vice versa) in a position at which the main gamma-beam would pass through the centre of the film holder. No objects whatsoever may be placed between the source (container) and the article to be inspected.

In cases where gamma-radiography is performed without special equipment, the source must be set in a manner which excludes the possibility of vibration or shifting during exposure, otherwise, the film image will be blurred.

Exposure set-ups. The most diverse exposure set-ups may be practised in gamma-radiography. Cylindrical or sphere-shaped welded (or cast) articles up to 2 m in diameter may be radiographed during one exposure, placing the radiation source inside the article (Figs. 74 and 75), or by sections, at several exposures, placing the source inside or outside the inspected article, as shown in Fig. 76. A weld seam is inspected through two walls, if it is impossible to place the source or holder inside the inspected article.

To inspect several objects at a time, the articles are arranged circumferentially and the radiation source is placed in the centre of the circle, as shown in Fig. 77. When several articles are inspected at a time, the difference in the thickness of the individual articles is compensated for by choosing the respective film-source distance for each thickness, or small parts are removed consecutively, as the exposure time set for the articles expires. The size of a radiographed section of an article should not exceed the values specified in Table 22.

Radiographing an article. The preparatory work having been completed, the article is then exposed to gamma-rays. If the inspection is carried out with the aid of a special apparatus, the source is handled and the gamma-beam directed in accordance with the

Table 22

Diameters of Exposure Field Depending on Film-Source Distance

Gamma-beam divergence angle, degrees	Thickness of inspected metal, mm	Diameter of exposure field on film and on entering inspected articles depending on film-source distance, cm			
		25	50	75	100
30	Unexposed film	13.5	27.0	40.0	54.0
	20	12.5	26.0	39.0	52.5
	40	11.5	25.0	38.0	51.5
	60	10.0	24.0	37.0	50.5
	80	9.0	22.5	36.0	49.5
	100	8.5	21.5	35.0	48.0
	150	5.5	18.5	32.0	46.5
	200	2.5	16.5	29.0	45.5
40	Unexposed film	18.0	36.0	54.0	72.5
	20	16.5	35.0	53.0	71.5
	40	15.5	33.5	51.5	69.5
	60	14.0	32.0	50.0	—
	80	12.5	30.5	48.5	—
	100	11.0	29.0	47.5	65.5
	150	7.5	25.5	43.5	62.0
	200	3.5	22.0	40.0	58.0
50	Unexposed film	23.5	47.0	70.5	93.0
	20	21.5	47.0	68.0	91.5
	40	19.5	43.0	66.5	89.5
	60	17.5	41.0	64.5	88.0
	80	16.0	39.0	62.5	86.0
	100	14.0	37.0	60.0	84.0
	150	9.5	32.5	55.0	79.0
	200	4.5	28.0	51.5	84.0
60	Unexposed film	29.0	57.5	86.5	115.0
	20	26.5	55.5	84.5	110.5
	40	24.5	53.5	82.0	109.5
	60	22.0	51.0	80.0	108.5
	80	19.5	48.5	77.5	106.0
	100	17.5	46.0	75.0	104.0
	150	11.5	40.5	69.5	98.5
	200	5.0	35.0	63.5	92.5
70	Unexposed film	35.0	70.0	105.0	140.0
	20	32.5	67.5	102.5	137.5
	40	29.5	65.5	100.0	134.5
	60	27.0	61.5	96.5	132.5
	80	24.0	59.0	94.0	129.0
	100	21.0	56.0	91.5	126.0

Continued

Gamma-beam divergence angle, degrees	Thicknees of inspected metal, mm	Diameter of exposure field on film and on entering inspected articles depending on film-source distance, cm			
		25	50	75	100
70	150	14.0	42.0	84.0	129.0
	200	7.0	42.0	77.0	115.0
80	Unexposed film	41.5	83.0	124.0	166.0
	20	38.5	80.5	122.5	164.5
	40	35.0	77.5	119.5	161.5
	60	32.0	74.0	116.0	158.0
	80	28.5	70.5	112.5	154.5
	100	25.0	67.5	109.0	151.0
	150	17.0	58.5	100.0	142.5
	200	8.5	50.5	92.5	134.5
90	Unexposed film	50	100	150	200
	20	46	96	146	196
	40	42	92	142	192
	60	38	88	138	188
	80	34	84	134	184
	100	30	80	130	180
	150	20	70	120	170

operating instructions issued for the apparatus. When operating with low-activity gamma-sources which have no special source manipulator, the source is handled with the aid of special-type tongs which make it possible to manipulate the source rapidly, so that the radiation dose received by the attending worker will not exceed the maximum permissible dose per working day. After the source is bared, the attending personnel must immediately move away to a safe distance. When the exposure is completed, the source is placed back into the protective container. The holder is then removed from the article and the film processed.

Photographic processing of gamma-graphs. The personnel of X-ray laboratories are sufficiently familiar with the photographic processing of X-ray films. However, in many cases radiography is carried out in places where no X-ray laboratories are available and special personnel must be trained. Therefore, photographic processing of gamma-graphs is considered here in detail.

Photographic processing of gamma-graphs includes: development, spray rinsing, fixing, final washing, and drying. The processing quality depends on the developer formula and the conditions of de-

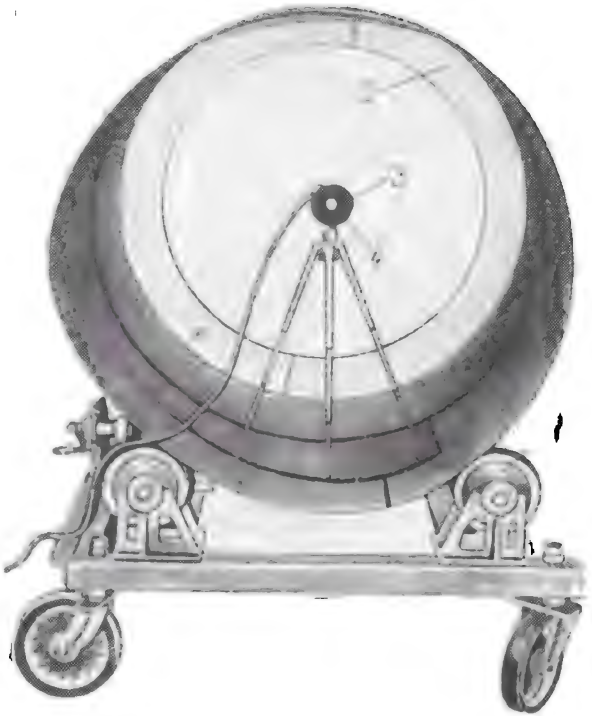

Fig. 74. Arrangement of the radiation source at the centre of a cylindrical article making possible examination of a circular weld in one exposure:
1—stand; 2—welded joint; 3—coordinator (manipulator); 4—radiation source

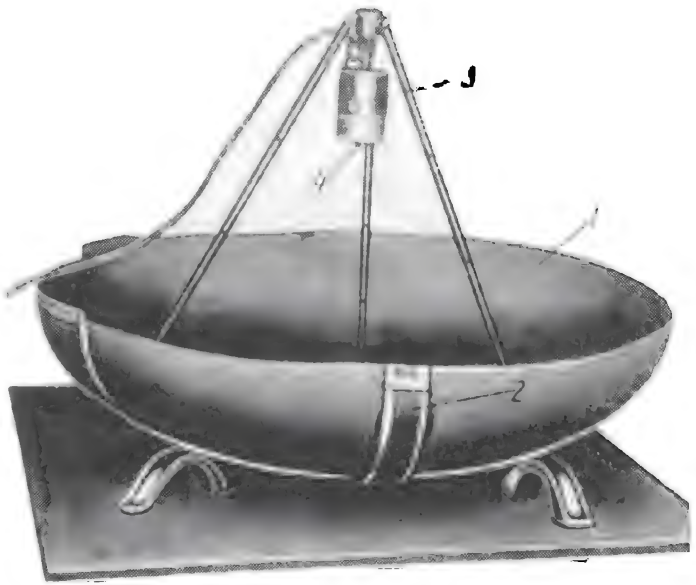

Fig. 75. Examination of a weld in a sphere-shaped welded article in one exposure:
1—welded article; 2—film-charged holder and holder clamping device; 3—coordinator-manipulator; 4—radiation source

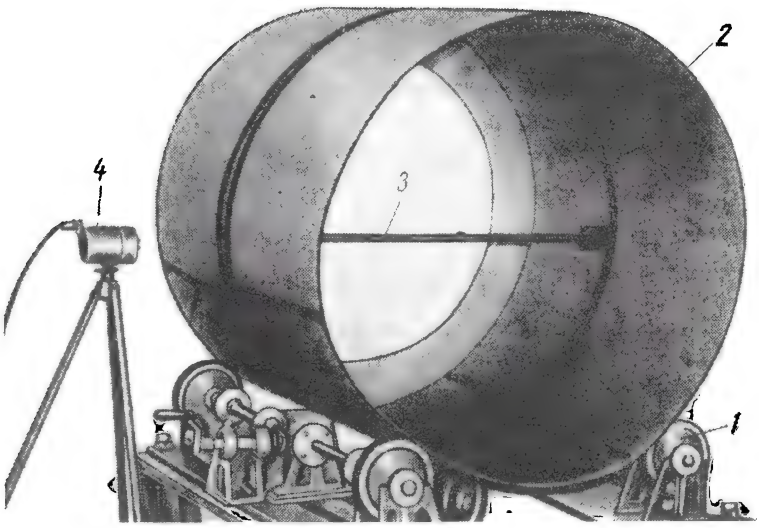

Fig. 76. Examination of a weld section of a cylindrical welded article, placing the gamma-source outside the inspected object:
1—stand; *2*—welded unit; *3*—holder clamping device; *4*—manipulator with radiation source

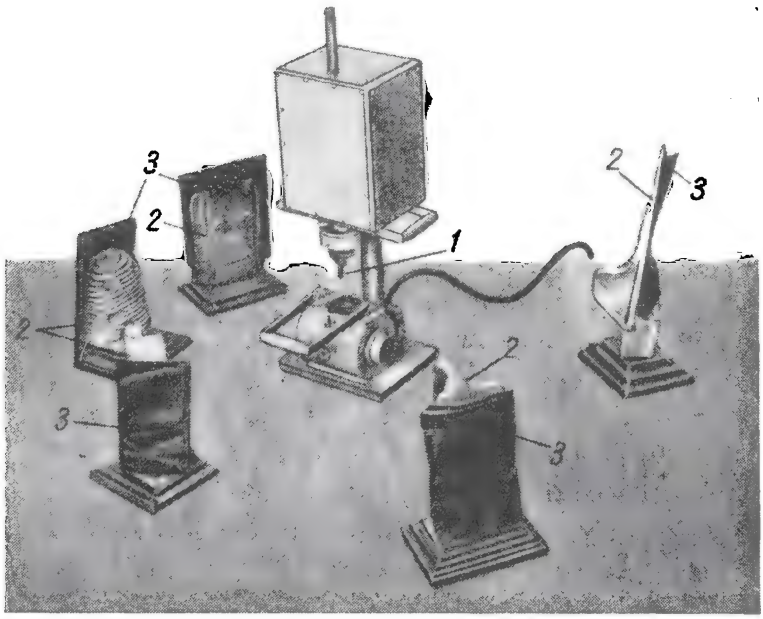

Fig. 77. Simultaneous inspection of several cast articles:
1—radiation source; *2*—part; *3*—film charged holder

velopment. X-ray film producers recommend the following developing solution:

Warm water (50-52°C), cu cm	500
Metol, g	2
Hydroquinone, g	8
Sodium sulphite, crystalline, g	178
or anhydrous sodium sulphite, g	88.5
Sodium carbonate, crystalline, g	118
or anhydrous sodium carbonate, g	43.5
or potash, g	57
Potassium bromide, g	5
Cold water (added to full volume), cu cm	1,000

This metol-hydroquinone developer is quite satisfactory for gamma-graph processing. Its most important component is the developing agent which acts as a reducing agent, transforming silver bromide (ionised) into metallic silver. In the specified solution, hydroquinone is the principal developing agent. Hydroquinone by itself develops slowly and unsharply; the chemical is very sensitive to temperature and the development proceeds slowly, if the solution temperature is below 15°C. Hydroquinone developers must be used at temperatures from 19 to 21°C. The metol component of the solution accelerates development; metol is a rapid and soft developing agent which brings out image details well at the gamma-graph density ensured by the hydroquinone. When development is carried out with metol alone, the image appears rapidly, but image density is insufficient; so, metol is used together with hydroquinone which ensures higher densities, but diminishes the definition of image details.

The alkali component actuates the developability of the solution and accelerates development. Without the alkali component the metol-hydroquinone developer lacks developability.

The sodium sulphite protects the developer from rapid aerial oxidation and participates in the reduction of the colloidal silver by the developing agent. An oxidised developer rapidly loses its properties and acquires a characteristic colouring. With sodium sulphite added the developer may be stored for a long time.

The potassium-bromide component is added to diminish fog. When in normal concentration, the potassium bromide does not affect development speed, but a large potassium-bromide component acts as a restrainer.

The developer components are dissolved in boiled water or distillate at a temperature not exceeding 52°C; at a higher temperature the developer loses some of its activity due to disintegration of the developing agents.

The components are dissolved in the order listed above, each component being introduced into the solution after the preceding component has been fully dissolved.

The chemicals are dissolved in 500-600 cu cm of warm water, then cold water is added to make one litre of the developing solu-

tion. It is not advisable to filter the solution, or this results in oxidation and loss of valuable properties. Impurities penetrating into the solution are removed by settling. Developing solutions should be kept in corked glass bottles.

The composition of a developer changes gradually in the course of usage, for a certain portion of the developing agents is spent in the process of transforming silver bromide into metal silver. In addition, aerial oxidation of the developer occurs. As a result the activity of the developer diminishes, as the number of the developed films increases.

Table 23 indicates the number of films that is possible to develop in one litre of the developing solution.

Table 23

Number of Films Developed in 1 Litre of Developer

Size of "Roentgen X" film, cm	Total number of films	Number of films of different lots *		
		I	II	III
13×18	46	26	12	8
18×24	28	14	6	8
24×30	15	8	4	3
30×40	9	5	2	2

* Lot I films placed into a fresh developer at 18-19°C are developed in 5 min, lot II films placed into a partially exhausted developer are developed in 6 min, and lot III films—in 7 min.

It is advisable in order to maintain the activity of the primary developer to use a replenishing solution. The composition of both developer and replenisher are given in Table 24.

The replenishing solution is used in the following manner. The level is marked on the developer bottle. The solution is poured into a developing tank and 10-12 films of any size are developed; then, the developer is poured back into the bottle and the replenishing solution added to the initial level. This replenishment is based on the rate at which one litre of the primary developer becomes exhausted. Evaporation losses in the primary developer are compensated for by adding water to the initial level, the replenishing solution not being used for this purpose. The employment of replenishing solutions gives a 40% saving in chemicals without impairing the quality of film processing.

Gamma-graphs are developed in a dark room, generally in ruby light, provided the type of film permits such development. The development is carried out in trays or deep tanks. Sufficient developer solution should be poured into a horizontal tray. The film is sub-

merged in the developer and turned several times in succession. In doing so, care must be taken that no air bubbles remain on the

Table 24

Composition of Developer and Replenishing Solutions

Components	Primary developer solution	Replenishing solution
Warm water (52°C), cu cm	600.0	600.0
Metol, g	2.2	4.0
Hydroquinone, g	8.8	16.0
Sodium sulphite, crystalline, g	144	144
or anhydrous sodium sulphite, g	72	72
Sodium carbonate, crystalline, g	130	130
or anhydrous sodium carbonate, g	48.3	48.3
or potash, g	63	63
Potassium bromide, g	4	—
Sodium hydrate, dry, g	—	7.5
Cold water (added to required volume), cu cm	1,000	1,000

film, otherwise, spots will form on it. Uniform development is ensured by rocking the tray periodically. One must avoid removing the film from the bath too often for viewing, as this results in film oxidation and fogging. Care must be taken that films do not stick together when several films are developed together.

For deep-tank development the film is secured in a special frame and submerged in the developer-filled tank. Air-bubble traces are removed several times by moving the frame and film up and down below the developer level. In deep-tank development films do not stick together, for they are separated by clamping frames. The developer lasts longer than in horizontal bath development. In deep-tank development 12 litres of the developer are sufficient to process 150 films, 30 × 40 cm in size.

The quality of gamma-graphs depends to a considerable extent on the development time and the developer temperature. A temperature of 19-21°C is considered normal for metol-hydroquinone developers. The activity of the developer is low at temperatures below 19°C and the rate of development is excessive at temperatures above 21°C.

Table 25 gives the development time for a metol-hydroquinone developer at various temperatures.

The metol-hydroquinone developer may be used at 24°C, provided crystalline sodium sulphate is added, 120 g per litre. The development time for such a hardening developer is indicated in Table 26.

Table 25

Variation of Development Time with Temperature

Film	Development time, min, at a temperature, °C								
	16	17	18	19	20	21	22	23	24
"Roentgen X"	8	7.5	7	6.5	6	5.5	5	4.5	4
"Roentgen XX"	12	11.0	10	9.5	9	8.5	8	7.0	6

Note: Grade "Roentgen XX" film requires a longer development time, for its emulsion is thicker, compared with that of "Roentgen X" film.

Table 26

Variation of Development Time with Temperature for a Metol-Hydroquinone Developer with a Sodium Sulphate Addition

Film	Development time, min, at a temperature, °C						
	24	25	26	27	28	29	30
"Roentgen X"	6	5.5	5	4.5	4	3.5	3
"Roentgen XX"	9	8	7	6.5	5.75	5	4.5

The development time specified for gamma-graphs must be strictly observed, and the films should not be examined in ruby light during development. The films are removed from the developer 15-20 sec ahead of the set time and rapidly rinsed in running water, so that the remaining developer is removed from the film. If a hardening developer containing a sodium sulphate additive is used, it is necessary to place the films for 2 min in an intermediate bath of the following composition:

Chrome alum, g	30
Sodium sulphate, crystalline, g	120
Water (to the required volume), l	1

The films are then fixed in an acid fixing bath of one of the following recommended compositions:

Boric acid fixing bath

Warm water, cu cm	500
Hyposulphite, g	400
Sodium sulphite, crystalline, g	50
Boric acid, g	40
Cold water (to required volume), cu cm	1,000

Acetic acid fixing bath

Warm water, cu cm	500
Hyposulphite, g	400
Sodium sulphite, crystalline, g	50
Acetic acid (30%), cu cm	40
Cold water (to required volume), cu cm	1,000

Sometimes fixing is done with hyposulphite only, but the fixing bath colours gradually as the developer left on the film gets into the bath and the fixed films acquire a yellow tint. An acid fixing bath stays transparent for a long time, for the acid and sodium sulphite neutralise developer residues. To avoid the appearance of yellow spots on gamma-graphs, care must be taken that films do not float to the surface of the bath where air contact is possible, and film sticking must be prevented.

The fixing process lasts 10-12 min (doubled development time) at a bath temperature of 15-18°C. Gamma-graphs fixed insufficiently cannot be preserved for a long time.

The fixed gramma-graphs are rinsed in running water for 20-25 min then allowed to dry thoroughly prior to proceeding with the interpretation of the gamma-graphs in order to evaluate the quality of the inspected articles.

The fog density of a given film is determined by submerging several strips of unexposed film into a developing bath for 4, 5, 6, 8 and 10 min. These strips are fixed, rinsed and dried, then the fog density of the film is determined with the aid of a photometer. It is not recommended to use film, the fog density of which D_0 is 0.25, this density having been obtained by developing film strips for 6 min in a developing solution at 20°C.

A heavy fog may be the result not only of poor-quality film, but of an excessively bright ruby light, or the presence of slits through which light passes. The ruby light is checked by using it in the dark room to expose sections of one and the same film for various periods of time (1, 2, 4 and 8 min). The exposed film is normally developed in complete darkness. The ruby light is considered fully reliable, if there is no difference in the density of the individual film sections, and the ruby light is rejected outright, if there is any difference in the densities at exposures of 2 min and less.

Interpretation of gamma-graphs and evaluation of the quality of inspected articles. The evaluation of the quality of an article with the aid of its gamma-graphs is the most important stage in gamma-radiography. The interpretation aims at determining the reasons for the varying density on the gamma-graph.

The interpretation of the dry gamma-graphs is carried out on a negative viewer or illuminator. The illuminator is a device fitted with lamps covered with a frosted glass plate and a scattered (uniform) light. The gamma-graph is placed on the plate and examined in transmitted light.

The illuminator must conform to the following requirements:

1. It must allow of wide-range control of light intensity, and ensure uniform illumination of the frosted glass plate; the normal density of a dry negative may vary from 1 to 2 and an illuminator without light intensity control must produce a light of an intensity allowing inspection of images within the specified density range;

to evaluate the density of a negative, it is recommended to have available a set of standard densities.

2. The frosted glass of the illuminator should allow viewing of 30 × 40 cm gamma-graphs.

3. The illuminator should incorporate a shutter which will produce a lighted field of a size equal to that of the gamma-graph.

In viewing a gamma-graph it is necessary to distinguish the defects due to poor quality of the film or improper film handling from the actual defects of the inspected material.

Tails running along the entire negative or round spots are usually easily identified and leave no doubt.

Sometimes, in looking for cavities and inclusions in castings or welds spots of different density and irregular shape as well as small round spots due to reasons which have nothing to do with metal quality may be taken for images of defects. Doubts of this kind are removed by repeated inspection or by loading two films into one holder. If the second negative is free from such spots, it may be assumed that on the first negative they were due to film defects or other reasons not related to the inspected material.

The inspection certificates for ingots, cast and welded articles are drawn up in accordance with specification requirements for a given article. The quality of an article is appraised if:

1) the inspected article or reinforced weld distinctly appears on the gamma-graph along its entire length;

2) the markers are visible;

3) the image is free from spots, scratches, fingerprints or the white deposit due to poor washing and other film defects.

Record keeping and the filing of gamma-graphs.

Proper attention must be devoted to record keeping and the filing of gamma-graphs, for frequently the need arises to find a filed gamma-graph of a certain section of a previously inspected article (part).

The following data on gamma-graphs are usually entered into a special register: name and number of inspected article, gamma-graph number, exposure set-up, film-source distance, activity of radioactive source employed, grade of film and type of intensifying screens, exposure time and the conclusion regarding the quality of the inspected article based on gamma-graph interpretation.

The storage time for gamma-graphs is fixed according to the nature of the inspected articles and the operating conditions.

§ 7. Examples of industrial gamma-radiography

Gamma-radiography of industrial products makes it possible to reject seriously defective articles and to perfect the processes which make for the manufacture of flawless articles. Articles which are subjected to gamma-radiography may be divided into various categories, depending on the technological processes employed to manu-

facture the articles (for instance, welded, cast, rivetted articles, etc.). Assembled units and aggregates may be subjected to gamma-inspection as well.

Inspection of welded and soldered joints. The following defects may be encountered in welds: lack of fusion (incomplete penetration), porosity, slag inclusions and cracks.

Porosity is one of the defects most common in welds. The pores may be filled with gas or slag, their diameter varying from the microscopic to 3 mm. Large pores are usually classified as cavities or blowholes. The distribution of pores in the built-up metal may vary in character from individual pores to uniform scattering of pores over the entire welded section, or there may be heavy accumulations in one part of the seam. A great number of pores, evenly distributed along the entire length and cross-section of a weld (more than five per 1 sq cm approximately), is often identified as a net of pores. Pores and slag inclusions appear on gamma-graphs as dark roundish spots. In most cases it is not possible on gamma-graphs to distinguish gas-filled pores and cavities from pores and cavities filled with slag. But this is of minor importance, for defects of both kinds almost equally diminish the working cross-section, and, therefore, the strength of a weld.

Lack of fusion is very frequent in welds. This imperfection may be revealed as lack of fusion between the parent and filler metal, lack of fusion along the edges, and lack of fusion between individual beads of the built-up metal.

Lack of fusion diminishes the working (effective) cross-section of a weld and gives rise to local stresses which are particularly dangerous for a fluctuating and dynamic load. Lack of fusion along the welded seam is most dangerous, such a defect being equivalent to a crack.

On gamma-graphs, lack of fusion of a different nature appears as regular dark lines of a different density, depending on the length of the defect. Location of lack of fusion in a weld depends on the nature of the welded joint. In open square butt joints (Fig. 78,*a*) or in open and closed single-V butt joints (Fig. 78,*b*, *c*) the most probable defect is lack of fusion at the root of the weld. Lack of fusion may also be detected along weld sides. Lack of root fusion is detected best when the film is placed on the side of the root and the direction of inspection is perpendicular to the weld (Fig. 78, *a*, *b*), this being called perpendicular radiography of a weld. Other weld defects such as pores and slag inclusions are also effectively revealed when such an exposure set-up is adopted. In the case of open square butt joints (Fig. 78,*d*) the most probable defect is lack of fusion at the centre of the weld, while lack of fusion in open double-V joints appears as illustrated in Fig. 78,*e*,*f*, at the root. Since both joints are symmetrical, the film may be placed on either side of the seam. The direction of inspection must be parallel to the perpendicular to the weld axis

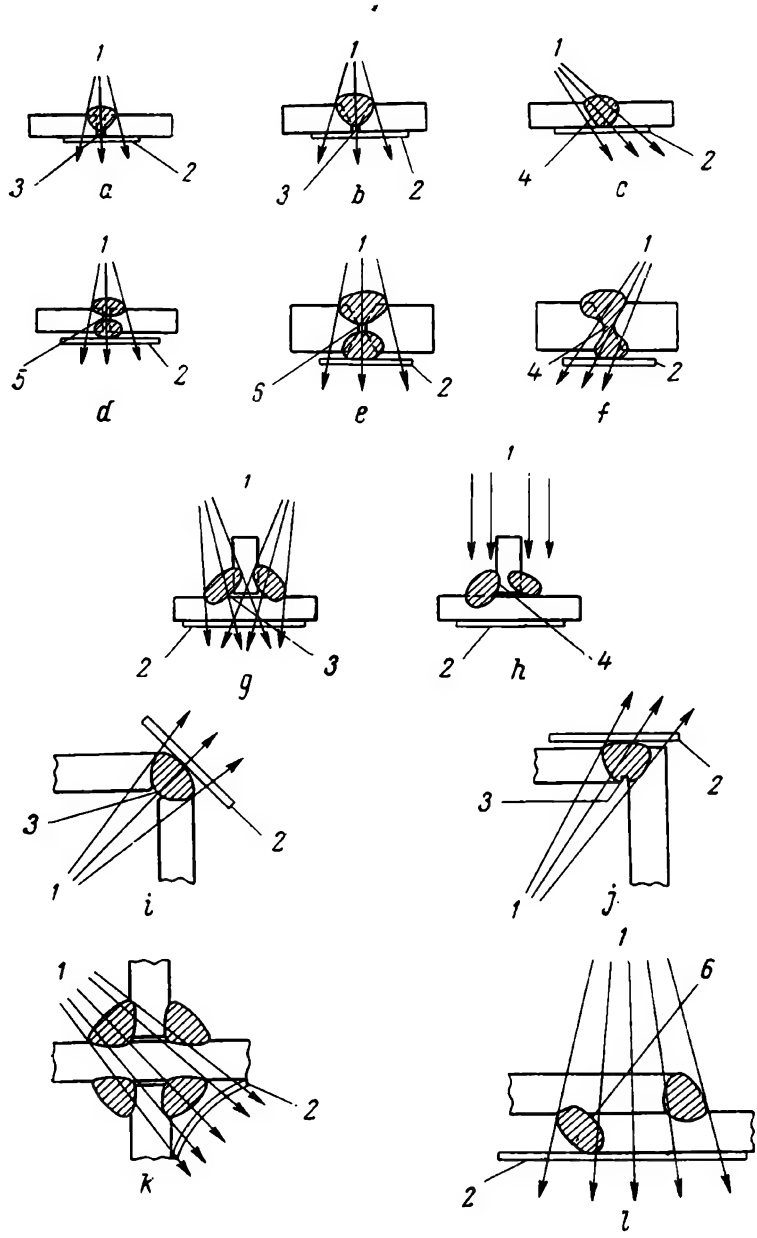

Fig. 78. Different exposure set-ups for welds:

1—radiation beam; *2*—holder; *3*—lack of root fusion (incomplete penetration); *4*—lack of side fusion; *5*—lack of fusion at centre of weld; *6*—lack of root fusion; *a*—one-sided open square butt joint; *b*—single V-butt joint; *c*—single V-butt joint with lack of side fusion; *d*—open double-joint; *e*—closed double-V joint; *f*—double-V joint with lack of side fusion; *g*—square tee-joint; *h*—square tee-joint; *i*—closed corner joint; *j*—bevel corner joint; *k*—closed double tee-joint; *l*—lap joint

(Fig. 78,*d*, *e*), as in the example treated above. When perpendicular gamma-raying is practised, lack of side fusion is far less well detected than lack of fusion at the root and centre of the weld. In such a case, lack of side fusion may be detected by radiographing along the welded surfaces in two stages, as illustrated in Fig. 78,*c*, *f*.

In square and bevel tee-joints, defects such as lack of root fusion and lack of side fusion are most often encountered. It is not easy to inspect such joints by gamma-radiography. Incomplete fusion at the root of a tee-joint is best detected by directing the central beam at a 10-15° angle to the surface of the vertical plate (Fig. 78,*g*). Such an exposure set-up also makes possible the detection of other faults, such as pores and slag inclusions. When a weld is thus inspected, lack of side fusion appears poorly in most cases. It is better to inspect such seams in the direction of the vertical web (Fig. 78,*h*).

In corner joints, as well as in butt joints, incomplete fusion at the root is very frequent. It is convenient to inspect plain corner joints by directing the central beam at a 45° angle to the surface of the plates; in such a case the film-loaded holder is arranged perpendicularly to the direction of the central beam (Fig. 78,*i*). For double bevel corner welds lack of side fusion may be detected by radiographing the joint as illustrated in Fig. 78,*j*.

Double-tee or cross welds are inspected as shown in Fig. 78,*k*. The effect of scattered radiation on the film is reduced by employing lead screens. In lap joints, defects such as incomplete fusion at the root, pores and slag inclusions, are detected most effectively when the gamma-rays are directed along the line perpendicular to the jointed plates (Fig. 78,*l*). These joints may also be radiographed by directing the beam at a 30-45° angle to the perpendicular.

Cracks cause a greater concentration of stresses than any other defect. In welds the cracks may be located in the built-up metal and in the transition zone. Gamma-radiography reveals only cracks the size of which falls within the limits of sensitivity of this technique of flaw detection. Cracks formed in the course of welding special steels or during the heat treatment of welds made from these grades of steel do not appear on gamma-graphs. Detection of longitudinal cracks in butt welds also presents considerable difficulties. If the central gamma-ray beam is directed perpendicularly to the seam surface, the direction of the cracks coincides with that of the rays, and the cracks may be detected. But, if the gamma-ray beam is directed at an angle, these cracks may not appear on the radiograph, for the size of the cracks in this direction may happen to be less than the sensitivity limit of gamma-radiography.

In order to detect longitudinal cracks in beads of tee-joint seams and in lap joints, it is most advantageous to direct the gamma-rays along the angle bisector.

Very often there are several defects in a weld, such as lack of fusion and pores, lack of fusion and cracks. The images of individual

defects may be superimposed on the gamma-graphs and this may lead to an incorrect estimation of the quality of the weld.

Large articles and articles of a complex shape should be examined in parts, in individual sections, accessible from the point of view of the correct arrangement of the gamma-ray source and film. For the purpose of inspection a complex welded unit should be divided into sections in a manner permitting to radiograph individual welds of the unit in accordance with the exposure set-ups illustrated in Fig. 78.

Of the total volume of welded joints a great proportion falls to the share of pipelines, such as steam pipes, boiler feed pipes, heating systems, gas mains, oil pipelines, etc. As stated above, three principal source-and-film set-ups may be used to inspect welded joints of pipelines: gamma-raying from the inside, gamma-raying from the outside through one wall; and gamma-raying through two walls simultaneously.

Gamma-raying from the inside offers the best possibilities, for, when the gamma-source is positioned at the centre of the pipe or reservoir, it is possible to radiograph the entire annular seam during one exposure or sections of several longitudinal seams (the seam is embraced by the film on the outside). In addition, the walls of the vessel partially absorb gamma-rays and, as a result, irradiation of personnel diminishes. The radiation source may be placed inside the vessel either with or without the container, as illustrated in Fig. 79. In the latter case the source is arranged in the required position with the aid of a manipulator or it is secured in a special holder in the centre of a sphere or pipe, as the case may be. When gamma-raying is carried out from the inside, the radiation source may be arranged not in the centre of a vessel, but nearer to the examined section, but in this case the difference in the film-source distances, measured in the centre and at the edges of the film holder, should not exceed 20-30 mm.

Pipes or spheres are radiographed from the outside in cases, when for one or other reason it is impossible to place the radiation source inside the vessel. When annular welds are inspected from the outside, it is possible to radiograph only a small section of the weld during a single exposure (see Fig. 76); therefore, this method is less efficient, compared with inspection from the inside (see Figs. 74 and 79). Radiography through two walls is practised in extreme cases, when it is not possible to inspect the object through one wall, for instance, because of the small diameter of the inspected object, or when it is not possible to drill a hole to enable the radiation source to be set up inside the pipeline. When such a set-up is adopted, the film-source distance is set equal to 1.5-2.0 pipe diameters. In order to prevent superimposition of the top-section image upon that of the bottom section, the radiation source is placed so that the angle between the beam and the weld axis is not more than 10° (Fig. 80).

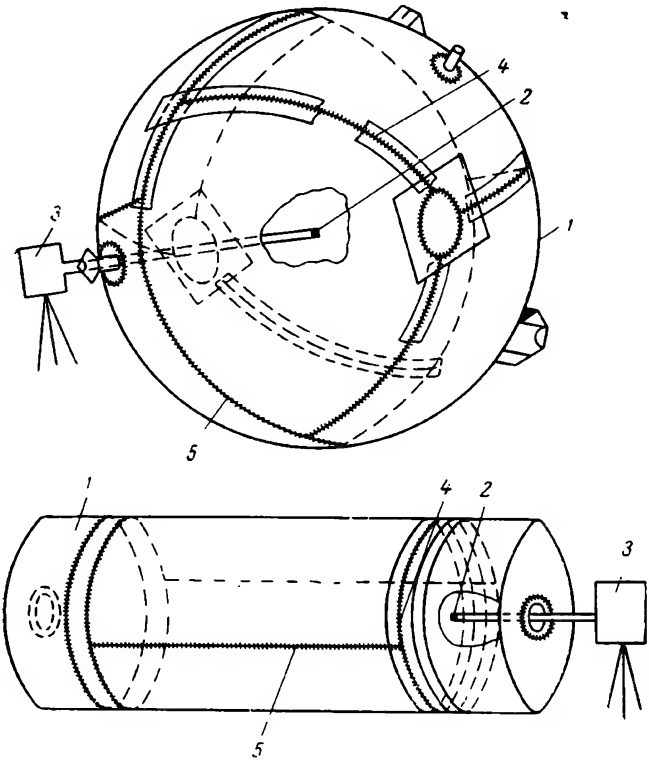

Fig. 79. Exposure set-up for cylindrical and sphere-shaped articles:

1—examined object; *2*—radiation source; *3*—manipulator; *4*—film-loaded holder; *5*—weld

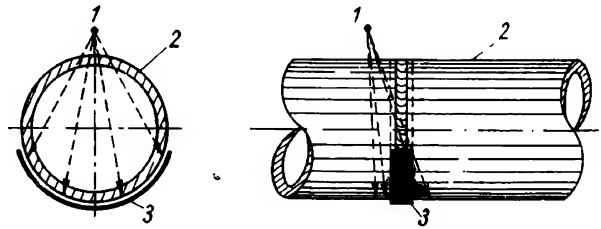

Fig. 80. Exposure set-up practised in radiographing a circular pipe weld through two walls:

1—radiation source; *2*—welded pipe; *3*—film-loaded holder

A circumferential seam is radiographed in this way in several stages. The part is turned through a certain angle around its longitudinal axis for each exposure. The number of radiographed sections depends upon the outer diameter of the inspected cylinder and its wall thickness; however, the weld ought to be divided into not less than four sections, if a 100% inspection of the weld is practised.

If thick-walled tubes of a large diameter are radiographed through two walls, the radiation source may be placed directly on top of the seam reinforcement. In such a case the top section of the seam will not appear on the radiograph. The entire annular seam is radiographed in several stages, as in the preceding case.

Welds may be radiographed with the aid of different radioactive isotopes, the choice of a particular isotope depending upon the thickness of the seam and density of the metal.

Welding defects detected by means of X-ray radiography may also be revealed with the aid of gamma-radiography, provided the radioactive isotopes and the exposure set-ups are correctly chosen. In practice, the length of the weld to be inspected is determined by the nature of the article. In addition, it has to be borne in mind that spots where circumferential welds mate longitudinal welds should be inspected without fail since formation of defects such as cracks and lack of fusion in these spots is most probable.

Figs. 81 and 82 show gamma-graphs of welded steel and duralumin articles with typical welding defects.

In soldered (or brazed) joints as in welds defects such as lack of fusion and cracks are most frequent. On gamma-graphs lack of fusion appears as a spot darker than the soldered seam, and cracks—as dark lines.

The technique of radiographing soldered seams is similar to that practised for the inspection of welded joints. The direction of gamma-raying is usually selected so that the central beam is perpendicular to the direction of the joint. As an example, Fig. 83 shows the radiograph of a soldered seam executed on a flame tube. The detected flaws are a crack and lack of fusion.

Quality requirements for welds executed by means of various welding techniques on parts manufactured from all weldable materials and alloys are fixed by the respective standards or specifications covering welded articles.

Radiography of ingots and castings. The following defects are frequently encountered in ferrous and non-ferrous metal ingots and castings: gas cavities, shrinkage cavities and looseness, sand and slag inclusions, cracks and junctions. A gas cavity is a void in the metal with a correct sphere-shaped inner surface sometimes covered by an oxide film. Depending upon the reasons for the formation of gas cavities, the latter are concentrated in groups at individual sections or are distributed over the entire ingot or casting. Sand and slag inclusions are voids in the metal, partially or entirely

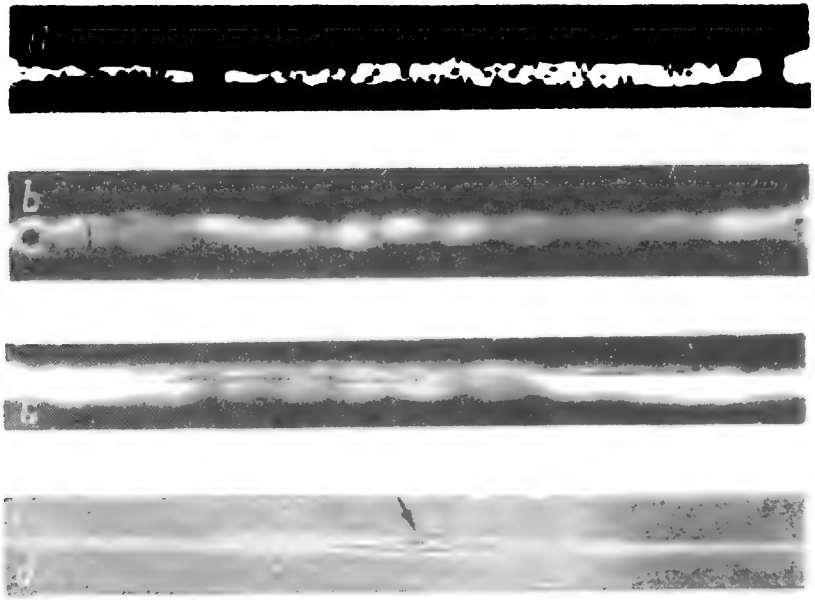

Fig. 81. Eu^{155} gamma-graphs of steel welds 4 mm thick, including reinforcement (*a*, *b*) and duralumin reinforced welds 4 mm thick (*c*, *d*) Porosity (*a*), cracks (*b*), chain of blowholes (*c*) and crack (*d*) appear on the gamma-graphs

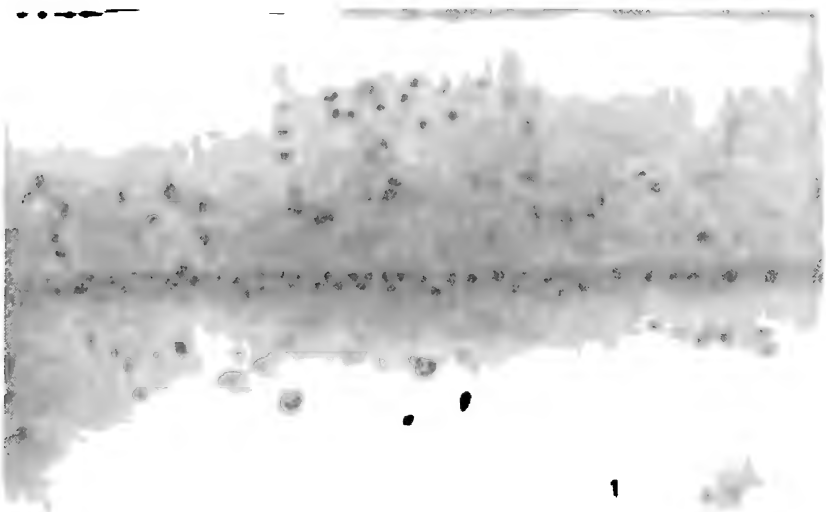

Fig. 82. Gamma graph of grade 30ХГСНА steel weld 80 mm thick (Cs^{137} source) revealing the presence of lack of fusion, porosity and shrinkage cavities in the parent cast material

filled with sand or slag. Shrinkage cavities are voids of various sizes and of most varying shapes, having a rough surface of a coarse crystalline structure. Shrinkage cavities appear as individual and group formations; usually, they are located in the solid sections of a casting near to spots where thick sections develop into thin sections. Cracks are most often encountered in spots where the cross-section of a casting changes abruptly; they are considered as the gravest kind of spoilage.

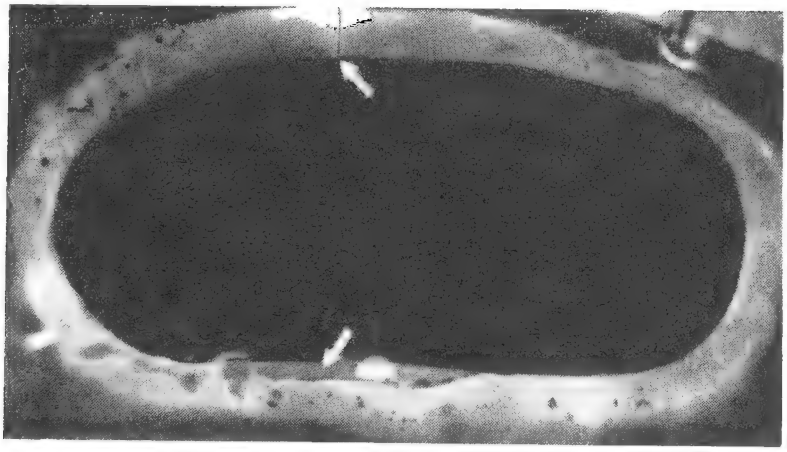

Fig. 83. Gamma-graph of soldered flame tube made of a heat resistant alloy 2.5 mm thick (Eu^{155} source). Lack of fusion and crack in the soldered seam are revealed

A junction formed as the result of nonmonolithic adherence of solidified metal flaws, appears on the surface of a casting as a seam with defective edges. When ingots and castings are inspected by means of gamma-radiography, gas and shrinkage cavities as well as sand and slag inclusions are reliably detected. On gamma-graphs gas cavities appear as circular black spots and shrinkage cavities as black spots of most varying outlines and sizes; sometimes these spots are lengthened at the end and blurred.

Sand and slag inclusions appear on gamma-graphs as spots and points of irregular shape, but not as dark as gas and shrinkage cavities.

Gamma-radiography makes it possible to detect cracks in castings if the direction in which the cracks run coincides with that of the gamma-rays, and provided the cracks are of a sufficient width and depth. Thus, some cracks may remain unrevealed by gamma-radiography. Defects such as loosenesses and junctions are also poorly detected.

Inspection of ingots is of great importance, for defective ingots are not allowed to be subjected to further processing. An ingot defect may be exactly located by means of a double-exposure technique providing two mutually perpendicular projections. Fig. 84 shows

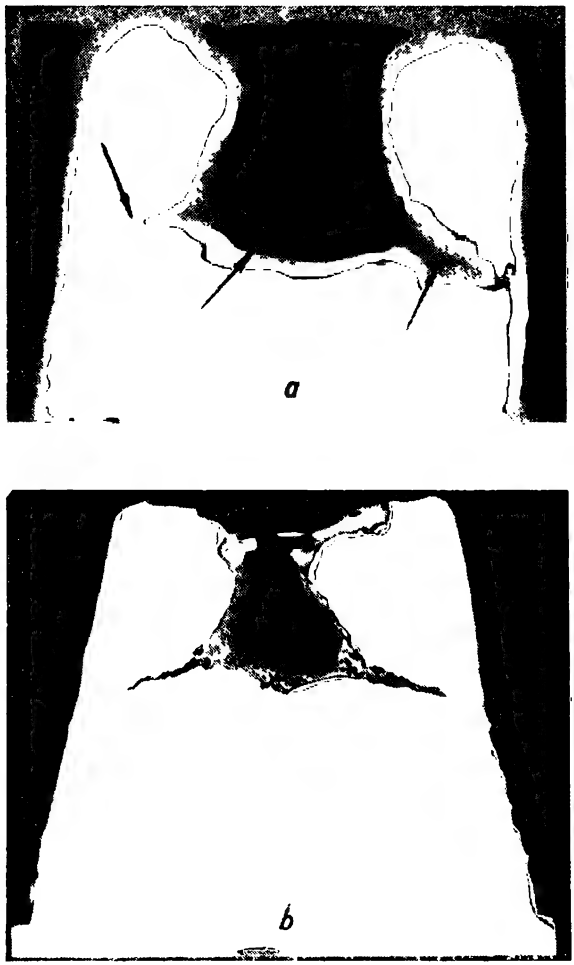

Fig. 84. Gamma-graph of the head section of an ingot showing a shrinkage cavity (*a*); cross-section over the defective spot (*b*)

a gamma-graph and the cross-section of the head discard of an ingot weighing about 500 kg. The gamma-ray source employed was a Co^{60} preparation of an activity of 50 gram radium equivalent.

Exposure set-ups for castings are chosen so as to inspect objects through one wall only. Sections of a casting in which defects are most

frequently encountered, and also heavily-loaded sections, are inspected first. Large castings of complex configuration are inspected in sections. The gamma-beam is directed at a certain angle depending on the conditions of inspection. When inspecting hollow castings, it is an advantage to place the radiation source inside the article. Fig. 85,*a* illustrates the exposure set-up used to inspect a cast tee-piece in sections. Having placed the radiation source inside the article in position *I*, the entire sphere-shaped section of the tee-piece

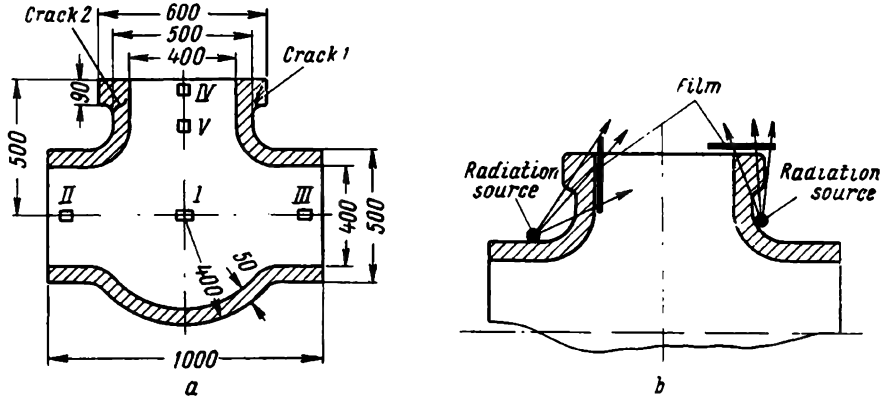

Fig. 85. Exposure set-up adopted to radiograph a cast tee-piece (*a*) and arrangement of film holders (*b*) to detect cracks near flanges of the tee-piece

is radiographed at one exposure. To radiograph side branches, the radiation source is placed inside the branches along the horizontal axis, first in the left-hand branch (position *II*), then in the right-hand branch (position *III*). To radiograph the top branch, a fourth exposure is required, the radiation source being placed now at the centre of the branch, along the vertical axis (position *IV*). It is not possible to radiograph the flange and branch at one exposure, for the flange of the top branch is about twice as thick as the walls of that branch. In such a case another radiograph is taken, placing the radiation source into position *V*. It should be borne in mind that some defects, for instance, cracks located at spots where thin sections develop abruptly into thick ones, cannot be detected if this exposure set-up is employed. These cracks can be detected by additional inspection, the radiation source being arranged as shown in Fig. 85,*b*. Gamma-graphs of cast articles possessing typical casting defects are shown in Fig. 86 (also see Fig. 82).

At present there are no instructions, nor general methods which would govern the rejection of cast articles on the basis of gamma-radiography. This may be explained by the wide diversity in shape, size and application of castings. It should be mentioned, however, that articles, in which there are detected cracks of any size or defects

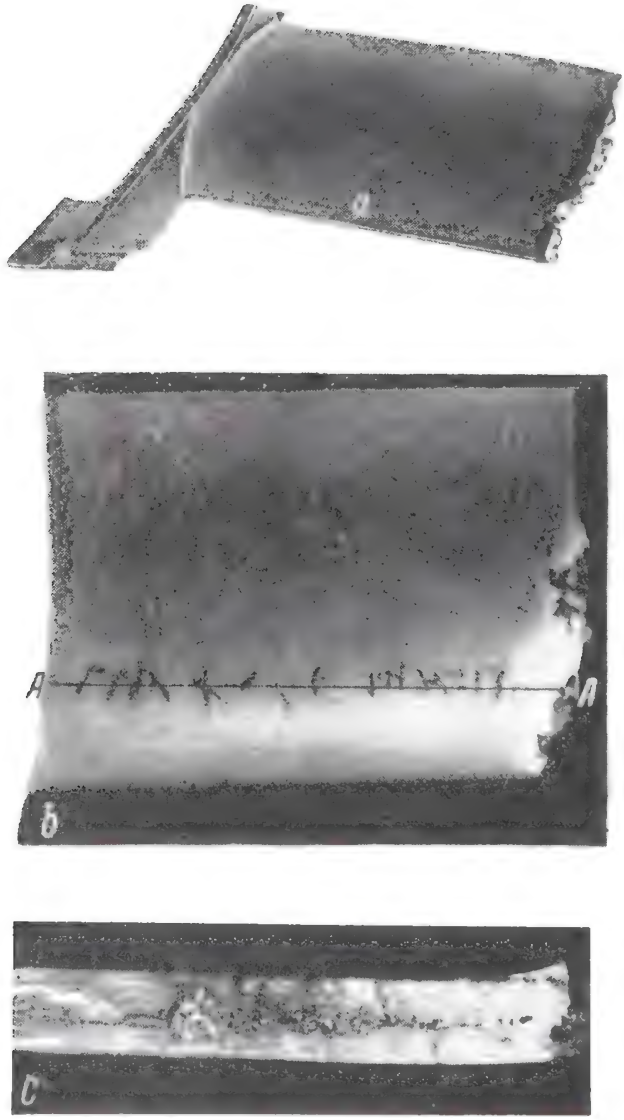

Fig. 86. Inspection of a nozzle box blade:
a—blade; *b*—Ir^{192} gamma-graph; *c*—macrograph of defective spot (2x magnified, AA section)

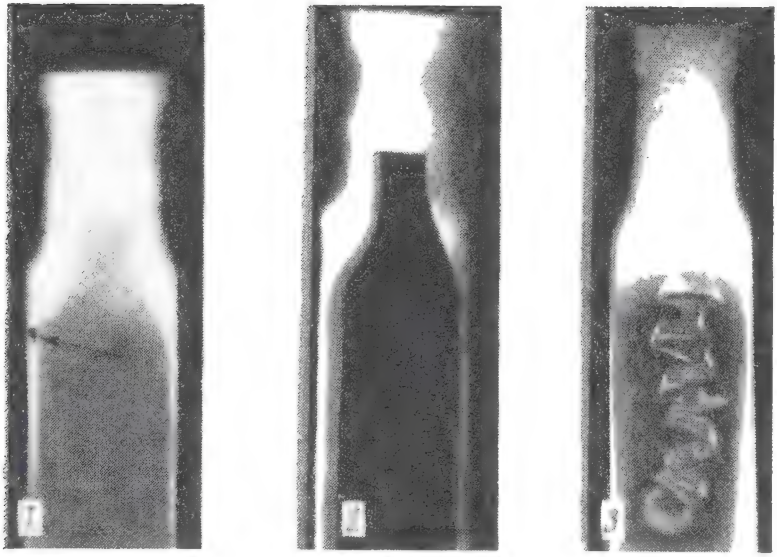

Fig. 87. Cs^{137} gamma-graphs of valves:
1—corroded inner surface of valve stem; *2*—variation in wall thickness; *3*—presence of chips in the inner space of a stem

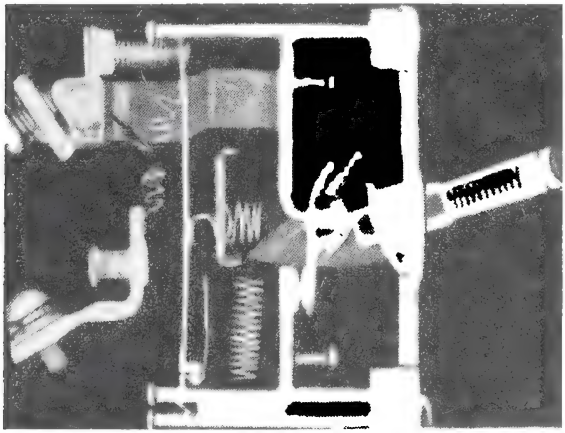

Fig. 88. Eu^{155} gamma-graph of a switch showing a broken current supply wire

such as cavities (both gas and shrinkage), slag and other inclusions of a total area exceeding certain safety margins, should be rejected.

Radiographing parts and units with a view to determining their internal geometry. Sometimes parts and units are manufactured with degrees of inaccuracy and irregularity which cannot be discovered by external examination. For instance, variations in wall thickness, variations in the shape of the inner outlines from that prescribed in the drawings of parts featuring enclosed cavities, incorrect assembly of parts in individual units the stripping of which presents difficulties, etc.

In all such cases it is advisable to practise gamma-radiography. Gamma-ray inspection of parts and units for condition is of great importance too, the aim of such inspection being to determine the nature of the defects which occur in the course of operation, as, for instance, corrosion of the inner surface of parts, internal faults in units, disturbance of the mutual arrangement of component parts of a unit, etc.

The technique (the choice of the radiation source and exposure set-up) employed to inspect one part or another depends on the material from which the given part is made, its thickness, size, shape, and also the purpose of the inspection. In addition it should be borne in mind that when complex units of a considerable variation in thickness are inspected a sharper definition of defects is obtained by gamma-radiography, compared with X-ray radiography.

Figs. 87 and 88 show gamma-graphs of defective parts and units.

§ 8. Locating a defect in an article and determining the size of the defect in the direction of inspection

Locating a defect. In some articles the presence of surface defects is permissible, while defects located at a large distance from the surface are inadmissible. Surface defects can be eliminated when the part is being machined. In other articles, surface defects are also inadmissible. It is frequently necessary not only to detect internal defects, but to locate them as well. Defects may be located by radiographing the part from two mutually perpendicular positions. However, this technique cannot be applied to sheets, plates and parts of a complex shape. In such cases X-ray radiography uses a double-exposure technique (Fig. 89), based on making two exposures of the part on one film, placing the X-ray tube in two different positions parallel to the film, as illustrated in Fig. 89.

If the first exposure is made with the source placed in point S_1, and the centre of the defect—in point O, then the centre of the defect image will be projected in point A_1. The second exposure is made on the same, film the radiation source having been shifted parallel to the film to point S_2. On the film the centre of the second image moves into point A_2. The distance from the X-ray source to the film

is equal to f in positions S_1 and S_2; the distance from the lower surface to the film is denoted c and from the centre of the defect to that surface—x.

From the similarity of the triangles S_1OS_2 and A_1OA_2 it follows that

$$\frac{f-(x+c)}{a}=\frac{x+c}{b}, \tag{58}$$

where a—the displacement of the radiation source;
b—the displacement of the defect image.

Hence, the distance from the defect to the surface at which the rays leave the object is

$$x=\frac{f}{\frac{a}{b}+1}-c \quad \text{or} \quad x=\frac{f}{k+1}-c, \tag{59}$$

where $k=\frac{a}{b}$—the ratio of the displacement of the X-ray source to the displacement of the defect image in the radiograph.

The accuracy with which x is determined depends upon the accuracy with which f, c and k are measured. Under conditions of a given measurement, accuracy for f and c and a constant film-source distance f, a larger displacement a brings about a larger b, thus increasing the accuracy with which these values are measured, and, therefore, the accuracy of the final result. However, this technique of flaw detection has not found application in gamma-radiography, for two exposures on one film result in a considerably diminished image contrast.

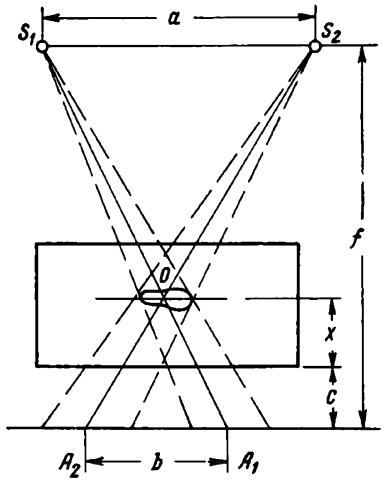

Fig. 89. The method of locating a defect by the double-exposure technique, shifting the source parallel to the film

In gamma-radiography the depth at which a defect is located is determined by taking two gamma-graphs with the radiation source placed in two different positions.

For the first exposure two markers are placed on the film holder so that the straight line connecting the markers is perpendicular to the direction in which the source is being shifted. For the second exposure the markers are arranged on the holder in the same way as for the first exposure. This makes it possible to match the gamma-graphs for interpretation. After the negatives have been developed and dried the centre of the defect on the first gamma-graph is pierced with a pin, then both gamma-graphs are

matched according to the markers and the centre of the defect in the first gamma-graph is marked on the second gamma-graph. The distance between this mark and the centre of the defect on the second gamma-graph is equal to the displacement b of the defect image, corresponding to the displacement a of the source for the second exposure.

Determining the size of a defect in the direction of inspection. When articles are inspected for quality (mostly welds), the need frequently arises to determine not only the depth at which a defect is

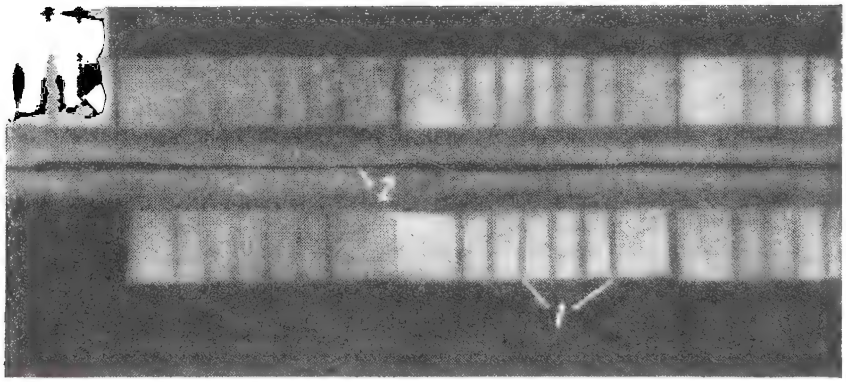

Fig. 90. Tu^{170} gamma-graph of a weld; parent metal is 3 mm thick
1—penetrameter notch; *2*—lack of fusion

located, but the size of the detected fault in the direction of gamma-raying. This problem can be solved within certain limits of accuracy by one of the known methods.

First method. Determining the length of lack of fusion with the aid of penetrameters.

A set of penetrameters of different thicknesses with grooves of various depths and widths (Fig. 90) is arranged next to the section of the weld being inspected. Then a gamma-graph is taken. The length of the lack of fusion is determined by comparing visually the density of the grooves with that of the defective spot. The length of lack of fusion is evaluated with the aid of the penetrameter which caused an image density similar to that produced by the seam reinforcement. If the thickness of the penetrameter coincides with the height of seam reinforcement and the width of the imperfection approaches that of the penetrameter groove, then the length of lack of fusion will be determined by the depth of the respective penetrameter groove.

Second method. Determining the length of lack of fusion by means of two gamma-graphs taken with sources of a different radiation energy.

This method is based on the relationship existing between the revealment of defects and radiation energy (hardness). In order to determine the length of lack of fusion, the sensitivity of the gamma- or X-ray picture to minimal defects in a metal of a given thickness and density with radiation sources of different energies is discovered. One gamma- or X-ray picture is then taken with a source of normal hardness ensuring the best revealment of defects, and another picture—with a harder radiation source producing a poorer revealment of defects in the same article. If the gamma- or X-ray picture taken with the radiation source of a higher energy does not show the defect, this signifies that the length of the defect is smaller than the length which could be detected on a picture taken with a radiation source of a higher energy (Fig. 91).

Third method. Determining the length of lack of fusion with the aid of a photometric curve. First the gamma-graph or X-ray picture showing the defect is investigated with the aid of a recording microphotometer. Then, the obtained photometric curve (Fig. 92) is used to determine the ratio of the peak l, corresponding to the defective section, to the peak L, corresponding to the seam reinforcement on the section adjoining the defective one. This ratio is multiplied by d which represents the reinforcement of the seam on the examined section. The length of lack of fusion is determined by means of standard curves on which the length of the defect h (as a percentage to the total thickness of the weld) is plotted versus the revealment factor $d\frac{l}{L}$ (Fig. 93).

This method was checked for accuracy by plotting such a standard curve for lack of fusion of a length maintained within certain limits in welded low-carbon steel plates 10 mm thick; the gamma-graphs of the welds were studied with the aid of a recording microphotometer. The actual length of lack of fusion in welds was checked on micrographs. It was found that the dependence of h on $d\frac{l}{L}$ may be expressed by the following empirical relationship

$$h = 10 + 15\left(d\frac{l}{L} - 0.60\right), \tag{60}$$

(d, l and L being expressed in mm).

Experimental checking has shown that the width of a lack-of-fusion defect is one of the determining factors in establishing the dependence of $d\frac{l}{L}$ on the length of lack of fusion. It was shown that while inspecting a welded seam imitating lack of fusion (Fig. 94) the examined relationship is true for a weld with an artificial defect of a width (gap) $S = 0.1; 0.3; 0.5; 1.0; 2.0; 3.0$ mm.

The minimum width of lack of fusion, for which the value of $d\frac{l}{L}$ is simple (within the limits of permissible error) and related to the length of such defect, is approximately 0.3-0.5 mm.

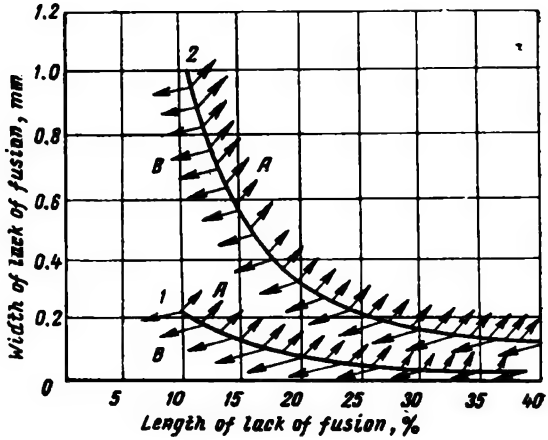

Fig. 91. Curves expressing revealment of lack of fusion depending on radiation source; steel, parent metal 6 mm thick:
1—Tu^{170}; *2*—Co^{60}; *A*—lack of fusion is seen; *B*—lack of fusion is not revealed

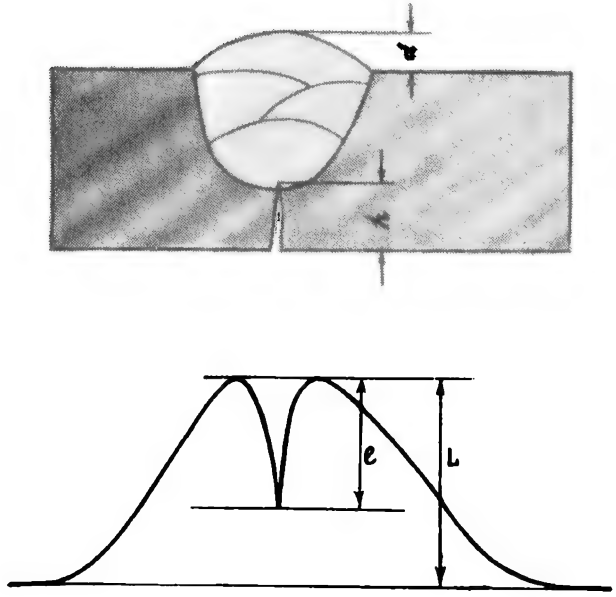

Fig. 92. Photometric curve of a gamma-graph of a defective (lack of fusion) weld

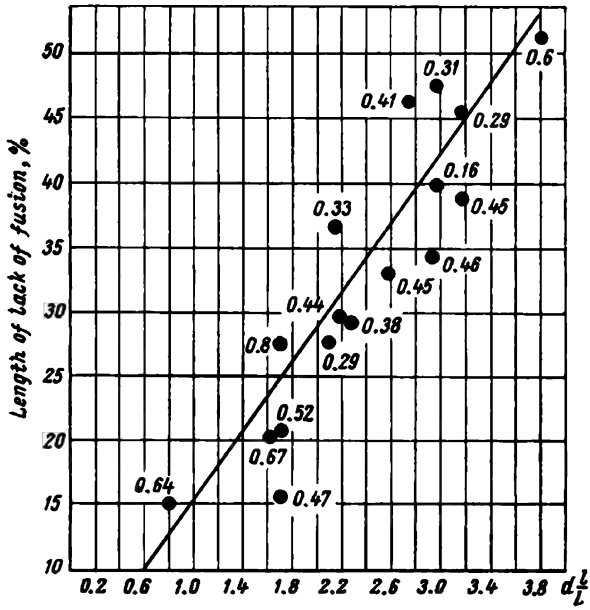

Fig. 93. Length of lack of fusion as a function of the revealment factor $\left(d\frac{l}{L}\right)$. The figures at points indicate width of lack of fusion in mm

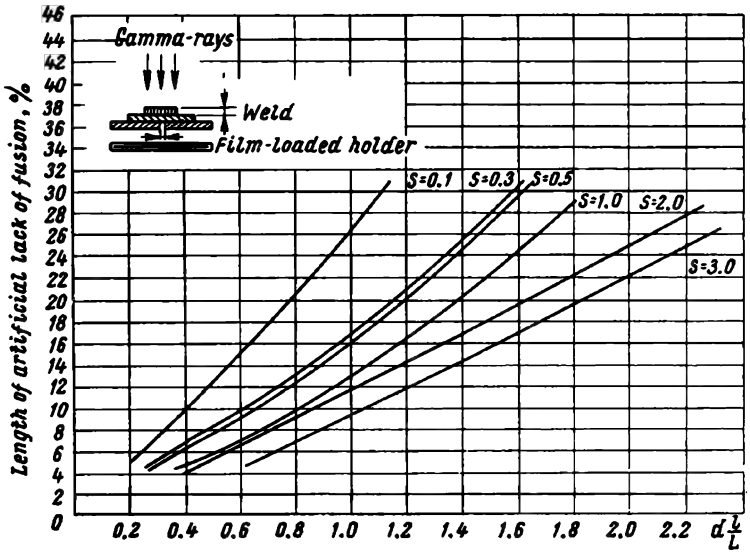

Fig. 94. Dependence of imitated lack of fusion on the revealment factor $\left(d\frac{l}{L}\right)$ for defects of different width

The attempt to establish a similar relationship for welded test plates with narrow bands of lack of fusion (<0.1 mm) was not successful, owing to a wide scattering of points.

Table 27 gives the control measurement data characterising the accuracy with which the length of lack of fusion in a weld (the parent metal is 10 mm thick) was determined with the aid of a photometric curve.

Table 27

Control Data Characterising the Accuracy of the Length of Lack of Fusion in Welds Determined with the Aid of a Photometric Curve

Specimen No.	Width of defect, mm	Weld reinforcement, mm	True fracture measured length of defect, % of parent metal thickness	Length of defect determined by formula, %	Absolute error, %	Relative error, %
7-1	0.20	3.00	31.9	28.7	—3.2	—10
7-2	0.35	1.80	32.5	24.2	—8.3	—25
7-3	0.42	2.25	42.3	39.1	—3.2	—7.5
7-4	0.46	2.25	43.0	44.5	+1.5	+3.5
7-5	0.38	2.70	50.0	41.5	—8.5	—17.0
8-1	0.59	3.50	16.3	18.7	+2.4	+14.7
8-2	0.40	2.93	17.0	19.4	+2.4	+14.1
8-3	0.30	2.95	23.2	19.7	—3.5	—15.2
8-4	0.43	3.15	29.0	25.1	—3.9	—13.5
8-5	0.34	2.90	25.8	32.4	+6.6	+25.6
8-6	0.41	2.45	27.4	32.4	+5.0	+18.3
8-7	0.53	3.0	31.7	36.2	+4.5	+14.5
9-1	0.46	2.0	21.4	20.5	—0.9	—4.3
9-2	0.38	2.2	29.1	22.4	—6.7	—23.0
9-3	0.28	2.8	29.1	21.1	—8.0	—27.5
9-4	0.25	2.75	36.6	33.1	—3.5	—9.8
9-5	0.20	2.20	37.8	29.9	—7.9	—21.0
9-6	0.54	2.10	39.5	35.5	—4.0	—10.0
9-7	0.49	1.85	43.3	34.6	—8.7	—20.0
10-1	0.54	1.50	15.9	15.8	—0.1	—0.6
10-2	0.50	1.90	15.9	15.2	—0.7	—4.4
10-3	0.51	2.10	14.1	15.7	+1.6	+11.3
10-4	0.78	2.65	23.0	22.0	—1.0	—4.3
10-7	0.96	2.90	17.2	20.3	+3.1	+18.0
10-9	0.93	2.90	18.4	24.7	+6.3	+34.0
10-10	1.00	2.70	27.9	32.2	+4.3	+15.5

As an example, let us determine the length of lack of fusion in a welded sample No. 8-3 with the aid of formula (60): the height of the seam reinforcement $d = 2.95$ mm, the width of the lack of fusion

$S = 0.3$ mm; the maximum lack of fusion on the photometric curve $l = 13$ mm, and the maximum seam reinforcement $L = 30.5$ mm. The length of the lack of fusion is

$$h = 10 + 15\left(d\frac{l}{L} - 0.6\right) = 10 + 15\left(2.95 \times \frac{13}{30.5} - 0.6\right) = 19.75\%.$$

The actual length of the lack of fusion (see Table 27) for the given sample is 23.2%. The error amounts to 3.5% of the thickness of the parent metal. According to data listed in Table 27, the mean absolute error is equal to 3.5% and the mean relative error—15.2%.

Thus when dealing with welded joints of steel plates about 10 mm thick, this method makes it possible to determine the length of the lack of fusion in welds with a 5% accuracy, provided the imperfection is not less than 0.3 mm wide. Certain corrections should be introduced into the calculations when this method is used to inspect other welds, differing in plate thickness and the density of the welded metal.

The detection and location of a defect does not make it possible, however, to determine to what extent a given defect affects the mechanical properties of the inspected article. For this it is necessary to take into consideration the effect of flaws on the workability of the parts (joints) under loads of a different nature.

CHAPTER II

EQUIPMENT FOR GAMMA-RADIOGRAPHY

§ 1. Classification of equipment

Equipment intended for the inspection of various objects by means of gamma-rays from radioactive isotopes must meet operating and safety requirements.

All radioactive isotopes used for gamma-radiography are divided into three groups, depending on the gamma-energy. The first group includes radioactive isotopes of a gamma-energy of about 1 Mev, the second group—isotopes of a gamma-energy ranging from 0.3 to 0.7 Mev, and the third group—soft gamma-emitters of an energy below 0.3 Mev.

As the thickness of the protective barrier ensuring safe handling of radioactive isotopes is determined primarily by radiation energy, it is also expedient to divide all inspection units, portable, mobile and stationary, into three types, conforming to the three groups of radiation sources.

The first type includes units employed to inspect heavy metals of a large thickness (steel and metals of similar density, 80-200 mm thick). These units are used mostly with Co^{60} preparations of an activity of 5.0 and 50 gram radium equivalent.

Units of the second type are employed to inspect heavy metals of medium thickness (steel and metals of similar density, 15-80 mm thick), also thicker light alloys, for instance, aluminium alloys from 50 to 300 mm thick. These units are used with Cs^{137} and Ir^{192} radioactive sources of an activity up to 30 gram radium equivalent and $Eu^{152, 154}$ emitters of an activity up to 20 gram radium equivalent.

The third type includes units employed to inspect thin heavy metals (steel and other metals of similar density, up to 15 mm thick; light alloys—for instance, aluminium, up to 50 mm thick). These units utilise Tu^{170}, Eu^{155} and other gamma-active isotopes of an energy below 0.3 Mev.

Inspection units which allow the use of radioactive sources of the 1st, 2nd and 3rd groups are known as combined-type units.

§ 2. Hard gamma-radiation inspection units

Let us consider here two units of this type: ГУП-Co-5-1 (gamma-radiography unit with a Co^{60} source of an activity equal to 5 gram

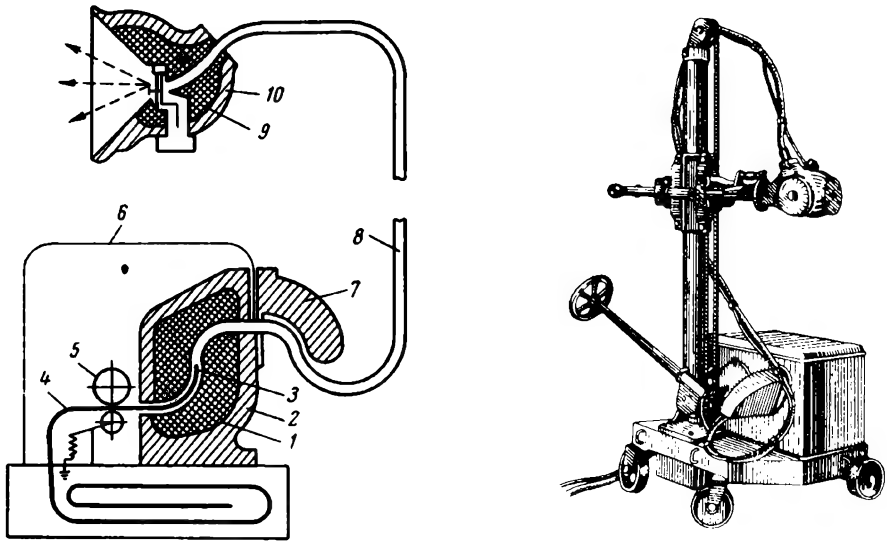

Fig. 95. General view and layout of a ГУП-Co-5-1 (ГУП-Co-50-1) inspection unit:

1—lead; *2*—cast-iron storage container; *3*—radioactive source; *4*—steel rope; *5*—electromagnetic mechanism shifting the rope and source from the storage into a working container; *6*—steel case; *7*—cast-iron protective hield; *8*—hose for shifting the source; *9*—lead; *10*—cast-iron case of the working container

radium equivalent), and ГУП-Co-50-1 unit employing a 50 gram radium equivalent Co^{60} source. These units are mostly used as stationary. They may be shifted from place to place only within a shop (laboratory). These are remote-control units and permit to inspect

parts in any direction. Operating safety is ensured by lead protective shields 20 and 23 cm thick respectively.

The two units are of similar design (Fig. 95), each having two containers: one working and the other used to store the radioactive preparation. The preparation is shifted from the working into the storage container and vice versa with the aid of a flexible hose-clad steel rope and a remote-controlled electric motor.

The ГУП-Co-5-1 unit weighs 550 kg and is 2.2 m high; the required floor space is 1.0 × 1.5 m. The ГУП-Co-50-1 unit of similar overall dimensions weighs 700 kg.

§ 3. Medium gamma-radiation inspection units

Units of this type are used both under stationary and field conditions, depending on application. The units allow gamma-raying in any direction, including circular (panoramic) inspection. With medium radiation units, safety in operation is ensured by lead shields not less than 10 cm thick.

The ГУП-Co-0.5-1 unit, which is in regular production, is intended for the inspection of parts under shop conditions. The pear-shaped source container of this unit is mounted on the stand of the РУП-2 X-ray apparatus. When the unit is not in use, the source of radiation is kept in the thickened storage section of the container; the working section of the container has a taper opening through which gamma-rays pass. The source is shifted to the taper opening and back into the storage section of the container with the aid of a rope up to 3 m long. For panoramic (circular) inspection the source may be drawn out of the container. The total weight of the unit is 165 kg, the height is 2.2 m and the required floor space is 1.4 × 1.3 m.

The УР-1 unit, intended for the inspection of one or several articles (or a section of an article) by a directed gamma-beam, and for simultaneous inspection of cylindrical parts and parts arranged in a circle, may also be considered as a medium gamma-energy unit.

The УР-1 inspection unit contains the following components: 1) protective container; 2) a device for lifting and lowering the radioactive source; 3) stand; 4) trolley.

The protective container is used to store and transport the radioactive preparation, and also to obtain a pencil gamma-beam. The container consists of a cylindrical lead-filled steel case.

The container is used either with a device for lifting and removing the preparation, or mounted on a stand, depending on the exposure set-up, selected to suit definite operating conditions.

Simultaneous panoramic inspection of several parts and inspection of annular parts can be carried out by means of the special device shown in Fig. 77.

This unit consists of a support on which the source container is placed, the column, box, and separately mounted control board.

The box contains the mechanism which lifts and lowers the radioactive preparation from and into the storage container, a 220/36 v, 50 w step-down transformer, selenium rectifiers and limit switches.

The lifting and lowering mechanism consists of a reversible d.c. motor (26 v, 12 w, 11,000 rpm), a reducing gear (gear ratio 1 : 650) and a rack with guide rollers. The lifting mechanism is operated

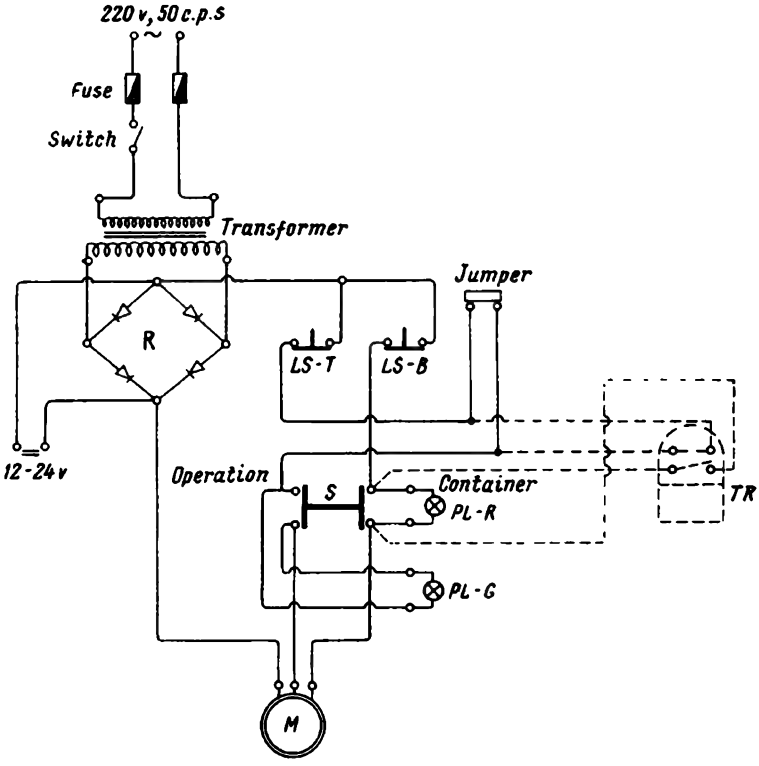

Fig. 96. Electric circuit diagram of mechanism for lifting and lowering the radioactive source into the container

from the control board arranged at a safe distance from the spot where gamma-raying is performed. Mounted on the control board are: the main switch, electric-motor reversing switch, pilot lamps and fuses.

The circuit diagram of the lifting and lowering mechanism is shown in Fig. 96. The mechanism is supplied from 220 v a.c. mains. The reversible electric motor is connected to the supply mains through the step-down transformer and selenium rectifiers *R* by means of the mains switch. The electric motor is reversed with the aid of switch *S*. The electric motor can be cut-off by using the switches

LS-T and LS-B; when the motor is cut-off by the limit switch LS-T the red pilot lamp PL-R lights; the PL-G green pilot lamp lights up when the limit switch LS-B cuts off the electric motor. Under field conditions 12-24 v storage batteries may be used as a supply source for the lifting mechanism.

The electric curcuit of the lifting mechanism allows the required exposure time to be fixed automatically by means of a time relay. In this case the jumper must be removed.

The overall dimensions of the source lifting and lowering mechanism are 220 × 250 × × 650 mm; weight—23 kg.

It takes 7 sec to lift the radioactive preparation or lower it into the protective container.

The stand fitted with two racks (Fig. 97) allows the capsulated radioactive source to be set in any position required for inspection. The stand is turned around its axis by means of a hand wheel. The carriage holding the lifting mechanism can be shifted in the vertical direction along stand racks.

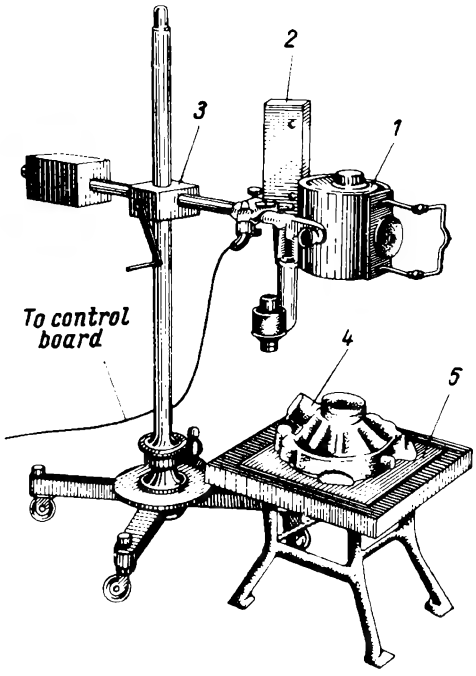

Fig. 97. Column-type inspection unit (part of the УР-set):

1—container with radioactive source; *2*—mechanism for removing the container plug; *3*—mechanism adjusting the source-film distance; *4*—cast part; *5*—film-loaded holder

The lifting mechanism is a worm reducing gear, the shaft of which is rotated by means of a handle; the worm wheel is set on the shaft on which gears meshing the racks are set. The fork, which carries the protective container and the mechanism which removes the plug from the container, is jointed to the carriage by means of a pipe. The protective container is balanced by a counterweight set on a lever welded to the carriage.

The plug-removing mechanism consists of a reversible electric motor, the reducing gear, the output gear of which meshes a rack, and a cam gear. The housing of the mechanism is strapped to two parallel arms of the fork and the reducing gear and electric motor are attached to vertical walls of the housing which, besides guide rollers, carry racks and limit switches. The lower end of the rack is supported in taper ball-bearings set in the sleeve of the cam gear.

The sleeve has a shaped slot. As the rack moves, the roller, firmly fixed in relation to the rack by the bracket welded to the mechanism casing, moves along the shaped slot. The lever welded to the cam gear sleeve carries a lock which secures in place the plug of the protective container. The protective container is attached to the fork by two screws. In the nonworking position the end plugs of the protective container are locked in place. The plug-removing mechanism is controlled from a panel situated at a safe distance from the spot where gamma-raying is to be performed. The panel is similar to that used to control the lifting mechanism. The electric circuit controlling the plug-removing mechanism is similar to that of the source lifting and lowering mechanism. The protective container can be moved horizontally over the floor without restriction, but vertical displacement of the container is limited to 105 cm (the lowest position is 35 cm and the uppermost 140 cm from the floor). The stand and container can be turned through 360°; the container can be turned through ±45° from the horizontal axis (from a beam directed vertically downwards parallel to the stand).

All preparatory operations (arrangement of inspected articles, attachment of film holders and markers) are carried out with the radioactive source kept inside the container.

§ 4. Soft gamma-radiation inspection units

Let us consider the portable ПУР-1 and РК-1 units and the ГУП-Tu-0.5-1 apparatus.

The portable ПУР-1 inspection unit. This unit (Fig. 98) consists of a container (manipulator) holding the capsulated radioactive source, remote-control panel with electric equipment and tripod.

The gear diagram of the manipulator is given in Fig. 99. Capsule *2*, holding the radioactive source and arranged inside the manipulator, is reliably isolated from the ambient medium by a lead can *3*. Opening and closing of cover *1* of the manipulator and shifting of the source is done automatically from the remote-control panel which can be placed at any required distance. The manipulator cover and source are handled by means of the d.c. electric motor *4* located inside the manipulator. From the electric motor, through the gear train, motion is imparted to screw *5* which carries capsulated source *2* on one end and two fingers *7* and *8* on the opposite end. The free end of finger *8* enters into a slot in drum *9*, turns the drum, thus opening or closing cover *1* of the manipulator. Through microswitch *6*, finger *7* controls the electric motor and the displacement of the radioactive source *2*. The opening and closing of the manipulator cover is fully synchronised with the displacement of the radioactive source. It takes not more than 10 sec for all the mechanisms to operate. The unit is supplied from either a.c. mains or a d.c. storage battery.

The sectional tripod allows the container to be fixed in any required position by rotation round the horizontal and vertical axes; the source-article distance may be varied from 250 to 1,000 mm.

Portable inspection unit РК-1. The unit shown in Fig. 100 is designed for gamma-raying welded and cast articles, also articles with defects acquired in the course of service (corrosion, cracks,

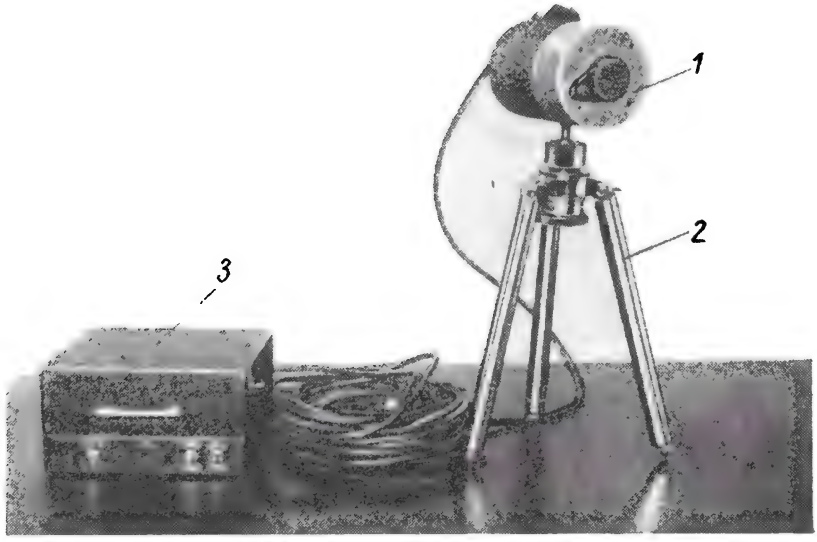

Fig. 98. Portable type ПУР-1 inspection unit:
1—container-manipulator; *2*—adjustable tripod; *3*—control board

mechanical injuries, etc.). The thickness of the inspected articles is: for steel articles—from 1 to 15 mm; titanium-alloy articles—from 2 to 30 mm; aluminium-alloy articles—from 5 to 50 mm and magnesium-alloy articles—from 10 to 150 mm.

The design of the unit permits its employment under both stationary and field conditions (Figs. 101 and 102). The unit can be dismantled and assembled in 15-20 min by one man.

The unit is used for inspection of flat parts and shaped cast parts with a pencil gamma-beam emitted at a 40-50° angle, for simultaneous panoramic (circular) inspection of several parts, and for inspection of cylindrical articles of an inner diameter ranging from about 400 to 2,000 mm.

A РК-1 unit comprises: the container (manipulator); the dismantled stand; the case (which serves as a table during inspection); the remote-control mechanism and an electro-mechanical timer.

The container-manipulator (Fig. 103) is a case accommodating a spherical lead container offering protection from gamma-radiation

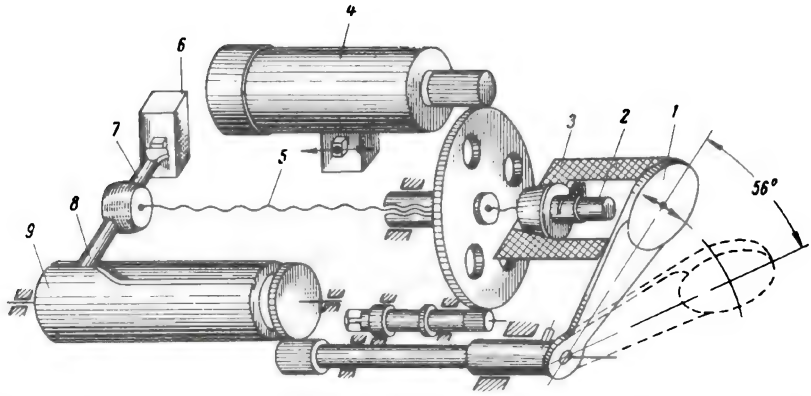

Fig. 99. Gear diagram of manipulator of type ПУР-1 inspection unit

and the mechanism controlling the capsulated radioactive preparation. On the outer top section of the manipulator there are two handles for carrying and turning the manipulator, and two trunnions

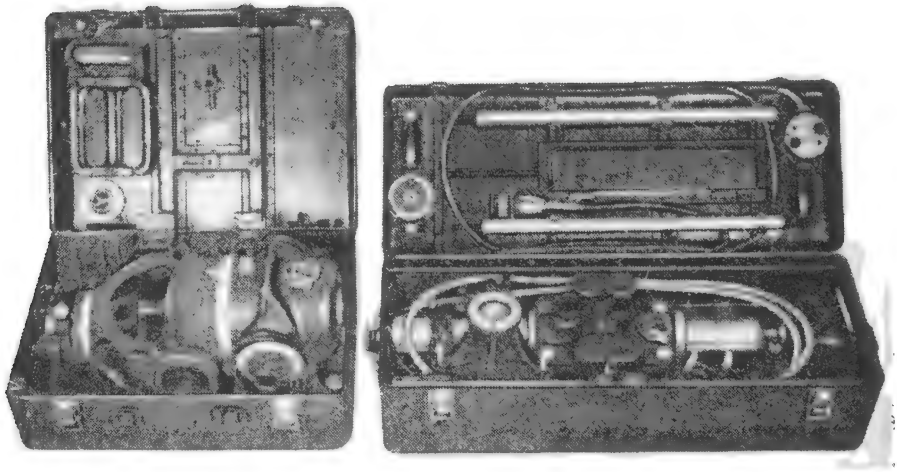

Fig. 100. Dismantled portable type РК-1 inspection unit placed in two transportation cases. The case to the left serves as base for the inspection unit and as table for the examined articles

which serve as an axis of rotation. The bottom section of the manipulator serves as a protective cap and removable telescopic indicator. The ring placed between the top and bottom sections of the manipulator determines the position of the capsule and the gamma-emission angle.

The capsule containing the radioactive source *24* secured in a cartridge lampholder is reliably shielded by the lead sphere *23*.

Flaps *17* and *18* of the manipulator shutter are opened or closed, and displacement of the capsule is controlled automatically from the control panel.

From the 27 v, MH-145 a, d.c. electric motor, through friction clutch *11* and gear train *20*, motion is transmitted to screw *14*, the

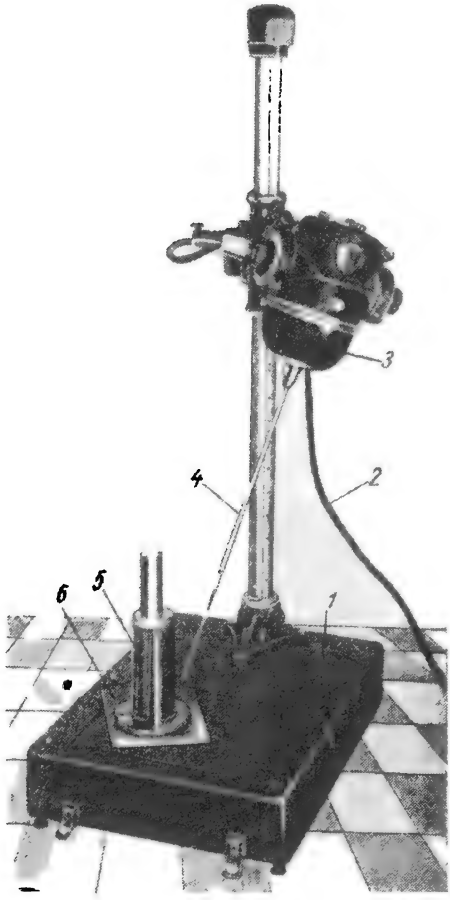

Fig. 101. Preparation of part to be radiographed on type PK-1 inspection unit:

1—case; *2*—cable running to timer and control board; *3*—container-manipulator; *4*—detachable centering device; *5*—welded article; *6*—film-loaded holder

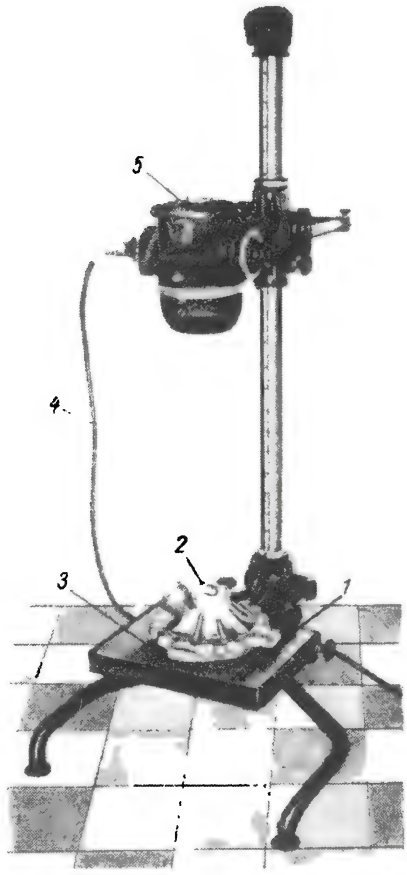

Fig. 102. Inspection of cast article on type PK-1 inspection unit:

1—table for articles; *2*—cast article; *3*—film-loaded holder; *4*—cable running to timer and control board *5*—container-manipulator

bottom end of which carries the capsule; three fingers are arranged on the top end of the screw. Two fingers *12* entering into slots provided in drums *13* and *22*, and moving downwards turn the two drums

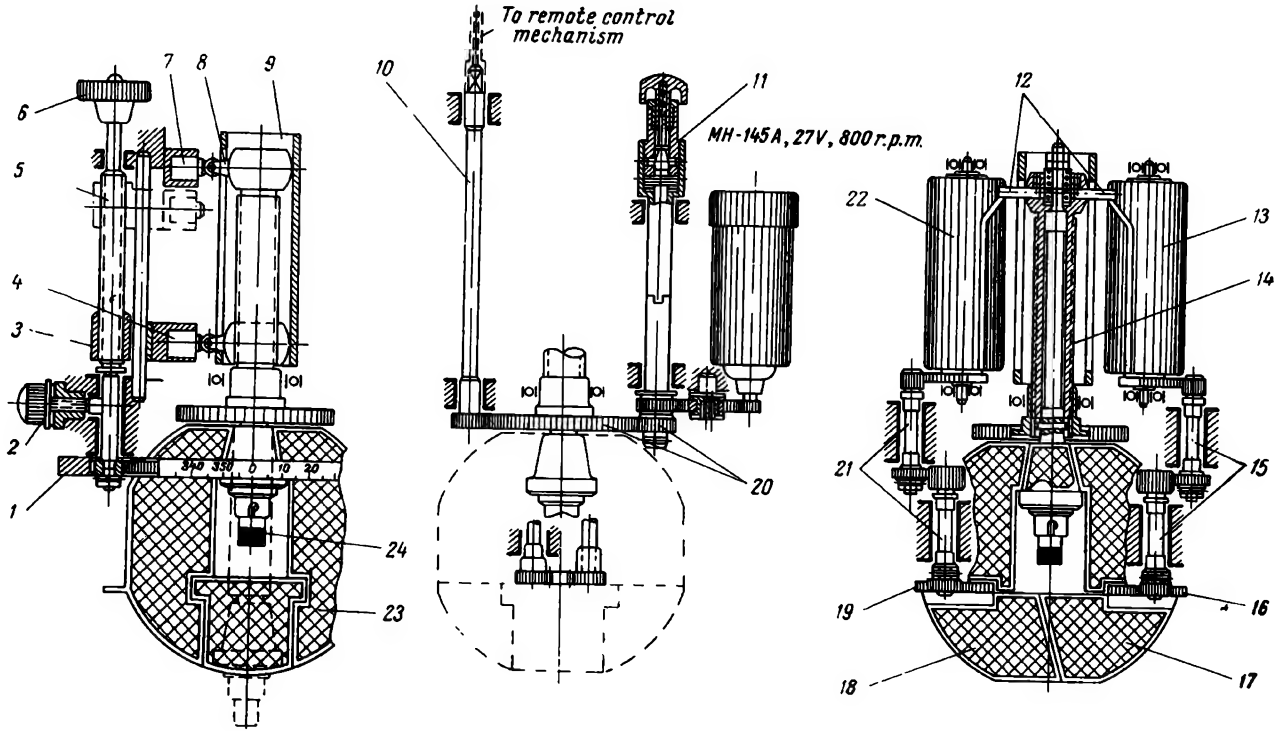

Fig. 103. Kinematic diagram of container-manipulator

and open or close flaps *17* and *18* of the manipulator shutter, motion being transmitted through gear drives *15* and *21* and racks *16* and *19*.

As it moves along the slot in guide cup *9*, finger *8* switches on and off the microswitches *4* and *7* which control the work of the motor and capsule displacement. The microswitches limit displacement of the capsule within 20 to 80 mm, depending on the conditions of inspection. Microswitch *4* is shifted by turning handle *6*, through screw *5* and nut *3*. The position of the microswitch and capsule is determined by the readings on scaled ring *1* jointed to screw *3* by a gear drive. The microswitch is kept from self-displacement by screw *2*. Friction clutch *11* is used to cut off the electric motor, when it is necessary to control the manipulator by hand, by means of the remote-control mechanism, through output shaft *10*.

The electro-mechanical timer (Fig. 104) is designed to set exposures ranging from 1 min to 24 hrs. It is possible to set the timer to operate after a given delay in time. The timer functions in the following manner: the hands of the timer rest always at zero, i.e., the top position from which the timer operates. The given exposure is set in hours and minutes by turning handle *7*. The cam of disc *11* follows the minute hand *5* and the cam of disc *10*—the hour hand *4*.

In order to remember the chosen exposure time, the painted hand *12* is set to indicate the given hours by turning the mounting of glass *9*, and hand *6* is set to indicate the given minutes by turning handle *8*.

After the timer is started the hands, rotating counterclockwise, come to zero position at which the cam of disc *11* closes contact *2*, and the cam of disc *10*—contact *3*; thus, both series-connected contacts are closed and motor *1* of the timer is shut-off. The electric circuit of the container-manipulator is controlled from the panel, fitted with two pilot lamps.

The exposure slide rule, shown in Fig. 105, is employed to determine the exposures for gamma-raying all kinds of objects using Tu^{170} and Eu^{155} radioactive sources. The slide rule enables one to determine the exposures for the inspection of articles made from iron-, titanium-, aluminium- and magnesium-base alloys, 0.5 to 60 mm thick, at source-film distances of 25, 50 and 75 cm, using "Roentgen X" film and two lead foils 0.05 mm thick. Negative density is 1.5.

The ГУП-Tu-0.5-1 unit is designed for the inspection of articles with a gamma-beam emitted at 40° angle, for simultaneous panoramic inspection of several articles, also for the inspection of cylindrical objects with an inner diameter of from 400 to 2,000 mm. This gamma-inspection unit may be employed under both stationary and field conditions.

The unit (Fig. 106) comprises a manipulator, stand, control panel, junction cable, a.c. mains cable, mains cable for connecting

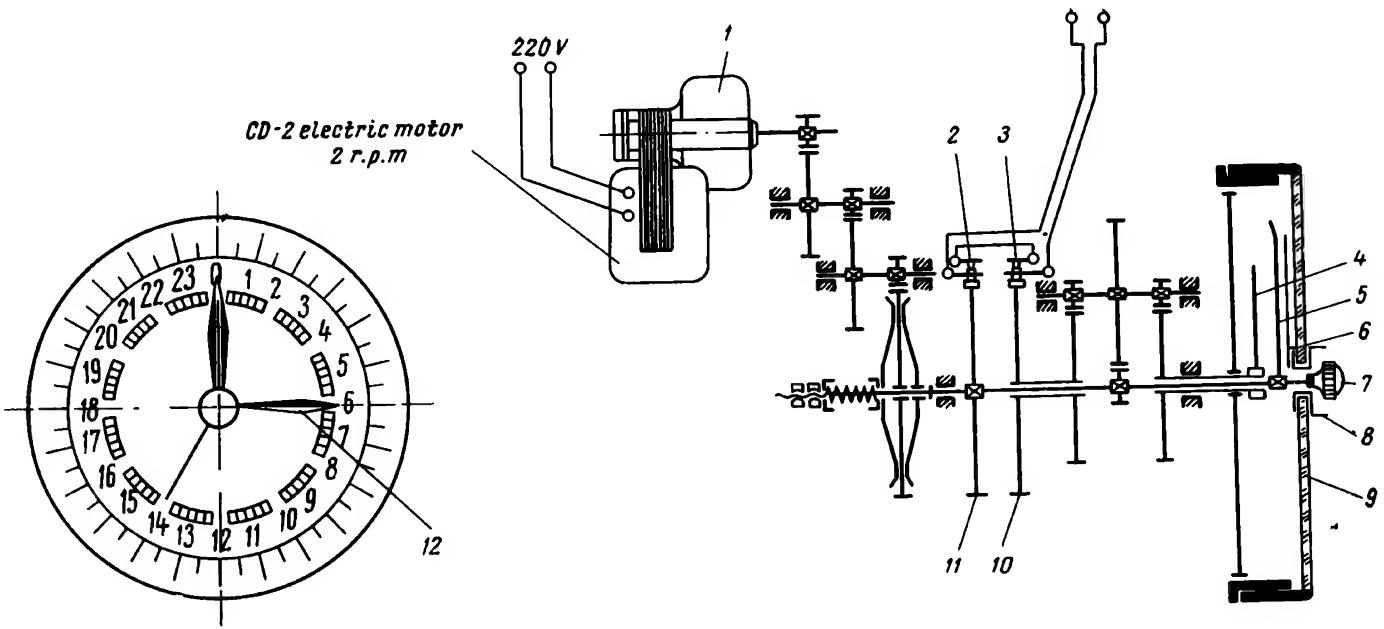

Fig. 104. Schematic layout of electro-mechanical timer

side line, detachable centering device, detachable guides and a special wrench.

The manipulator is a case housing the pressed-lead container, shutter control mechanism, source shifting mechanism, flexible shaft and cartridge.

The pressed-lead container is sphere-shaped. The cartridge with a capsule and shutter is fitted into a round passage in the container. In the shutter—a cylinder rotating on two trunnions—there is a passage through which the source passes.

The schematic layout of the apparatus and the interaction of its component elements are shown in Fig. 107. The cartridge holding the radioactive source *3* is secured to the end of the flexible shaft *8* and is stored in the centre of the main protective case *2*. The gamma-ray emission port is closed by shutter *1*. When the source is shifted into the position at which the inspection is performed, the shutter turns into position "Open". The shutter is controlled by the SM *12* reversible electric motor. After the shutter is opened, the friction mechanism receiving motion from the second reversible electric motor PM *11* shifts the cartridge and source into the position required for inspection. For the purpose of inspection with a 40° beam the socket may be shifted into the centre of the shutter working cone; the source may also be shifted along tubular guides outside the protective case for a distance from 40 to 1,500 mm.

Prior to starting inspection work, after the supply source and conditions of inspection have been selected and certain switchings have

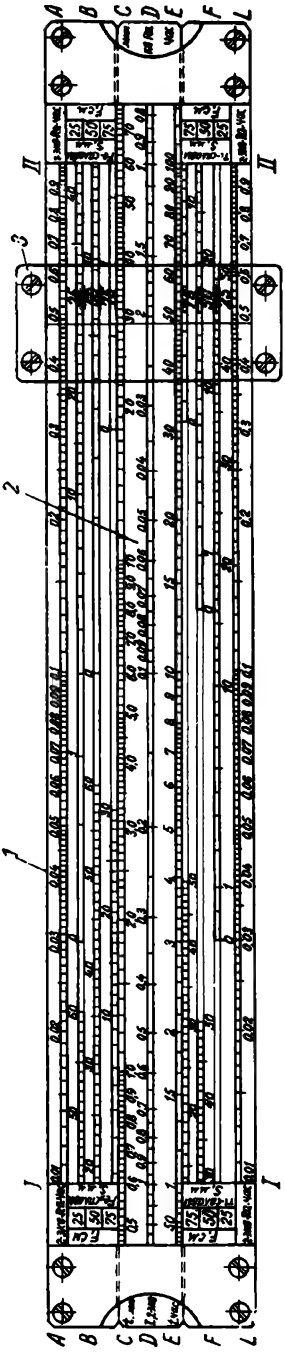

Fig. 105. Exposure slide rule:

1—case; *2*—slide; *3*—movable frame with indicator. *A* and *L* correspond to exposure values expressed in gram radium equivalent-hrs; *B* and *F* scales correspond to the thickness of iron-, titanium-, aluminium- and magnesium-base alloys; slide *C* is graduated in values representing exposure time in minutes; scale *D* divisions correspond to the activity of the radioactive source expressed in gram radium equivalent; scale *E* divisions indicate exposure time in hours

been made on the control panel, and also after the control circuit has been switched on, a green lamp PL lights up on the MS switch, the green light indicating that the source is kept in storage.

Motor SM, switched on by pressing the push-button marked "Start", brings the shutter into position "Open". At the same time the semicircular segment *15*, engaged with the worm wheel of the shutter-turning mechanism, switches the SM_1 microswitch from the n.o.

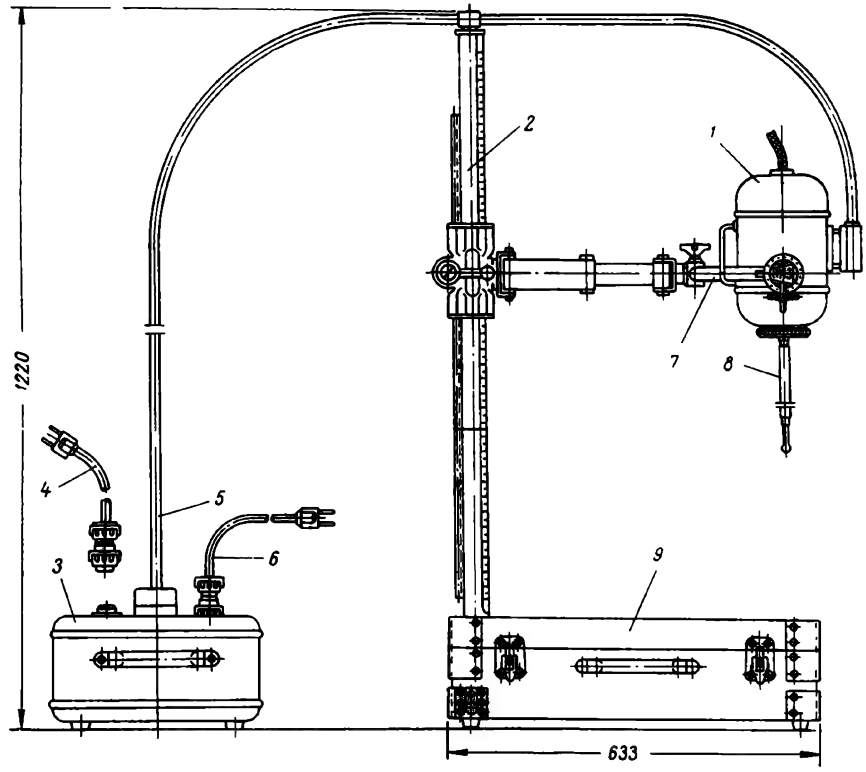

Fig. 106. Type ГУП-Tu-0.5-1 gamma-inspection unit:
1—container-manipulator; *2*—stand; *3*—control panel; *4*—mains cable for connecting side line; *5*—junction cable; *6*—a. c. mains cable; *7*—detachable guides; *8*—detachable centering device; *9*—case

into the n.c. position in which the microswitch remains until the end of the exposure. When turned through 105°, the segment switches microswitch SM_2 and the latter shuts down the electric motor SM. Simultaneously, the auxiliary relay IR_2 switches on the motor PM which shifts the flexible shaft and source cartridge through the friction device of the shifting mechanism *5*. The moment the flexible shaft starts moving, the microswitch SM_1 is switched, thus preparing the SM motor for reverse running.

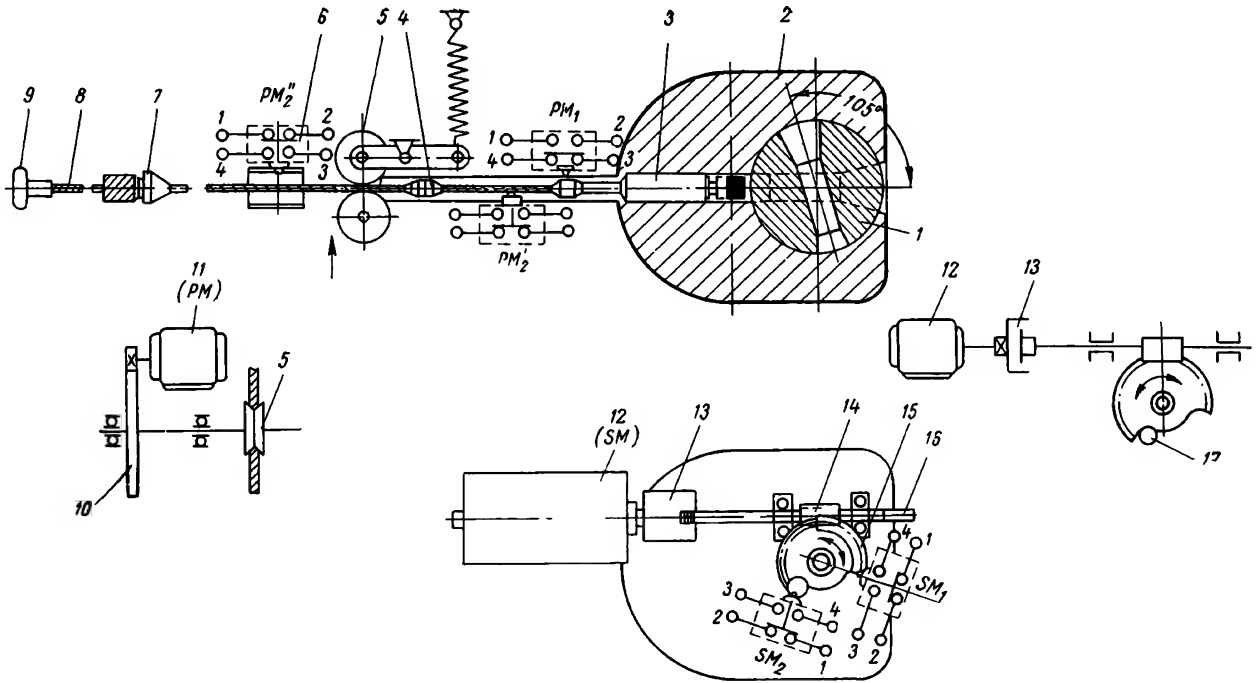

Fig. 107. Schematic layout of type ГУП-Tu-0.5-1 gamma-inspection unit:

1- shutter; *2*- lead container; *3*--source attachment cartridge; *4*—limit; *5*- friction device; *6*—microswitch; *7* movable limit; *8*—flexible shaft; *9*—knob; *10*—gear drive; *11*—source-shifting reversible electric motor; *12* shutter control reversible electric motor; *13*—friction plate clutch; *14*—worm and wheel; *15*—segment; *16*—square end to accommodate wrench to turn the shutter in case of emergency; *17*—mechanical stop

With further movement of the flexible shaft, limit *4* approaches the microswitch SM_2, and the switch will shut-off the circuit of motor PM, if the source displacement switch PM_1 is in position "Cone" The red lamp PL_2 lights up, indicating that the radioactive source is in the "Cone" position and is emitting a gamma-beam. But if the source displacement switch PM is shifted into the position marked "40-1,500", the PM motor will come to a standstill only after the microswitch PM_2 has been switched over with the aid of the movable limit *7*.

§ 5. Combined-type units

Pneumatic radioactive-source manipulators and the portable three-positional gamma-radiography unit ГУ-2 are classified as combined-type units.

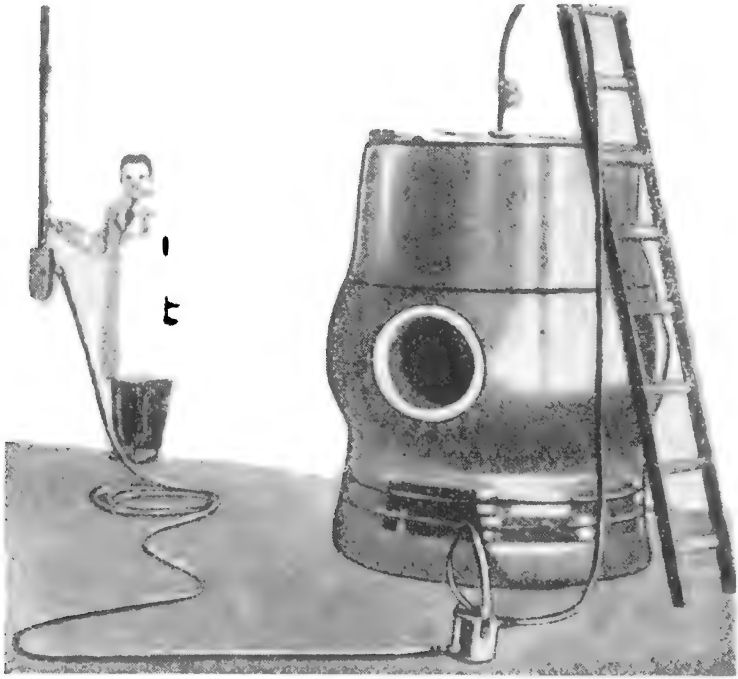

Fig. 108. Pneumatic manipulator (control may be effected from another room)

In Czechoslovakia the pneumatic manipulator (Fig. 108) suggested by Pajer is widely employed. This manipulator offers reliable protection for the attending personnel, and in addition has a convenient signalling system indicating whether the radioactive isotope is in

the working container or in the position for inspection. The manipulator is remote-controlled from a safe distance.

A pneumatic manipulator for small-diameter sources (Fig. 109). Prior to extracting the source from the container *2*, the end *10* of

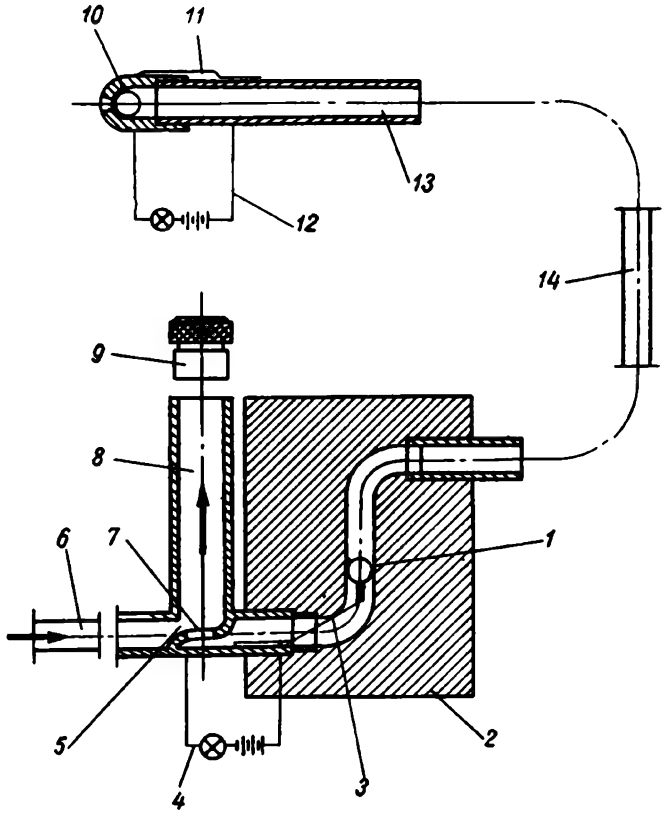

Fig. 109. Schematic layout of a pneumatic manipulator for small-diameter sources:

1—aluminium-clad radioactive source; *2*—lead storage container; *3*—contact isolated from container walls; *4*—signalling device; *5*—narrow passage; *6*—rubber hose; *7*—opening in partition; *8*—suction pipe; *9*—plug; *10*—aluminium end piece; *11*—contact isolated from aluminium end piece; *12*—signalling device; *13*—pipe; *14*—thick-walled hose for source displacement

the hose *14* is secured at a certain point, taking into account the film-source distance and the selected exposure set-up; the control signalling device *12* is cut into the circuit and the suction pipe is closed by plug *9*. Then, compressed air is admitted into the container via hose *6*; the air flows through the hose *14*, to the aluminium end of the pipe and pushes out the radiation source. The source capsule closes the electric circuit of the signalling device *12* which indi-

cates the beginning of the exposure. After the exposure is completed the plug is taken out of the pipe *8*, and compressed air is admitted through the hose *6*; the stream of compressed air draws the air out of the container and hose through the opening *7*, and the radioactive source is drawn into the container. The contacts *3* of the signalling device *4* close and the signalling device *4* indicates that the radioactive source has returned to the container.

Two-passage pneumatic manipulator (Fig. 110). Prior to inspection a signalling device *6* is attached next to the radiographed sec-

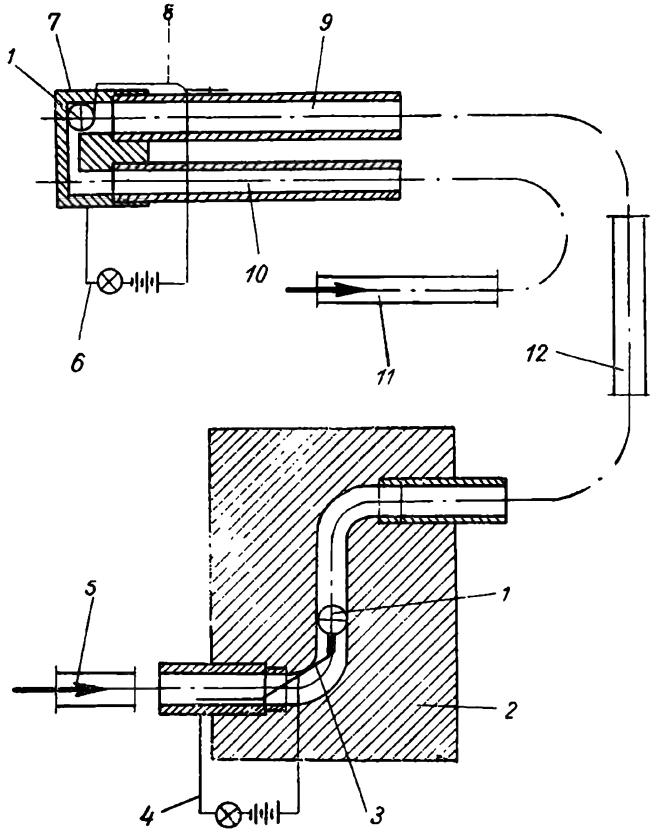

Fig. 110. Schematic layout of a two-passage pneumatic manipulator:

1—radioactive isotope; *2*—lead storage container; *3*—contact isolated from container walls; *4*—signalling device; *5*—hose; *6*—signalling device; *7*—aluminium end piece; *8*—contact; *9* and *10*—pipe; *11*—vent hose; *12*—thick-walled hose

tion and compressed air is admitted through the hose *5*. The air pushes the isotope capsule into the aluminium end piece which closes the electric circuit of the signalling device *6*. At the end of the

exposure the compressed air introduced into the hose *11* forces the radioactive isotope back into the container and the contacts close the electric circuit of the signalling device *4*.

The inside diameter of the thick-walled hose must be large enough to ensure free passage of the capsulated radioactive isotope. The contacts situated at the end of the tube are arranged to keep the source from falling out. The plugs used to close the suction tube may be replaced by rope-suspended cones. If no compressor is available, compressed air or gas may be obtained from an oxygen or sometimes from an acetylene cylinder, or a two-passage hand pump or other compressed air (or gas) sources may be employed.

Portable, three-positional industrial gamma-inspection unit, model ГУ-2. This unit is mainly designed for the inspection of stationary or bulky items with sections which are difficult of access

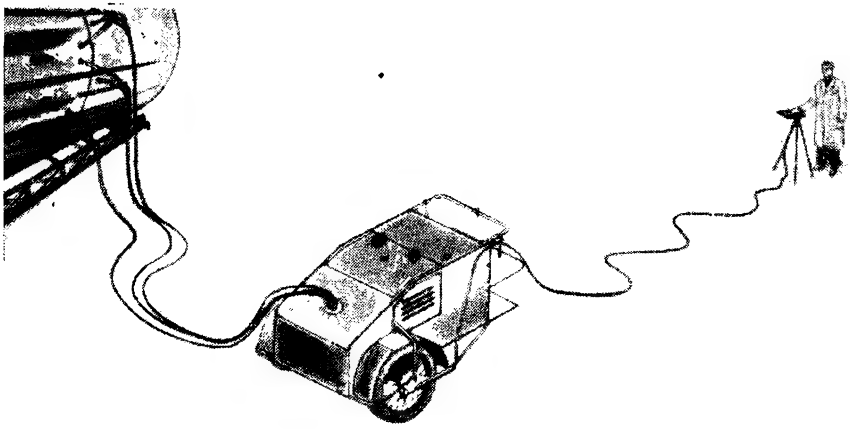

Fig. 111. General view of an industrial gamma-inspection unit, type ГУ-2

(ship hull welds, erected boilers, all kinds of trusses, etc.). In these cases, inspection is performed using simultaneously three Co^{60} gamma-sources with a total activity of 6 gram radium equivalent or three Ir^{192} gamma-sources of 15 gram radium equivalent.

The gamma-sources from the container are pneumatically shifted to the spot of inspection and back; the unit is controlled from a portable remote-control post.

The ГУ-2 unit is shown in Figs. 111 and 112. The unit, mounted on a three-wheel trolley *7*, includes the following component parts: storage container *1* with three flexible metal hoses for source shifting, the hoses being attached to the inspected object by means of electromagnetic brackets *6*; compressor assembly *2* with two receivers, switchgear with three switches and remote-control board *4* with cable *5*.

The storage container (Fig. 113) is a sectional lead block *2*, *4* and *5* in the centre of which the drum *3* is fixed accommodating three gamma-sources in aluminium cigar-shaped capsules. The metal

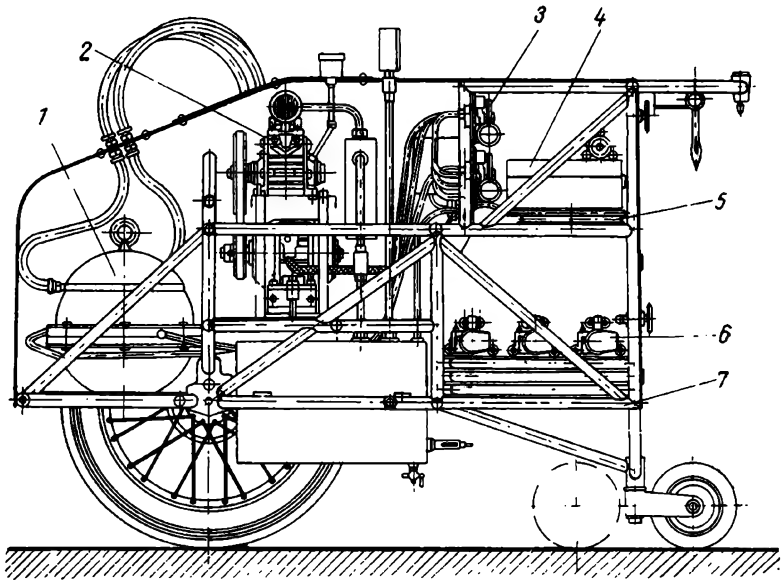

Fig. 112. Type ГУ-2 inspection unit cross-section

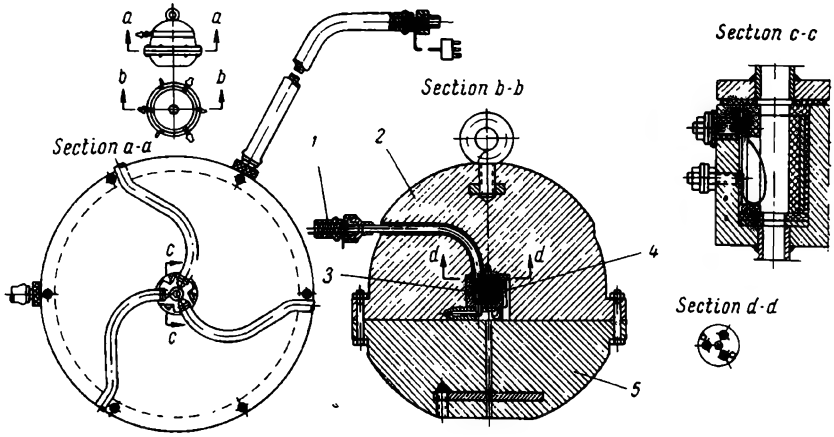

Fig. 113. Storage container of type ГУ-2 inspection unit

hoses *1* through which the sources are shifted are 8 m long, with an 8 mm inside diameter; air-tightness is ensured by vacuum rubber.

The storage container and electromagnetic brackets are equipped with signalling devices. Three green lights on the control board

indicate that the gamma-sources are inside the container, three yellow lights indicate that the electromagnetic brackets are mounted on the object to be inspected and three red lights signal that the gamma-radiation sources are exposed.

The three switches on the switchgear make it possible to connect the storage container and the three hoses to either a compressed-air receiver or to a vessel in which there is a vacuum. In the first case, the radiation sources are shifted out of the container for the purpose of exposure, while in the second, they are returned to the container. The switching-over is done from a remote-control panel by means of an electromagnetic device.

The overall dimensions of the unit are 1,715 × 1,185 × 1,035 mm; the weight does not exceed 350 kg.

Flexible hoses make possible the radiographing of large articles at spots difficult of access.

Remote-control and air-shifting of the gamma-sources reduce the irradiation of personnel to 0.01 r per 6 hours of work, which is five times less than the maximum permissible dose.

The container is pneumatically recharged so that full safety of operation is ensured.

§ 6. Basic principles of development, design and production of gamma-inspection units

Gamma-inspection units must ensure high efficiency of inspection, be economic, provide manoeuvrability in usage and operational safety. Therefore, in designing and producing radiography equipment it is necessary to take into account the experience obtained from using gamma-units in various branches of industry, and to select the most rational kinematic set-ups that ensure operational manoeuvrability, that is, inspection of sections of a radiographed object which are difficult of access and sending the gamma-beam in the required direction. The development of such units requires simultaneous work on designs and a study of the technological requirements, which the units must meet. To develop more perfect units, technological problems and problems pertaining to hte construction of individual components of a unit, standardisation and unification of parts and individual sub-assemblies must be solved. In addition correct classification should be made of the units according to their sphere of application and the radiation source employed.

It is impossible to develop and design one single inspection unit which would satisfy the needs of the various branches of industry. However, by changing one or another of the requirements of one user, so as to combine them with the requirements of other users, and also by widening the operating range of the units, by introducing auxiliary elements or spare parts (sub-assemblies), it is possible to develop and construct a group of typical units, taking into consid-

eration the radiation energy and activity of the radioactive sources employed.

In order to save metal and improve the quality of operation it is of great importance to cut down the weight of the units, taking into account, in doing so, the application of the units of a given type, since stationary and portable units must conform to different requirements. The weight of portable units must ensure ease of transportation from site to site and technological manoeuvrability under complex industrial conditions. As for the stationary units, the weight-reducing requirement is dictated mainly by the desire to save metal in general and scarce materials in particular. Lighter units may be created with plastics which are a good construction material, possessing high durability and good mechanical properties.

The units must be reliable and trouble-free in operation.

The finish of the units acquires great importance. In their endeavour to create inspection units with a pleasing outer appearance, designers are prompted towards more rational and economical designing work.

CHAPTER III

IONISATION, XERORADIOGRAPHIC AND METAL-VISION METHODS OF INSPECTION

In the U.S.S.R. the radiographic method of inspection is successfully used in hundreds of industrial establishments. But radiography, like X-ray inspection, has a number of disadvantages (long exposure time, and the time spent on arranging articles for exposure and film development), which prevent inspection becoming an automatic operation. Another shortcoming is the large consumption of costly roentgen film. These shortcomings may be eliminated by practising other methods of inspection, using radio isotopes, such as: ionisation, xeroradiographic and metal-vision techniques.

The ionisation method of control has been developed considerably, especially in the field of thickness measurement, and is widely used in industry. The xeroradiographic and metal-vision methods of inspection are for the present at the development stage.

§ 1. Ionisation method of inspection

Unlike the radiographic method of inspection in which the film registers the intensity of radiation that has passed through individual sections of the examined object, in the ionisation method the intensity of radiation is recorded by various radiation meters and ionisation chambers. The employment of such detectors is based on the ionisation action produced by radiation as it interacts with matter. By means of a detector alpha-, beta-, gamma- or neutron-radiation creates a flux of charged particles which it is easy to register.

Ionisation gamma-inspection units or measuring instruments have the following main component elements: the radiation source, radiation detector and electronic device which serves to amplify the electrical signal created in the detector by the passing gamma-rays.

There are several types of ionisation flaw detectors, all operating on practically the same principle as that illustrated in the diagram shown in Fig. 114. Having passed through the inspected object *3*, the gamma-ray flux *2* falls on the orificed shutter *4* and indicator *5*.

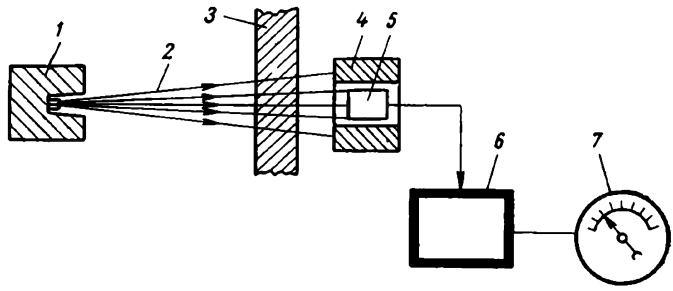

Fig. 114. Schematic layout of an ionisation inspection unit:
1—radiation source; *2*—gamma-rays; *3*—inspected object; *4*—orificed shutter; *5*—intensity indicator; *6*—amplifier; *7*—output instrument

The output indicator signal is converted by the amplifier *6* into tension or ionisation current, the intensity of which is proportional to the intensity of radiation falling on the detector (meter). Usually, a galvanometer, milliammeter, mechanical impulse counter, oscillograph, or a light or sound signalliser is used as an output instrument. If there is an imperfection in the inspected article, the registering device will record an increase in radiation intensity. The presence of a defect in the inspected articles may be indicated by a deflecting instrument pointer, by a recording instrument or by a tripped relay, etc.

The radiation source and registering instruments are placed on opposite sides of the object to be inspected and shifted parallel to its surface, maintaining the source-object and object-indicator distances constant. Individual sections of the article are inspected in turn as the radiation source and indicator are shifted in this way. Sometimes the procedure is reversed: the inspected article is shifted, while the radiation source and detector remain stationary.

The sensitivity of an ionisation flaw detector in revealing defects is one of the principal factors which determine the field of its application. Therefore, the choice of a detector is of great importance.

The most important properties of a detector are: sensitivity characterised by the ability of the detector to register reliably low-

intensity radiation; maximum radiation intensity which may be measured with the aid of a given detector; registration efficiency characterised by the ratio of registered particles or gamma-quanta to the total number of particles which penetrate into the detector. The requirements which supply sources must satisfy, such as reliability in operation and service life, etc., are also of great importance.

Ionisation chambers. The principal elements of the ionisation chamber are two isolated electrodes and a gas (usually air) filling

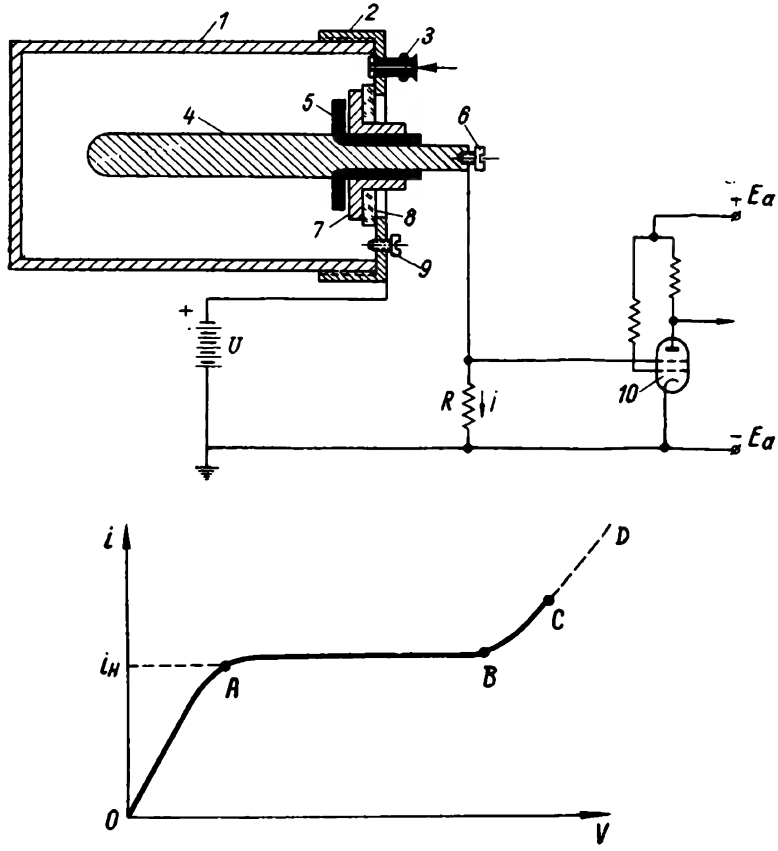

Fig. 115. Schematic layout, connection and volt-ampere characteristic (dependence of ionisation chamber current on the potential difference applied across chamber terminals) of an ionisation chamber:

1—cylinder (high-voltage electrode); *2*—base; *3*—passage; *4*—internal electrode; *5*—quartz or amber insulator; *6* and *9*—terminals for amplifier wires; *7*—protective metal sleeve; *8*—glass washer; *10*—electrometer tube

the space between the electrodes (Fig. 115). One of the electrodes of the ionisation chamber is a hollow thin-walled metal cylinder *1* or a cylinder made of an insulating material; its inner surface is metal

coated. The other electrode is a metal rod *4* arranged along the cylinder axis. Ionisation chambers operate with a current tension ranging from tens to several hundred volts, depending on the nature of the radiation and the construction of the chamber.

As radiation penetrates into the chamber, positive and negative ions form in the gas filling the chamber and an ionisation current is induced in the chamber circuit. The induced current is measured by means of sensitive galvanometers or an electron-tube instrument.

The induced current varies, depending on the energy and intensity of the radiation penetrating into the ionisation chamber, and on the tension applied across the electrodes. Part of the produced ions does not reach the electrodes (the initial inclined region of the characteristic curve), if the potential difference applied across the electrodes is small. The ionisation current increases (*OA* region) as the chamber voltage is increased, the ionising radiation intensity remaining unchanged. At sufficiently high tensions the current intensity becomes constant (*AB* region) and equal in value to the saturation current at which all the formed ions accumulate on the electrodes; the current intensity hardly depends on the applied voltage.

The saturation current is proportional to the intensity of radiation penetrating into the chamber. Further increase in the potential difference across the electrodes results in an increase in current intensity (*BC* region). The following phenomenon takes place in this case. As a result of the high potential difference applied across chamber electrodes the ions formed in the gas acquire such a high kinetic energy that when they collide with neutral molecules they split the latter into ions (collision ionisation). In this case, the ionisation chamber functions as a particle counter—a Geiger-Müller counter, for instance. Further increase in the applied tension (*CD* region) results in a breakdown.

As a rule, ionisation current intensity ranges from 10^{-9} to 10^{-16} a and the resistance of the high-ohmic resistor—from 10^{8} to 10^{11} ohm. The ionisation current may be intensified with the aid of special electrometer tubes possessing a low grid current.

The efficiency with which an ionisation chamber registers ionising alpha- and beta-radiation is 100%, because each alpha- and beta-particle ionises the gas. Ionisation chambers make possible the measurement of radiation fluxes of a very high density, which is of great importance in cases where it is necessary to conduct rapid and precise measurements. Ionisation chambers are of simple construction, reliable in operation and possess practically an unlimited service-life. That is why ionisation chambers are widely used in the instrument-making industry to register alpha- and beta-radiation.

As is known, gamma-radiation does not give rise to ionisation; the ionisation is caused by the secondary electrons knocked out of the chamber walls by gamma-radiation. But this process occurs rarely, therefore, only a small percentage of the gamma-radiation

is registered. This is the serious drawback of ionisation chambers, as far as the measurement of gamma-fluxes is concerned. Therefore, ionisation chambers find limited application in gamma-inspection.

Let us consider the sensitivity of a gamma-flaw detector fitted with an ionisation chamber. From the volt-ampere characteristic of an ionisation chamber (Fig. 115) it follows that saturation current intensity does not depend, within a certain range, on the potential difference applied across chamber electrodes and changes (for a given chamber volume) only as the gamma-radiation intensity varies.

The intensity of saturation current is

$$i_s = en, \tag{61}$$

where e—the electron charge,

n—the number of ion pairs formed by ionising radiation in the chamber volume per unit time.

In the AB region of the curve the ionisation current is the measure of the amount of energy E absorbed in the gas-filled space of the chamber per unit time. If ε is the average amount of energy required to form one ion pair, then, the ionisation current is

$$i_s = e\frac{E}{\varepsilon}. \tag{62}$$

Under conditions of uniform ionisation over the entire chamber volume the saturation current is proportional to the chamber volume V

$$i_s = en_0V, \tag{63}$$

where n_0—the number of ion pairs formed in 1 cu cm of the chamber volume per second.

The ionisation current i induced in the chamber is related to its volume V and to the physical radiation dose P by the following equation:

$$i = 3 \times 10^9 V \times P. \tag{64}$$

The sensitivity to minimum-size defects of a gamma-detector fitted with an ionisation chamber is defined by the difference

$$h = i_d - i_0, \tag{65}$$

where i_d—the chamber ionisation current induced by rays passing through the defective section of the inspected article;

i_0—the ionisation current induced by rays passing through the section of the inspected article free from defects.

The usually employed amplifying devices permit the registration of the minimum ionisation current i_{min} of about 2×10^{-13} a. Thus, the sensitivity limit of the inspection method in question may be expressed by the equation

$$i_d - i_0 = 2 \times 10^{-13}, \tag{66}$$

or

$$3 \times 10^9 VP_d - 3 \times 10^9 VP_0 = 2 \times 10^{-13}, \tag{67}$$

where P_d and P_0—the dose rates pertaining respectively to the defective and flawless sections of the inspected article.

By rearranging the equation (67) we get

$$3 \times 10^9 V (P_d - P_0) = 2 \times 10^{-13}. \quad (68)$$

Assuming $P_d - P_0 = P$, we get

$$3 \times 10^9 VP = 2 \times 10^{-13}. \quad (69)$$

From the equation (69) it follows that in order to obtain the maximum sensitivity, it is necessary for P to be as large as possible under conditions of a small chamber volume V. However, the physical dose rate P_g and, hence, the source activity must be large, if the volume V of the ionisation chamber is small. When dealing with 1 cu cm ionisation chambers, it is necessary in order to ensure the minimum saturation current sensed by the amplifier, to expose the chamber to gamma-radiation of a physical dose rate equal to

$$P_\gamma = \frac{3 \times 10^9 \times 2 \times 10^{-13}}{1} = 6 \times 10^{-4} \text{ r/sec} = 600 \ \mu\text{r/sec}.$$

This dose is 27 times larger than the permissible safe dose. Consequently, the use of such chambers for flaw detection would require the employment of a remote-controlled device to shift the inspected object or the ionisation chamber and gamma-source.

When employing a 3,000 cu cm ionisation chamber under similar conditions of inspection, the dose rate amounts to

$$P_\gamma = \frac{3 \times 10^9 \times 2 \times 10^{-13}}{3 \times 10^3} = 2 \times 10^{-7} \text{ r/sec} = 0.2 \ \mu\text{r/sec}.$$

This dose is 115 times smaller than the safe dose. However, employment of large-volume ionisation chambers is accompanied by a decrease in the sensitivity of this method of inspection. Hence, gamma-detectors featuring ionisation chambers may be employed mostly to detect large defects such as shrinkage cavities in castings. Counters of a higher sensitivity to gamma-radiation are more widely employed for the inspection of metals.

Counters employed to register radioactive radiation. *Discharge counters.* In considering ionisation chambers, it was stated that if the tension applied to an ionisation chamber is increased above point B (see Fig. 115), the chamber will function as an ionising particles counter. Counters are classified as proportional and self-maintained discharge counters, depending upon the nature of the discharge.

Proportional counters operate under tensions somewhat exceeding point B, the counter impulse at low gas-amplification factors* being proportional to the initial ionisation formed in the counter by the

* The gas-amplification factor is the ratio of the total number of ions formed in the counter to the initial number of ions.

ionising particle. In this case a smaller initial ionisation will result in a smaller output pulse.

In self-maintained discharge counters the potential difference applied across the electrodes is so high that the counter can operate under conditions of a self-maintained discharge, as the name of the counter implies. The output pulse of such a counter is of a constant amplitude, irrespective of initial ionisation, i.e., breakdown between electrodes occurs (corona discharge—in ring counters, sparking or arc striking—in point counters). Conventional discharge counters (Fig. 116) consist of a hollow cylindrical cathode (glass, aluminium) inside which an anode is placed—a thin wire 0.1-0.2 mm in diameter arranged along the cylindrical tube axis and secured at the ends of the tube in insulating plugs. The inner surface of the glass tube is coated with a current-conducting layer (copper, tungsten, graphite). The tube is filled with various gases (air, hydrogen, argon with oxygen, nitrogen, etc.) under a pressure of several tens of millimetres of mercury. A tension ranging from 1,000 to 2,000 v, depending upon the type of a counter, is applied to the counter electrodes. Such a counter ensures the formation at the anode of an electric field of a high gradient under relatively low tensions; as a result the electrons are highly accelerated in the vicinity of the wire filament and form an avalanche of collision ions.

Depending on the manner in which the discharge caused by the ionising particle is quenched, discharge counters are divided into self-quenching counters, the quenching in which is caused by internal reasons, and nonquenching counters in which the formed discharge lasts till it is quenched by an external effect.

In self-quenching counters the discharge becomes quenched after the passage of one or several ion avalanches when the wire filament potential is restored to initial value. Another ionising particle appearing in the counter may initiate a repeated process. Owing to the multistage nature of the discharge, these counters possess a long-duration pulse (about 10^{-3} sec) and that is why counters of this type are rarely employed in automatically controlled devices, where fast response is required. Quenching of the discharge in the first stage is attained with the aid of special admixtures—polyatomic gases—introduced into the counter. In the course of the discharge, molecules of the polyatomic gas split into simpler molecules, thus retarding the further development of the discharge. In self-quenching counters pulse duration usually does not exceed 10^{-4}-10^{-5} sec and the time during which the counter is not able to register radiation being restored after the discharge (dead time) does not exceed 10^{-4} sec. Counters filled with a polyatomic gas have a limited period of service. Usually, the polyatomic molecules disintegrate to a considerable extent after 10^{8}-10^{9} pulses, resulting in the failure of the counter. This shortcoming restricts the employment of polyatomic gas-filled counters.

The so-called halogen-quenched counters filled with inert gases (argon, neon) and a small halogen admixture (chlorine, bromine) have been widely used in automatic-control devices. Unlike collision-ionisation counters, the action of halogen-quenched counters is based on the formation of metastable (not quite stable) atoms of the primary filling gas. These atoms become destroyed as they collide with halogen molecules and for an avalanche ionisation. Halogen-quenched counters are distinguished for their long service, and operate under low tension.

Fig. 116 shows the counting rate-voltage characteristic of halogen counters. The curve expresses the relation between the counting rate (the number of output pulses) and the voltage applied to the counter. The section of the curve to the left of point U_1 is the range of proportional counting. Along the section of the curve between points U_1 and U_2, the counting rate depends only a little on the voltage. This section of the curve, called the plateau, covers the range of working voltages of a counter and is considered to be the principal characteristic of the latter. The plateau section of the curve is somewhat inclined. The smaller the incline and the longer the plateau, the better the counter. Some types of halogen counters used in automatic-control devices possess a plateau extending from 60 to 100 v, the incline of the plateau not exceeding 0.125% per volt.

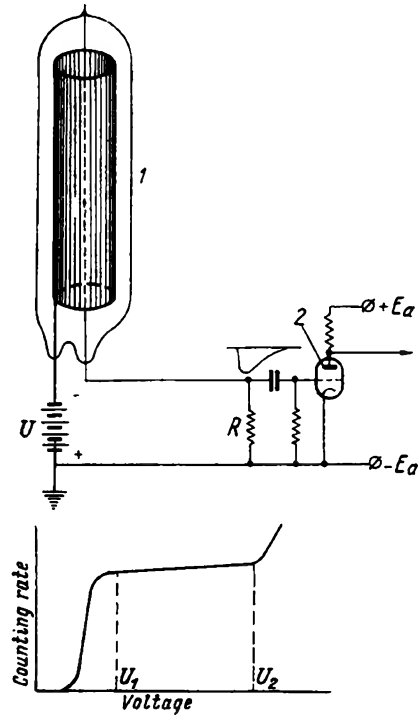

Fig. 116. Connection diagram and counting rate characteristic of gas discharge counter:
1—counter; *2*—amplifying tube

The design of a counter depends on the kind of radiation for which the counter is intended. Alpha-particle counters have a thin face window, 3-5 mg/sq cm thick, through which alpha-particles pass. Beta-particle counters are thin-walled counters of a high penetration for beta-particles of an energy ranging from tens of kilo-electron-volts to several Mega-electron-volts. Beta-counters are made of metal (usually, the cathode is made of aluminium up to 0.1 mm thick). Counters employed to register gamma-radiation of different energies, in which the discharge initiation is traced to the ionising influence

of the secondary electrons ejected from the counter walls by gamma-quanta, have either metal-coated glass walls or metal walls.

The first electron formed as a result of interaction between gamma-quanta and counter walls penetrates into the counter and ionises the gas. As the counter electrodes are energised the formed electron acquires an amount of energy sufficient to ionise the atoms of the filling gas. The secondary electrons are accelerated as they move towards the filament and acquire sufficient energy to produce further ionisation of other atoms of the gas. The initial ionisation process is avalanche-like—gas amplification takes place. This results in the appearance of a gas discharge along the entire length of the counter filament. A discharge in the counter may be observed when a voltage pulse occurs on the counter's loading resistance R. The avalanche-like ionisation increases the sensitivity of the gamma-intensity measurement.

Experience has shown that the efficiency of gas-filled counters is low (it is practically impossible to attain a counting rate exceeding several thousands per second), therefore, at present, gas-filled counters are replaced by scintillation counters, sometimes called luminescent counters.

Scintillation counters. A scintillation counter (Fig. 117) combines a scintillation crystal or luminescent screen M and a multiplier

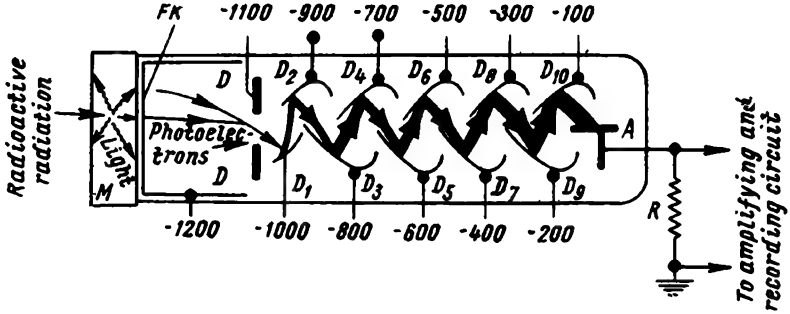

Fig. 117. Schematic layout of scintillation counter

phototube in a common opaque case. Crystals of anthracene, naphthalene, sodium iodide, etc., are used as scintillation crystals. Light flashes (scintillation) occur in the scintillation crystals under the influence of ionising radiation. The photomultiplier picks up the crystal scintillation and gives out corresponding current pulses into the anode circuit. Having passed through a tube magnifier, discriminator and scaling unit, these pulses are registered by an electromechanical counter. The efficiency of scintillation counters in counting gamma-quanta exceeds the resolving power of gas-filled discharge counters by several orders of magnitude. Scintillation counters have an important advantage over gas-filled counters in that

their dead time (de-excitation time) is very short. This makes it possible to count hundreds of thousands of gamma-quanta per second, to operate with high-intensity gamma-rays and to create ionisation flaw detectors with a fast response and a high sensitivity.

Gamma-radiation detectors of any kind may be used with ionisation inspection units, provided the detectors possess the following properties: a sufficiently high efficiency (the probability that the counter will register a gamma-photon of a given energy) and a resolving power determined by the duration of a pulse in the course of photon registration and, consequently, by the maximum counting rate for a given counter. For this purpose, scintillation counters and in some cases self-quenching counters are most suitable.

Scintillation counters use highly-sensitive type ФЭУ-19М photomultipliers for detectors and, usually, monocrystal NaI(Tl) (sodium iodide) for the scintillation crystal. This monocrystal is thallium-activated and possesses a high absorption coefficient, a high light yield and a short fluorescent lifetime. As compared with scintillation detectors, self-quenching counters are less efficient, therefore they are used in flaw detection only when inspection efficiency is of no essential importance.

When registering gamma-radiation, the power of the output signal of the photomultiplier is low and an intermediate magnifying circuit is used to have the signal picked up by any output instrument (recording potentiometers, relays, pointer instruments, indicators, etc.).

Gamma-inspection units using self-quenching and scintillation counters are considered below.

Flaw detectors using counters. An inspection unit possessing a self-quenching counter consists of the following main components: the container holding the gamma-source and a screened counter firmly attached to the container; a mechanically and electrically controlled device for shifting the radiation source-counter unit in relation to the object under inspection; registering instruments. The general schematic layout of such an inspection unit is similar to that shown in Fig. 114.

On the curves plotted by means of such a flaw detector defects appear as peaks corresponding to the change in wall thickness of the inspected article. The relation between sensitivity and steel thickness is graphically shown in Fig. 118. This curve has been plotted from data obtained in gamma-raying artificial defects, the cross-sections of which are larger than those of the gamma-beams, employing Co^{60} as the radiation source. The output of the flaw detector is about 10-20 sq cm/min.

As mentioned above, scintillation counters possess a higher resolving power and a higher efficiency, compared with self-quenching counters. Scintillation counters increase the sensitivity of the flaw detector. From the curves shown in Fig. 119 it follows that in in-

specting steel articles up to 100 mm thick the sensitivity of the flaw detector using a cobalt gamma-source of small activity (0.175 curie)

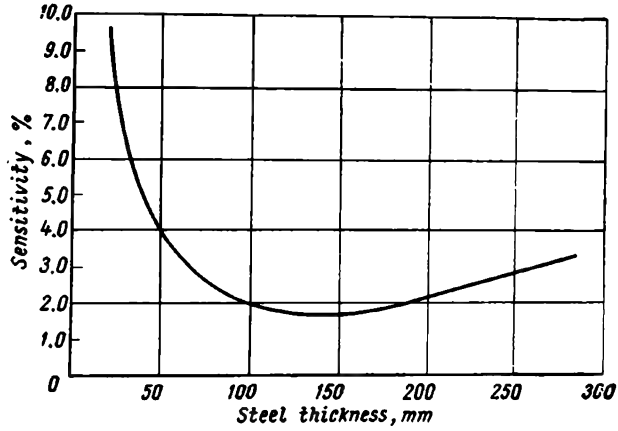

Fig. 118. Sensitivity curve of gamma-inspection unit fitted with self-quenching counter

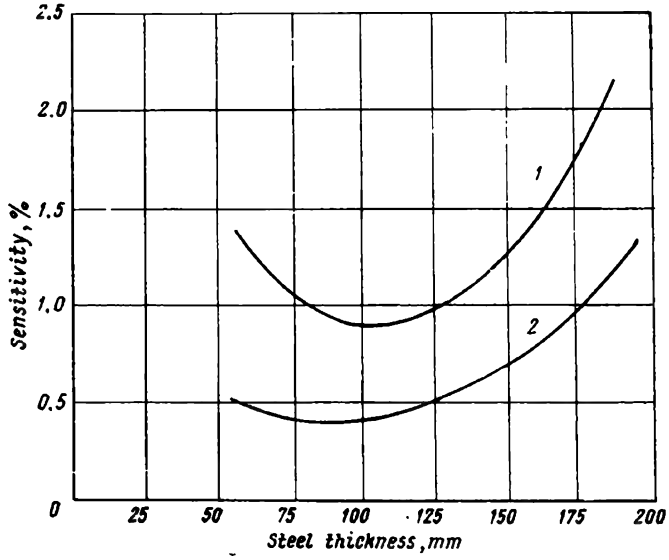

Fig. 119. Sensitivity curves of gamma-inspection unit fitted with scintillation counter:
1—source activity 0.175 curie; *2*—source activity 0.6 curie

makes possible the detection of variations in thickness beginning with 0.6-0.8 mm (0.6-0.8%). An increase in the activity of the source up to 0.6 curie almost doubles the sensitivity of the unit—a 0.3-0.4 mm (0.3-0.4%) variation in thickness is detected.

An analysis of the curves shown in Figs. 118 and 119 proves that, other conditions being equal, a scintillation counter increases the sensitivity to variation in steel thickness by about 2-4 times. When operating with a 0.6 curie Co^{60} gamma-source, inspection output ranges from 20 to 30 sq cm/min. Consequently, compared with a flaw detector fitted with a self-quenching counter, a scintillation counter inspection unit possesses a higher sensitivity and efficiency.

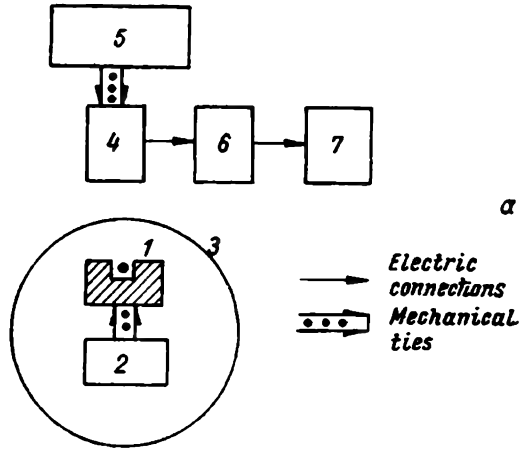

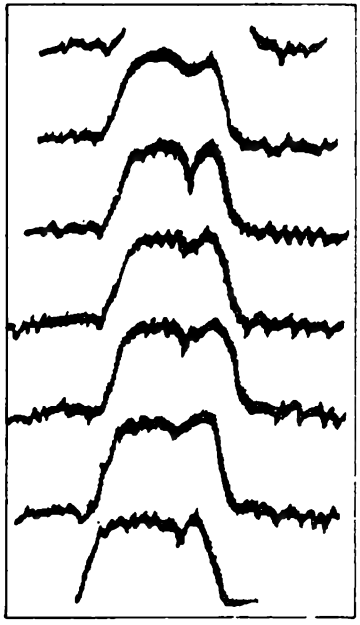

Fig. 120. Key diagram of type ИД-3 ionisation flaw detector (*a*) and image of a defective weld (lack of fusion) (*b*)

Fig. 120,*a* shows the schematic layout of a type ИД-3 ionisation gamma-inspection unit intended for flow-line inspection of welds in steel gas mains 560-720 mm in diameter. The gamma-ray source *1* bound to the shifting mechanism *2* is placed inside the welded steel tube *3* which moves in the axial direction during the course of inspection. Mechanism *5* puts the radiation detector *4*, consisting of a luminescent crystal and a photoelectron multiplier, into reciprocating (scanning) motion in the plane perpendicular to the weld axis. The output signal of the radiation detector passes through the amplifier *6* to the recorder *7*. Inspection data are recorded on thin graphite-base paper. When the current passes through the pen the paper burns out and a dark strip appears. The degree of darkening is proportional to the current intensity. The flaw diagram

obtained characterises the internal macro-structure of the inspected weld. Fig. 120,*b* shows the flaw diagram of a defective tube weld (lack of fusion) recorded with the use of an Ir^{192} gamma-source. The flaw detector can examine 0.6 m of a weld per minute. Unfortunately, the ionisation method in spite of its many advantages has not been developed as much as it should in the inspection of welded joints and castings. In industry this method is widely employed to measure the thickness of materials, walls of articles, coatings, etc.

The measurement technique is based on the dependence of the absorption and scattering rates of alpha-, beta- and gamma-radiation on the properties of the inspected articles, such as: density, thickness, temperature, humidity and also the rate of shifting.

Instruments, the action of which is based on radioactive radiation, can perform measurements without direct contact with the measured article and also through thick walls of metal vessels, pipelines and other similar structures. Such instruments are most suitable for modern industry with its tendency towards a sharply increased rate of various technological processes, high temperatures, pressures, etc.

The action of float level gauges, torqueless tachometers, which can measure the speed of rotating articles enclosed inside various mechanisms and, therefore, inaccessible to any other devices, radiation balances and other transmitters, sensing minute displacements and vibration, is based on the change in the distance between the radiation source and the detector.

The action of instruments such as thickness gauges, liquid or pulp flow density gauges, production-line article counters, etc., is based on the variation in radiation absorption and scattering. The change in the ionisation effect produced by radiation and the rearrangement of the produced ions underlie the action of such instruments as absolute pressure gauges, gas flow meters, etc.

Below we shall examine typical examples of the use of radioactive isotopes to measure the thickness of various materials and coatings, because these problems are directly related to flaw detection.

Measuring the thickness of materials by the ionisation method. The ionisation method of thickness measurement is based on the different absorption of radiation by various materials, or on the utilisation of scattered gamma-radiation.

To measure thickness by registering the absorption of the radiation by the measured material, one must have a beta- or gamma-radiation source and a detector for registering the radiation that has passed through the checked material. Usually, a scintillation counter is employed as the detector. The radiation source is chosen according to the thickness to be measured, the kind of radiation and its energy, the half-life and other properties of the isotopes.

Fig. 121 shows the schematic diagram of a radiation thickness gauge and curves characterising the absorption in steel of beta

and gamma-radiation respectively from Tl^{204}, Sr^{90} and Co^{60}, Ir^{192} sources.

In measuring thicknesses by this method, the following relation is employed

$$d = \frac{1}{\mu} \ln \frac{h_0}{h_d},$$

where h_d and h_0—the beta-particle or gamma-quanta fluxes, respectively, which passed through the material and by-passed it;

μ—the linear absorption coefficient;

d—the thickness of the material.

The error of measurement by this method does not exceed, as a rule, 1% of the measured thickness, and the maximum accuracy of

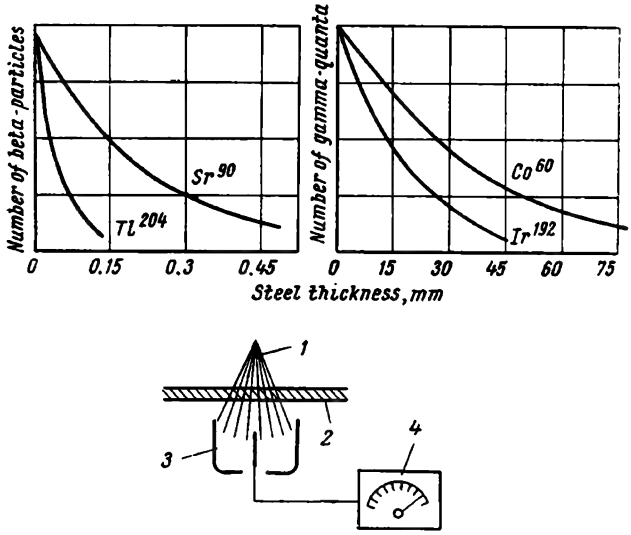

Fig. 121. Beta- and gamma-absorption curves and schematic layout of thickness, density or weight gauge based on radiation absorption:

1—radiation source; *2*—measured material; *3*—radiation detector; *4*—amplifier and indicator

measurement ranges from $\frac{1}{\mu}$ to $\frac{2}{\mu}$. The instrument determines the mass and not the geometric thickness, therefore, the error of measurement depends on the variation in the density of the measured material. This limits the use of such instruments for measuring thickness and does not allow them to be used to measure, for instance, pulp density in metallurgical works, the density of process solutions, etc.

Instruments based on the compensation principle (Fig. 122) are widely employed to measure the thickness of hot- and cold-rolled stock, plastics, rubber, paper, textiles, etc. The radiation detector of such instruments is a differential ionisation chamber *1*. The current arising at the exit of this chamber is proportional to the difference between the two radiation fluxes. The flux coming from the main radiation source *2* transverses the material being checked on its way to the chamber, while the flux of the compensating radiation source *4* passes through the shutter *3*. The vibration rectifier *6* con-

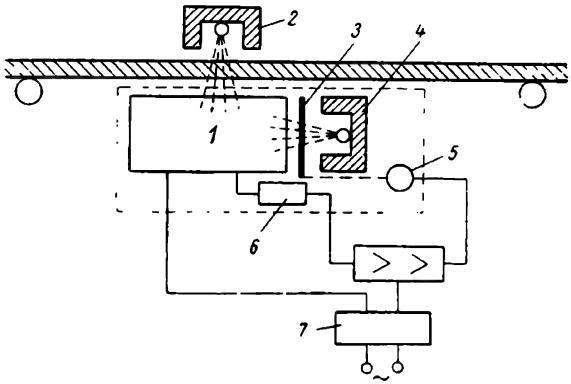

Fig. 122. Key diagram of thickness gauge based on the compensation principle:
1—differential ionisation chamber; *2* and *4*—main and compensating radiation sources; *3*—shutter; *5*—servomotor; *6*—vibration rectifier; *7*—rectifier

verts the differential ionisation current into alternating current. The amplified current actuates the servomotor *5* which shifts the shutter until both radiation fluxes become equal and the chamber output current tends towards zero. The position of the shutter bound to a secondary indicator makes it possible to determine the measured thickness and also to estimate both the density and weight of the measured material.

At present scintillation counters which, in most cases, possess a considerably higher efficiency and require radiation sources of a smaller activity, as compared with ionisation chambers and ionisation counters, are being ever more widely used.

The method of measuring the thickness of a material by measuring the intensity of the scattered gamma-radiation is based on the fact that the number of gamma-quanta scattered from the checked material at a 180° angle increases with the increase in the thickness of the irradiated material, and reaches saturation at a definite thickness.

Fig. 123 shows the schematic layout of such a thickness gauge and the curve, expressing the dependence of the intensity of back scat-

tered radiation on the thickness of the reflector. The value d_s, called saturation thickness, represents the maximum thickness which can be measured by this method. If the wall of an article is thinner than d_s, this method can measure the thickness of the article accessible for measurement from one side only, the gamma-radiation source and detector being arranged, in this case, on one side of the checked article. The thickness of the material is determined by evaluating the flux of back-scattered gamma-radiation.

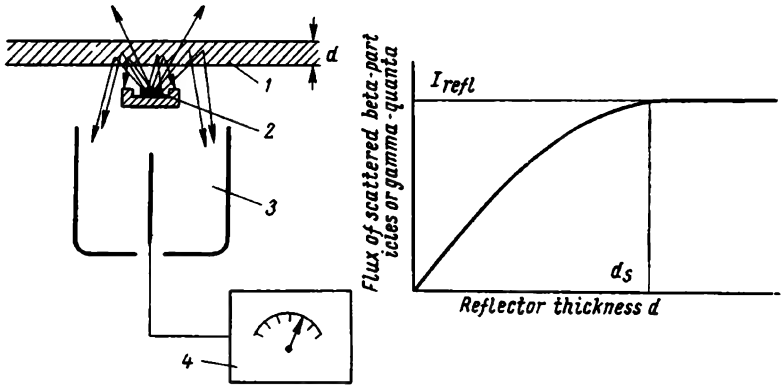

Fig. 123. Key diagram of a thickness gauge based on scattered radiation intensity and curve showing the dependence of scattered radiation on material thickness:

1—checked material; *2*—radiation source; *3*—radiation detector; *4*—amplifier and recording instrument

Scattered gamma-quanta differ in energy from incident gamma-radiation. Thus, the energy of direct gamma-radiation emitted by a Co^{60} source is 1.17 and 1.33 Mev, while the energy of scattered gamma-quanta ranges from 0.209 to 0.214 Mev. Owing to this, there is no need to protect the detector from the radiation source, and so sources of a lower activity can be used. The radiation source is placed on the case of the scintillation counter at a short distance from the sodium iodide crystal, the source being set inside a protective case. The source and counter constitute the measuring head of the gauge which is placed on the checked article or at a small distance from it. These radiation back-scattering thickness gauges fitted with a Co^{60} source can measure the thickness of steel walls up to 20 mm thick and ensure a measurement accuracy up to $\pm 3\%$. They can also detect corroded sections in boilers, tubes, cylinders, tanks, etc.

Measuring the thickness of coatings by the ionisation method. The radioactive method of measuring the thickness of coating is based on the registration of beta-particles back-scattered from the measured substance (Fig. 124). The amount (or proportion) of the back-scattered beta-particles depends on the nature of the

checked substance and its thickness and reaches a constant value when the thickness of the material is equal approximately to three half-value layers. Depending upon its atomic number, each substance has a definite back-scattering constant. The thickness of a paint or any other kind of coating can be measured by registering the amount of beta-particles back-scattered from the material, providing the coating is thinner than the saturation layer. The measurement is performed without contact with the material. The design of a number of thickness gauges widely used in the production of galvanised

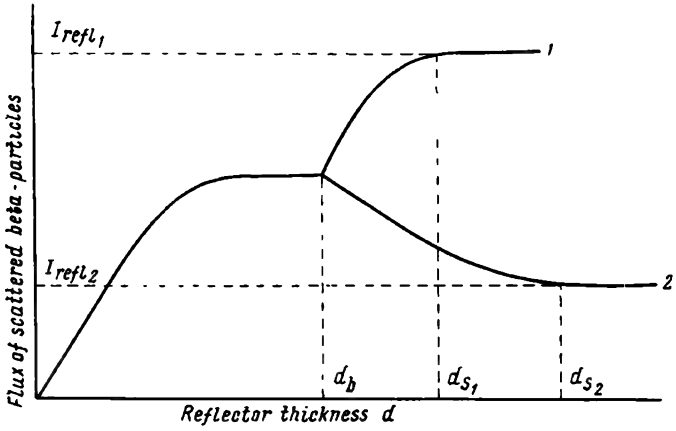

Fig. 124. Dependence of scattered beta-flux on coating thickness:

1—the atomic number of the coating is larger than that of the base; *2*—the atomic number of the coating is smaller than that of the base; d_{s_1} and d_{s_2}—saturation thickness

sheetiron, tin, radio parts, plastic-clad sheet materials, heat-resistant, electric conducting, water-proof, adhesive and other substances, is based on this principle.

The dependence of the intensity of back-scattered beta-radiation on the atomic number of the irradiated substance is expressed by the formula

$$\frac{I_{refl_1}}{I_{refl_2}} = \left(\frac{Z_1}{Z_2}\right)^n,$$

where I_{refl_1} and I_{refl_2}—the maximum radiation fluxes scattered from materials of Z_1 and Z_2 atomic numbers respectively;

n —the factor ranging from 0.7 to 0.8 and determined experimentally.

If we take a material with the Z_1 atomic number and cover it with thin layers of a substance with the atomic number Z_2, then the intensity of back-scattered radiation would change from I_{refl_1} to I_{refl_2}, if

the applied coating is sufficiently thick. The operating range of the thickness gauge is limited to the section of the curve (Fig. 124) along which the value of the back-scattered flux depends upon coating thickness. It is possible to check the thickness of a great number of conventional coatings by using several beta-sources. If the thickness of the base exceeds d_b (see Fig. 124), then any variation in the base thickness introduces no error into the coating thickness measurement. The larger the difference in the atomic numbers of the base and coating, the higher the accuracy of the coating thickness measurement. In practice, it is possible to measure the thickness of a coating, if the difference in the atomic numbers amounts to two unities. Measurement runs up to tenth fractions of a micron, if the difference in the atomic number is larger than two.

One of the disadvantages of thickness gauges based on back-scattered radiation is that the measurement of the thickness of the coatings is performed on sections of a considerable area. This disadvantage means that such gauges cannot be used to check small parts or parts with curved surfaces. Scintillation counters can be used to measure the thickness of a coating on an area of 0.75 sq cm. The economic advantage of using radiation thickness gauges may be illustrated by the following examples.

§ 2. Xeroradiographic method of inspection

Principles. The xeroradiographic method of inspection is based on the property of some materials, good insulators under normal conditions, to conduct electricity under the influence of X-ray or gamma-ray irradiation. If a plate made of such a material is electrically charged to a definite level and then exposed to gamma-radiation, which has already passed through an inspected object, the residual charge on the plate will be directly dependent on the intensity of the radiation falling on a given section of the plate, the residual charge being the smaller (at a given exposure time) the higher the intensity of incident gamma-radiation. Consequently, the residual charge on the sections of the plate exposed to radiation which passed through a defect (lack of fusion, cavity, porosity) will be smaller than the charge on other sections of the plate. Thus, the electrical charges become distributed on the plate in a certain way, maximum charge density occurring on sections of the plate subjected to minimum irradiation.

In the xeroradiographic method of inspection the xeroradiographic plate holders are arranged in relation to the inspected object in the same way as in gamma-radiography. In the course of X-ray or gamma-ray irradiation the charged layer of the plate turns into a conductor and, as a result, the electric charge leaks from the surface of the xeroradiographic plate. The rate of charge leakage depends on the intensity of the incident radiation, i.e., on the thickness and densi-

ty of the inspected material. The conductivity of the sections of the plate influenced by only slightly attenuated gamma-rays, i.e., by rays which have passed through defective spots in the inspected article, greatly increases and the charge leakage from these sections considerably exceeds the leakage from sections influenced by gamma-radiation attenuated to a greater extent.

Thus, the influence exerted by gamma-radiation on xeroradiographic plates is of a photoelectric nature, as distinct from the conventional X-ray film, the reaction of which is of a photochemical nature. As soon as the exposure is completed, an invisible electrostatic image appears on the surface of the plate in the shape of a distribution of electric charges over the sensitive layer of the xeroradiographic plate. The residual charge density is greatest on sections subjected to minimum gamma-irradiation. The sections of the plate influenced by the most intensive gamma-rays are almost fully discharged. After the exposure is completed the sensitive layer of the xeroradiographic plate returns to its normal state, which is characterised by a high specific resistance, but the electric charge distribution resulting from gamma-irradiation of the inspected article and plate remains unchanged.

This distribution of electric charges may be fixed with the aid of pigments (dry paints), and this is what gives the name xeroradiography to the method (the Greek word *xeros* means "dry"). Xeroradiographic inspection can be carried out with the equipment employed for radiographic inspection.

The xeroradiographic method of inspection is distinguished for a number of features: 1) a xeroradiographic plate may be used repeatedly (hundreds and thousands of times), if it is not damaged; 2) a xeroradiographic plate does not become spoiled by accidental exposure to light, roentgen or gamma-rays; 3) a xeroradiographic image can be made visible in several seconds after the exposure is completed, no solutions of any kind being necessary for the development operation.

The process of obtaining a xeroradiographic image includes the following stages: electric sensitising of the xeroradiographic plate; gamma-raying of the articles; development of the xeroradiographic plate to render the latent image visible; transferring the image from the plate to another surface, paper, for instance, to secure a permanent image; removal of the old image from the plate and preparing the latter for repeated usage. In some cases the last stages of the described process may be omitted.

Xeroradiographic plates. The most important component of the xeroradiographic method of inspection is the xeroradiographic plate.

At the present time xeroradiographic plates consisting of a polished conducting material bearing a thin layer of a radiation-sensitive substance are widely employed. The conducting material must

ensure a high mechanical strength and the sensitive ayer must firmly adhere to the surface of the plate. Sheet aluminium, brass, glass or paper bearing a conductor coating, steel foil or any other suitable material may be used as a conducting base. The sensitive layer may be produced from selenium, sulphur or other semiconductors. Aluminium is most widely used as a conducting material for xeroradiographic plates. The amorphous selenium layer is sprayed in vacuum on to the surface of aluminium plates which are up to 350 × 450 mm in size. When there is no radiation, the plates serve as good insulators with a specific resistance ranging from 10 to 15 ohm/cm, but under the influence of X-rays or gamma-rays they turn into an electric conductor (the specific resistance diminishes 100-100,000 times).

General procedure in xeroradiographic inspection. As xeroradiographic plates are not sensitive to X-rays without preliminary treatment, they are not spoiled under the influence of radiation. In order to make a xeroradiographic plate sensitive to radiation, it must be specially treated—sensitised. The process of sensitising a plate consists in covering the top sensitive surface of the plate with a uniform layer of electric charge. Usually, during the charging operation the conducting backing plate is grounded. The plate is sensitised either by shifting it below thin wires to which a 7,000 v potential is applied, or by arranging the plate above an electrode (at a distance of 110-120 mm from the electrode) with a positive potential of 12 kv. A free electric charge forms on the selenium layer in the process of emission. The charging takes from 10 to 120 sec.

A charged xeroradiographic plate is sensitive not only to X-rays and gamma-radiation, but to visible light as well; therefore, charged plates should be kept in the dark or in red light.

The charged surface of xeroradiographic plates must not be touched with the hands or any other articles, for touching removes the electric charge from the surface of the plate and causes the appearance of white and other spots on the developed image. Therefore xeroradiographic plates are placed in special holders, the cover of which does not contact the sensitive layer of the plate. A charged xeroradiographic plate loses its electric charge with time, even if kept in full darkness. The rate of discharge is especially high when the charging has been done rapidly. The experience gained in using xeroradiographic plates in X-ray laboratories shows that charged plates may be kept in the dark for 1 hour without any considerable loss in plate sensitivity and image definition. Longer storage of charged plates (up to 24-50 hrs) is undesirable, for such plates produce images of a smaller density.

It is desirable to use lead foils, when xeroradiographic inspection is performed with a gamma-ray source. Lead foils, as in the case of X-ray film, increase the definition of the image and the rate of in-

spection and are particularly effective when the inspection of articles is carried out with the aid of hard gamma-radiation.

In xeroradiographic inspection, it is undesirable to use conventional fluorescent screens, for the latter diminish image definition because of the presence of a coarse-grained fluorescent layer, and the impossibility of making close contact between the fluorescent screen and the sensitive layer of the charged plate (such contact would discharge the plate).

To render the latent image visible, exposed plates are developed preferably within several hours after exposure to radiation. The images are subject to distortion, if the plates are kept undeveloped for a longer period of time. Like X-ray film, exposed xeroradiographic plates are fogged if affected by light, X-rays, gamma-rays or any other kind of radiation that can discharge the plate.

The distribution of electrostatic charges on the surface of an exposed xeroradiographic plate can be measured with an electrometer. However, this method is costly and complicated.

The simplest and cheapest way to develop exposed xeroradiographic plates is to ensure in some way that the pigment particles settle on the surface of the plates in amounts proportional to the density of the charge remaining in each area of the plate. These particles may be charged in the conventional way or by the triboelectric effect, and be fixed on the latent image by electrostatic forces acting between the image charge and that of the fine particles.

At present there are two methods of depositing charged pigment particles on xeroradiographic plates: the cascade development method, and the method of development with a powdery cloud.

In cascade development the powdery developer is a mixture of the finest (0.1 to 2.0 microns in diameter) pigment particles possessing suitable triboelectric properties and a coarse-granulated carrying agent 200-300 microns in diameter. The carrying agent is selected from the triboelectric series, so as to give the pigment powder the greatest charge of triboelectricity, after the powder is separated from the coarse carrying particles. It is convenient to cover the exposed plate with the powdery developer in a swinging trough. As it rolls along the surface of the plate, each carrying particle leaves behind a trace consisting of pigment particles that have adhered to the surface of the charged plate.

Repeated swingings (2-10 times) distribute the developer fairly uniformly, in amounts proportional to the potential of the plate sensitive layer, and so the latent electrostatic image is developed. The larger the charge of the plate sensitive layer the larger the density of the adhered layer of powder. Development is completed as soon as the image becomes visible and the process lasts from 5 to 10 sec.

At the present time development by means of the powdery cloud is extensively used. The holder with the xeroradiographic plate is placed in a special compartment over a vibrator so that the sensi-

tive layer of the plate with the hidden image faces downwards. Then the holder is opened. The plate begins to be developed as soon as its sensitive layer comes into contact with the cloud of finely-ground white powder; the cloud is created by a special vibrator supplied from a 6.5-9.5 v source. The vibrator throws out the powder through a hole 3 mm in diameter. Owing to friction, part of the particles becomes positively charged and part of them negatively charged. A round electrode 37.5 mm in diameter connected to a 12 kv potential is placed in the path of the white powder, between the vibrator and the plate. This electrode, placed at a distance of 120 mm above the vibrator, serves as a filter for the negatively charged particles which are attracted by the electrode and adhere to it. Consequently, only positively charged particles remain suspended. These particles adhere to the charged layer of the xeroradiographic plate in amounts proportional to the distribution of the electric charge, and develop the latent electrostatic image. Development time ranges from 30 to 40 sec. From the xeroradiographic plates the images may be transferred to paper by various methods.

The first gum-printing method is similar to the method employed to obtain images in magnetic flaw detection. The other gum-printing method requires the use of special materials.

The electrostatic method is simple in use and printing can be done on any kind of paper. The printing is done by placing a sheet of writing paper on top of the developed xeroradiographic plate. Then, the plate and paper are placed under a positively-charged 12 v electrode in a manner similar to that practised in charging plates. When the electrified paper is removed from the plate, it carries off part of the powder and only $^1/_3$ to $^1/_4$ of the initial amount remains on the plate. The powder is transferred from the plate to the paper under the influence of the electric field induced between the paper and the plate. The powder particles have then to be fixed to the paper and this is done by giving the image obtained a coat of resinous powder which is made to stick to the paper by heating. The fixing time is 2-3 sec. The image transferred in this way may be used as long as the paper lasts.

In a number of cases the process of transferring the image to paper does not clean the xeroradiographic plates sufficiently. Therefore, plates must be thoroughly cleaned before being used again. The powder can be removed from the plates by means of solvents like acetone or carbon tetrachloride and a soft rag or brush. If handled with care, xeroradiographic plates can be used hundreds and even thousands of times.

Two different xeroradiographic units for charging and developing plates are shown schematically in Figs. 125 and 126. A replaceable stationary pointer (sharp-pointed probe) is fitted into the plate-charging chamber at a distance of 10-12.5 cm from the plates, depending on the size of the latter. The potential applied to the probe is main-

tained at about 15 kv, by connecting the probe to a high-voltage transformer. At the base of the development compartment there is a powder-filled taper chamber with an opening of about 3 mm in diameter. The powder, forced violently through the opening by a vibrator, settles on the walls of the chamber. The tension applied to the vibrator is regulated by means of an autotransformer. The charge carried by a powder particle is determined by means of a disc electrode about 4 mm in diameter, placed in the path of the powder stream. The potential applied to the disc electrode is equal to that brought to the

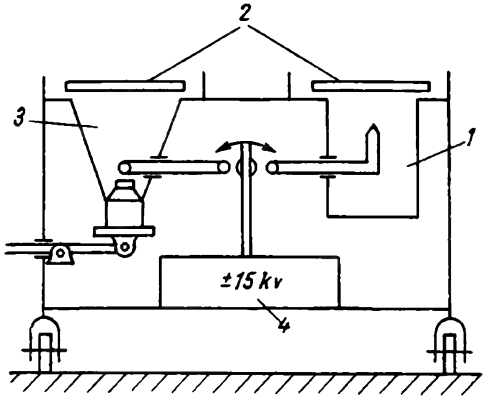

Fig. 125. Schematic layout of a xeroradiographic unit with chambers arranged horizontally:

1—charging chamber; *2*—xeroradiographic plate-loaded holders; *3*—development chamber; *4*—supply source

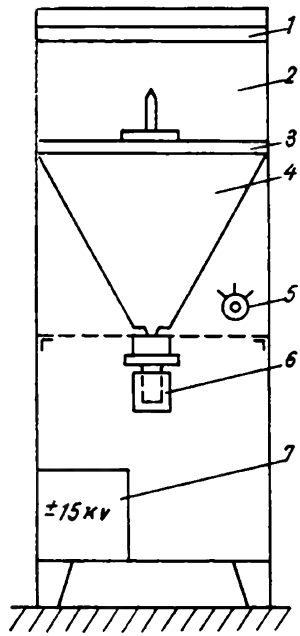

Fig. 126. Schematic layout of xeroradiographic unit with chambers arranged vertically:

1 and *3*—slots for holders; *2*—charging chamber; *4*—powder spraying chamber; *5*—polarity switch; *6*—membrane-type powder sprayer; *7*—supply source

stationary charging probe. This disc, which, in addition, sprays the powder stream into a cloud, is placed at a distance of 12 cm above the opening. A negative image can be obtained by changing the polarity of the powder charge.

Exposure time and sensitivity in xeroradiographic inspection. As in the case of X-ray and gamma-radiography, in xeroradiographic inspection the exposure time depends on the energy of the gamma-rays, the source activity, the density and thickness of the inspected article, source-plate distance, sensitivity (electric) of the employed xeroradiographic plate to radioactive emission of a given energy, and the nature of the foils and screens used. The rate of xeroradiography

also depends on the thickness of the selenium coating and the plate charge. Under similar conditions of inspection (one and the same radiation source, similar exposure set-up and intensifying foils) the exposure time in xeroradiographic inspection is always shorter than in film radiography. The difference in the respective exposure times is the larger the lower the gamma-ray energy.

In addition it should be kept in mind that, although xeroradiographic plates are sensitive to X-ray and gamma-radiation in a wide energy range (from 50 kev to several Mega-electron-volts), the density and definition of xeroradiographic images diminish with the increase in radiation energy.

When using X-ray or gamma-ray sources of an energy up to 100 kev, xeroradiography exposure time is 4-7 times shorter than that required for inspection with fine-grain X-ray film (under similar conditions of inspection, without lead foils and intensifying screens). Within the specified range of gamma-ray energy the density and definition of images obtained on xeroradiographic plates and X-ray film are about the same. With radiation energies ranging from 100 to 400 kev xeroradiography exposure time is 2.5-4 times shorter than the exposure time required for inspection with fine-grain X-ray film (without intensifying foils and screens). Within the specified energy range the density and definition of xeroradiographic images are inferior to those obtained with softer gamma-radiation (up to 100 kev).

Xeroradiographic images obtained with gamma-radiation of a higher energy (up to 1,000 kev and above) possess a lower density and a weak definition. With such energies xeroradiographic exposure time is twice as short as that for fine-grained film, the density and definition of xeroradiographic images being somewhat lower and weaker respectively.

Lead foils (screens) 0.025 mm thick used in conjunction with hard gamma-radiation considerably reduce the exposure time and increase the definition of xeroradiographic images. When loading holders, close contact between the lead foil and the sensitive layer of the plate must be ensured.

The sensitivity of xeroradiographic inspection depends on the gamma-radiation energy, the resolving power of the plates and the method of development (properties of the developing powder and the way it is used). The sensitivity in transferring the image to paper also depends on the printing technique employed. In practice, the resolving power of a xeroradiographic plate is determined by the size of the fine powder particles and is equal to 8-12 lines per millimetre.

It is generally accepted that the sensitivity of xeroradiographic inspection is of roughly the same order as that of radiographic inspection (when the inspection is performed with fine-grain X-ray film). However, xeroradiographic plates have certain advan-

tages over film, when employed to detect fine cracks inside metal articles.

It has been shown by experiment that in xeroradiographic inspection of materials of various thicknesses and densities using gamma-sources of different energies defects of a length of up to 2% of the thickness of the inspected material (provided the inspection is correctly carried out) are detected.

The definition of a xeroradiographic image can be considerably diminished by the so-called skiagraph images which may be traced to the presence of mechanical defects (scratches) in the sensitive layer of the plate. Sometimes a skiagraph image is the result of a deteriorated selenium layer, this, in turn, being caused by long exposure to high-intensity radiation or insufficient discharge of the plate by exposure to light (the preceding residual image appears on the plate). To ensure proper discharge, xeroradiographic plates must be heated to about 40°C, then cooled rapidly in a stream of air.

The method of xeroradiographic inspection is in the development stage. The manufacture of plates is the essential factor hampering further development of this inspection technique. Another inconvenience is the need to store sensitised and exposed plates in full darkness. At present investigations are conducted to introduce screens nonsensitive to luminescent light.

§ 3. Metal vision

Automation is one of the most important factors of technical progress. The highest economic effect of introducing automation is gained where the technological process is continuous. In this connection the problem of ensuring continuous and rapid quality control of metal stock and metal articles in the course of production is very urgent for metallurgical and machine-building works.

This problem can be solved by introducing continuous and remote flaw detection. The most essential element here is the introduction of gamma-electron and gamma-optical converters and amplifiers, arranged in the plane of the radiation fluxes.

Methods of converting latent gamma-images into optically visible images. There are three known methods of converting the latent gamma-image into an optically visible image: the scintillation method; the method based on the employment of semiconductor light sources; and the method based on the preliminary conversion of gamma-radiation into an electron flux, followed by conversion of the flux into visible light on a fluorescent screen.

The scintillation method is based on the fact that the passage of high-energy gamma-quanta through an optically transparent crystal is followed by scintillation, i.e. by the appearance of visible light flashes.

The passing gamma-ray flux can be converted into a visible image by selecting a crystal of a definite chemical composition, size, etc. The brightness of the crystal glow reaches its maximum brilliance, when the rays pass through a defective spot in the inspected material and the gamma-ray flux is, therefore, of a higher intensity and, vice versa, minimum brilliance is traced to spots where the weakest gamma-fluxes have passed.

Semiconductor light sources (often called electroluminescent light sources) intensify the brilliance of glow under the influence of penetrating gamma-radiation. The bright and shadowed spots on the screen and their distribution indicate the presence and the nature of the defects in the inspected material.

The method based on the employment of image converters is considered to be the most universal. This method magnifies the signal to the required value both by varying the applied voltage and by the employment of secondary-electron emitters. The use of electroluminescent gamma-converters makes it possible to combine amplifying and conversion, although not as effectively as in the case of electron conversion.

The image converter is an instrument based on the photoelectric effect and is designed to convert gamma- or X-ray emission into electron radiation which is further converted into a visible image.

The image converter consists of the following main parts: an electric vacuum tube; luminescent screens and an electron emitter (photoelectric cathode); focusing and optical systems; and a 20-25 kv constant-voltage supply source. The schematic layout of the image converter is shown in Fig. 127. The X-rays or gamma-rays *3* emitted by the radiation source *1* pass through the lead diaphragm *2* toward the inspected object *4*, behind which the image converter is placed. Having passed through the glass wall of the cylindrical vacuum tube *5*, the gamma-rays fall on the luminescent screen *7*, the luminescent compound of which is applied in a thin layer on an aluminium base *6*. The luminescent screen is optically bound to the photoelectric cathode *8*. The gamma-rays falling on the fluorescent layer of the screen make the latter luminescent, this causing the photoelectric cathode to emit electrons. The number of electrons freed per second at any point of the photoelectric cathode is proportional to the intensity of the incident light, hence, to the intensity of gamma-radiation. In this particular case the latent gamma-ray (or X-ray) image is converted into an electron image representing the distribution of the intensity of gamma-radiation after passage through the inspected material. Thus, the distribution of electron flux density directly depends on the variation in material thickness or the presence of defects in the inspected material. The photoelectrons *9* are accelerated by 25 kv voltage from an independent supply source. Special focusing excludes the possibility of electron flux distortion as it moves towards anode *10*. The electron image is

concentrated on the second output luminescent screen *11* and is converted into a visible luminous flux *12*. The output screen serves as an observation screen.

The image obtained is considerably smaller than the image on the fluorescent screen but its brightness is increased 1,000 times. The image may be enlarged by means of the optical arrangements *13*. The image appearing on the output screen may be observed through a binocular microscope *14* which magnifies the image about 9 times

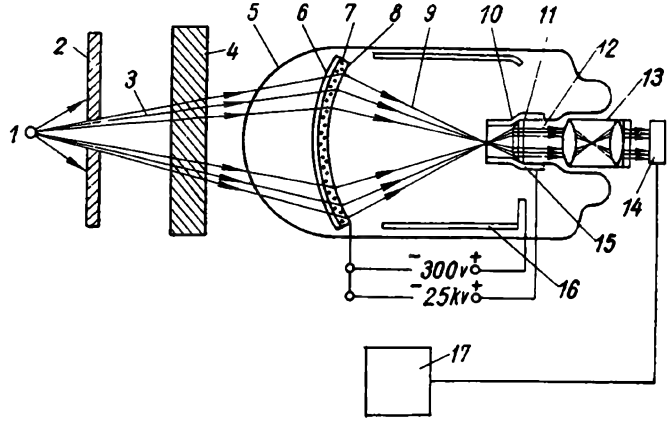

Fig. 127. Key diagram of an image converter:
1—radiation source; *2*—lead diaphragm; *3*—gamma- or X-rays; *4*—inspected object; *5*—glass vacuum tube; *6*—aluminium base; *7*—luminescent screen; *8*—photocathode; *9*—photoelectrons; *10*—anode; *11*—output luminescent screen; *12*—light flux; *13*—optical lens; *14*—ocular, cine or photographic camera or television-camera display tube; *15*—special electrode; *16*—metal-coated screen; *17*—picture screen

without loss of light, thus making it possible to observe the inspected objects or individual sections of the inspected object at almost their full size.

The image received by the metal vision technique may be televised on screen *17*. This offers good prospects for organising remote inspection from any distance of articles on the production line.

Remote vision in metals. The schematic layout of the system for remote vision in metals is shown in Fig. 128. Usually, all gamma-image converters have a mirror-reflecting surface on the side of the light beam propagation. This surface allows the direction of the light propagation to be adjusted. The mirror is arranged so that it is possible to observe the obtained light image from an adjacent room or, employing a television camera, to transmit the image on to the observation screen which can be placed at any distance from the site of inspection or even in several places simultaneously.

Recently several metal vision systems were developed at the Introscopy Institute under the direction of Prof. P. K. Oshchepkov,

D. Sc. (Eng.). With the aid of this equipment it will be possible to achieve remote metal vision to a depth exceeding 500 mm, the inspected article being in continuous motion. The process of inspecting parts for condition may be made automatic with the aid of radio-equipment used in other automatic systems. This provides new vast possibilities in the organisation of control of technological processes.

The systems of remote metal vision described above may be applied even with relatively weak gamma-ray sources to check for quality

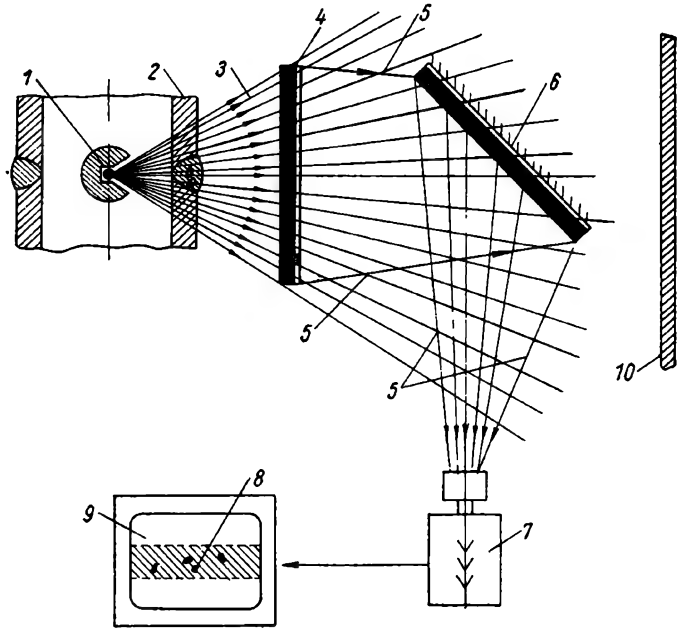

Fig. 128. Schematic layout of a remote metal vision unit:
1—container-manipulator holding gamma-source; *2*—checked welded article; *3*—gamma-rays; *4*—image converter and amplifier; *5*—light rays; *6*—mirror; *7*—video transmitter; *8*—image of defective weld; *9*—picture screen; *10*—shield made of high gamma-absorption material

small size parts or blanks, welded steel piping, rails, etc. It may be possible to use such set-ups to investigate dynamic processes in materials, for example, destruction zone studies.

The application of remote metal vision provides better working conditions for the personnel coming into direct contact with gamma-radiation sources. Undoubtedly, remote metal vision systems based on electron conversion and gamma-image amplification will find wide application in industry within the next few years.

Stereoscopic metal vision flaw detector. The diagram in Fig. 129 shows a system which may be used to obtain three-dimensional

images of defects in metals. Work is going on to develop a stereoscopic metal vision flaw detector. A flaw detector of this kind has two radioactive sources, two pick-up tubes (iconoscopes), two electron amplifiers, an oscillator, two picture tubes (kinescopes) and a binocular. The pick-up tubes feature a special photocathode which converts gamma-radiation into electron radiation.

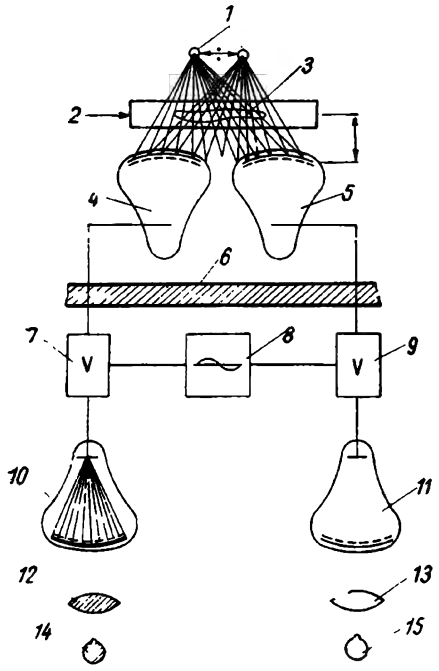

Fig. 129. Diagram of flaw detection unit for metals:

1—radiation source; *2*—inspected article; *3*—defect; *4* and *5*—pick-up tubes (iconoscopes); *6*—protective shield; *7* and *9*—amplifier channels; *8*—oscillator; *10* and *11*—picture tubes; *12* and *13*—optical system; *14* and *15*—observer's eyes

The photocathode of the pick-up tube is a $CaWO_4$, ZnS (or other material) fluorescent screen, the convex surface of which carries a thin cesium-coated silver layer. When a part is inspected by means of two radiation sources arranged at a definite distance from one another (the transmission base), the pick-up tubes will operate in pairs, synchronously with the picture tubes, i.e., the right half of the system and the left half will function alternately.

The alternating operation of the pick-up-and-picture-tube pairs is controlled by the oscillator which releases the left or right half of the system at a frequency equal to that of the a. c. supply source. Such alternating frequency eliminates picture-tube flicker.

The dose rate of the gamma-rays coming out of the inspected object varies, depending upon the thickness of the absorption layer at the inspected spot. Under the influence of gamma-radiation, the photocathodes of the pick-up tubes glow with a different brilliancy, the brilliancy being a function of the radiation dose rate. The fluorescence, in turn, influences the photocathode to imitate photoelectrons according to fluorescent screen brilliancy, therefore the left image will differ from the right image, and vice versa.

As the left image is seen by the left eye only and the right image by the right eye, then, owing to the presence of a transmission basis and a reception basis the object will appear as a three-dimensional image and the internal defects will be seen at the depth at which they are actually located. The appearance of a doubled stereoscopic image

may be prevented with the aid of a shutter system which would, firstly, alternate with the aid of electric motors, the action of the left and right radiation sources and, secondly, make the image visible in turn to the left and right eye of the observer. Image converters may also be employed in such systems.

These flaw detectors make possible the achievement of continuous and remote vision (detection) of faults in inspected articles and determination of the shape, size and location of the defect.

Part Three

LABOUR PROTECTION IN GAMMA-RADIOGRAPHY

§ 1. The effect of radioactive radiation on the human organism

Alpha-, beta- and gamma-radiation from radioactive isotopes ionise the medium in which the rays are absorbed. The ionisation caused by alpha-, beta- and gamma-radiation in live tissue has a definite biological effect. Under the influence of ionising radiation, proteins turn into compounds which are foreign to the human organism and toxic.

Water which constitutes $^3/_4$ of the entire human organism decomposes under the influence of radiation, forming negative and positive ions and active radicals which possess a great oxidation capacity. These radicals destroy protein in molecules.

The biological effect of ionising radiation is determined only by the density of ionisation which occurs in the irradiated live tissue and does not depend upon the kind of radiation. However, because of their different penetrating ability, known kinds of radiation cause ionisation of a different density and of nonuniform distribution in the tissue, thereby causing different biological changes in the human organism.

The ionising capacity of alpha-particles is hundreds of times greater than that of beta-particles and gamma-rays. However, the penetrating power of alpha- and beta-particles is insignificant and the particles are fully absorbed in the integument causing destruction chiefly of the skin, mucous membrane and cornea of the eye. Gamma-rays possess a high penetrating power and may be fatal for the living organisms, without causing changes in the integument during irradiation.

The severity of gamma-radiation injury depends on the radiation energy, the total radiation dose, the size of the irradiated section, the radiosensitivity of the individual and age. Thus, a single dose of 25 r may result in a serious disturbance in the human organism. If acquired over a short period of time, a dose of 100-300 r causes a complex disturbance in the human body, which is defined as radiation sickness. A radiation dose of 400-450 r is lethal in 50% of the

cases. This dose is called the lethal 50% dose. A dose of 600 r is lethal for human beings. Small-dose irradiation over a long period is less dangerous. During their lifetime people are exposed to external irradiation caused by cosmic rays, radioactive admixtures in the earth's crust, atmospheric air, water and food. The dose received from this natural radiation background by a human being in the course of 50 years amounts to about 20-25 r and is, apparently, not injurious to normal vital activity.

Monthly irradiation by doses of 5-25 r results in radiation sickness only in 1.5-3 years. The size of individual doses, intervals between irradiation and the cumulative dose determine the final result of multiple irradiation.

No visible symptoms of radiation sickness appear after a small field (about 4 sq cm) has been exposed to radiation in doses amounting to hundreds and thousands roentgen. It should be borne in mind that under similar conditions of irradiation some individuals may contract radiation sickness and others remain unaffected. For some individuals a dose of 100 r is lethal, while others recover after a dose of 1,000 r. It has been proved that young people are more sensitive to radioactive radiation. In addition, the effect of radiation on the human organism depends on the general state of the health and the presence of other diseases. Individual peculiarities of the human organism are revealed very strongly with insignificant radiation doses. Moreover, a number of other factors pertaining to conditions of daily life and work are of importance: humidity, temperature and contamination of the air in working premises, physical exertion, systematic irregular diet, sleep, work, rest, etc.

The personnel handling radioactive isotopes may be subjected to two kinds of ionising radiation: internal when the radiation source penetrates into the human organism, and external irradiation—from some outside source.

The personnel handling artificial radioactive sources for the purpose of gamma-inspection may be exposed only to external gamma-irradiation. In gamma-inspection there is no danger of radioactive substances getting on the skin and clothing.

The injurious effect of irradiation can be minimised, if the sanitary rules governing the handling of radioactive emitters are strictly observed, and it is possible to be engaged in gamma-inspection for a long period of time without any harm to the health.

Medical practice has established concepts of safe or maximum permissible doses for different kinds and modes of radiation. This means that even systematic exposure to such radiation doses over a period of dozens of years does not cause essential changes in the human organism. For personnel dealing with ionising radiation, this safe or maximum permissible radiation dose amounts to 0.05 r per working day, which corresponds to a dose rate of 2.3 μr/sec and 3.5 μr/sec respectively for a 6-hour and 4-hour working day, etc.

The maximum permissible dose rate P_0 for working days of different duration t (hours) is calculated from the relation

$$P_0 \approx \frac{14}{t} \mu r/sec. \quad (70)$$

If only hands or feet are exposed to radiation, the maximum permissible dose may be increased 5 times provided the cumulative dose which the body as a whole receives per day does not exceed 0.05 r. In some cases an increase in the safe radiation dose is permitted, provided the cumulative dose received by the worker during the week does not exceed 0.3 r. For personnel engaged in gamma-inspection, the cumulative radiation dose received in the course of one year must not exceed 15 r, while for personnel not engaged in gamma-ray flaw detection the physical radiation dose should not exceed 0.01 r per day, this corresponding to a dose rate of 0.35 μr/sec in the case of an 8-hour working day.

The safety of personnel engaged in gamma-inspection is ensured by the construction of protection devices, the reduction of exposure time and by increasing the distance between gamma-sources and attending personnel.

§ 2. Protection devices

The devices offering protection from the harmful effect of gamma-radiation are divided into two categories: stationary and portable. Stationary devices include walls, ceilings and floors, door shielding, shielding of viewing windows. The following devices are classified as portable: protective cases of gamma-units, containers employed to transport and store radioactive preparations, various shields, screens, etc.

Stationary and portable protection devices serve different purposes. Stationary protection devices are designed to protect the attending personnel and people working in adjacent rooms from the harmful effect of gamma-radiation when actual inspection of materials or articles is conducted. The aim of portable protection devices is to protect personnel during storage and transportation of radioactive sources, in the course of preparatory work prior to the inspection and during the actual building of radioactive preparations.

Depending on the working conditions and the purpose of the protection devices, the latter should afford protection from direct or scattered gamma-radiation. Thus, portable devices must ensure reliable protection from direct gamma-radiation. When inspection is performed with the beam directed downwards stationary devices must offer protection only from scattered gamma-radiation.

According to the Sanitary Regulations Governing Transportation, Storage, Stock-Taking and Handling of Radioactive Substances" newly designed or reconstructed protection devices must ensure a reduction of the daily radiation dose to 0.01 r.

Portable protection devices—transportation, storage and handling containers—are calculated to ensure a reduction in the dose to the maximum permissible at a distance of 0.5 m from the radiation source, during a six-hour working day.

Calculation of head-on gamma-radiation shielding. Protective barriers are usually built of materials of a high atomic number and density, mostly of lead. Steel, cast iron, barytes concrete, concrete, lead glass, etc., are employed in a number of cases.

In calculating protective shielding, account has to be taken of the radiation spectrum, intensity, distance from the source and the time that attending personnel spend in the irradiation zone. It will be recalled that linear absorption coefficients diminish as radiation energy increases (to a certain limit, till the process of pair production acquires decisive importance), therefore the thickness of the required protective barrier increases. When dealing with soft and medium radiation, an increase in radiation intensity influences the thickness of the protective barrier to a considerably smaller degree than an increase in radiation energy. So, for instance, if radiation energy is doubled (from 200 to 400 kev), the thickness of the required lead protective barrier increases five times, while a doubled radiation intensity (source activity) requires only a 10-15% increase in the thickness of the required lead protection shield. The thickness of protective shielding against gamma-radiation from various radioactive isotopes can be determined by the several methods treated below.

First method. The thickness of the lead protective barrier for various radioactive isotopes may be determined with the aid of the chart plotted for Co^{60} gamma-rays (Fig. 130).* If the radiation energy of the given isotope differs considerably from the energy of the gamma-radiation emitted by a Co^{60} source, then the thickness of the protective barrier read off the chart should be multiplied by the appropriate correction factor K for the radiation energy of the given isotope (the correction factor method). Correction factors are listed in Table 28. Calculations of protective shielding for a given isotope are based on the mean effective radiation energy appropriate to the isotope in question.

It is not difficult to determine the value of the mean effective energy for some radioactive isotopes, and for these isotopes the protective barrier is easily calculated as for monochromatic radiation. However, the majority of the radioactive isotopes employed in gamma-radiography possess a complex gamma-spectrum, and determination of the mean effective energy for such isotopes is a very laborious procedure, for it is rather difficult to determine by calculation the changes occurring in the radiation spectrum due to filtration.

---

* A protective layer of a thickness read off the chart ensures a decrease in the radiation dose to 0.05 r during 6 hours.

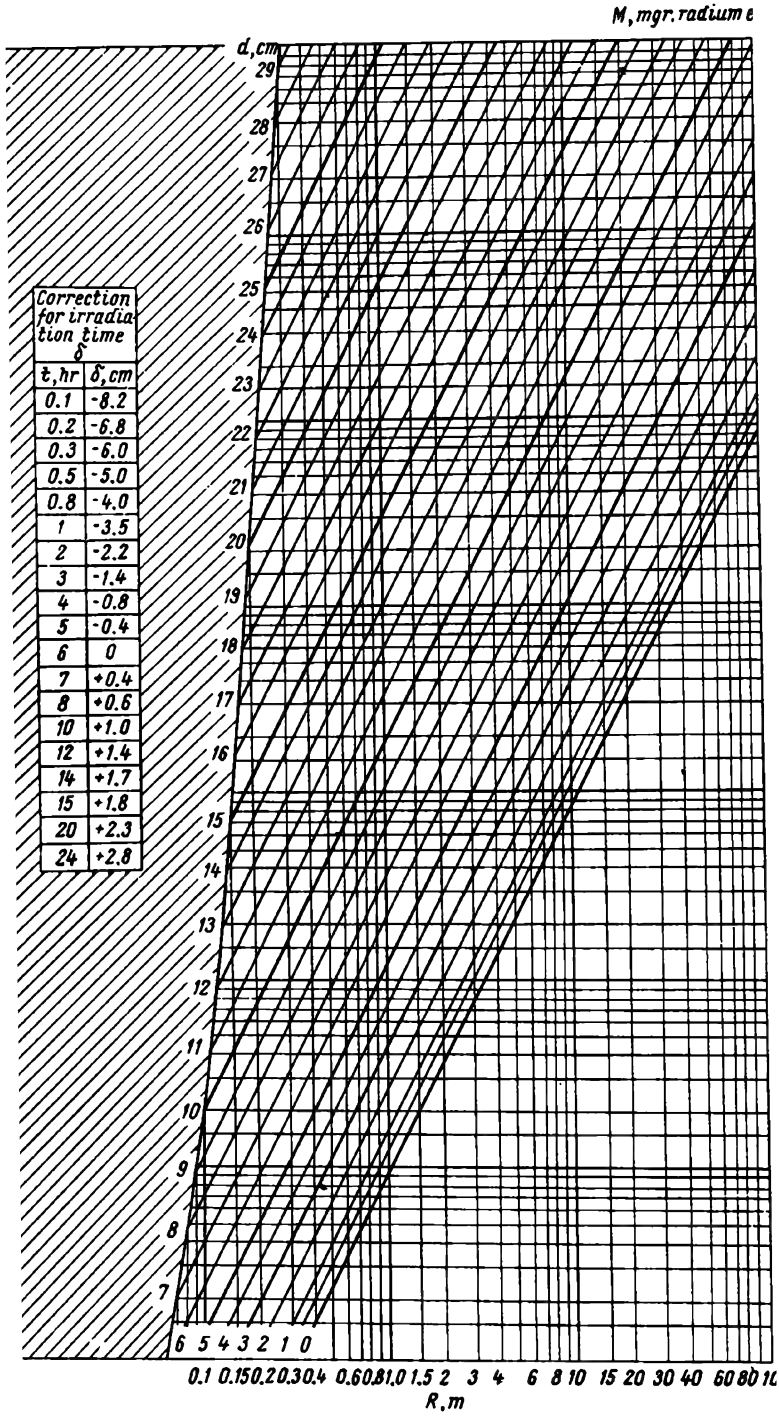

Correction for irradiation time δ

t, hr	δ, cm
0.1	-8.2
0.2	-6.8
0.3	-6.0
0.5	-5.0
0.8	-4.0
1	-3.5
2	-2.2
3	-1.4
4	-0.8
5	-0.4
6	0
7	+0.4
8	+0.6
10	+1.0
12	+1.4
14	+1.7
15	+1.8
20	+2.3
24	+2.8

Fig. 130. Chart used to calculate lead protection from broad-beam gamma-source

Table 28

Energy Correction Factor K

E_γ, Mev	K	E_γ, Mev	K
0.10	0.011	1.3	1.03
0.125	0.019	1.4	1.08
0.15	0.022	1.5	1.13
0.175	0.043	1.8	1.25
0.20	0.057	2.0	1.32
0.3	0.15	2.2	1.35
0.4	0.27	2.4	1.37
0.5	0.38	2.6	1.40
0.6	0.49	2.8	1.42
0.7	0.60	3.0	1.45
0.8	0.66	4	1.42
0.9	0.77	5	1.37
1.0	0.84	6	1.30
1.1	0.90	8	1.30
1.2	0.97	10	1.10

Because of this, and taking into account the fact that even in cases where correction factors may be chosen as for monochromatic radiation, one has usually to resort to interpolation because the correction factor method leaves a considerable margin of error.

Second method. According to this method the thickness of protective shielding from gamma-radiation emitted by various radioactive isotopes is determined by means of charts plotted for each particular isotope. Each of these charts is based on the radiation spectrum of the given isotope. The charts shown in Figs. 131 to 135 can be used to determine the thickness of the lead protective barriers for the following radioactive isotopes widely used in gamma-inspection: Co^{60}, Cs^{137}, Ir^{192}, $Eu^{152,154}$, Tu^{170} and Eu^{155}. The charts are plotted for a point source, an exposure time $t = 6$ hrs/day and maximum permissible dose $D_0 = 0.05$ r.

The charts shown in Figs. 130-132 are plotted on logarithmic cross-section paper. The source activity M is plotted on the ordinate and the distance from source R—on the abscissa. The inclined lines represent the thickness d of lead protection. The radiation level in the region to the right of the line of zero thickness ($d = 0$) is below the maximum permissible dose, therefore, this region represents safe operating conditions.

In the charts shown in Figs. 133-135, preparation activity M is plotted on the abscissa in the logarithmic scale and the thickness d of the lead protective layer—on the ordinate in the linear scale. The

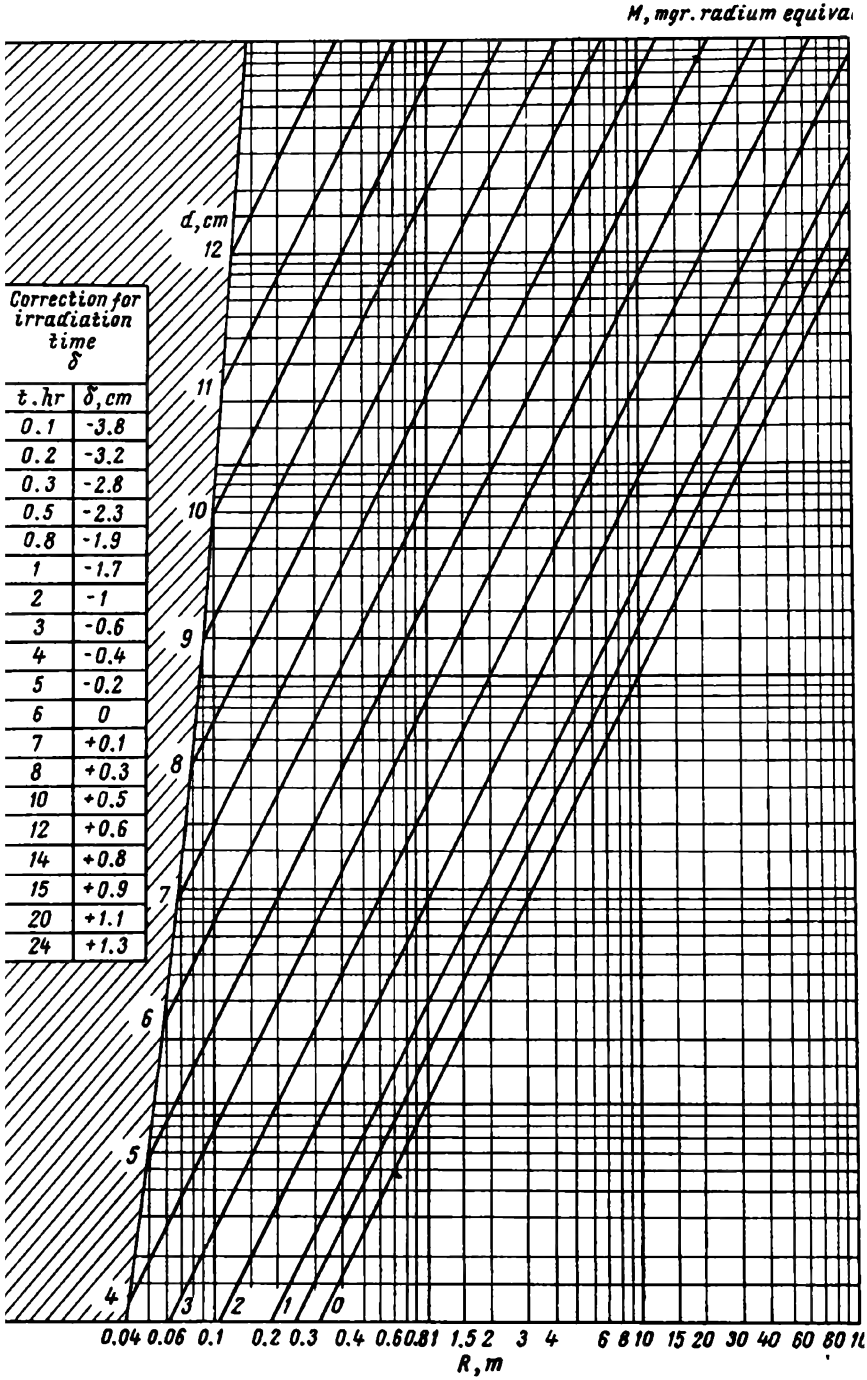

Correction for irradiation time δ

t, hr	δ, cm
0.1	-3.8
0.2	-3.2
0.3	-2.8
0.5	-2.3
0.8	-1.9
1	-1.7
2	-1
3	-0.6
4	-0.4
5	-0.2
6	0
7	+0.1
8	+0.3
10	+0.5
12	+0.6
14	+0.8
15	+0.9
20	+1.1
24	+1.3

Fig. 131. Chart used to calculate lead protection from broad-beam Cs^{13} gamma-source

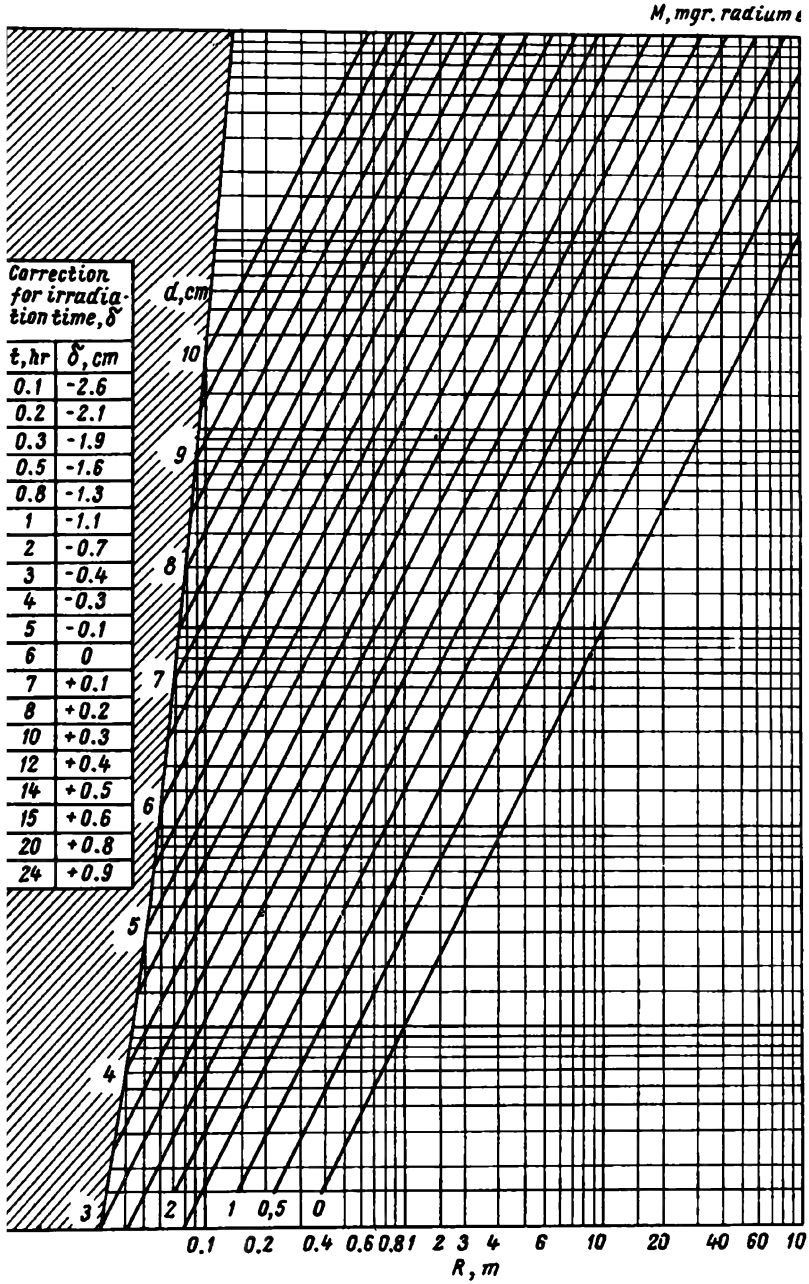

Fig. 132. Chart used to calculate lead protection from broad-beam l gamma-source

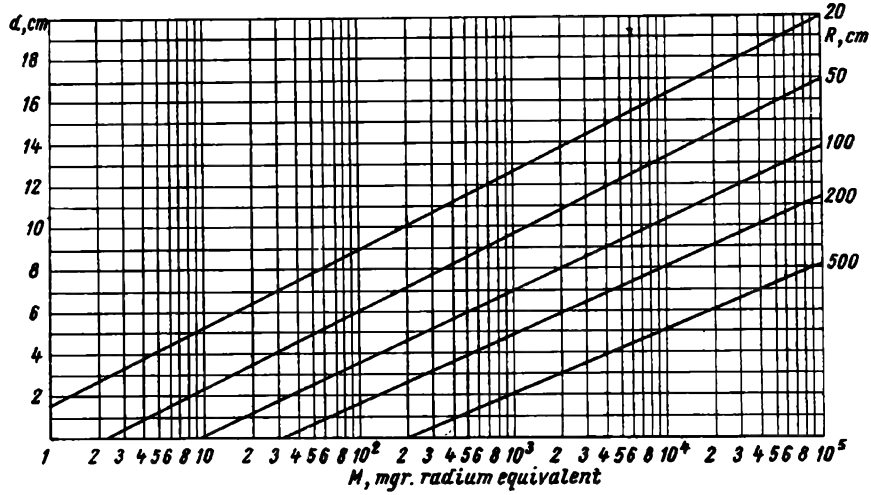

Fig. 133. Chart used to calculate lead protection from broad-beam $Eu^{152,154}$ gamma-source

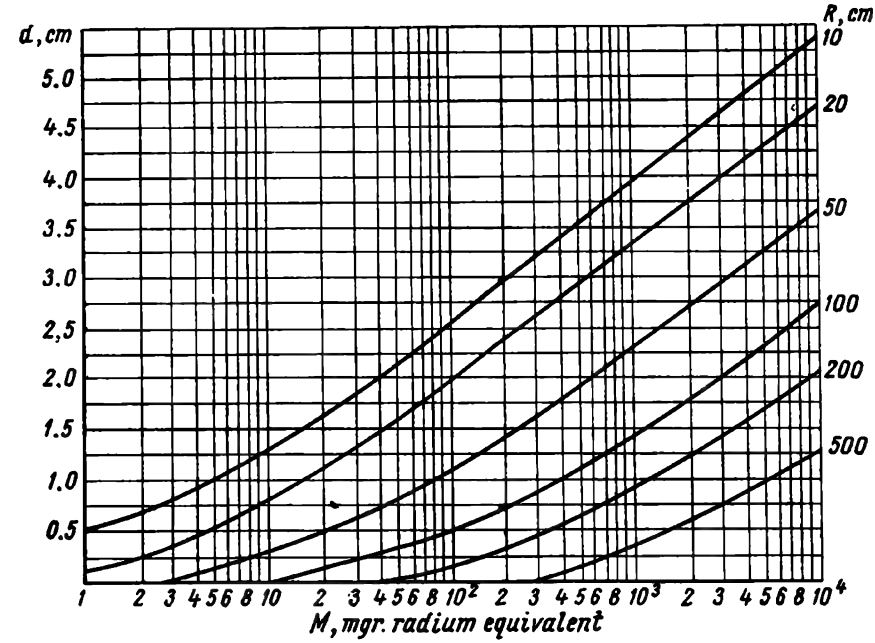

Fig. 134. Chart used to calculate lead protection from broad-beam Tu^{170} gamma-source

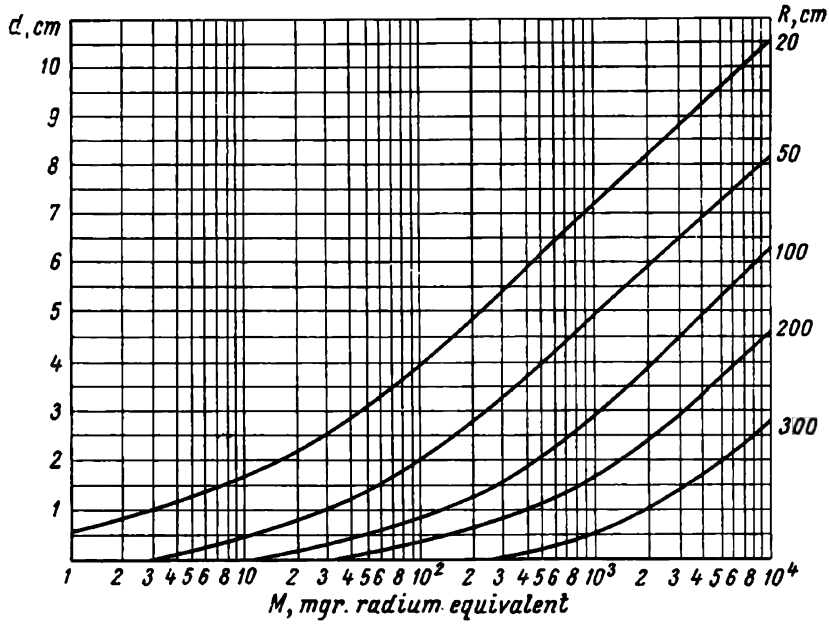

Fig. 135. Chart used to calculate lead protection from broad-beam Eu^{155} gamma-source

third parameter—the distance from the source R—is read off the inclined lines; the distance between the lines also changes on a logarithmic scale. The charts are plotted in this way for the sake of convenience.

Examples.

1. Find the thickness d of a lead barrier to offer protection from gamma-radiation emitted by a Co^{60} source, if $t = 6$ hrs, $R = 3$ m and $M = 3{,}000$ mg radium equivalent.

On the chart (Fig. 130) we find the point at which the horizontal line representing the energy M is $3 \cdot 10^3$ mg radium equivalent intersects the vertical line representing $R = 3$ m. The intersection point lies on the inclined line which represents a lead thickness $d = 7$ cm.

2. Find the thickness d of a lead protective barrier against Co^{60} gamma-radiation, if $t = 2$ hrs, $R = 3$ m and M is 3,000 mg radium equivalent.

On the chart (see Fig. 130) we find $d = 7$ cm, corresponding to $t = 6$ hrs. The radiation time correction $\delta = -2.2$ cm. Thus, the required thickness of the lead protective layer $d = 7-2.2 = 4.8$ cm.

3. Calculate the thickness of a protective barrier with a fivefold safety factor ($D_0 = 0.01$ r), if $t = 6$ hrs, $R = 1$ m and M is 40,000 mg radium equivalent.

In this case a fictitious activity $M_0 = \omega M$, where ω is the safety factor used in calculations. Thus, M_0 is $5 \times 40{,}000 = 200{,}000$ mg radium equivalent, and $d = 18.4$ cm Pb. For a radiation activity $M = 40{,}000$ mg radium equivalent $d = 15.4$ cm Pb.

4. Calculate the protective barrier for a radiation dose $D_0 = 0.1$ r/day, if $t = 6$ hrs, $R = 1.5$ m and M is 20,000 mg radium equivalent.

Let us determine the fictitious activity $M_0 = \frac{M}{\omega}$, where ω, the ratio of the given radiation dose to the maximum permissible dose 0.05 r, is equal to $\frac{0.01}{0.05} = 2$; $M_0 = \frac{M}{\omega} = \frac{20{,}000}{2} = 10{,}000$ mg radium equivalent, hence $d = 11.6$ cm Pb.

5. Determine the permissible activity of Co^{60}, Cs^{137} and Ir^{192} radiation sources, if $t = 6$ hrs, $R = 1$ m and $d = 8$ cm Pb.

On the chart shown in Fig. 130 we find the activity of the cobalt source $M = 600$ mg radium equivalent; on the chart in Fig. 131 the activity of the cesium source $M = 60{,}000$ mg radium equivalent and on the chart in Fig. 132 the activity of the iridium source M is 300,000 mg radium equivalent.

6. Find the maximum permissible distance to source R, if $t = 6$ hrs, the activity of Co^{60}, Cs^{137} and Ir^{192} M is 50,000 mg radium equivalent and $d = 8$ cm Pb. Using the same charts we find the distance R equal to 9.5, 0.8 and 0.4 m respectively for cobalt, cesium and iridium.

7. Find the permissible activity M of a cobalt source, if $t = 6$ hrs, $R = 10$ m and $d = 0$.

From the inclined line marked $d = 0$ in the chart shown in Fig. 130, we read off $M = 800$ mg radium equivalent.

8. A Co^{60} source emits radiation under the following conditions: $t = 6$ hrs, M is 10,000 mg radium equivalent, $R = 15$ cm. Is such radiation dangerous?

Under the given conditions radiation is dangerous, for the point at which the line $R = 15$ m and the line $M = 10^4$ mg radium equivalent cross is located in the dangerous zone (to the left of the inclined line marked d_0).

9. Determine the thickness of a lead barrier required to protect from gamma-radiation emitted by a 10,000 mg radium equivalent Co^{60} source, an adjacent room housing the personnel who are not involved in the radiation work. For such personnel the maximum permissible dose must not exceed 0.01 r during an 8-hour working day. The distance from the source to the wall is 3 m.

For a different maximum permissible dose and other working hours the thickness of the lead protective barrier is determined in the following way. The activity of the source, for which protection is calculated, is multiplied by the ratio of the maximum permissible dose (0.05 r) to the new dose and by the ratio of the new number of working hours to the specified. The thickness of the shield is then determined on the chart for the energy calculated, as described above.

The calculated activity of the source is $\frac{10{,}000 \times 0.05 \times 8}{0.01 \times 6} = 6.7 \times 10^4$ mg radium equivalent.

For a 6.7×10^4 mg radium equivalent Co^{60} gamma-source the chart in Fig. 130 specifies a lead shield 12.5 cm thick, placed at a distance of 3 m.

Containers intended for the transportation and storage of a definite radioactive isotope are frequently employed to transport and store a different source. In such a case, it is important to know the activity of the preparations which may be stored in such a container. For example, a container, the purpose of which is to store a Co^{60} preparation of an activity equal to 0.1 gram radium equivalent, reduces the dose to 0.05 r during 6 hrs at a distance of 0.5 m. It is desirable to know the activity of Cs^{137} and Ir^{192} sources which may be placed in that container, the same safety factor being maintained.

On the chart in Fig. 130 we find that the walls of a container ensuring the specified safety factor for a 0.1 gram radium equivalent Co^{60} source are 7 cm thick. The charts shown in Figs. 131 and 132 make it possible to determine that the same safety factor is preserved, if a 5.0 gram radium equivalent Cs^{137} source or a 30 gram radium equivalent Ir^{192} source is placed in this container.

Third method. The use of the above-mentioned charts plotted for radioactive gamma-sources of a definite activity is somewhat

restricted, for they are based on fixed distances, definite exposure time, maximum permissible doses, etc.

At present, Gusev's universal tables (Appendix II, Tables 1, 2, 3) which make possible the determination of the thickness of protective barriers as a function of the dose reduction factor, are widely used. These tables are based on the theory of attenuation of a broad gamma-beam and include the whole range of radiation energies of natural and artificial isotopes possessing a linear gamma-spectrum. The initial data required to determine protective layer thickness by means of these tables include gamma-ray energy and the dose-reduction factor required to ensure a desired radiation level behind the protective barrier.

The universal tables make it possible to calculate gamma-shielding in practically all important cases: to ensure radiation of any level; to ensure any maximum permissible physical dose; for sources of any shape, activity and spectrum complexity, placed at any distance; for any exposure time; and for the most important building materials.*

The discrepancy between the thickness of protective barriers determined with the aid of the universal tables (according to the dose-reduction factor) and the thickness found experimentally does not exceed 5-10%.

Shielding calculations based on the physical dose-reduction factor. For a calculated or measured dose D, whether with or without a protective shielding and an assumed maximum permissible dose $D_0 = 0.05$ r the dose-reduction factor is expressed by

$$k = \frac{D}{D_0}. \tag{71}$$

The thickness of the protective barrier is determined on the basis of this dose-reduction factor and the given gamma-radiation energy.

Example. A cobalt source produces at the site of work a dose of 6 r in a 6-hour workday. Find the thickness of a lead screen which would reduce the actual dose to the maximum permissible ($D_0 = 0.05$ r).

The required reduction factor $k = \frac{6}{0.05} = 120$. In Table 1 (Appendix II) we find that for a 1.25 Mev Co^{60} source and a dose-reduction factor $k = 120$ the lead protective barrier must be 8.7 cm thick.

Shielding calculations based on the physical dose rate reduction factor. If the calculated or measured physical dose rate is P and the maximum permissible dose rate P_0, the reduction factor is expressed by

$$k = \frac{P}{P_0}. \tag{72}$$

* The application of different building materials for gamma-shielding is considered below.

Example. The activity of a cobalt source M is 50 gram radium equivalent. The source is stored in a protective lead container, but during operation the source has to be shifted through an unshielded hose into a lighter container. The source remains in the unshielded hose for 6 min. Find the thickness of a steel shielding to be placed between the control desk and source, if the distance from the source to the control desk $R = 2$ m.

The protection should be calculated with a safety factor 5.0, e. g., for a dose $D = 0.01$ r.

The dose rate from an unshielded source is obtained from the following equation:

$$P = \frac{8.4 \times M \times 10^6}{3{,}600 \times R^2} = \frac{8.4 \times 50 \times 10^3 \times 10^6}{3{,}600 \times 4 \times 10^4} = 2{,}900 \ \mu r/sec.$$

For $t = 6$ min (0.1 hr) and $D = 0.01$ r the maximum permissible dose rate is

$$P_0 = \frac{0.01 \times 10^6}{0.1 \times 3{,}600} = \frac{100}{3.6} = 30 \ \mu r/sec.$$

The dose-reduction factor $k = \frac{2{,}900}{30} = 100.$

To ensure a dose-reduction factor of 100 with a 1.25 Mev gamma-source the steel shield must be 16.1 cm thick (Appendix II, Table 2).

Protective shielding calculations based on the reduction of radioactive source activity M. It is known that to ensure safe operation, the relation between source activity M_0, expressed in mg radium equivalent, daily irradiation time t in hours and the distance from the source R in metres must be equal to

$$\frac{M_0 t}{R^2} = 60.* \tag{73}$$

Thus, the maximum activity M_0 which permits unshielded operation during t hours is

$$M_0 = 60 \frac{R^2}{t} \text{ mg radium equivalent.}$$

So, for $R = 1.0$ m and $t = 6$ hrs, M_0 is 10.0 mg radium equivalent.

Therefore, for a given total source activity, expressed in mg radium equivalent, the required reduction factor is

$$k = \frac{M}{M_0}. \tag{74}$$

Example. Find the thickness of a lead protective barrier for a 1.0 gram radium equivalent Co^{60} source if $R = 2$ m, $t = 3$ hrs.

---

* The ratio (73) is derived from formula (14). For a maximum permissible dose $D = 0.05$ r and distance R is expressed in metres.

$$0.05 = \frac{8.4 \times M \times t}{R^2 \times 10^4} \quad \text{or} \quad \frac{Mt}{R^2} = 60.$$

For different permissible doses the ratio of source activity M_0, expressed in mg radium equivalent, and daily irradiation time t, hrs, to the distance from source R, m, is different.

So, for $D = 0.01$ r for one working day $\frac{Mt}{R^2} = 12.$

Under the specified conditions the maximum permissible amount of the Co^{60} source is

$$M_0 = 60 \times \frac{2^2}{3} = 80 \text{ mg radium equivalent.}$$

Hence, the required reduction factor

$$k = \frac{1 \times 10^3}{80} = \frac{1{,}000}{80} \simeq 13.$$

To ensure the required dose-reduction factor for 1.25 Mev gamma-energy, it is necessary to provide a lead barrier about 5 cm thick.

Shielding calculations based on changes in exposure time and distance. If the existing protective shielding ensures safe operation for t_0 hours and operation must be prolonged to t_1 hours, the thickness of the existing barrier should be increased to accord with the additional dose-reduction factor k to be ensured

$$k = \frac{D_1}{D_0} = \frac{\dfrac{Mk_\gamma \times t_1}{R_0^2}}{\dfrac{Mk_\gamma \times t_0}{R_0^2}} = \frac{t_1}{t_0}. \tag{75}$$

Example. The existing protective barrier meets safety requirements for an operation time $t_0 = 4$ hrs. Find the thickness of lead to be added to ensure safe work during 8 hours with a Co^{60} radioactive source.

The additional dose-reduction factor $k = \frac{t_1}{t_2} = \frac{8}{4} = 2$.

The additional lead screen must be 1.5 cm thick (Appendix II, Table 1) to ensure a dose-reduction factor $k = 2$ for gamma-rays from a Co^{60} source.

If the existing shield ensures safe operation at a certain distance R_0 from the radioactive source and it is necessary to work at a distance R_1 smaller than R_0, the protective shield must be made thicker to ensure the required additional attenuation of gamma-radiation

$$k = \frac{D_1}{D_0} = \frac{\dfrac{Mk_\gamma \times t_0}{R_1^2}}{\dfrac{Mk_\gamma \times t_0}{R_0^2}} = \frac{R_0^2}{R_1^2}. \tag{76}$$

Example. The existing protective barrier ensures safe operation for 6 hours at a source-barrier distance $R_0 = 4$ m. Find the thickness of the lead barrier required to ensure safe work for 6 hours at a distance of 2 m, using a Cs^{137} radioactive source.

The required additional dose-reduction factor is

$$k = \frac{R_0^2}{R_1^2} = \frac{4^2}{2^2} = 4.$$

A lead shield about 1.7 cm thick (Appendix II, Table 1) is required to ensure fourfold attenuation of gamma-radiation from a Cs^{137} source.

Approximate shielding calculations based on half-value layers. The half-value layer $\Delta\frac{1}{2}$ is the thickness of a shield which reduces the dose rate to one half of the initial value.

The half-value layer for both monoenergetic broad-beam gamma-radiation and gamma-radiation of a complex spectrum depends upon protective-shield thickness, all other conditions being equal. Therefore, it is difficult to suggest an exact and rapid method for shielding calculations based on half-value layers. However, in practice, it is often necessary to determine the approximate thickness of a protective shield and no precise tables or charts are available.

In such cases it is necessary to know at least the approximate half-value layer $\Delta\frac{1}{2}$ for broad-beam gamma-radiation from corresponding radioactive sources. Knowing this value and the reduction factor (obtained by any of the methods described above), the total number of half-value layers, i. e., the summary protection, has then to be found.

It should be noted that it is easy to find the half-value layer from the universal tables, by comparing the thicknesses for two reduction factors, one of the factors being numerically twice as large as the other.

The approximate values expressing the relation between the reduction factor k and the number of half-value layers n is given below:

Reduction factor	The number of half-value layers	Reduction factor	The number of half-value layers
2	1	64	6
4	2	125	7
8	3	250	8
16	4	500	9
32	5	1,000	10

For $k > 1{,}000$ this regularity repeats. For example, for $k = 2{,}000 = 2 \times 10^3$, the number of half-value layers $n = 1 + 10 = 11$; for $k = 500{,}000 = 500 \times 1{,}000$, $n = 9 + 10 = 19$; for $k = 10^6$, $n = 20$, etc.

The number of half-value layers may be found from the general expression $2^n = k$.

Example. It is necessary to reduce 30,000 times the gamma-radiation from a Co^{60} source. Determine the required protection, if $\Delta\frac{1}{2}$ of lead is 1.3 cm.

$5 + 10$ half-value layers are required to reduce radiation 30,000 ($30 \times 1{,}000$) times. Hence, the protective-shield thickness $d = 15 \times 1.3 = 19.5$ cm lead. The thickness of a protective lead shield as determined by experiment is 19 cm.

Calculations of shielding for radioactive sources of a complex spectrum. It was mentioned above that shielding for radioactive gamma-sources of a complex spectrum may be determined with the aid of

charts plotted for each isotope. However, owing to the large number of isotopes employed, this method is very inconvenient, for it requires a large number of different charts.

The protection calculation method (with the aid of the universal tables) for complex-spectrum sources consists in the following. First, the physical radiation dose produced by the entire gamma-radiation spectrum is determined. Then, one proceeds to find the summary dose-reduction factor k required to reduce the dose to the maximum permissible and the differential dose-reduction factors for each spectrum line individually (k_1, k_2, k_3, etc.), according to their respective dose contribution.

The relative dose contribution of individual lines of the spectrum is expressed in percentage values and is determined as the ratio of the dose rate created by gamma-quanta of the given energy $k_{\gamma i}$ to the dose rate created by the entire gamma-radiation spectrum k_γ.

$$k_1=\frac{P_1 k}{100}; \quad k_2=\frac{P_2 k}{100}, \quad \text{etc.}$$

where k_1 and k_2 - differential dose-reduction factors for gamma-quanta of different energies (of different lines);

P_1 and P_2 — the dose contribution, in percentage, for these gamma-quanta;

k— the summary dose-reduction factor.

Knowing the differential dose-reduction factor, it is possible, using the universal tables, to find the required barrier thickness for each spectrum component. The maximum thickness of the protective barrier found by this method may be considered as the total thickness of the protective barrier for the entire given polyenergetic source of gamma-radiation.

If the isotope radiation spectrum consists of a great number of lines, there is no need to determine the differential dose-reduction factor for each line. In such a case it is sufficient to discover the lines which produce the largest radiation dose in comparison with the summary dose; the differential dose-reduction factor and respective thickness of the protective shield are determined only for these lines.

Sometimes it is advisable to combine lines of a similar energy into groups and determine the differential dose-reduction factors according to the relative dose contribution of each group; then, it is possible to calculate the thickness of the required protective shield, proceeding as indicated above.

If the calculated thickness of the protective shield is similar for several lines (or groups of lines), then, to determine the thickness of the barrier of protection from the entire gamma-spectrum of a given isotope, it is necessary to add a corresponding number of half-value layers to the thickness arrived at. Otherwise, the radiation dose behind the shield will be larger than that specified by the corresponding number of times.

The thickness of the half-value layer for the most penetrating spectrum component is determined as the difference in the thicknesses of protective shields calculated for two reduction factors nearest to that required.

In most cases the protective thickness required for other lines differs essentially from the maximum thickness; nevertheless, one half of the half-value layer for the most penetrating component must be added to the maximum thickness of the protective shield to eliminate the influence of these lines.

Example. Find the thickness of a lead protective barrier which would reduce the gamma-radiation from a 3.0 gram radium equivalent Ir^{192} source to the maximum permissible dose (0.05 r) at a distance from the radiation source to the protective barrier $R = 1$ m for a 6-hr working day. The Ir^{192} isotope is a polyenergetic radiation source.

The radiation spectrum for the isotope is given below.

Gamma-quanta energy, E_γ, Mev	Relative dose contribution, percentage	Gamma-quanta energy, E_γ, Mev	Relative dose contribution, percentage
0.885	0.6	0.316	29.5
0.613	2.8	0.308	11.85
0.604	7.1	0.296	10.85
0.588	2.85	0.283	0.6
0.484	1.2	0.206	0.8
0.468	22.7	0.201	0.4
0.416	6.2	0.136	—

From the Ir^{192} gamma-spectrum data listed above it follows that in this case only five lines may be considered as the most intensive: $h\nu_1 = 0.885$ Mev (0.6%); $h\nu_2 = 0.613$ Mev (2.8%); $h\nu_3 = 0.604$ Mev (7.1%); $h\nu_4 = 0.468$ Mev (22.7%) and $h\nu_5 = 0.316$ Mev (29.5%).

The physical radiation dose for the entire gamma-spectrum of the given source can be found from the following formula

$$D = \frac{Mk_\gamma \times t}{R^2} = \frac{3 \times 10^3 \times 8.4 \times 6}{10^4} = 15 \text{ r.}$$

The following dose-reduction factor is required to reduce this dose to the maximum permissible dose $D_0 = 0.05$ r

$$k = \frac{D}{D_0} = \frac{15}{0.05} = 300.$$

The differential dose-reduction factors k for the specified spectrum lines and the thicknesses of the lead shields* to provide protection can be determined from the following expressions:

For $h\nu_1 = 0.885$ Mev; $P_1 = 0.6\%$; $k_1 = \frac{P \times 300}{100} = \frac{0.6 \times 300}{100} = 1.8$; $d_1 = 1$ cm lead.

For $h\nu_2 = 0.613$ Mev; $P_2 = 2.8\%$; $k_2 = \frac{2.8 \times 300}{100} = 8.4$; $d_2 = 2.0$ cm lead.

For $h\nu_3 = 0.604$ Mev; $P_3 = 7.1\%$; $k_3 = \frac{7.5 \times 300}{100} = 22.5$; $d_3 = 2.75$ cm lead.

* Protective thickness d is determined from Appendix II, Table 1.

For $h\nu_4 = 0.468$ Mev; $P_4 = 22.7\%$; $k_4 = \frac{22.7 \times 300}{100} = 67.1$; $d_4 = 2.55$ cm lead.

For $h\nu_5 = 0.316$ Mev; $P_5 = 29.5\%$; $k_5 = \frac{29.5 \times 300}{100} = 89$; $d_5 = 1.7$ cm lead.

From the data obtained it follows that the $h\nu_3$ and $h\nu_4$ lines determine the thickness of the protective shield from gamma-radiation emitted by an Ir^{192} source. The two lines require protective shields of about equal thickness. Therefore, if protection in this case is provided by a lead screen 2.75 cm thick, a double dose will exist behind the protective shield. To reduce the double dose to the maximum permissible dose it is necessary to add a half-value layer $\Delta\frac{1}{2}$ calculated for the most penetrating spectrum component $h\nu_3 = 0.604$ Mev with a dose-reduction factor $k = 23$; this layer will be about 0.5 cm thick. (This value of $\Delta\frac{1}{2}$ is obtained as the difference between the thicknesses of the protective shields calculated for the two dose-reduction factors nearest to $k = 23$, i.e., for $k = 20$ and $k = 40$.)

To eliminate the effect of the $h\nu_2$ line it is necessary to add about one half of a half-value layer, i.e., about 0.25 cm.

Thus, the thickness of the lead protective barrier determined by means of the universal tables is equal to $2.75 + 0.5 + 0.25 = 3.5$ cm.

Let us consider one more example. Find the thickness of a lead container intended for transporting a $Eu^{152, 154}$ source of an activity 5 gram radium equivalent. Transit duration is 24 hours, the shortest distance between the container and forwarding agent is 1.5 m. The container must be designed with a fivefold safety margin, i.e., protection must be calculated on the basis of a maximum permissible dose equal to 0.01 r. The $Eu^{152, 154}$ isotope is a polyenergetic radiation source.

The isotope possesses the following radiation spectrum:

Gamma-quanta energy, E_γ, Mev	Relative dose contribution, percentage	Gamma-quanta energy, E_γ, Mev	Relative dose contribution, percentage
0.344	5.5	0.866	4.6
0.442	1.17	0.963	16
0.550	1.23	1.116	26
0.720	3.0	1.240	9.5
0.778	8.3	1.405	24.7

From the spectrum data it follows that the only two lines of maximum intensity are: $h\nu_1 = 1.116$ Mev (26%) and $h\nu_2 = 1.405$ Mev (24.7%).

The physical radiation dose of the entire spectrum can be obtained from the formula

$$D = \frac{Mk_\gamma t}{R^2} = \frac{5 \times 10^3 \times 8.4 \times 2.4}{1.5^2 \times 10^4} = 45 \text{ r.}$$

The following dose-reduction factor is required to reduce the above dose to the maximum permissible value (0.01 r):

$$k = \frac{45}{0.01} = 4{,}500.$$

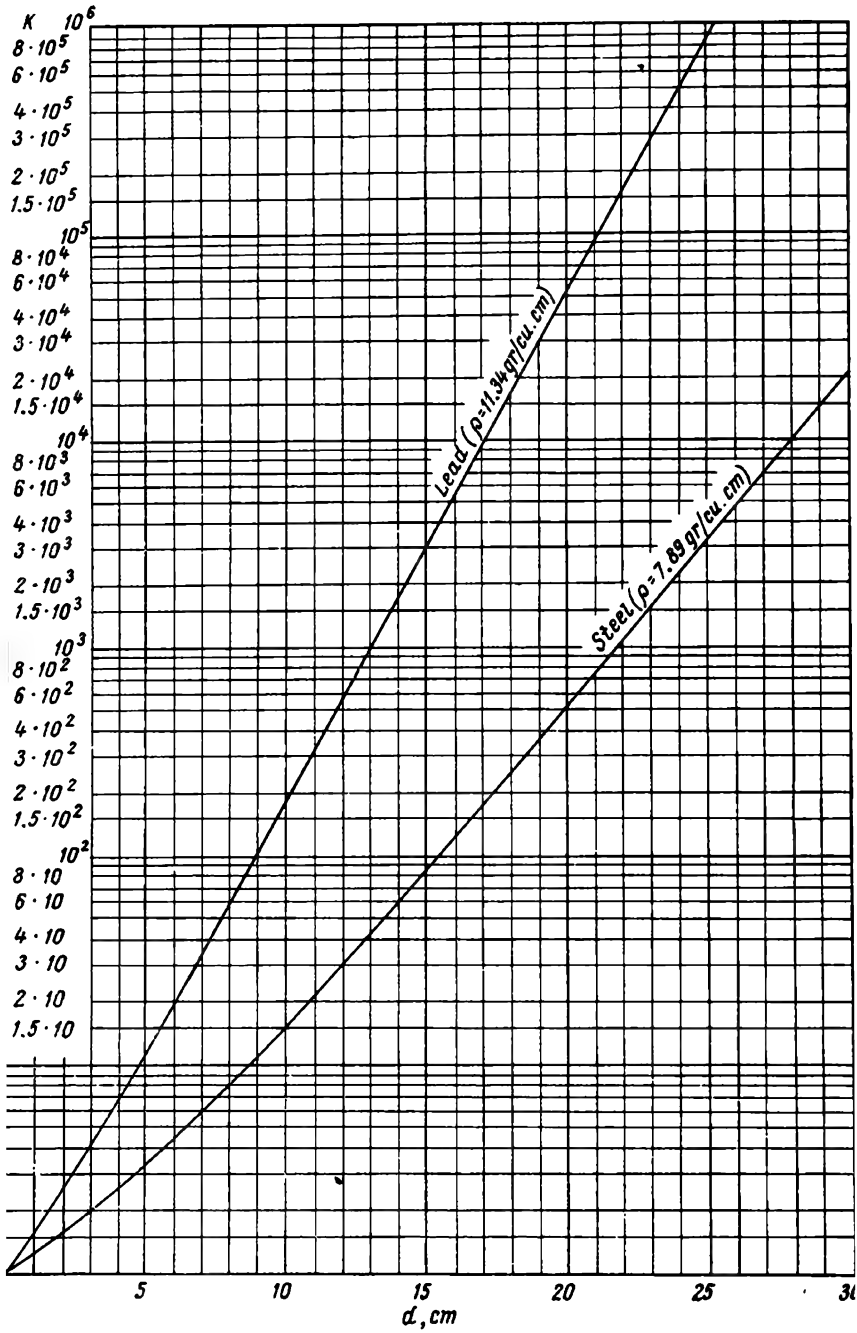

g. 136. Chart used to calculate protection from Co^{60} gamma-source ba on dose-reduction factors of lead and steel

The differential dose-reduction factors k for these lines and required thickness of lead shields d can be obtained from the following formulas:

For $h\nu_1 = 1.116$ Mev; $P_1 = 26\%$; $k = \frac{26}{100} \times 4{,}500 = 1{,}170$; $d_1 = 11.4$ cm lead.

For $h\nu_2 = 1.405$ Mev; $P_2 = 24.7\%$; $k = \frac{24.7}{100} \times 4{,}500 = 1{,}112$; $d_2 = 13.5$ cm lead.

The results obtained show that the $h\nu_2$ line determines the thickness of the protective barrier from the $Eu^{152, 154}$ source. The $h\nu_1$ line is weaker by about one and a half half-value layers, and its shield is thinner by 2.1 cm. To eliminate the

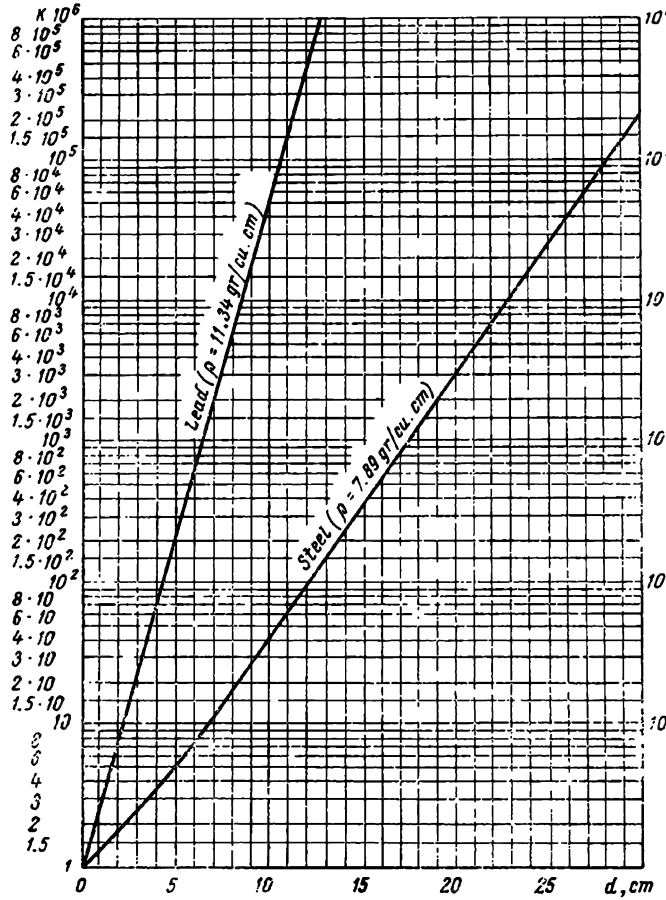

Fig. 137. Chart used to calculate protection from a Cs^{137} gamma-source based on dose-reduction factors of lead and steel

effect of this line behind the protective shield, it is necessary to add about one half of a half-value layer to d_2, i.e., 0.7 cm. Hence, the protective shield calculated by the differential method must be 13.5 + 0.7 = 14.2 cm thick.

The accuracy of this method can be determined by comparing the calculated protective thickness with the thickness determined experimentally and read off the chart shown in Fig. 132.

Thus, for 3 gram radium equivalent Ir^{192} source with $R = 1$ m and $t = 6$ hrs the calculated thickness of the protective barrier is 3.5 cm.

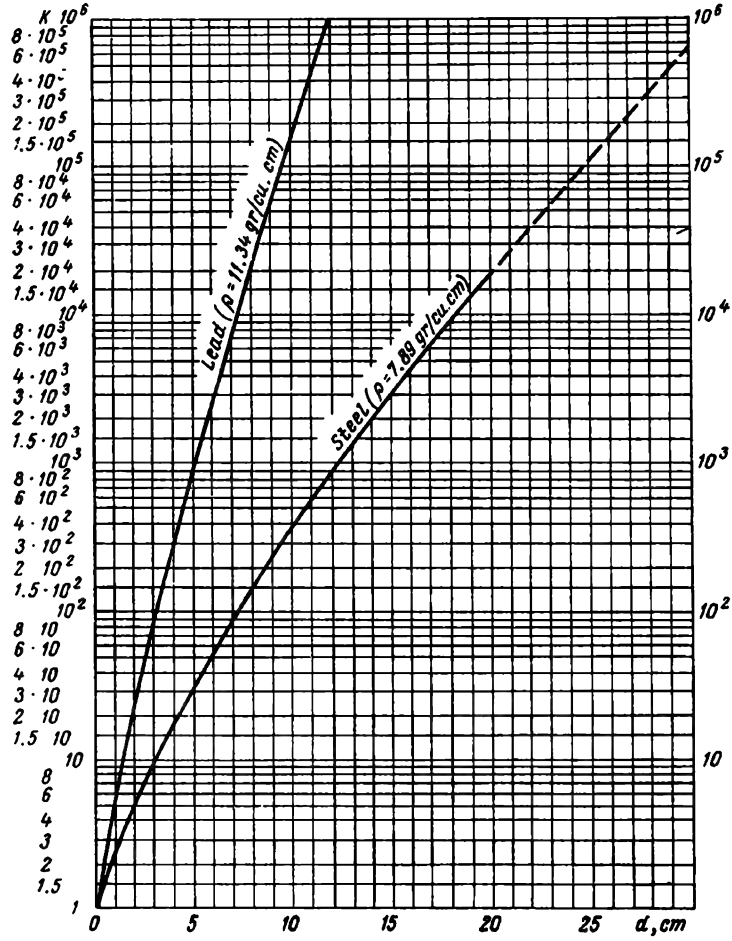

Fig. 138. Chart used to calculate protection from Ir^{192} gamma-source based on dose-reduction factors of lead and steel

On the chart (Fig. 132) it is found that for this source the thickness of the lead protective barrier is 3.6 cm.

Hence, this method of determining the thickness of protective shielding for polyenergetic gamma-ray sources by calculation is sufficiently accurate. The discrepancy between the calculated and the

experimental values does not exceed 5-10%, providing all the factors are properly considered.

However, the disadvantages of this method should be mentioned: firstly, time-consuming calculations, secondly, it is necessary to possess exact data on the isotope radiation spectrum, yield of gamma-quanta per disintegration and percentage contribution of individual lines.

Calculations of protection by means of universal charts. The charts in Figs. 136-139 may be used to determine protection from gamma-radiation emitted by Co^{60}, Cs^{137} and Ir^{192} sources on the basis of

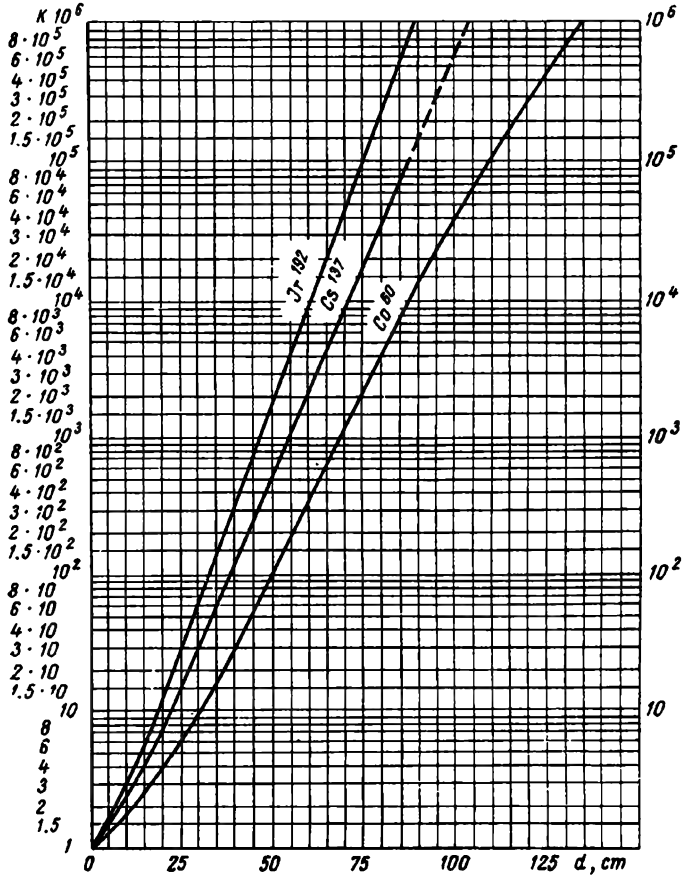

Fig. 139. Chart used to calculate protection from Co^{60}, Cs^{137} and Ir^{192} gamma-sources based on dose-reduction factor of concrete ($\rho = 2.35$ g/cu cm)

dose-reduction factors of lead, steel and concrete. These charts are called universal, for any protection problem may be reduced to the problem of finding the required dose-reduction factor. The charts are

plotted in semilogarithmic coordinates; the gamma-dose-reduction factors are plotted on the ordinate and the thickness of a protective barrier d required to ensure the given dose-reduction factor—on the abscissa.

Examples.

1. The calculated dose rate of a Cs^{137} source P is 460 μr/sec. It is necessary to reduce this dose to the maximum permissible dose if $t = 6$ hrs with a steel or lead barrier.

The maximum permissible dose rate (for $t = 6$ hrs) $P_0 = \frac{14}{6} = 2.3$ μr/sec and the required dose-reduction factor $k = \frac{P}{P_0} = \frac{460}{2.3} = 200$. From the chart (see Fig. 137) we read off $d = 5$ cm for lead and $d = 13.5$ cm for steel (or $d = 13.5 \times \frac{7.89}{7.2} = 14.8$ cm for a cast-iron barrier).

2. The calculated dose rate emitted by a Cs^{137} source P is 460 μr/sec. It is necessary to reduce this dose rate to the maximum permissible in $t = 6$ hrs ensuring the safety factor $k_1 = 5$ with a lead or steel barrier.

If $k_1 = 5$ is required, we have to reduce gamma-radiation to a dose rate of 0.01 r/day; $k = k_1 \frac{P}{P_0} = 5 \times \frac{460}{2.3} = 1{,}000$. From the chart (see Fig. 137) we read off $d = 6.5$ cm and $d = 17.5$ cm respectively for lead and steel shielding.

3. Find the thickness of a lead or steel protective barrier from a Cs^{137} source, if $t = 7$ hrs and the measured dose rate $P = 800$ μr/sec.

$P_0 = \frac{14}{t} = \frac{14}{7} = 2$ μr/sec; $k = \frac{800}{2} = 400$; hence, for lead $d = 5.5$ cm and for steel $d = 15.2$ cm.

4. A steel protective barrier 12 cm thick installed in a laboratory where a Cs^{137} source is handled ensures safe operation at a distance $R = 2$ m. To what thickness should the existing barrier be built up to ensure safe operation at a distance $R = 0.5$ m?

With $R = 0.5$ m the dose rate increases $k_0 = \left(\frac{2}{0.5}\right)^2 = 16$ times. On the chart (Fig. 137) we find that the existing barrier, 12 cm thick, ensures a dose-reduction factor $k_1 = 100$, while the new required dose-reduction factor $k_2 = k_0 \times k_1 = 16 \times 100 = 1{,}600$. This factor requires a barrier 18.2 cm thick. Thus, the existing steel barrier must be made thicker by 18.2—12 = 6.2 cm.

5. The dose-reduction factor $k = 1{,}000$. Find equivalents for lead with a Cs^{137} source. From the charts shown in Figs. 137 and 139 it follows that for $k = 1{,}000$, $d = 6.3$ cm lead, 17.5 cm steel and 55 cm concrete. Hence, for $k = 1{,}000$, 1 cm of lead is equivalent to 2.8 cm of iron and 8.7 cm of concrete.

6. Find the thickness of the concrete barrier required to reduce by 10,000 times the gamma-radiation from Co^{60}, Cs^{137} and Ir^{192} sources.

From the chart Fig. 139 we find that the thickness of the concrete barrier is 87 cm, 7i cm, and 62 cm respectively.

Charts used to determine the thickness of protective barriers by the measured dose rate. The charts shown in Figs. 140-142 are usually employed to determine the thickness of a lead barrier according to the measured dose rate. The charts are plotted in semilogarithmic coordinates, the measured (or calculated) dose rate P being plotted along the ordinate and the thickness d of the lead barrier—along the abscissa, while the irradiation time is represented by the inclined

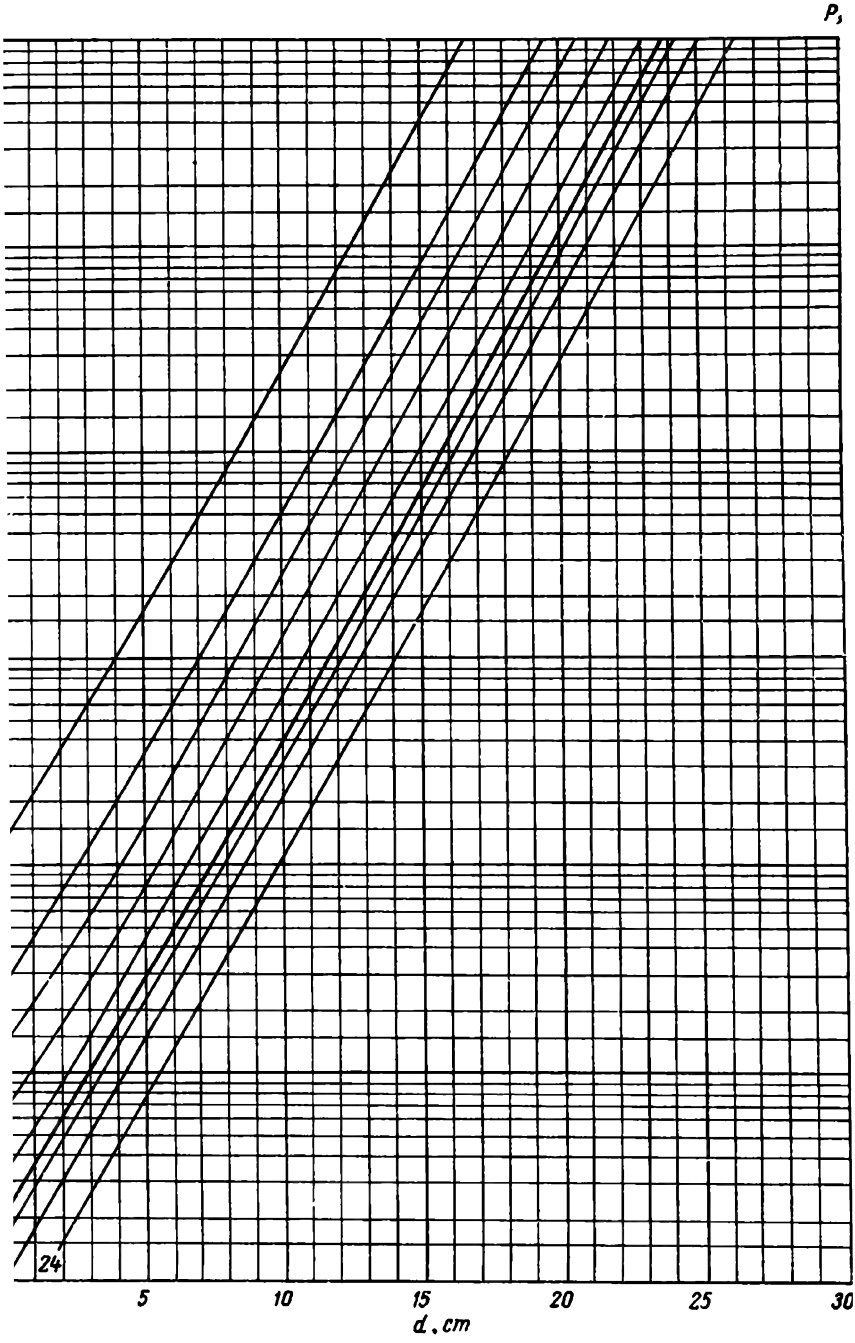

Fig. 140. Chart used to calculate lead protection from Co^{60} gamma-so depending on the dose rate and irradiation time

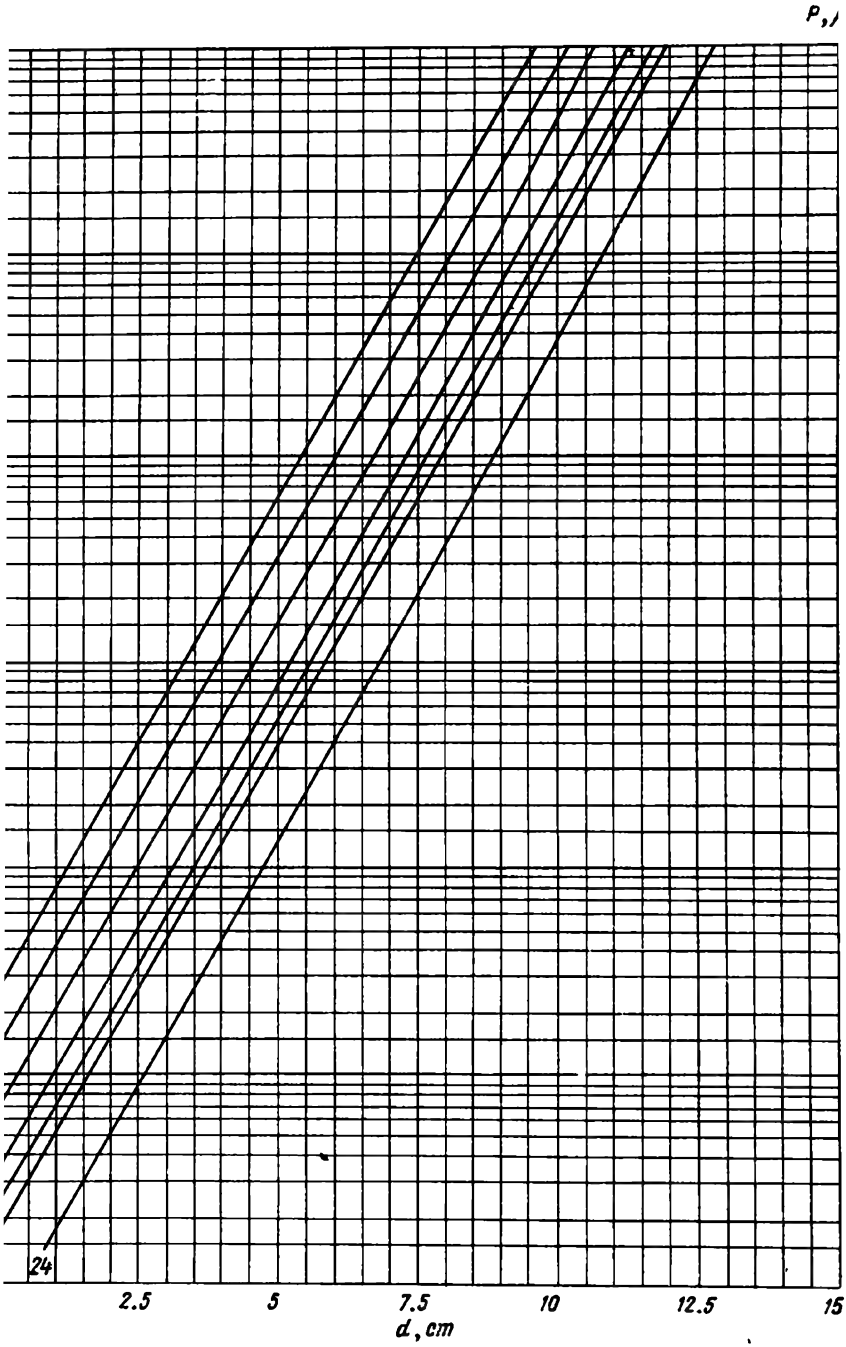

ig. 141. Chart used to calculate lead protection from Cs^{137} gamma-so
depending on the dose rate and irradiation time

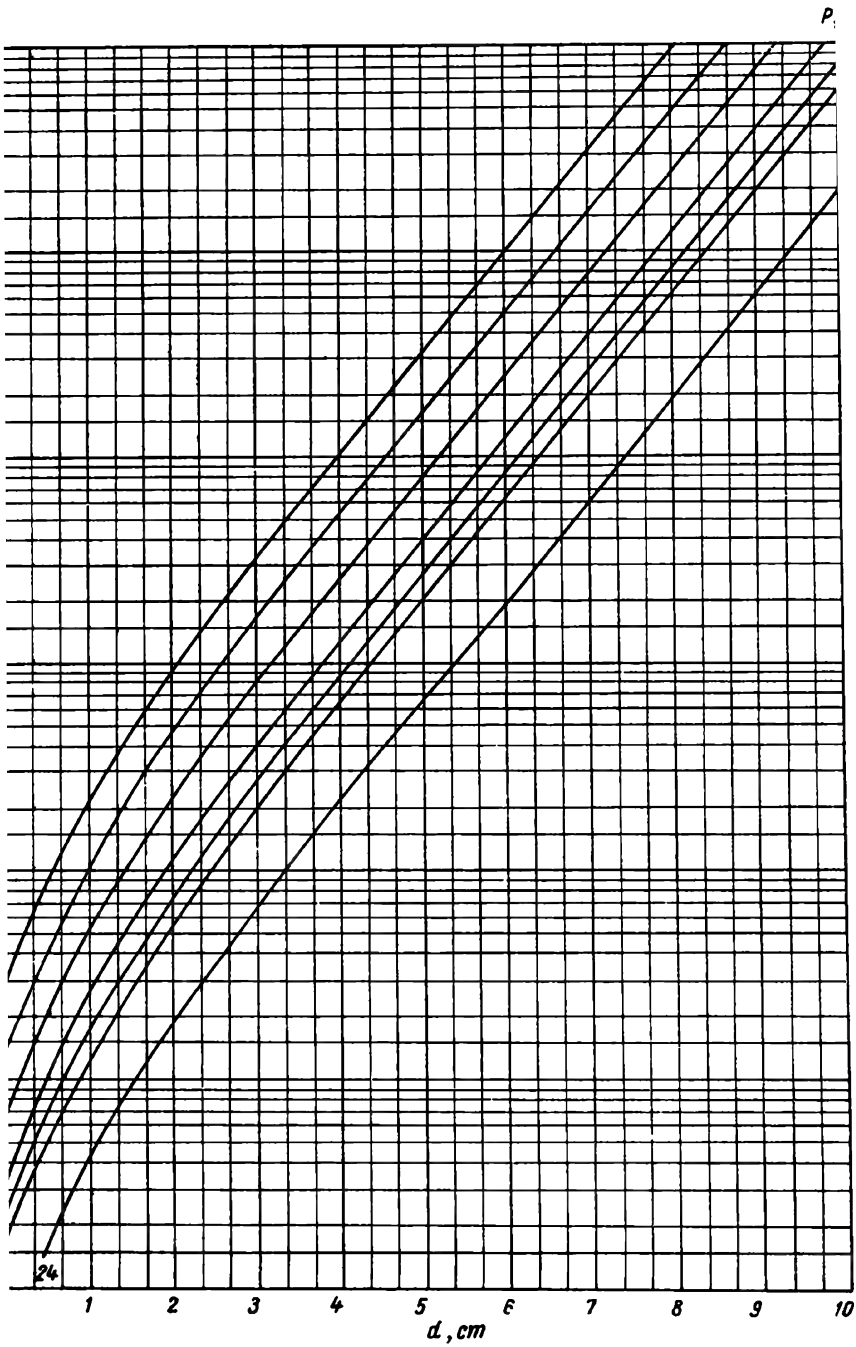

Fig. 142. Chart used to calculate lead protection from Ir^{192} gamma-sou depending on the dose rate and irradiation time

lines. For an irradiation time exceeding 24 hours (which is possible during transit) protection thickness is determined along the line corresponding to $t = 24$ hrs. The points at which the vertical axis $d = 0$ intersects the inclined lines correspond to the maximum permissible dose rate for the given irradiation time.

Examples.

1. Determine the thickness of a lead protective barrier from a Co^{60} gamma-source, if irradiation time $t = 6$ hrs and the measured dose rate $P = 200$ μr/sec.

On the chart in Fig. 140, the point is found at which the horizontal line $P = 200$ μr/sec intersects the inclined line $t = 6$ hrs. The thickness $d = 8.7$ cm is found by dropping a perpendicular from the intersection point on to the abscissa.

2. Calculate the thickness of a lead barrier offering protection from a Co^{60} source, ensuring a threefold safety factor for a dose $D_0 = 0.1$ r/week under the following operating conditions: $t = 6$ hrs; measured (or calculated) dose rate $P = 200$ μr/sec.

Multiply the measured dose by the safety factor $P = 3 \times 200 = 600$ μr/sec; then, using the value obtained, find the corresponding protective barrier thickness $d = 11.7$ cm (Fig. 140).

3. Find the thickness of a lead barrier offering protection from Co^{60} radiation for a measured dose rate (an accident rate) $P = 3{,}600$ μr/sec. In this case an irradiation dose $D_0 = 0.3$ r during $t = 0.5$ hr is permissible.

Find the over-irradiation factor $\omega = \frac{D_0}{0.05}$ and divide the given activity M (see charts, Figs. 130-132) by ω; then, find the dose-reduction factor k (see charts, Figs. 136-139) or the dose rate (see charts, Figs. 140-142). Use the fictitious values of these parameters to find the required thickness of the protective barrier.

In the problem under consideration an irradiation dose exceeding 0.05 r is permissible and the over-irradiation factor $\omega = \frac{0.30}{0.05} = 6$. Hence, the fictitious dose rate $P = \frac{3{,}600}{6} = 600$ μr/sec. For such a dose rate and the time $t = 0.5$ hr the required lead layer must be 6 cm thick (see a chart, Fig. 140).

Calculation of scattered gamma-radiation shielding. Up to now we have been considering calculation methods for direct gamma-radiation shielding. However, in practice, it is often necessary to protect attending personnel from scattered radiation. For example, when metal articles are inspected with a directed beam of gamma-rays, scattered radiation originates at all spots exposed to the incident gamma-beam: walls, floor, ceiling, inspected object, etc.

There are two kinds of scattered radiation: single scattering, coming from objects hit by a direct gamma-beam; and multiple scattering caused by incident scattered radiation.

The laws of angular distribution of scattered radiation in space, depending on the energy of primary radiation, state that the higher the energy the larger the fraction of radiation scattered forwards, in the direction of the primary gamma-beam, and the smaller the fraction scattered at a large angle. In addition, the larger the scattering angle, the lower the energy of the scattered radiation.

As a rule the path of a direct gamma-beam behind the inspected object is restricted by a protective barrier which reduces the intensity of direct radiation to the safety level over the entire beam cross-section. Therefore, usually radiation scattered at an angle smaller than 90° is reduced by the protective barrier. Thus, radiation single-scattered at an angle of 90° or near to it is the most dangerous.

The problems of protection from scattered gamma-radiation have not been sufficiently investigated. It has been proved experimentally that the intensity of gamma-radiation from a Co^{60} source scattered at a 90° angle does not exceed 1% of the initial intensity.

Thus, it can be assumed, with a certain margin of safety, that the intensity of the scattered gamma-radiation is equal to the intensity of the direct radiation emitted by a fictitious source of an activity 100 times smaller than that of the radioactive source employed. Thus, for instance, for a 400 gram radium equivalent Co^{60} source, emitting a head-on beam, the intensity of the scattered radiation is equal to the head-on radiation from a fictitious 4.0 gram radium equivalent Co^{60} source.

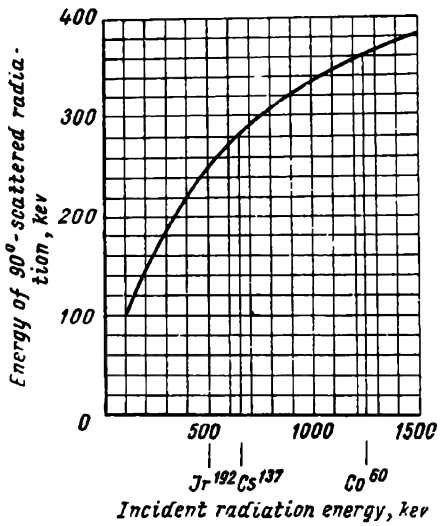

Fig. 143. Dependence of the energy of 90°-scattered radiation on incident radiation energy

In the first approximation, the intensity of back-scattered radiation for other isotopes may be determined in a similar way. However, calculations of protective barriers based on head-on radiation from a fictitious source may result in an excessive safety margin, if no corrections for the change in the scattered-radiation spectrum are introduced.

The energy of scattered radiation (at angle $\theta = 90°$) for any isotope may be determined from the curve (Fig. 143) expressing the dependence of the scattered-radiation energy on incident radiation energy. The curve shows scattered-radiation energy for Co^{60}, Cs^{137} and Ir^{192} sources. In this case one can depart from an effective energy of direct radiation equal to 500 kev and 1.1 Mev respectively for Ir^{192} and $Eu^{152, 154}$ sources.

Thus, in the first approximation protection from scattered gamma-radiation can be calculated as protection from direct radiation emitted by a fictitious source of an activity 100 times smaller, and of a radiation energy equal to the energy of 90°-scattered radiation

from the given source. Protection can be calculated by any of the methods considered above, using tables and charts employed to calculate protection from direct gamma-radiation.

For example, parts are radiographed with a downward-directed gamma-beam from a 400 gram radium equivalent Co^{60} source (the source is kept in a protective container). Determine the thickness of a protective barrier from scattered radiation produced by this source at a distance of $R = 3$ m during a 6-hour working day. The maximum permissible dose is 0.05 r/day.

First calculate the thickness of a protective barrier from a fictitious source of an activity $\frac{400}{100} = 4$ gram radium equivalent and a radiation energy of 365 kev.

The dose D created by such a source at a distance $R = 3$ m during 6 hours will be equal to

$$D = \frac{4 \times 10^3 \times 6 \times 8.4}{3^2 \times 10^4} = 2.24 \text{ r.}$$

The required dose-reduction factor

$$k = \frac{D}{D_0} = \frac{2.24}{0.05} = 45.$$

The thickness of a lead protective barrier which would ensure the required dose-reduction factor is 1.6 cm (see Appendix II, Table 1).

§ 3. Protection ensured by placing the source at a safe distance and reducing irradiation time

In a number of cases considerations of economy restrict the construction of protective devices, therefore, gamma-radiography should be so organised that the personnel are stationed at a safe distance from the source during exposure.

This requirement is of special importance in the case of small-activity sources, and when articles are radiographed with a pencil gamma-beam and it is necessary to provide protection from scattered radiation (usually, the direction of the beam is selected to avoid excessive protection, for example, downwards or to the side, where no personnel are stationed at any considerable distance).

The safe distance may be calculated for the various cases. From the curves in Fig. 144 it is possible to determine safe distances for direct and 90°-scattered radiation from radioactive isotopes of different activity. The curves are plotted for the safe dose of 0.05 r during a 6-hour working day.

Frequently the attending personnel have to handle exposed radioactive sources at short distances (charging, setting up the source for operation, actual radiography, etc.).

In all such cases, care should be taken that the personnel are exposed to direct radiation for the shortest possible time. From the chart in Fig. 145 it is possible to determine the time during which it is safe to operate with exposed sources of different activity at a given distance and also the safe distance at a given working time. The dose during that time will be equal to 0.05 r.

The chart in Fig. 145 is true for any radioactive source, provided the source activity is expressed in mg radium equivalent. The chart

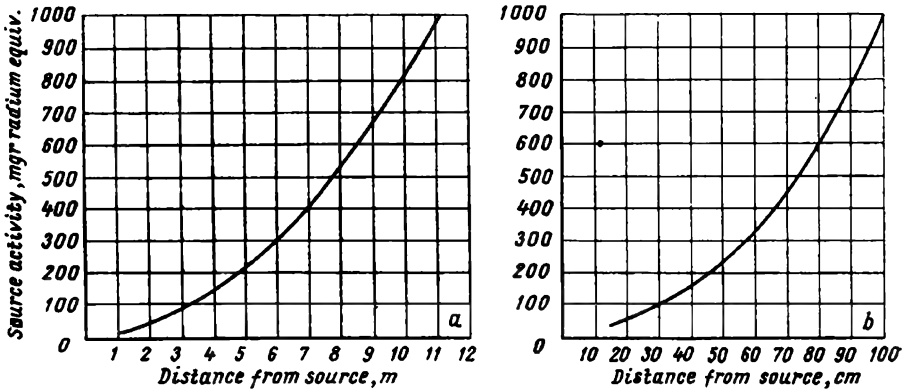

Fig. 144. Curves used to determine safe distance when handling radioactive sources:
a—for head-on radiation; *b*—for scattered radiation

relates to three principal parameters (source activity M, exposure time t and distance from source R), the combination of which ensures the maximum permissible radiation dose of 0.05 r in the absence of protective shields.

Examples.

1. Find the safe distance R from the radioactive source under the following conditions: source activity $M = 1{,}000$ mg radium equivalent; $t = 6$ hrs.
On the chart find the safe distance $R = 11$ m.
2. The activity of the radioactive source M is 5,000 mg radium equivalent. For how long may a worker be stationed at a distance $R = 3$ m from the source?
On the chart find the time $t = 0.1$ hr.
3. A source of what activity M may be handled without protection during $t = 0.5$ hr at a distance $R = 1.5$ m?
On the chart find M which is 300 mg radium equivalent.

All the principal methods of calculating protection from gamma-radiation that have been dealt with above are usually employed in combinations. Thus, for example, in calculating a protective container to be used to carry a radioactive source to the place of operation there is no reason to provide a protective shield of a thickness which would ensure safe operation during the entire working day, for the

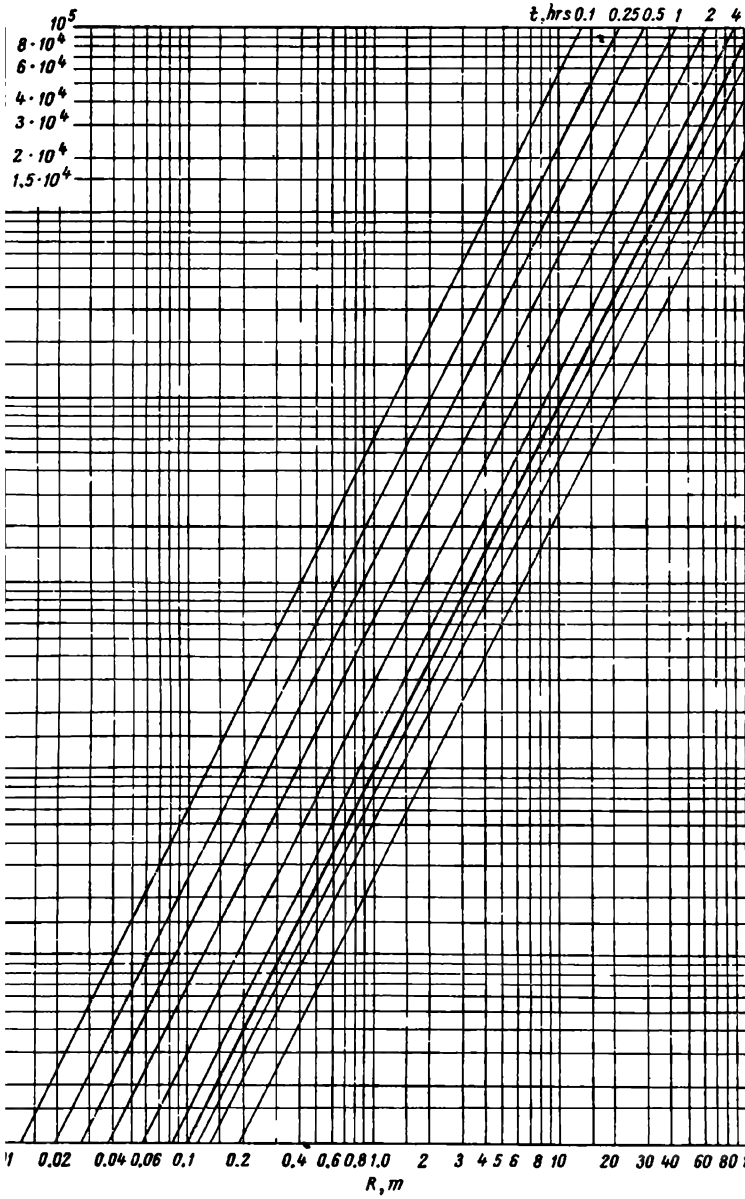

145. Chart used to determine permissible time of working wit
ion with radioactive sources of various activity at a given dista
safe distance for a given time (the maximum permissible radia
is 0.05 r/day)

source is usually carried for a short time and, in addition, the portable container can be fitted with long handles, ensuring safe distance from the radioactive source for the personnel.

§ 4. Protective materials

So far we have been considering lead protective barriers. However, it is very often possible to replace lead by cheaper materials, such as concrete, steel, etc. The proper selection of material for protective shielding contributes to less costly protective devices and more reliable protection.

The conditions under which lead may be replaced by other materials in portable and stationary protection devices differ. In portable protection devices such as containers, barriers, screens, etc., lead may only be replaced by materials which meet certain construction requirements. Therefore, as a rule, the lead in portable protection devices is replaced by steel, cast iron, copper, tungsten and other metals. In stationary protection devices preference is given to such construction materials as brick, concrete, barytes concrete, sand, earth and water.

It should be borne in mind that at energies exceeding 600-700 kev attenuation of radiation due to photoelectric absorption diminishes with the increase in radiation energy. Attenuation in this case is mostly due to scattering, which depends to a considerably lesser degree on the element atomic number Z. In this connection, when dealing with hard radiation, the difference in the thickness of the protective barriers made of lead and other protective materials diminishes; consequently, the advantage of lead as a protective material diminishes as well. Therefore, it is advisable to use materials of a smaller atomic number for protective barriers against hard radiation.

Let us consider the properties and applications of the principal protective materials.

Lead is used to manufacture protective barrels for inspection units, storage and transit containers for radioactive isotopes, door * protection devices, protective shields, as well as lining material for containers intended for X-ray film storage, i.e., in all cases where reliable protection has to be combined with the minimum size and weight.

Lead is used in bars and sheets of various thickness. Protective containers are cast from pig lead. Lead specific weight $\rho = 11.34$ g/cu cm.

---

* Lead may be used only with soft gamma-radiation as a protective material for doors. When operating with hard gamma-sources (over 1 Mev), concrete labyrinths are constructed so as to block both direct and single-scattered radiation.

Lead glass is used in all cases where the protection medium must be transparent to visible light. The specific weight of lead glass ranges from 3.4 to 4.6 g/cu cm. Glass plates 10 and 20 mm thick are available for the following sizes: 18 × 24; 24 × 30; 30 × 40; 40 × 50 cm.

Lead rubber (specific weight 3.3-5.8 g/cu cm) 3 mm thick is equivalent as regards protection properties to lead sheet 1 mm thick.

Tungsten of a specific weight ranging from 17 to 19 g/cu cm is machined with difficulty, and is, therefore, employed as a copper impregnated powder sintered at a high temperature. The specific weight of sintered tungsten is reduced to 15-16 g/cu cm. It is an advantage to use tungsten in devices offering protection against hard radiation, and for the manufacture of sphere-shaped protection containers for inspection units, designed for very important service.

Black metals: steel $\rho = 7.86$ g/cu cm, low-alloy steel $\rho =$ $= 7.5\text{-}7.9$ g/cu cm, grade РФ1 steel (containing 17-20% tungsten) $\rho = 10$ g/cu cm are employed to make external layers of protective containers, for floor protection, when operating with gamma-rays permanently directed downwards, for door protection, etc.

Barytes is used as plaster or as barytes concrete which is a mixture of barytes and cement. Barytes concrete can be made from natural barytes—a mineral containing 80-95% $BaSO_4$, Salaar barytes concentrate containing 80-95% $BaSO_4$, as well as tails of a low $BaSO_4$ content—barytes slag, for instance (50% $BaSO_4$).

As regards grain size, the following grades of barytes are available:

1) Powdered barytes leaving no residue on a sieve having 400 openings per square centimetre. The specific weight of powdered barytes is about 2.0 g/cu cm.

2) Lump barytes, 5 to 10 mm size pieces (crushed barytes), of a specific weight 2.6 g/cu cm.

3) Sand barytes, 5 mm size grain, of a specific weight 2.4 g/cu cm. The specific weight of barytes concrete made from powdered barytes is 2.7 g/cu cm; lump barytes concrete has a specific weight of 3-2 g/cu cm.

In constructing protection devices the fact that barytes concrete shrinks heavily as it cools must be taken into consideration, because of the cracks that result in nonreinforced constructions. Barytes concrete is the most advantageous material for protection against gamma-radiation of an energy up to 400 kev only.

Protective walls can also be constructed from ordinary concrete made up of portland cement, sand and gravel in a 1 : 2 : 4 proportion by volume, or 1 : 3 : 6 by weight. The specific weight of concrete is 2.1-2.4 g/cu cm. It is advisable to use concrete to build protective devices against gamma-radiation above 400 kev, because with energies of this magnitude the difference between the thickness of a barytes-concrete protective shield and a concrete shield is not large,

while the strength and reliability of an ordinary reinforced-concrete construction is considerably higher.

It is often an advantage to build protective barriers out of red or white brick. The specific weight of brick ranges from 1.4 to 1.9 g/cu cm.

In calculating the thickness of protective shields built of different materials the first step, usually, is to determine the thickness of the lead shield under the given conditions and then proceed to find the required thickness of the protective layer using the given material, the protective properties of which are generally compared with those of lead. In this case the lead-equivalent method is often employed. The lead equivalent is defined as the thickness, in millimetres, of a lead shield (d_{Pb}) which reduces a dose rate in air to the same degree as a shield of a given thickness made of the given material

$$\frac{P_1}{P_0} = e^{-\mu_x d_x} = e^{-\mu_{Pb} d_{Pb}},$$

$$\mu_x d_x = \mu_{Pb} d_{Pb}, \tag{77}$$

$$d_{Pb} = \frac{\mu_x d_x}{\mu_{Pb}}.$$

In the case of a Co^{60} source, for instance, the lead equivalent of a concrete wall 600 mm thick is equal to

$$\frac{600 \times 0.140}{0.672} = 120 \text{ mm Pb.}$$

The term "equivalent in lead" is often used in calculations. It is the thickness of a given material equivalent to a given thickness of lead shield in relation to the protective properties, i.e.,

$$d_x = \frac{\mu_{Pb} d_{Pb}}{\mu_x}. \tag{78}$$

Sometimes calculations are made on the basis of 1 mm lead equivalent. This is the thickness, in millimetres, of a protective layer built of a given material and equivalent to 1 mm of lead, i.e., the ratio $\frac{d_x}{d_{Pb}}$.

From the above definitions it is clear that the lead equivalent increases with the improvement in the protective properties of the given material, while the equivalent in lead and the 1 mm lead equivalent diminish.

The value of lead equivalents (equivalents in lead) for a given protective material depends on the energy of the isotope radiation (Table 29).

It should be mentioned that little information has been published on the lead equivalents of building materials used for protection against the gamma-radiation emitted by different radioactive isotopes.

Table 29

Equivalents in Lead for Various Protective Materials Against Co^{60} Gamma-Radiation

Gamma-radiation source	Material thickness, mm				
	Lead ρ=11.34, g/cu cm	Steel ρ=7.85, g/cu cm	Barytes concrete ρ=2.7, g/cu cm	Concrete ρ=2.3, g/cu cm	Brick ρ=1.6, g/cu cm
Radium	0.2	0.5	1.5	2	5
	0.6	1.4	3	5	8
	1.0	2.5	5	8	11
Radium-mesothorium	2.0	4.1	7	10	15
Cobalt-60	3.0	6.0	11	15	25
Radium	4.0	8.0	16	25	35
Radium-mesothorium	5.0	9.2	21	30	50
	6.0	10.8	26	35	50
Cobalt-60	7.0	12.7	29	41	57
	8.0	16.0	36	55	65
	10.0	19.0	45	65	80
	20.0	35.0	85	120	150
	50.0	80.0	200	280	
	100.0	150.0	400	550	

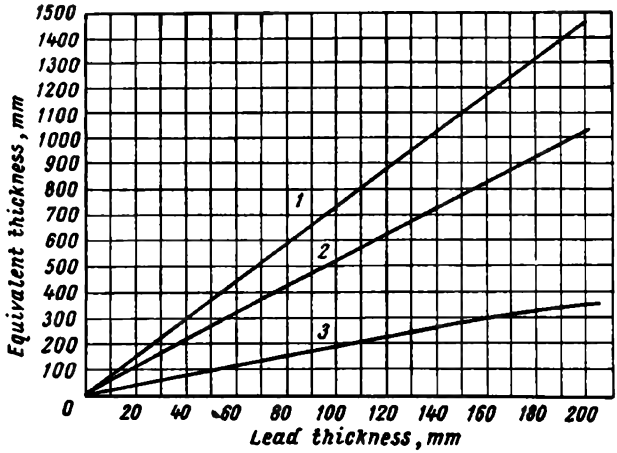

Fig. 146. Equivalent thicknesses of steel, concrete and brick protective layers for a broad-beam Co^{60} gamma-source:

1—brick (ρ = 1.6 g/cu cm); *2*—concrete (ρ = 2.3 g/cu cm); *3*—steel (ρ = 7.8 g/cu cm)

The curves shown in Figs. 146-148 determine the relation between the thickness of protective barriers built from steel, concrete and

brick and the thickness of a lead protective shield against the broad beam gamma-radiation emitted by Co^{60}, Cs^{137} and Tu^{170} sources. The curves shown in Fig. 147 can also be used to calculate protective shielding against broad-beam gamma-radiation from an Ir^{192} source with sufficient accuracy.

If we know the lead equivalent of any building material of a certain specific weight, concrete, for instance ($\rho = 2.2$ g/cu cm), then the lead equivalent of another building material, concrete of a different specific weight, for example, or brickwork, may be determined for hard radiation according to the specific weights ratio.

Let d_{Pb} represent the lead equivalent of a concrete barrier ($\rho = 2.2$ g/cu cm) d_{con} thick, then the lead equivalent of a barrier of similar thickness, but constructed from a different material, for instance, brick of a specific weight $\rho = 1.6$ g/cu cm, will be equal to $d_{Pb}\frac{1.6}{2.2}$.

For one and the same lead equivalent, in the case of medium and hard gamma-radiation, the thickness ratio of protective layers constructed from different building materials is inversely proportional to the specific weights of the materials.

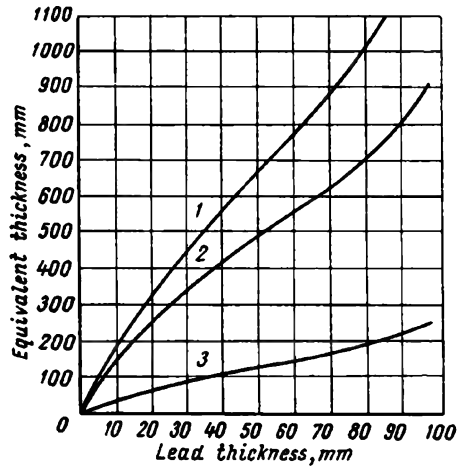

Fig. 147. Equivalent thicknesses of steel, concrete and brick protective layers for a broad-beam Cs^{137} gamma-source:
1—brick ($\rho = 1.6$ g/cu cm); *2*—concrete ($\rho = 2.3$ g/cu cm); *3*—steel ($\rho = 7.8$ g/cu cm)

The thickness of a protective barrier constructed from different materials may be calculated on the basis of the dose-reduction factor using the universal tables (Appendix II, Tables 2 and 3). From these tables it is possible to determine the thickness of the protective barriers constructed from different materials for all the important cases considered above. The tables contain data for lead ($\rho = 11.34$ g/cu cm, $Z = 82$), steel ($\rho = 7.89$ g/cu cm, $Z = 26$) and concrete ($\rho = 2.3$ g/cu cm, $Z_{ef} = 14$). The thickness of protective barriers built from other materials can be recalculated on the basis of the specific weights ratio, maintaining maximum approximation to the effective atomic numbers of the materials. The higher the energy and the lighter the protective material the smaller the error in recalculating protective shielding according to the specific weights of materials. Thus, for example, for radiation energies above 1.0 Mev, protective barriers may be recalculated according to specific weights without any substantial error, when passing not only from certain

grades of concrete to other grades, or from concrete to brickwork and earth, but from concrete to cast iron as well.

It is often necessary to calculate protective structures made up of several layers of different materials. With multilayer protection it is possible partially or fully to replace lead by other materials. When

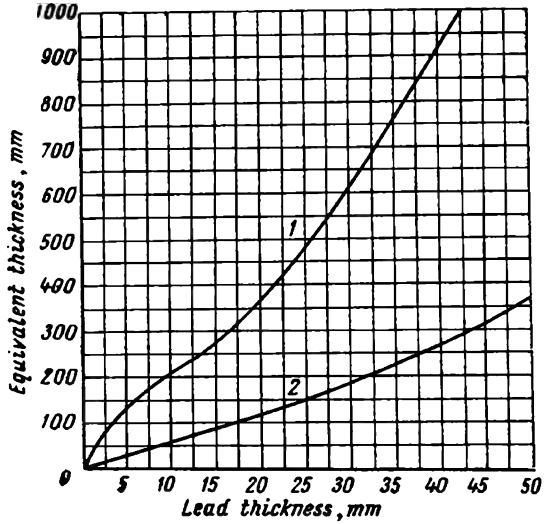

Fig. 148. Equivalent thicknesses of steel, lead and concrete protective layers for a broad-beam Tu^{170} gamma-source:
1—concrete ($\rho = 2.3$ g/cu cm); *2*—steel ($\rho = 7.8$ g/cu cm)

lead is replaced by materials of a smaller atomic number and specific weight, the total weight of the protective barrier, as a rule, increases, the difference in weight being the larger the softer the radiation against which the protection is required.

A multilayer protective device is either flat (shields) or sphere-shaped (containers for radioactive materials).

Let us consider the replacement of lead by steel in a flat protective barrier:

1. A lead barrier 4 cm thick or a steel shield 12 cm thick are required for a 100-fold reduction in the radiation dose emitted by an Ir^{192} gamma-source. 1 sq m of lead, 4 cm thick, weighs 455 kg and the weight of 1 sq m of the steel barrier is 940 kg, which is about twice the weight of the lead barrier.

2. A lead barrier 8.45 cm thick or a steel one 16.1 cm thick are required to reduce 100-fold the dose of gamma-radiation emitted by a Co^{60} source. 1 sq m of lead, 8.45 cm thick, weighs 960 kg and the weight of 1 sq m of the steel shield 16.1 cm thick is 1,250 kg, i.e., only 25% more than the weight of the lead barrier. Thus, in dealing

with hard radiation, lead should always be replaced by lighter materials, for the replacement will not result in any appreciable increase in the size and weight of the protective barrier.

The weights ratios are different with sphere-shaped protective devices intended for hard-radiation sources. In the latter case, if lead is replaced by materials of a lower specific weight, the radius of the protective device will increase in inverse proportion to the specific weight of the material, and its volume—in proportion to the cube of the radius. This results in a considerable increase in weight. The total weight of the protective device will increase approximately in inverse proportion to the square of the material specific weight. For example, a lead protective container for a high-energy Co^{60} source with a wall thickness of 16 cm, and a 2 cm inner diameter, weighs about 230 kg, while a cast-iron container possessing similar protection properties weighs about 500 kg.

Thus, the replacement of lead by other materials of a smaller specific weight in sphere-shaped and cylindrical protection devices results in a considerable increase in weight, even in the case of hard radiation emitted by a Co^{60} source. However, proper partial replacement of lead by a material of a smaller specific weight leads to a considerable saving in lead and results in only a small increase in the total weight of the device. In this case only the external layers of the protective containers should be replaced, leaving the internal lead layer intact. As an example, let us consider the same sphere-shaped container with a lead wall 16 cm thick intended for a Co^{60} source (with the internal lead layer 9 mm thick, the external steel layer should be 12.7 cm thick, this thickness being equivalent to a 7 cm lead layer). In this case the total weight of the container is about 300 kg; with only about 45 kg of lead expended, instead of 230 kg.

It should be borne in mind that it is an advantage to use multilayer cylindrical and sphere-shaped containers, as well as flat multilayer barriers, only when dealing with hard gamma-radiation.

§ 5. Gamma-radiation health monitoring

In gamma-inspection, operational safety depends to a great extent on the correct organisation of work and timely control. This includes checking protective barriers for reliability, measurement of the radiation dose received by the personnel under the given working conditions, and periodical medical examination of the servicing personnel.

At present the following principal methods of health monitoring are practised: the ionisation method, luminescent and photographic methods.

The ionisation method of health monitoring consists in measuring the ionisation caused by gamma-radiation in air with the use of the ionisation chambers described above. An ionisation chamber is of very simple construction and can be used to measure the absolute

dose and dose rate. It should be mentioned that the international unit of radiation dose was based on the method of measuring it with the aid of an ionisation chamber. By determining this unit it is possible to establish the relationship between the dose rate, measured in roentgens per second, the volume of the ionisation chamber, expressed in cubic centimetres, and the intensity of the chamber saturation current. Current intensity is very low and amounts to 0.77×10^{-13} amperes for a chamber with a volume of 1 litre and a dose rate of 2.31 μr/sec; under conditions of continuous 6-hour irradiation this corresponds to a maximum permissible radiation dose of 0.05 r. The measurement of currents of so low an intensity is difficult and can only be carried out with the aid of special electron amplifiers.

Gas-discharge counters are more sensitive monitoring instruments, although their accuracy is not very high.

If a counter is exposed to an incident constant-energy gamma-beam, the counting rate, i.e., the number of pulses per unit time, will vary, depending on the tension applied to the counter.

A disadvantage of gas-discharge counters consists in the poor efficiency of the gamma-quanta registration and the fact that this efficiency is dependent on gamma-quanta energy.

Gas-discharge counters are widely employed in health monitoring, notwithstanding a number of shortcomings. At the present time very sensitive scintillation counters fitted with simple counting devices are also employed to register radiation. Besides high efficiency, scintillation counters possess another essential advantage, as against gas-discharge counters: the dead time of a scintillation counter is very short. Its dead time is determined by the de-excitation time of the crystal which ranges from several fractions of a microsecond to 10^{-8} sec and often to 10^{-11} sec for different crystals. Owing to this, it is possible to register hundreds of thousands of gamma-quanta per second with the scintillation counter.

The photographic method of health monitoring is often used to register ionising radiation. This method is based on the relationship that exists between the density of an X-ray film and the dose of gamma-radiation to which the film was exposed. This relationship is expressed by a characteristic curve true for the given grade of film. the manner the holder was loaded and a definite radiation spectrum. It should be borne in mind that, all other conditions being equal, the density of film of a certain lot also depends upon storage time, developer composition and temperature, and development time. In addition, account should be taken of the phenomenon of the ageing of the latent image, for the density of the exposed film depends on the time interval between exposure and development, and film density diminishes gradually as the time interval is prolonged.

Health monitoring with the aid of X-ray film is performed in the following manner. Rectangular badges 30 × 50 mm in size are cut

from a piece of film, the fog of which must not exceed 0.2-0.25. Each worker is handed two badges, properly marked and placed in light-tight paper holders fitted with a stiff cover to protect the badge from damage. The workers wear the film-badges during working hours for 10 days. At the same time ten film-badges of a similar size cut from the same film are preserved as a standard. Five or six days later the standard film-badges, also kept in light-tight holders, are irradiated with doses ranging from 0.1 to 1.0 r to form ten different standard badges. The irradiation is carried out with a gamma-source of a corresponding energy and known activity. The radiation dose intended for each of the ten badges is varied by changing the exposure time and the film-source distance. The conditions of ageing must be similar for all badges.

When the ten working days are over the film-badges worn by the personnel are developed in a normal developer together with the standard film-badges. The developed badges are fixed and dried by conventional procedure. The standard badges are studied with the aid of a photometer. With the densities of the standard badges it is possible to plot a curve expressing the film density, as a function of the radiation dose (characteristic curve). The radiation dose received by the personnel in ten working days is determined with the aid of the plotted curve by estimating the density of the film-badges worn. The density of the film-badge worn in the breast pocket characterises the total radiation dose and the density of the film-badge worn on the sleeve—local arm irradiation. If no instruments are available, with which to measure film density the radiation dose is determined visually by comparing the film-badges worn with the standard badges.

The quantitative and qualitative measurement of gamma-radiation doses and dose rates is carried out by means of special instruments: dosimeters, roentgenometers, radiometers, etc. According to the purpose for which they are used, the instruments are divided into two categories: personnel monitoring instruments and instruments to measure gamma-radiation dose rates.

The personnel monitoring instruments are used to measure the cumulative radiation dose received by a worker during a workday or working week, while the dose rate measuring instruments are designed, as a rule, for general health monitoring. The same instruments can be employed to check adjacent premises for the presence of radiation, to search for radioactive preparations, etc.

Brief specifications of some of the typical instruments are given below.

Instruments employed to measure the dose rate of gamma-radiation. The *model ПМР-1 portable micro-roentgenometer* is designed to measure the dose rate of gamma-radiation emitted by sources of an energy ranging from 0.2 to 2.0 Mev under laboratory and field conditions. Its measuring range is from 0 to 5,000 μr/sec. The instrument

has four sub-ranges: 0-5; 0-50; 0-500 and 0-5,000 μr/sec. Main measurement error ±10%. Additional measurement error: for a change in ambient temperature from +20 to +35°C—15%; from +20 to —20°C —40%; and after continuous operation for 60 hours from one supply source ±10%.

Supply sources: a 1.6 v dry cell and 22.5 v storage battery.

The instrument and supply sources weigh 3.5 kg. The instrument is mounted inside an air-tight aluminium case on the bottom of which a flat ionisation chamber with a plate-like central electrode is placed. The chamber volume is 1 litre. The sub-range setting splines, control knobs and handle for carrying are arranged on the front panel. The duration of continuous operation from a single supply source is 60 hours. Overall dimensions are 220 × 130 × 170 mm.

The *type MPM-1 medical micro-roentgenometer* is designed to measure the dose rates of X-ray and gamma-radiation of energies from 0.1 to 1.2 Mev. The instrument features an ionisation chamber for a radiation detector. The instrument, designed to measure radiation doses ranging from 0 to 1,000 μr/sec, has four sub-ranges: 0-2; 0-10; 0-100 and 0-1,000 μr/sec. Its main measurement error is ±10%. The additional measurement error: for a change in radiation energy from 0.1 to 1.2 Mev is ±10%; for a change in ambient air temperature from 5 to 35°C±5%; for variation in supply voltage from 7 to 15 v±10%. Normal operating conditions for this monitoring instrument are: ambient air temperature is from 5 to 35°C; relative air humidity up to 75%.

The instrument is supplied from 50 cps, 127 or 220 v a.c. mains. Overall dimensions are 370 × 268 × 200 mm; weight is 5 kg.

The *Cactus micro-roentgenometer* is a stationary instrument designed to measure gamma-radiation dose rates. Any ionisation chamber that can be removed from the control board to a distance of 100 m with the aid of a connection cable may serve as a radiation detector for the instrument. The Cactus micro-roentgenometer is chiefly used in conjunction with a 5 litre model ДИГ-5 ionisation chamber.

The measurement range (with a ДИГ-5 chamber) is from 0 to 20,000 μr/sec. The instrument has five sub-ranges: 0-2; 0-20; 0-200; 0-2,000 and 0-20,000 μr/sec.

The main measurement error is ±10%, daily drift of the instrument pointer (at an ambient air temperature of 25 ± 5°C, 75% relative air humidity and six-hour continuous work) ranges within ±4%.

The instrument is supplied from 50 cps, 110, 127 and 220 v a.c. mains. Power consumed is 75 w.

Overall dimensions are 355 × 195 × 335 mm, weight (without the 100 m connection cable and chamber) is 17 kg.

The *PM-2 small-size pocket radiometer* is designed for the detection, under laboratory and field conditions, of radioactive substances emitting gamma- and beta-radiation. Indication is by sound—ear-

phone clicks, and visual—indicator lamp flashes. CTC-1 counters are used as detectors.

The measurement range is from 0 to 1,000 μr/hr, the main error is ±20%.

The instrument is supplied from a 200 v storage battery. Continuous operation time without change of battery is 500 hours. Overall dimensions are 125 × 101 × 39 mm, weight is 0.35 kg.

The *СД-1М alarm meter* is designed to control and give warning of an increase in the gamma-radiation dose rate above that permissible in working premises. The radiation detector is a model CTC-1 gas counter. Normal operating conditions are: ambient air temperature—from 5 to 40°C; relative air humidity—up to 98%.

The smooth adjustment range for the alarm meter operating threshold is within 2 to 10 μr/sec; the main operational error is under ±20%; the additional summary operational error (due to different factors) is under ±20%.

The instrument is supplied from 50 cps, 220 v a.c. mains. The power consumed is 40 w.

The instrument is fastened to a wall by means of a special connector box. The signalling is done either with red and green alarm lights, or with a bell. When the dose rate of gamma-radiation falls below the threshold value, the signalling device is cut-off automatically. With this instrument the alarm section can be installed at a distance of 250 m from the counter.

Overall dimensions are 185 × 500 × 170 mm; weight is 8.5 kg.

Personnel dosimeters. These are mostly electrostatic instruments with which it is possible to determine the dose-rate of gamma-radiation at any moment.

It is known that in a charged electroscope the thin metal strips suspended from the insulated electrode are mutually repulsed and come together gradually, as the received charge is being lost. The better the central electrode is insulated, the longer the charge remains on the strips. If the electroscope were subjected to ionising irradiation, the air in the electroscope would become an electric conductor, the charge would leave the strips more quickly and the strips would come together sooner.

The *КИД-1 personnel dosimeter* is employed to measure the cumulative dose from hard gamma- and X-ray radiation under laboratory conditions. Its measuring range is from 0.02 to 2.0 r.

The instrument consists of a charging-measuring device and 20 pocket dosimeters. It has two sub-ranges of measurement: 0.02-0.2 r; and 0.2-2.0 r. The main error of the instrument is ±0.02 r and ±0.3 r for the first and second sub-ranges respectively.

The pocket dosimeter consists of a double ionisation chamber enclosed in a case resembling a fountain pen. The operating principle of the instrument is based on the change in the charge of the capacitor. The selfdischarge of the chamber does not exceed 3-5% of the scale

in 24 hours (at a temperature of +20±5°C and a relative air humidity up to 80%).

The instrument is portable. A set including 100 chambers (packed) weighs 22 kg; the overall dimensions are 325 × 225 × 200 mm. The size of a double ionisation chamber is 15 × 120 mm. The charging-measuring unit is supplied from 50 cps, a.c. mains of a voltage of 127 or 220 v ± 10%. The charging device is a table instrument with a panel accommodating the measuring instrument, scale setting adjuster, charging and measuring jacks, mains block, supply mains tumbler switch and two pilot lamps.

The *ДК-0.2 personnel dosimeter* is designed to measure the cumulative dose of X-ray and gamma-radiation under both laboratory and field conditions. Its measuring range is from 0 to 200 μr (for radiation energy from 0.2 to 2.0 Mev). The maximum permissible gamma-radiation dose rate is 100 μr/min. The dosimeter main error is ±10%. The selfdischarge of dosimeters of this type does not exceed 10% per 24 hours.

The instrument functions normally at an ambient air temperature of —30 to +35°C (for the dosimeter) and —20 to +50°C (for the charging unit) and a relative air humidity—up to 98%.

The instrument consists of a charging device and personnel dosimeters. The ЗД-3 charging unit is supplied from a 105 v storage battery and 1.48 v dry cells. The continuous operation time, without changing the batteries, is 500 hours, without changing the dry cells—45 hours.

A dosimeter looks like a fountain pen and its aluminium case accommodates a sensitive system (electroscope), consisting of a quartz fibre and stationary loop, an ionisation chamber and a three-lens microscope. When the fibre and loop are charged, the fibre moves away from the loop. The dosimeter is charged before starting work. To charge the ionisation chamber, the protective cap has to be unscrewed and the dosimeter placed into the opening in the charging unit which is supplied from storage batteries.

The dosimeter functions on the discharge principle. The electrometer readings are proportional to the lost charge. From the number of scale divisions through which the fibre shifts it is possible to determine the dose received by a worker during a definite period of time. The scale of the electrometer is graduated in roentgens, a scale division amounting to 10 μr. If there is no radiation, the electrometer fibre will deflect, merely owing to charge leakage. This fibre deflection must not exceed 1% per 24 hours.

The overall dimensions of the charging unit are 128 × 128 × × 115 mm; the dosimeter is 15 mm in diameter and 115 mm long.

The dosimeter weighs 23 g, the charging unit and storage batteries—1,650 g.

The *ДК-50 personnel monitoring set* is designed to measure the cumulative dose of gamma-radiation to which the servicing person-

nel are exposed under laboratory and field conditions. The measurement range of the instrument is from 0 to 50 r. The permissible gamma-radiation dose rate is 0.5-200 r/hr. The maximum selfdischarge of the dosimeter is 10% per 24 hours.

Normal operating conditions are: ambient air temperature from —40 to +50°C for the dosimeters and from —20 to +50°C for the charging unit; relative air humidity—up to 98%.

The personnel monitoring set consists of a ЗДМ-1 charging unit and 55 personnel dosimeters, type ДК-50. The charging unit is supplied from a 105 v storage battery and 1.48 v dry cells. The continuous operation time without changing the batteries or dry cells is 500 and 45 hours respectively.

The overall dimensions of the charging unit are 128 × 128 × × 120 mm; a dosimeter is 132 mm long and 15 mm in diameter. A packed personnel-monitoring set weighs 6.2 kg; one dosimeter— 25 g, and the charging unit (without storage batteries and dry cells)— 600 g.

§ 6. Gamma-inspection laboratories

In gamma-inspection laboratories, radioactive preparations are stored and used in special inspection units or containers ensuring the required protection. Therefore, in laboratories where inspection is not carried out with bare gamma-sources, stationary protective shielding is required to safeguard only against scattered radiation. In laboratories where inspection is carried out by panoramic setups with the aid of a bare source, stationary barriers should be calculated to absorb a direct gamma-beam.

In building new flaw-detection laboratories intended for industrial inspection, research work and experimental work on testing cast, welded and other metal articles for quality, it should be borne in mind that it is possible to effect reliable control of different articles only by using different methods of flaw detection.

Fig. 149 shows the typical layout of a flaw-detection laboratory. The laboratory is a separate one-storey building. To make the flaw-detection laboratories more universal in operation, the project envisages the use of various methods of flaw detection based on the magnetic field, ultrasonic techniques, X-ray and gamma-radiation. The project assumes that the gamma-inspection will be employed for both thick-walled articles, using Co^{60} sources (ГУП-Co-50 and ГУП-Co-5 inspection units), and parts which are not so thick, with the aid of Tu^{170} and Eu^{155} sources (РК-1 inspection units). Accordingly, there is a storage room for radioactive substances and three inspection rooms. The walls of the storage and gamma-inspection rooms are calculated to provide reliable protection against head-on gamma-radiation emitted by a Co^{60} source of an activity of 50 gram radium equivalent at a distance of 0.5 m. Protective shielding has been calculated on the basis of a tenfold safety margin, i.e., source activity

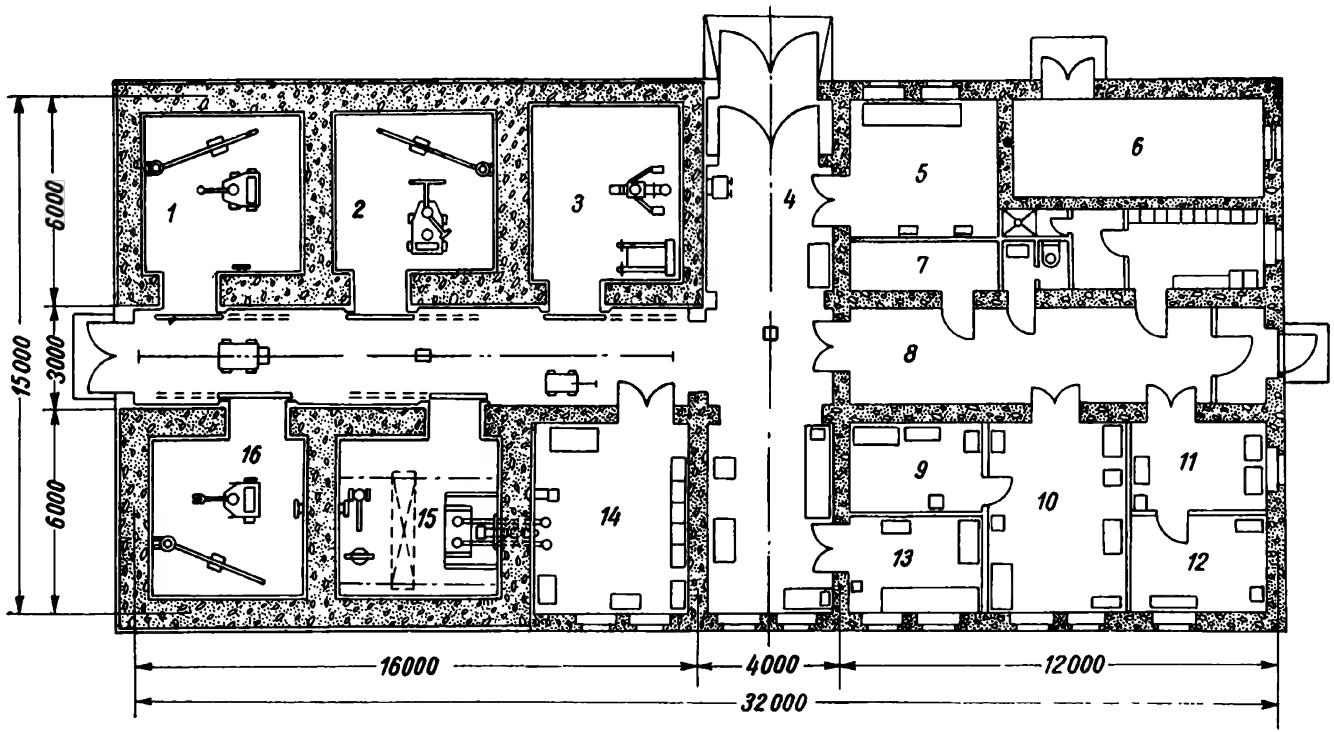

Fig. 149. Typical layout of a complex flaw-detection laboratory:

1—room for gamma-radiography with sources of an activity 50 gram radium equivalent (19.3 sq m); *2*—X-ray inspection room (20.4 sq m); *3*—soft gamma-source inspection room (20 sq m); *4* and *8*—corridors (33.1 sq m); *5*—magnetic flaw-detection room (16.8 sq m); *6*—plenum ventilation chamber (20.8 sq m); *7*—store-room; *9* and *10*—photographic laboratories (33.2 sq m); *11*—working room (10.7 sq m); *12*—study of the head of the laboratory (9.6 sq m); *13*—instrument repair shop (10.6 sq m); *14*—control board room (22.7 sq m); *15*—source storage and recharging room (20.4 sq m); *16*—room for gamma-radiography with sources of an activity 5 gram radium equivalent (19.8 sq m)

was assumed to be 500 gram radium equivalent, instead of 50. Accordingly, the thickness of the concrete walls in both the gamma-inspection rooms and the source storage premises was set at 840 mm and 2 × 130 mm for brickwork. These protective barriers diminish the dose rate to 0.25 μr/sec on the outside, thus ensuring adequate protection for personnel not engaged in handling radioactive sources.

A fivefold dose-rate safety margin is admissible for personnel directly engaged in radiography. Under these conditions concrete walls will be 740 mm thick and brickwork—2 × 130 mm. The thickness of cast-iron doors is 300 mm (see charts and tables, § 2). Since a cast-iron door 300 mm thick weighs about 15 t and is, therefore, very inconvenient to use, it is necessary to build labyrinths (additional partitions) in inspection rooms which would exclude the possibility of head-on and single-scattered gamma-radiation hitting the door. These partitions can be constructed from cast iron 200-250 mm thick, barytes concrete—500 to 550 mm thick or concrete—650 to 700 mm thick. In order to protect adjacent rooms from scattered radiation, the labyrinth door must be lined with lead sheet 3-5 mm thick.

For Co^{60} sources of a smaller activity or other isotopes ($Eu^{152, 154}$ sources of an activity of 5 and 0.5 gram radium equivalent, Cs^{137}—15, 10 and 2 gram radium equivalent, Ir^{192}—15 and 2.0 gram radium equivalent, Tu^{170}—1.0 and 0.5 gram radium equivalent and others) the thickness of the walls may be correspondingly reduced.

The floors and ceilings of the inspection rooms do not have to be protected from gamma-radiation, since the flaw-detection laboratory under consideration is designed as a separate one-storey building.

Radiation sources are to be kept in safes and special wells in storage room *15*. Source handling is to be carried out by means of typical M15-A master-slave manipulators. The manipulators are operated from the adjacent room *14*. The articles are prepared for radiography in room *4* in which ultrasonic flaw detection may be conducted, if required. From this room, articles are removed into rooms *1*, *2*, *3* and *16* for gamma- or X-ray inspection or into room *5* for magnetic flaw detection. The design provides for cold- and hot-water supply.

Three kinds of health-monitoring are planned: firstly, stationary gamma-background control with the aid of СД-1М alarm meters; secondly, periodic control of gamma-background distribution in all laboratory rooms with the aid of ПМР-1, МПР-1 portable microroentgenometers and other instruments and, thirdly, personnel dosimetric control to check the cumulative radiation dose received by each laboratory worker effected with the aid of type КИД-1, ДК-0.2 and ДК-50 personnel dosimeters.

Such laboratories may be set up at large industrial establishments and research institutes. The individual elements of this comprehensive laboratory could be used in small laboratories, and control posts in existing or newly built industrial enterprises.

Where it is impossible to build a special flaw-detection laboratory a radiographic room is set up. In a number of cases existing X-ray

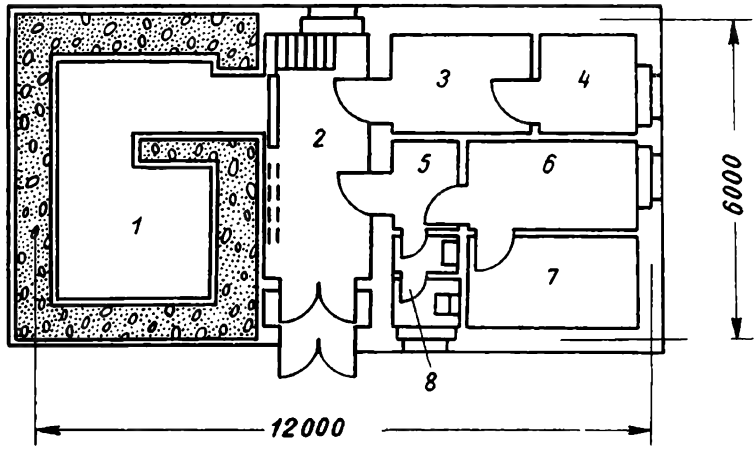

Fig. 150. Layout of a laboratory designed for small-part inspection:

1—exposure room; *2*—corridor and vestibule; *3*—storage room; *4*—plenum ventilation room; *5*—cloak room; *6*—light room; *7*—dark photographic room; *8*—lavatory

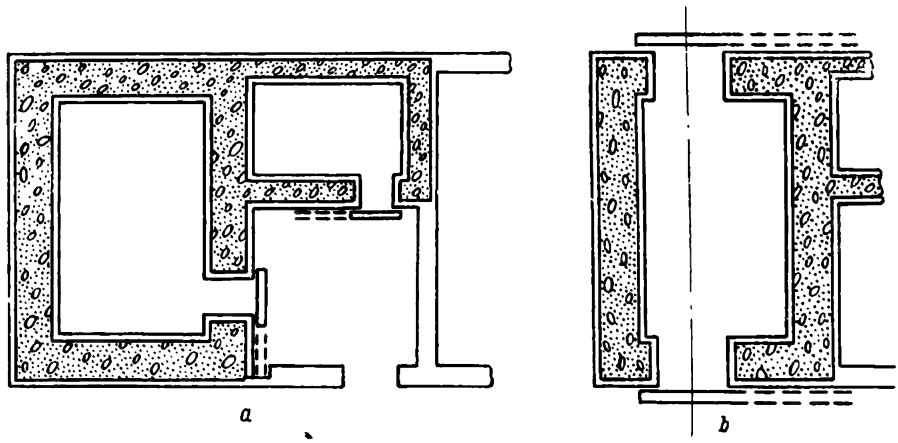

Fig. 151. Layout of a shop laboratory for large-part inspection

rooms are refitted for gamma-radiography. In this case the thickness of the protective shielding must be correspondingly augmented.

Fig. 150 shows the layout of a laboratory intended for the inspection of small articles. Similar layouts may be used for small-part inspection rooms set up directly in shops.

The layouts shown in Fig. 151 may be used for inspection rooms where large parts are to be inspected. The radiographic room shown in Fig. 151,*a* has no ceiling, and articles are delivered for inspection by means of a crane; in the case of the inspection room shown in Fig. 151,*b* a trolley is used for this purpose.

In inspection rooms with no ceilings it is desirable to radiograph articles only with a gamma-beam directed downwards, or sideways, by way of exception. In this case, apart from wall and door protection, account should be taken of the dose rate of the upward scattered radiation, as well as of the radiation scattered from the shop ceiling and directed downwards.

If gamma-inspection is to be practised in workshops, on erection sites, as well as in the control of operating equipment, where it is impossible to conduct gamma-inspection at a safe distance from the servicing personnel, safety is ensured by means of special protective shields, calculated with the aid of the charts and tables, given in § 2 in accordance with the activity of the employed radioactive sources and source-to-personnel distances.

Part Four

THE EFFECT OF DEFECTS ON MECHANICAL PROPERTIES OF ARTICLES AND WELDS

§ 1. The effect of defects of metallurgical origin on the strength of articles

The task of determining the fitness of welded, cast and other articles with the aid of gamma-graphs is complicated by the necessity to take into account the effect of the defects on the mechanical properties of the inspected articles.

A Soviet handbook entitled *Evaluation of the Effect of Metal Flaws on the Strength of Articles* throws light on the effect of metallurgical flaws such as hair cracks, foreign inclusions and other surface and internal imperfections on the strength of articles. It is pointed out that in the evaluation of metal flaws it must be determined how they affect the strength of articles; account should be taken of the sensitivity of the metal to the defects, their location, and orientation in the field of stressed state, as well as the peculiarities of the stressed state and the operating conditions (kind of service, rate and duration of loading, surrounding conditions, nature and concentration of stresses, etc.).

Very elongated and sharply outlined defects are considered the most dangerous; rounded defects are less dangerous. The orientation of a defect is considered dangerous, if the maximum tensile stress acts in a direction perpendicular to that of the elongated defect. The least dangerous orientation is when the tensile stress acts in the direction of the defect. Alloys of a medium strength and a sufficiently high plasticity (many grades of steel of $\sigma_b = 120$ kg/sq mm and less), low-plasticity materials of a considerable internal heterogeneity (cast iron, light cast alloys) are characterised by a low sensitivity to defects. Materials of higher strength and limited plasticity, for instance, grades of steel of a strength exceeding 140-150 kg/sq mm, aluminium-base alloys of a strength exceeding 40-50 kg/sq mm, some magnesium alloys, etc., are characterised by a higher sensitivity to defects.

The effect of imperfections is minimum under a static load. It becomes more dangerous if repeated loading with a limited number of cycles is practised. Under continuous and repeated loadings the danger increases greatly. Symmetric cycles make defects particularly

dangerous and the danger diminishes, as cycle asymmetry increases. The danger increases the longer the parts operate in a stressed state and especially in a corrosive environment.

However, the handbook does not deal with welding defects, for the authors consider welding a very important field requiring special examination.

In view of the large volume of welding work done in machine-building and other branches of industry, let us examine the effect of welding defects on the working efficacy of welds.

§ 2. The effect of welding quality on the strength of welds

A number of papers published both in the U.S.S.R. and abroad have been devoted to the effect of welding quality on the mechanical properties of welds. Since 1930 research has mostly aimed at evaluating the effect of welding defects on the strength of welds from the point of view of accepted standards. In a number of investigations great attention was paid to establishing the relation existing between defects revealed on a roentgenograph and the mechanical properties of the welds.

The effect of pores and slag inclusions on static, vibratory and impact strength. Under a static load the main effect of pores and slag inclusions consists in the weakening of the cross-section. If the built-up metal possesses high mechanical properties, these defects, up to a certain point, have no noticeable effect on the static strength of the weld. Weld reinforcement largely compensates for the weakening of the weld cross-section by the defects.

Under a vibratory load the effect of pores and slag inclusions is quite different. These defects may noticeably diminish the fatigue limit of a weld under a vibratory load. Welds are most seriously affected by pores and slag inclusions arranged in rows, large defects, as well as by defects coming to the surface of welds. In most cases concentration of stresses caused by weld reinforcement affects the fatigue limit of a weld more than internal porosity.

The resistance of welds to impact loads gradually diminishes with the increase in porosity and slag inclusions. These defects reduce weld metal density, so resulting in poorer plastic properties. Large defects decrease the resistance of welds to impact loads to a greater extent than very many (according to the area on radiographs) pores and slag inclusions of a smaller size.

The effect of cracks and lack of fusion on static, vibratory and impact strength. The main harmful effect of lack of fusion and cracks on low-carbon steel welds subjected to static loads is that these defects diminish the useful area of the weld, with a resultant reduction in its static strength. The concentration of stresses occurring in these zones disappears under conditions of plastic deformation.

Lack of fusion at the centre of a double X-joint is less dangerous than lack of root fusion in single V-joint welds. Lack of fusion in open butt welds, up to 25% long, does not appreciably diminish the static strength of a weld. A longer defect of this kind diminishes the strength of a weld approximately in proportion to the further weakening of the cross-section. The reinforcement of a weld very largely compensates for lack of fusion.

Lack of fusion of a small length (10-15% of weld thickness) only slightly diminishes the static strength of a single V-weld. With an increase in the length of the defect (to about 50%), the static strength decreases on an average in proportion to the cross-section weakening. Reinforcement of such welds does not bring about a noticeable increase in the static strength of the welds.

It can be recorded that under vibratory loads the harmful effect of lack of fusion and cracks is that they cause concentration of the stresses. In the case of single V-welds even a slight lack of fusion (5-10%) halves the fatigue strength of the weld, as compared with similar but flawless welds. An increase in the length of the defect to 25% of metal thickness does not substantially alter the stress concentration factors, as compared with a slight lack of fusion, and the fatigue limits remain unchanged. With lack of fusion exceeding 25% of the weld thickness not only stress concentration, but the weakening of the cross-section begins to tell too, and the fatigue limit diminishes in proportion to the decrease in the working cross-section of tested specimens.

Fatigue bending tests show that in double X-welds lack of fusion does not very much affect the supporting ability of a weld. Fatigue tension-compression tests show that even slight lack of fusion reduces the fatigue strength of a weld.

Published data on carbon and low-alloy steel suggest that the more plastic the metal, the smaller the stress concentration effect of lack of fusion under repeated loads. In § 3 it will be shown, however, that with special grades of steel this conclusion is not corroborated.

Available data make it difficult to come to any general conclusion as to the effect of lack of fusion on the resistance of welds to impact loads.

It may be assumed, however, that lack of fusion and cracks considerably affect the resistance of welds to impact. In this connection published recommendations stating that 10-15% lack of fusion in welds subjected to impact loadings is permissible give rise to doubt.

The effect of weld structure on static and vibratory strength. For low-carbon steel the structure of a weld does not have any noticeable effect on static strength. Reinforcement of a weld of any size does not, as a rule, reduce static strength; however, reinforcement greatly affects the fatigue strength of welds (Fig. 152). The heavier the weld reinforcement and the larger the parent-to-build-up-metal

transition angle, the greater the affect of reinforcement on fatigue strength.

The fatigue strength of a weld increases considerably, if its reinforcement is removed and stress concentration is, consequently, eliminated, or if the parent-to-weld-metal transition surface is machined (or hand-worked).

Thus, weld reinforcement or improper structure of a weld may nullify all the advantages gained by improving the quality of the filler metal in welds intended for fatigue operation.

In conclusion it may be noted that the effect of welding imperfections on the mechanical properties of welds depends on the shape, size and depth of the imperfections, the grade of the parent metal and the quality of the filler metal, on the nature of the load and loading conditions.

Cracks and lack of fusion are most dangerous. Undercuttings, faulty edges and weld structure also greatly affect the mechanical properties of welds operating under vibratory and impact loads.

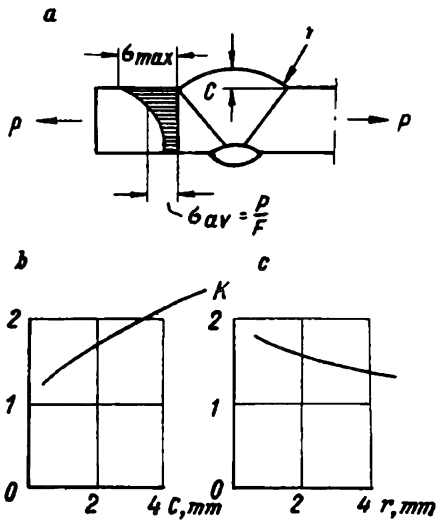

Fig. 152. Distribution of stresses in a butt weld:
a—stress sheet; *b*—variation of the concentration coefficient with bead height $K = \frac{\sigma_{max}}{\sigma_{av}}$ at $r = 0.5$ mm; *c*—variation of the concentration coefficient with the transition radius $K = \frac{\sigma_{max}}{\sigma_{av}}$ at $C = 2$ mm

As compared with lack of fusion, pores and slag inclusions are less dangerous and their effect depends not only on their shape, size and depth of penetration into the weld metal, but also on the mutual arrangement of such defects in the built-up metal. The effect of welding defects on the mechanical properties of welds was mainly investigated on low-carbon steel welds under static and vibratory loads. The results obtained do not characterise the effect of welding defects on high-strength steel welds under vibratory and dynamic loads, especially since the effect of such imperfections on the resistance of welds to impact has hardly been investigated at all.

So far in studying the relation between the defects revealed on radiographs and the mechanical properties of a weld, the fact that a three-dimensional defect appears on the radiograph as a two-dimensional image was not taken into account. From the roentgenograph it is only possible to estimate the area of the defect appearing

on the film. Therefore, the full extent to which a defect weakens the cross-section of a weld may be determined only when, besides the area of the defect, its length is known as well.

§ 3. The effect of lack of fusion on the workability of welded grade 30ХГСНА, 1Х18Н9Т steel and grade Д16-Т duralumin

In § 2 we considered the effect of welding imperfections established by means of tests on low-carbon steel welds. It is important to know how welding imperfections affect welds of other materials used for critical structures.

Many years of experience with welded articles (pipelines, reservoirs, aircraft welded units, etc.) have proved that lack of root fusion in single V-welds is the most frequent and dangerous defect.

Hence, let us consider the results of investigations conducted to find the effect of lack of root fusion on grades 30ХГСНА, 1Х18Н9Т steel and grade Д16-Т duralumin single V-welds subjected to various loadings. Grade 30ХГСНА is a high-strength steel, grade 1Х18Н9Т steel is an austenitic steel, while grade Д16-Т duralumin represents the aluminium alloys.

The effect of lack of root fusion on single V-welds * under static tension. Static tension tests like fatigue and static endurance tests were carried out with 10 × 20 mm specimens. Grade 30ХГСНА specimens were treated to $\sigma_b = 160 \pm 10$ kg/sq mm and grade Д16-Т duralumin specimens to $\sigma_b = 42\text{-}44$ kg/sq mm; grade 1Х18Н9Т specimens were not subjected to heat treatment.

The results obtained in testing at room temperature flawless butt welds and V-welds with lack of root fusion show (Fig. 153) that the imperfection affects grade 30ХГСНА and 1Х18Н9Т steel welds and grade Д16-Т duralumin welds in a different manner under conditions of static tension. The strength of flawless grade 1Х18Н9Т steel welds is equal to that of the parent metal. Lack of fusion does not affect the weld metal. The ultimate strength of the weld metal does not drop with the increase in the length of the defect. For grade 1Х18Н9Т steel welds lack of fusion is tantamount to cross-section weakening. Lack of fusion affects grade 30ХГСНА steel welds and grade Д16-Т duralumin welds to a considerably greater degree, especially grade 30ХГСНА steel. Lack of fusion not only weakens the cross-section of the welds, but acts as a stress concentrator, especially in the case of 30ХГСНА welds.

---

* In all cases 10 mm thick plates were welded automatically with a melting electrode. Grade 30ХГСНА steel specimens were welded by the hidden arc technique, using grade Св-18ХМА electrode wire 3.0 mm in diameter. Plates of grade 1Х18Н9Т steel and Д16-Т duralumin were welded in a stream of pure argon using grade Св-1Х18Н9Т electrode wire, 2.0 mm in diameter for steel and 2.5 mm grade АК electrode wire for duralumin.

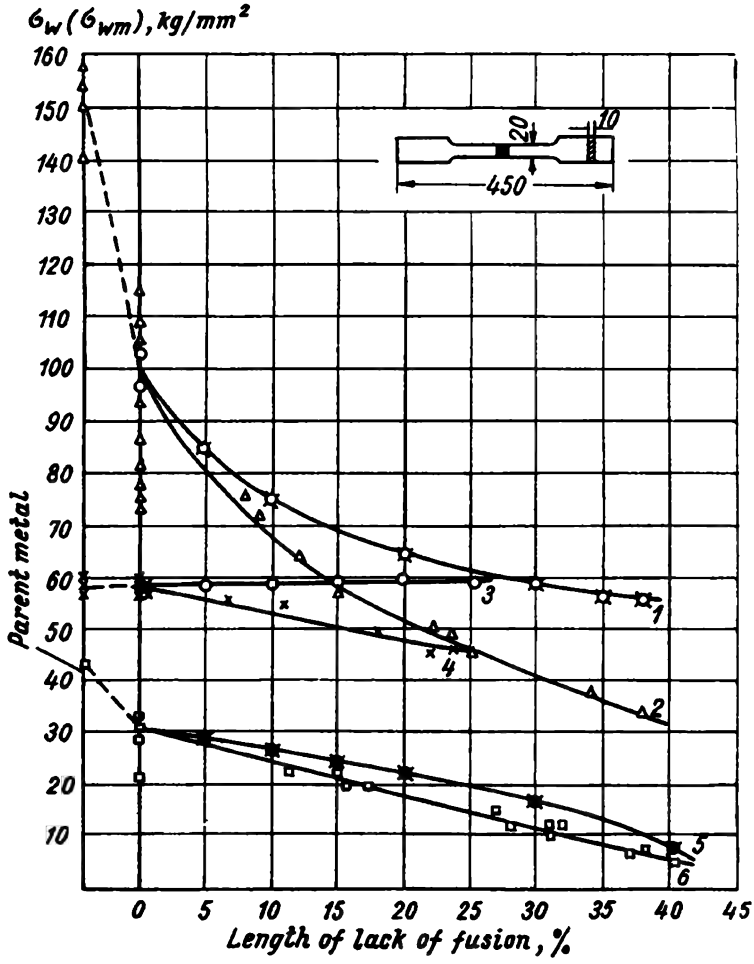

Fig. 153. Dependence of the ultimate strength on length of lack of fusion under static tension testing:

1—grade 30ХГСНА steel
3—grade 1Х18Н9Т steel
5—grade Д16-Т duralumin
} $\sigma_{wm} = \frac{P_{br}}{F_d}$,

2—grade 30ХГСНА steel
4—grade 1Х18Н9Т steel
6—grade Д16-Т duralumin
} $\sigma_w = \frac{P_{br}}{F_0}$

σ_{wm}—ultimate strength of weld metal; σ_w—ultimate strength of weld; P_{br}—breaking load; F_d—cross-section of test sample including lack of fusion; F_0—cross-section of test sample excluding lack of fusion

The effect of lack of fusion on welds under vibratory loads. The fatigue tests were carried out with a nonsymmetric loading cycle, maintaining a constant minimum stress of 2.5 kg/sq mm. Loading frequency was maintained at 700 cps. The fatigue limit σ_r was determined on the basis of 5×10^6 cycles for each lot of specimens.

An analysis of the experimental data (Fig. 154 and Table 30) shows that for grade 30ХГСНА and 1Х18Н9Т steel and grade Д16-Т

Table 30

Dependence of the Fatigue Limit of Welds on Lack of Fusion

Material, grade	Kind of specimen	Series No.	Length of lack of fusion, %		Fatigue limit σ_r, kg/sq mm	Effective concentration factors	
			Extent of defect in series	Average size of defect in series		For the faulty section, %	For the parent metal
30ХГСНА steel	With removed reinforcement	1	Parent metal		25.3	—	1.0
		2	0	0	18.2	1.0	1.4
		3	7-11	10	11.5	1.6	2.2
		4	20-26	23	7.0	2.6	3.6
		5	33-37	35	6.5	2.8	4.0
		6	0	0	10.3	1.76	2.5
	With reinforcement	7	19-24	22	8.5	2.14	3.0
1Х18Н9Т steel	With removed reinforcement	1	Parent metal		19.6	—	1.0
		2	0	0	17.1	1.0	1.1
		3	10	10	5.6	3.0	3.5
		4	20-25	23	4.0	4.26	5.0
	With reinforcement	5	16-27	22	5.0	3.42	4.0
Д16-Т duralumin	With removed reinforcement	1	Parent metal		8.5	—	1.0
		2	0	0	7.5	1.0	1.13
		3	6-17	8	4.8	1.56	1.8
		4	27-34	29	3.0	2.5	2.8
		5	35-45	40	2.75	2.72	3.1

duralumin an increase in the length of lack of fusion causes a nonlinear drop in the fatigue limit of welds. The rate at which the fatigue limit diminishes, determined as the change in the fatigue limit per 1% of lack of fusion, decreases with the increase in the length of the imperfection. A 5% lack of fusion reduces the fatigue limit of grade 30ХГСНА and 1Х18Н9Т steel and grade Д16-Т duralumin

welds by 23, 56 and 20%, respectively. The rate at which the fatigue limit drops with lack of fusion ranging from 0 to 5% amounts on an average to 0.84, 1.8 and 0.4 kg/sq mm per 1%, respectively.

As the length of lack of fusion increases from 5-10 to 25-30%, the fatigue limit of grade 1X18H9T steel and grade Д16-Т duralumin

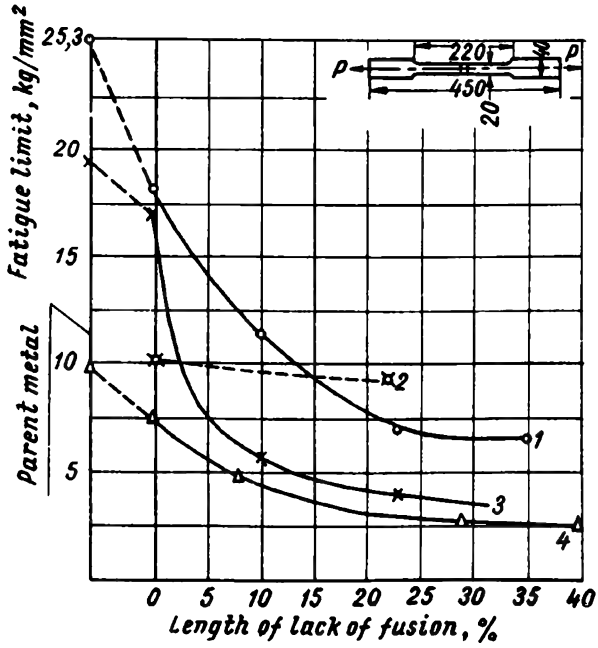

Fig. 154. Fatigue limit of welds as function of length of lack of fusion:

1—grade 30ХГСНА steel samples with removed reinforcement; *2*—grade 30ХГСНА steel reinforced weld samples; *3*—grade 1Х18Н9Т steel welds with removed reinforcement; *4*—grade Д16-Т duralumin welds with removed reinforcement

welds drops at the rate of 0.3-0.1 kg/sq mm per 1% and 0.5 to 0.1 kg/sq mm per 1% for grade 30ХГСНА steel.

As mentioned above, 5% lack of fusion reduces the fatigue limit of grade 30ХГСНА steel welds by 23%, whereas a 35% lack of fusion reduces the fatigue limit by 65%, i.e., only 2.8 times (65 : 23) and not 7 times (35 : 5). Hence, the rate at which the fatigue limit diminishes decreases rapidly with the increase in the length of the imperfection, being the maximum in small lengths of lack of fusion (5-10%)

A 10% lack of fusion reduces the fatigue limit by 38%, 67% and 36% respectively in grade 30ХГСНА and 1Х18Н9Т steel welds and grade Д16-Т duralumin welds. A lack of fusion of 20-25% brings about the following reduction in the fatigue limit of welds: grade

30ХГСНА steel welds—62%; grade 1Х18Н9Т steel welds—73%; and grade Д16-Т duralumin welds—57%.

The fatigue limit of flawless grade 30ХГСНА and 1Х18Н9Т steel welds and grade Д16-Т duralumin welds amounts to 18.2, 17.1 and 7.5 kg/sq mm respectively. Compared with the parent metal. the fatigue limit of flawless welds (with removed reinforcement) is 28, 13 and 24% lower for grade 30ХГСНА and 1Х18Н9Т steel and grade Д16-Т duralumin respectively.

For grade 30ХГСНА steel the ratio $\frac{\sigma_r}{\sigma_b}$ (of fatigue limit to ultimate strength) drops slowly as the lack of fusion increases from 0 to 30% and ranges from 0.18 to 0.15. For this grade of steel the $\frac{\sigma_r}{\sigma_b}$ ratio may be assumed constant, not depending on the length of this welding defect. This means that an increase in lack of fusion reduces both the fatigue limit and the ultimate strength equally. However, taken separately, for grade 30ХГСНА steel, the reductior in σ_r and σ_b, with an increase in lack of fusion is nonlinear, σ_r being about 5.5-6.5 times smaller than σ_b in the 0 to 30% range.

For grade 1Х18Н9Т steel welds the $\frac{\sigma_r}{\sigma_b}$ ratio diminishes most rapidly in the 5-10% range. The sharp drop in the curve, expressing $\frac{\sigma_r}{\sigma_b}$ as a function of the length of lack of fusion, indicates that for this grade of steel the fatigue limit diminishes more quickly than the static ultimate strength with an increase in the length of the imperfection.

Hence, although lack of fusion does not affect grade 1Х18Н9Т steel welds under static tension, under vibratory loads it affects such welds to a greater degree than grade 30ХГСНА steel and grade Д16-Т duralumin welds.

Reinforcement of flawless grade 30ХГСНА steel welds affects them negatively, reducing the fatigue limit by 35-45%. In the case of grade 30ХГСНА and 1Х18Н9Т steel, weld reinforcement of a size equal to 20-25% lack of fusion (in relation to parent metal thickness) does not bring about an essential increase in the fatigue limit.

Results of fatigue tests conducted on parent metal specimens, flawless weld specimens and defective welds with a lack of fusion of various lengths proved that this imperfection has a considerable effect on grade 30ХГСНА and 1Х18Н9Т steel welds and grade Д16-Т duralumin welds under vibratory tension loads. Most sensitive to small lack of fusion (5-10% of parent metal thickness) are grade 1Х18Н9Т steel welds.

The effect of lack of fusion on welds under repeated static load. The effect produced by this defect on welds under repeated static load was determined, as in the case of fatigue tests, by testing parent metal plates, flawless welds (0% lack of fusion) and defective welds with lack of fusion of different lengths.

Grade 30ХГСНА steel and duralumin samples were subjected to the same heat treatment as specimens intended for fatigue and static tension tests. Grade 1Х18Н9Т steel specimens were tested without heat treatment.

The static fatigue limit (σ_r^{st}) tests were carried out with 10,000 repeated loadings, observing a nonsymmetric tension cycle and maintaining a constant minimum stress of 2.5 kg/sq mm. Load application frequency was maintained within 4-6 cycles per minute.

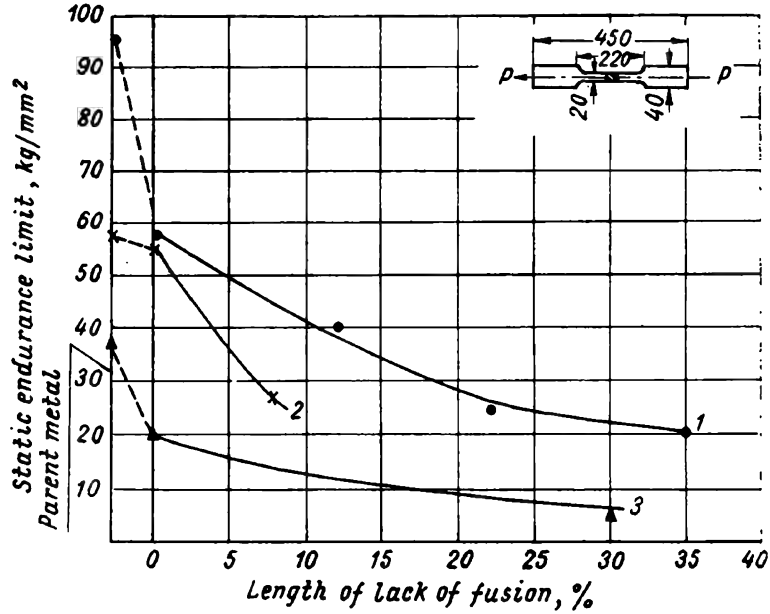

Fig. 155. Dependence of the static endurance limit of welds on length of lack of fusion:

1—grade 30ХГСНА steel; *2*—grade 1Х18Н9Т steel; *3*—grade Д16-Т duralumin.

Note: Curves are plotted on the basis of 10,000 cycles. For flawless Д16-Т duralumin welds—7,500 cycles, and for duralumin welds with lack of fusion ranging from 27 to 30%—4,000 cycles

The test data show that the static fatigue limit (Fig. 155) of grade 30ХГСНА and 1Х18Н9Т steel welds and grade Д16-Т duralumin welds drops nonlinearly with an increase in length of lack of fusion, and, as in the case of fatigue tests, the rate of the drop is maximum for small lengths of the defect and diminishes as the length increases.

In the 0 to 5-7% range of lack of fusion the static fatigue limit (σ_r^{st}) drops at an average rate of 2.0, 3.4 and 0.65 kg/sq mm per 1% of lack of fusion for grade 30ХГСНА and 1Х18Н9Т steel welds and grade Д16-Т duralumin welds respectively. 5% lack of fusion in grade 30ХГСНА steel welds reduces the static fatigue limit by about 17%, and a 35% imperfection—by 65%. Thus, a sevenfold increase

in the imperfection (35 : 5) reduces the static fatigue limit 3.8 times (65 : 17) and not 7. Hence, the rate at which the static fatigue limit drops diminishes with the increase in the length of lack of fusion.

A flawless weld from which reinforcement was removed shows the following reduction in the static fatigue limit, as compared with that of the parent metal: grade 30ХГСНА steel by 38%; grade 1Х18Н9Т steel—by 5% and grade Д16-Т duralumin—by 46%.

7% lack of fusion in welds from which reinforcement was removed reduces the static fatigue limit, as compared with flawless welds, by 25, 52 and 33% respectively for grade 30ХГСНА and 1Х18Н9Т steel and grade Д16-Т duralumin.

The dependence of the static fatigue limit-ultimate strength ratio $\left(\frac{\sigma_r^{st}}{\sigma_b}\right)$ on the length of lack of fusion was also analysed. For grade 30ХГСНА steel welds the ratio $\frac{\sigma_r^{st}}{\sigma_b} = 0.55$ remains constant in the 0 to 35% range.

For grade 1Х18Н9Т steel and Д16-Т duralumin welds the $\frac{\sigma_r^{st}}{\sigma_b}$ ratio diminishes with an increase in the length of the imperfection, and since σ_b diminishes with an increase in the length of the imperfection it follows that σ_r^{st} must diminish still more quickly. The static fatigue limit of grade 1Х18Н9Т welds drops at a comparatively higher rate. Thus, the static fatigue tests have shown that grade 1Х18Н9Т steel welds are also more sensitive to the stress concentration caused by lack of fusion of a small length (5-7%).

Reinforcement of grade 30ХГСНА steel welds with a 20-25% lack of fusion does not augment the resistance of these welds to repeated static loads, as compared with welds from which reinforcement has been removed.

Fatigue tests have made it possible to establish the sensitivity of the studied materials to welds and the effect of lack of root fusion in single V-welds in the high-stress region under repeated static load. It has been ascertained that the sensitivity of grades 1Х18Н9Т and 30ХГСНА steel and grade Д16-Т duralumin to welds and the effect of lack of fusion on the welds of these metals as determined by repeated static tension load testing is qualitatively the same as in dynamic endurance testing.

The effect of lack of fusion on welds under impact bend test. The effect of lack of fusion on welds was in this case investigated as a function of the length of the imperfection, test temperature, heat treatment, static hardening and a fatigue load.

Grade 30ХГСНА steel specimens were heat-treated to $\sigma_b = 160 \pm 10$ kg/sq mm and grade Д16-Т duralumin welds to a $\sigma_b = 42$-44 kg/sq mm. Grade 1Х18Н9Т steel specimens were not heat-treated.

The tests were conducted on a 75 kg m pendulum impact testing machine in a manner specified for notch bar-bending tests by the U.S.S.R. State Standard (ГОСТ) 1524-42. In welds the lack-of-fusion defect corresponded to a notch. Flawless welds and parent metal specimens were tested without notches, for comparison. 10 × 20 mm section specimens were freely placed upon supports arranged at a distance of 80 mm.

The results of the impact bending test of grades 30ХГСНА and 1Х18Н9Т steel and Д16-Т duralumin parent metal specimens, specimens of flawless single V-welds and single V-welds with lack of root fusion of different lengths (Figs. 156-158) lead to the following conclusions.

Grade 30ХГСНА steel welds manifested the greatest sensitivity to lack of fusion under impact bending. Lack of fusion of any length (from 3 to 75% of specimen thickness) sharply reduces the impact resistance of welded specimens. Heat treatment under various conditions only slightly affects the impact resistance of welded specimens with lack of fusion defects; lack of fusion causes such a high blue-brittleness of the built-up metal that the effect of temperature is very slight. There are no traces of blue-brittleness and cold-brittleness on the impact-vs-lack of fusion curve, whereas these phenomena occur in impact and static notch bar-bending tests.

The reason for the high sensitivity of welds to lack of fusion under impact bending is that slight lack of fusion (up to 10% of weld thickness) sharply reduces the plastic properties (the extent of the deformed field and maximum values of the relative longitudinal Δx and cross Δy deformations) of grade 30ХГСНА steel welded specimens (Fig. 159). Such an excessively heavy effect of lack of fusion on grade 30ХГСНА steel welds under impact test is not to be neglected in practical work.

Defective grade Д16-Т duralumin welds show a low impact resistance in the —60 to +300°C temperature range. As compared with flawless welds, lack of fusion reduces the impact resistance of such welds about 2-3 times.

Although grade 1Х18Н9Т steel welds show a noticeable sensitivity to lack of fusion ranging from 4 to 15% of specimen thickness under impact bending, destruction of the weld occurs with a considerable absorption of impact energy. The rate, at which the impact resistance of welds is reduced, diminishes with the increase in the length of the imperfection (to 40%). The impact resistance of defective welds at high temperature (from 100 to 700°C) is twice that of welds tested at room temperature.

At a temperature of about 500°C (the blue-brittleness phenomenon) the effect of lack of fusion on impact resistance is less pronounced than at room temperature. A drop in temperature (to —60°C) is not followed by any considerable increase in the brittleness of the weld metal.

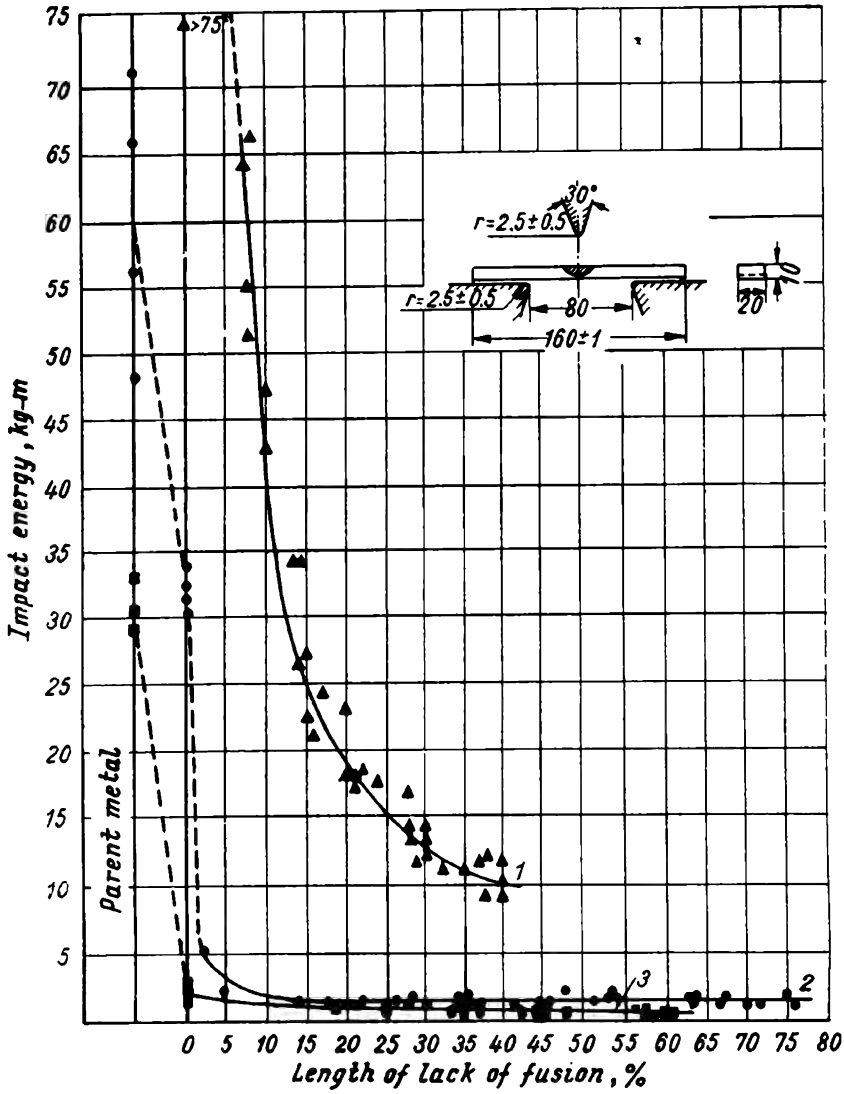

Fig. 156. Effect of lack of fusion on the impact resistance of welds: *1*—grade 1Х18Н9Т steel; *2*—grade 30ХГСНА steel; *3*—grade Д16-Т duralumin

The comparatively high strength of defective grade 1Х18Н9Т steel welds is due to the fact that slight lack of fusion (up to 10%) does not have a serious effect on the plastic properties of welds under impact bending. A further increase in the length of the imperfection is not followed by a sharp reduction in the deformed field and, hence, in the maximum relative longitudinal and cross deformations.

Static hardening by elongation (0.33% for grade 30ХГСНА steel and 1.25% for grade 1Х18Н9Т steel) and fatigue load (training at stresses constituting 0.6 of fatigue limit stress and $N = 10^5$ cycles) do not reduce the impact resistance of grades 30ХГСНА and 1Х18Н9Т

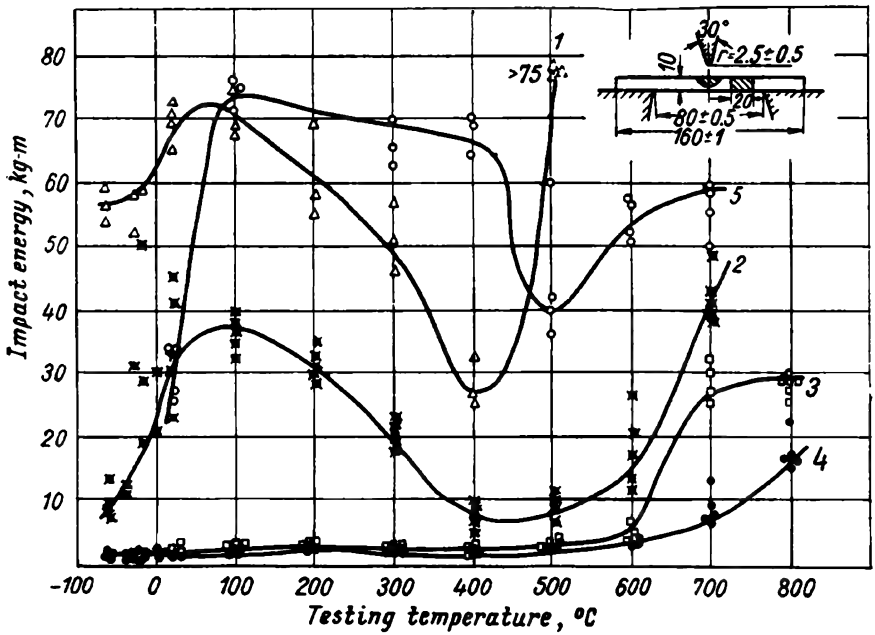

Fig. 157. Effect of welding quality and weld metal on the impact resistance of welds under different test temperatures:

1—grade 30ХГСНА steel, parent metal; *2*—grade 30ХГСНА steel, 0% lack of fusion; *3*—grade 30ХГСНА steel, 10-15% lack of fusion; *4*—grade 30ХГСНА steel, 20-30% lack of fusion; *5*—grade 1Х18Н9Т steel, 10-15% lack of fusion

steel welds with a 20-25% lack of fusion at temperatures from —60 to +20°C.

The investigations described above have shown that lack of fusion affects welds differently, depending on the kind of load.

As for the extent to which lack of fusion affects welds, the materials investigated can be arranged in the following order:

a) under static tension—grade 30ХГСНА steel, grade Д16-Т duralumin and 1Х18Н9Т steel;

b) under vibratory load—grade 1Х18Н9Т steel, 30ХГСНА steel and Д16-Т duralumin;

c) under repeated static load—grade 1Х18Н9Т steel, Д16-Т duralumin and grade 30ХГСНА steel;

d) under impact bending—30ХГСНА steel, 1Х18Н9Т steel and Д16-Т duralumin.

Hence, the sensitivity of welds to lack of fusion acting as stress concentrators is determined not only by the plastic properties of

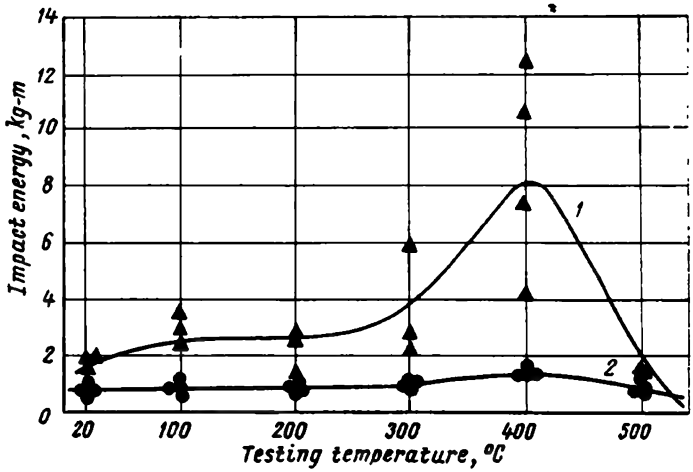

Fig. 158. Effect of temperature on the impact resistance of grade Д16-Т duralumin welds:
1—0% lack of fusion; *2*—30-50% lack of fusion

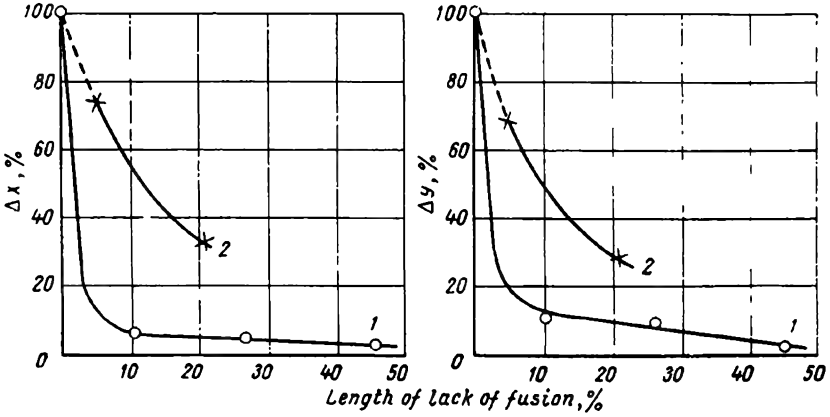

Fig. 159. Change in plasticity factors Δx and Δy under impact bending with a change in the length of lack of fusion:
1—grade 30ХГСНА steel; *2*—grade 1Х18Н9Т steel

welded material (and weld metal), but also by the kind of load. The way in which the load is applied is the main factor determining the sensitivity of welds to lack of fusion in the case of grade 1Х18Н9Т steel welds subjected to fatigue and static endurance tests.

It is advisable to take into account the effect of lack of fusion on welds in choosing materials for welded structures, especially in the

case of structures intended to operate under vibratory and impact loads. The preference should be given to grades of steel (or other metal) which, apart from other strength properties, show a comparatively lower sensitivity to lack of fusion and other welding defects under vibratory and impact loads.

The following considerations should be taken into account in estimating the quality of a weld with the aid of a gamma-graph. It is not advisable to determine the length of lack of fusion if the weld metal is highly sensitive to this imperfection under the given loading conditions, because, in practice, long and short lack of fusion is equally dangerous. Even a slight lack of fusion revealed on the gamma-graph must be considered as grounds for rejection.

In gamma-inspection, attention should chiefly be directed towards the detection of lack of fusion of the smallest possible linear dimensions in the direction of inspection.

In cases where lack of fusion in welds is admissible by manufacturing and acceptance standards for welded structures, it is advisable, besides using other known methods, to determine the length of the imperfection with the aid of the characteristic curve plotted for the weld gamma-graph.

Linear Absorption Coefficients for Narrow-Beam Monochromatic Gamma-Radiation

E, Mev	μ, cm^{-1}	σ, cm^{-1}	τ, cm^{-1}	χ, cm^{-1}	$d_{0.5}$, cm	$d_{0.1}$, cm
			Aluminium ($Z=13$; $\rho=2.7$ g/cu cm)			
0.102	0.444	0.384	0.0597	—	1.56	5.2
0.128	0.393	0.363	0.0297	—	1.76	5.85
0.170	0.347	0.335	0.0118	—	2.00	6.64
0.255	0.297	0.294	0.00335	—	2.34	7.75
0.340	0.265	0.264	0.00129	—	2.62	9.0
0.409	0.247	0.246	0.00077	—	2.8	9.3
0.511	0.224	0.224	0.000416	—	3.1	10.3
0.681	0.198	0.198	0.000195	—	3.5	11.6
1.022	0.165	0.165	0.0000778	—	4.2	14.0
1.362	0.143	0.143	0.0000467	0.000294	4.85	16.1
1.523	0.133	0.132	—	0.000502	5.20	17.3
2.043	0.115	0.113	0.000025	0.001890	6.02	20.0
2.633	—	—	—	—	—	—
3.065	0.094	0.089	—	—	7.37	24.5
4.086	0.0825	0.074	0.0000101	0.00856	8.4	28.0
5.110	0.0754	0.064	0.00000764	0.01140	9.2	30.6
6.130	0.0702	0.056	—	0.01380	9.9	32.8
			Steel ($Z=26$; $\rho=7.8$ g/cu cm)			
0.102	2.826	1.086	1.74	—	0.243	0.81
0.128	1.943	1.023	0.92	—	0.356	1.18
0.170	1.321	0.945	0.376	—	0.524	1.74
0.255	0.932	0.824	0.108	—	0.75	2.50
0.340	0.781	0.735	0.0464	—	0.89	2.94
0.409	0.720	0.694	0.0275	—	0.963	3.20
0.511	0.647	0.631	0.0158	—	1.07	3.55
0.681	0.565	0.558	0.0715	—	1.23	4.07
1.022	0.463	0.460	0.0029	—	1.50	4.97
1.362	0.393	0.390	0.00173	0.00167	1.76	5.86
1.533	0.380	0.374	0.00144	0.00362	1.82	6.05
2.043	0.330	0.315	0.000945	0.01070	2.20	6.98
2.633	—	—	—	—	—	—
3.065	0.280	0.250	0.000543	0.0292	2.48	8.2
4.086	0.256	0.209	0.000464	0.0486	2.70	9.0
5.110	0.253	0.189	—	0.0645	2.74	9.1
6.130	0.237	0.159	—	0.0780	2.92	9.7

Continued

E, Mev	μ, cm^{-1}	σ, cm^{-1}	τ, cm^{-1}	χ, cm^{-1}	$d_{0.5}$, cm	$d_{0.1}$, cm
		Lead ($Z=82$; $\rho=11.34$ g/cu cm)				
0.102	60.2	1.328	58.9	—	0.0115	0
0.128	33.6	1.255	32.3	—	0.0206	0
0.170	16.5	1.160	15.35	—	0.042	0.139
0.255	6.32	1.015	5.30	—	0.110	0.364
0.340	3.40	0.906	2.495	—	0.204	0.686
0.409	2.43	0.85	1.578	—	0.285	0.945
0.511	1.65	0.73	0.915	—	0.42	1.39
0.681	1.16	0.684	0.480	—	0.597	1.98
1.022	0.772	0.566	0.206	—	0.9	2.98
1.362	0.624	0.49	0.1275	0.00643	1.11	3.69
1.533	0.58	0.459	0.100	0.0109	1.20	4.0
2.043	0.50	0.391	0.0687	0.0424	1.39	4.6
2.633	—	—	—	—	—	—
3.065	0.423	0.307	—	0.1157	1.64	5.45
4.086	0.472	0.256	0.0287	0.187	1.48	4.88
5.1	0.493	0.221	0.0224	0.250	1.41	4.67
6.130	0.515	0.195	0.0220	0.298	1.39	4.65

E, Mev	μ, cm^{-1}	$d_{0.5}$, cm^{-1}	$d_{0.1}$, cm	μ, cm^{-1}	$d_{0.5}$, cm	$d_{0.1}$, cm
	Concrete ($\rho=2.4$ g/sq cm)			*Brickwork* ($\rho=1.7$ g/sq cm)		
0.10	0.410	1.69	5.62	0.29	2.39	7.93
0.15	0.360	1.92	6.39	0.256	2.70	9.00
0.20	0.330	2.04	6.98	0.233	2.97	9.9
0.30	0.286	2.42	8.05	0.202	3.43	11.4
0.40	0.254	2.73	9.06	0.18	3.85	12.8
0.50	0.234	2.96	9.83	0.164	4.23	14.0
0.60	0.214	3.24	10.8	0.152	4.57	15.2
0.80	0.189	3.66	12.2	0.133	5.22	17.3
1.00	0.170	4.07	13.5	0.120	5.77	19.2
1.50	0.138	5.02	16.7	0.098	7.06	23.4
2.00	0.119	5.83	19.3	0.084	8.23	27.4
3.00	0.095	7.3	24.2	0.0673	10.3	34.2
4.00	0.0815	7.5	28.3	0.0575	12.0	40.0
5.00	0.0725	9.56	31.8	0.0513	13.5	45.0
6.00	0.0665	10.4	34.6	0.0472	14.7	48.7
8.00	0.058	11.95	39.6	0.0410	16.9	56.0
10.00	0.053	13.1	43.5	0.0376	18.5	64.2

h	$h\nu$, Mev																			
	0.1	0.2	0.3	0.4	0.5	0.6	0.7	0.8	0.9	1	1.25	1.5	1.75	2.0	2.2	3	4	6	8	10
1.5	0.5	1	1.5	2	2	3	4	6	7	8	9.5	11	12	12	12	13	12	10	9	9
2	1.0	2	3	4	5	7	8	10	11.5	13	15	17	18.5	20	20	21	20	16	15	13.5
5	2	4	6	9	11	15	19	22	25	28	34	38	41	43	44	46	45	38	33	30
8	2	5	8	11	15	19.5	23.5	28	32	35	42	48	52.5	55	57	59	58	50	43	38
10	3	5.5	9	13	16	21	26	30.5	35	38	45	51	56	59	61	65	64	55	49	42
20	3	6	11	15	20	26	32.5	38.5	44	49	58	66	72	76	78	83	82	71	63	56
30	3.5	7	11.5	17	23	30	36.5	43	49.5	55	65	73	86	85	88	93	92	80	72	66
40	4	8	13	18	24	31	38	45	52	58	68.5	78	80	91	94	100	99	87	78	68
50	4	8.5	14	19.5	26	32.5	39.5	46	53	60	72	82	90	96	100	106	105	92	83	73
60	4.5	9	14.5	20.5	27	34.5	42	49.5	56	63	75	86	95	101	104	110	109	97	87	77
80	4.5	10	15.5	21.5	28	37	45	53	60	67	80	92	101	107	111	117	116	109	94	82
100	5	10	16	23	30	38.5	47	55	63	70	84.5	96.6	106	113	117	122	121	109	99	87
200	6	12.5	19	26	34	44	53	63	72	80	96.5	111	122	129	134	140	138	126	114	102
500	6.5	14	22	31	40	51	61	72	82	92	113	129	142	150	154	163	161	149	133	119
1,000	7	15	24	33	44	57	69.5	81	92	102	123	141	156	165	170	180	178	165	151	133
2,000	8.5	17	27	38	50	63	76	88	100	111	135	154	168	179	185	197	195	181	165	148
5,000	9	19	30	42	55	70	85	99	112	124	149	170	186	198	205	219	217	203	185	166
8,000	10	20	31.5	44	57	73.5	90	104	118	130	158	180	196	208	215	230	229	215	196	175
10^4	10.5	21	33	45.5	59	75	91	106	120	133	161	183	201	213	221	235	234	220	201	180
2×10^4	11	22	35	48.5	63	80	97	113	128	142	172	195	214	227	235	251	250	236	217	195
5×10^4	11.5	23.5	37	52	69	87	105	123	140	156	188	214	233	247	255	273	272	258	237	215
1×10^5	11.5	24	38	54	72	92	111	130	148	165	201	227	247	262	270	289	289	275	258	229

k	$h\nu$, Mev																
	0.1	0.2	0.3	0.4	0.5	0.6	0.7	0.8	0.9	1	1.25	1.5	1.75	2	2.2	3	4
1.5	5	9	12	14	16	17	18.5	20	20.5	21	21.5	22	23	24	25	27	28
2	7	12	17	22	25	27	29	31	32	33	34.5	36	38	39	41	44	45
5	14	25	34	41	48	51	55	51	61	64	69	74	78	81	83	89	94
8	17	31	42	51	58	63	67	71	75	78	85	91	96	101	103	112	116
10	19	35	46	56	63	68	73	77	81	85	93	100	106	110	114	122	126
20	23	43	57	68	77	83	88	94	98	103	113	122	130	136	141	153	159
30	24	45	62	75	85	92	98	104	109	114	126	136	144	151	156	170	177
40	25	48	66	80	91	98	105	111	117	122	133	144	153	161	166	182	191
50	29	52	71	84	95	103	110	116	122	127	139	151	161	169	175	191	200
60	31	56	75	88	98	107	114	121	127	132	145	157	167	176	182	199	210
80	32	59	77	92	104	112	120	127	134	140	155	163	178	187	194	212	222
100	34	61	81	96	108	117	125	132	139	145	161	173	185	195	202	221	233
200	42	70	91	107	120	131	140	148	156	163	180	196	208	220	228	250	266
500	44	77	101	120	134	149	160	170	179	187	206	223	237	250	259	288	306
1,000	45	82	110	132	150	163	175	186	196	205	226	244	261	275	286	317	337
2,000	49	90	111	144	162	177	193	202	212	222	245	265	283	300	312	346	368
5,000	56	101	134	158	177	193	207	220	232	243	270	294	314	333	343	382	407
10^4	68	115	147	171	190	207	223	236	249	260	288	313	336	355	369	409	437
2×10^4	80	129	160	183	202	219	234	248	263	276	306	332	356	378	392	434	465
5×10^4	86	138	170	196	218	236	252	269	284	299	330	359	384	408	423	472	504
10^5	100	158	182	208	230	249	267	284	300	315	349	380	407	432	447	500	534

k	$h\nu$, Mev																
	0.1	0.2	0.3	0.4	0.5	0.6	0.7	0.8	0.9	1	1.25	1.5	1.75	2	2.2	3	4
1.5	26	47	63	75	82	82	82	83	83	85	86	87	87	88	89	94	100
2	47	76	99	113	123	124	124	126	127	129	133	136	138	141	143	153	164
5	56	110	155	188	211	218	223	226	230	235	246	258	270	282	294	329	352
8	70	129	178	220	246	256	264	272	279	288	305	322	338	352	364	399	434
10	82	146	197	237	258	268	276	284	291	299	319	340	359	376	390	434	475
20	82	153	214	258	299	319	336	350	362	370	399	425	448	470	486	540	587
30	85	164	228	277	309	348	364	378	392	405	437	465	493	516	535	599	657
40	85	176	242	296	340	362	379	396	413	428	453	498	528	552	573	640	698
50	99	188	251	308	350	376	394	412	428	446	435	521	552	581	601	669	728
60	110	200	261	317	364	385	405	425	441	458	501	540	575	605	627	698	740
80	115	204	277	336	387	411	430	448	465	481	524	564	599	654	657	740	810
100	115	211	289	352	399	430	453	472	488	505	545	583	622	657	636	775	845
200	127	235	324	392	446	479	505	526	546	564	608	653	697	740	772	880	957
500	138	246	352	439	505	545	573	588	625	646	698	748	798	845	885	1,010	1,104
1,000	155	282	392	481	552	592	625	653	678	704	761	817	876	927	970	1,109	1,209
2,000	176	305	423	524	599	641	674	704	732	757	822	885	946	1,004	1,040	1,209	1,321
5,000	188	331	456	564	657	700	740	770	802	828	902	974	1,042	1,109	1,155	1,321	1,468
10^4	198	352	485	603	693	747	791	829	862	892	972	1,045	1,115	1,186	1,247	1,468	1,567
2×10^4	211	384	519	634	728	782	831	873	911	945	1,027	1,108	1,186	1,262	1,317	1,567	1,673
5×10^4	233	423	564	686	781	834	887	934	979	1,021	1,115	1,204	1,284	1,362	1,420	1,673	1,814
10^5	305	505	646	751	828	883	935	981	1,025	1,068	1,169	1,266	1,357	1,444	1,507	1,814	1,914

Specific Weight of Substances

Substance	Density, g/cu cm	Substance	Density, g/cu cm
Aluminium	2.70	Nickel	8.9
Beryllium	1.83	Tin	7.29
Concrete	2.2-2.35	Platinum	21.5
Paper	0.7-1.1	Rubber	0.91-0.93
Air	0.001293	Lead	11.3
Tungsten	19.3	Silver	10.5
Graphite	2.3	Glass	2.4-2.6
Duralumin	2.79	Thallium	11.9
Steel	7.1-7.9	Tantalum	16.6
Steel, pure	7.87	Titanium	4.5
Gold	19.32	Thorium	11.3
Indium	7.3	Uranium	18.7
Iridium	22.41	Phosphorus, red	2.20
Cadmium	8.64	Phosphorus, yellow	1.83
Cobalt	8.6	Chromium	7.1
Silicon	2.3	Celluloid	1.4
Leather	0.85-1.0	Cerium	6.92
Bone	1.8-2.0	Cast iron	7.2
Brass	8.4-8.7	Zinc	7.1
Magnesium	1.7	Ebonite	1.8
Copper	8.9	Quartz, melted	2.21
Molybdenum	10.0		

Lead Glass

Heavy flint glass	ТФ-1	3.86	Heavy flint glass	ТК-10	3.66
" " "	ТФ-2	4.09	" " "	ТК-11	4.01
" " "	ТФ-3	4.46	Barytes crown glass		
" " "	ТФ-4	4.65	БК	up to	3.12
" " "	ТФ-5	4.77	Flint glass Ф	up to	3.67
" " "	ТФ-7	4.52	Crown glass К	up to	2.53

Chemical Composition of Concrete

Compound	Content by weight, % in relation to		
	cement	sand	gravel
SiO_2	20.03	95.87	73.60
CaO	63.41	0.25	1.08
Al_2O_3	7.10	1.83	14.44
Fe_2O_3	3.14	0.04	0.43
FeO	—	0.27	1.49
NaO	—	0.88	4.20
MgO	2.84	—	—
SO_2	1.88	—	—
KO	—	0.61	4.46